CANADA
DEPARTMENT OF MINES AND TECHNICAL SURVEYS
DOMINION OBSERVATORIES

PUBLICATIONS

OF THE

Dominion Observatory

OTTAWA

VOLUME XX No. 2

THE MECHANICS OF FAULTING, WITH SPECIAL REFERENCE TO THE FAULT-PLANE WORK

(A Symposium)

JOHN H. HODGSON, *Editor*

INTERNATIONAL UNION OF GEODESY AND GEOPHYSICS
ASSOCIATION OF SEISMOLOGY AND PHYSICS OF THE EARTH'S INTERIOR
ELEVENTH GENERAL ASSEMBLY, TORONTO, CANADA

1957

55092-1—1½

TABLE OF CONTENTS

The Mechanics of Faulting, with Special Reference to the Fault-Plane Work

(A Symposium)

Foreword

The idea for this Symposium originated shortly after the Tenth General Assembly of the International Union of Geodesy and Geophysics. Several seismologists interested in the fault-plane work were present at those meetings but, under the pressure of the heavy program and in the absence of a session formally devoted to their subject, there was little opportunity for dis cussion. It was suggested to Prof. K. E. Bullen, President of the Association of Seismology and Physics of the Earth's Interior, that a fault-plane Symposium should be arranged at the Eleventh Assembly; with the concurrence of the Bureau of the Association Prof. Bullen agreed, and asked the writer to arrange the Symposium.

Because of the large number of papers presented at the Toronto meetings it was possible to assign only a morning session to the fault-plane Symposium. This gave each speaker about twenty minutes, too short a time for adequate presentation. It seemed desirable that the papers should be printed in a single volume so that the complete presentation of all the authors would be available for comparison. Because the meetings were to be held in Canada, and because the Symposium dealt with a subject in which it is very much interested, the Dominion Observatory offered to print the Symposium in its Publications. We are indebted to Dr. Marc Boyer, Deputy Minister, who agreed to this arrangement on behalf of the Department of Mines and Technical Surveys, to President K. E. Bullen and Secretary J. P. Rothé who gave the permission of the Association, and to the several authors who have allowed their papers to be published in this way.

The meetings in Toronto suffered from the absence of two important contributors to the fault-plane work, Prof. H. Honda and Dr. A. R. Ritsema. Dr. Ritsema submitted his manuscript for printing in this volume which, to some extent, filled the lack caused by his absence, but Prof. Honda had already had his paper printed in Japan for distribution at the meeting, so that no paper was available from him. In editing the Symposium I was repeatedly struck with the fact that no adequate treatment of fault-plane studies could be given without bringing in the work of the Japanese, and I therefore sought permission of Prof. Honda to reproduce his already-published paper. This permission was granted and the paper will be found reprinted in the present volume. I am very much indebted to Prof. Honda and to the editors of *The Science Reports of Tôhoku University* for permission to do this.

In arranging the Symposium it would have been desirable to have had the papers presented in a logical order: those dealing with theory or the fundamentals of method first, then those giving the summary of the results obtained by various working groups, and finally papers dealing with the interpretation of results. It was not possible to follow this order completely at Toronto because several titles were submitted after the program had been arranged; this has been rectified in these printed proceedings, which follow the order outlined above.

It is inherent in the nature of symposia that they do not provide final answers; the present volume can only present a survey of current fault-plane work and its interpretation. It seemed desirable however that a summary should be provided, to define areas of agreement and disagreement among the various authors and to point the direction of future research. As Editor, I have taken the liberty of providing this summary in a final paper. The manuscript of this paper was circulated to all the authors, and their comments have been incorporated as much as possible; nevertheless I must bear the responsibility for any inadequacies it may have as a survey of the present volume.

JOHN H. HODGSON,
Editor

Motion at the Source of an Earthquake

BY PERRY BYERLY AND WILLIAM V. STAUDER, S.J.
University of California, Berkeley, California, U.S.A.

ABSTRACT

NAKANO's theoretical development emphasizes the effect of seismic disturbances at large distances from the source and develops equations of first motion in P and S for several types of source mechanisms. These equations are compared to the methods of approach of various investigators, and two mechanisms in particular are singled out: a single couple, which represents motion along a fault, and a double couple, which represents a compressive and tensile stress at right angles. Methods of transformation and projection permit the application of the theory for an infinite homogeneous earth to the heterogeneous earth. Possible uses of S phases are noted. Single observations of the first motion of S offer the possibility of resolving the ambiguity in fault-plane solutions from P alone in which the single couple is the mechanism assumed. Identification of the second nodal surfaces of SV and SH offers a criterion for deciding which mechanism, the single couple or the double couple, is operative in particular earthquakes. Further, simple relations involving the ratios SH/SV, P/SH, P/SV suggest other approaches to the problem of motion at the source of an earthquake. S phases, however, are to be used with great care.

THEORY

The theory in back of the interpretation of the motion at the source of an earthquake from the first motions in the waves recorded on seismograms was first published by HIROSHI NAKANO in 1923. Departing from formulae developed by STOKES and assuming an infinite homogeneous elastic solid, he took a source of form $f(t)$ at the origin in a Cartesian reference system and computed the equations of wave accelerations for P waves and S waves at large distances.

These were of the form

$$\left.\begin{aligned} \delta_{ax} &= (lx + my + nz)\,\frac{x}{4\pi\rho a^2 r^3}\, f''\left(t - \frac{r}{a}\right) \\ \delta_{bx} &= -\,[(lx + my + nz)x - lr^2]\,\frac{f''\left(t - \frac{r}{b}\right)}{4\pi\rho b^2 r^3}\;. \end{aligned}\right\} \tag{1}$$

Here l, m, n are direction cosines of the force at the origin and r is the distance of the observing point from the source. The speeds of P and S are a and b and the density is ρ. There are three equations of each type, the three components of P and S. There is no assumption involved for a homogeneous medium. There is an assumption, perhaps, in extending the theory to a heterogeneous medium, but experience proves it justified as far as direction of first motion of P goes.

NAKANO then proceeded to extend the theory to several systems of forces. First he took a couple of lever arm Δs, the direction cosines of which were λ, μ, ν. The member $\vec{F}$ of the couple which has a downward component will be taken as acting at the positive end of Δs.

The equations for acceleration at a large distance were of form

$$\left.\begin{aligned} \delta_{ax} &= (\lambda x + \mu y + \nu z)\,(lx + my + nz)x\,\frac{\Delta s\, f'''\left(t - \frac{r}{a}\right)}{a^3 r^4} \\ \delta_{bx} &= -\,(\lambda x + \mu y + \nu z)\,[(lx + my + nz)x - lr^2]\,\frac{\Delta s\, f'''\left(t - \frac{r}{b}\right)}{b^3 r^4}\;. \end{aligned}\right\} \tag{2}$$

Note that the power of a (or b) in the denominator has increased by one, the function $f''(t-r/a)$ having been differentiated once. The Soviet seismologists speak of the order of the source, n. This quantity depends on the number of differentiations and therefore on the power of

a (or b). These speeds appear as a^{n+1} in their formulae. Two couples having moments about a common point are additive and do not increase the order. However, two couples whose moments are not about a common point increase the order again by one, another differentiation being involved.

NAKANO treated a number of cases. HONDA has also developed such equations, (HONDA *et al.*, 1956) preferring wave amplitude to acceleration. They have been developed in the Soviet Union also, as reviewed by KEYLIS-BOROK (1956).

A study of equations (2) reveals a number of means by which, given seismograms from stations well distributed over the earth, one can deduce the nature of the force system at the source. In theory one could do it with very few stations.

The pertinent relations are as follows:

1. The signs of the first motion in P and in S as they emerge form a pattern on the face of the earth which is dependent on the nature of the forces at the source.
2. The ratios of the earth amplitudes of the incident waves P, SH and SV bear a simple relationship to the source.

For example, a single impulsive force would send a P compression into one-half space and a rarefaction into the other. The nodal plane of P would bisect the force, which would be perpendicular to it. There would be a nodal line for S waves which would pass through the force.

However most seismologists have found more complex forces to be more reasonable and useful, in particular sources of a single couple or a pair of couples at right angles in a single plane.

The latter is equivalent to two forces in line directed toward the origin plus two others in line at right angles to the first, and oppositely directed. This latter type of source is favored by HONDA (*see* Figure 1).

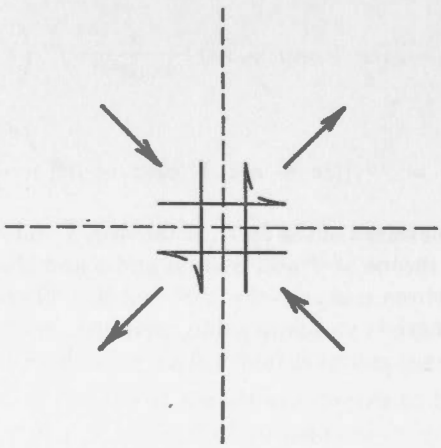

Figure 1. Pair of couples at right angles equivalent to tensions and compressions at right angles to each other and oblique to the pair of couples.

The single couple is used in North America, in Holland, and seems the most successful in the Soviet Union. The two types each give an identical quadrant distribution of P. The distribution of first motion of S, on the other hand, differs for the two cases (*see* Figure 2). A study of the distribution of S might discriminate between the two types of sources. The difficulties in finding the first motion in S, however, are grave.

The American view has been much influenced by the 1906 California earthquake and also the 1940 Imperial Valley earthquake. Both had long surface faults with horizontal slippage. To us it is the fling, the displacement along the fault, which is the source of the waves. To us who hold the elastic rebound theory, if HONDA's source is established, it will mean that the source of the waves is the release of strain in the large body of rock about the source, strain which had accumulated there due to external forces. Then the pairs of arrows representing strain need not be of the same length. Neither would the two possible fault planes necessarily coincide with the nodal planes of P. They would rather be inclined up to 15° to 20° toward the direction of the maximum compressive strain. Many Japanese seismologists consider faulting as a result of the earthquake—not its cause. They seem to have no difficulty in postulating a sudden application of force systems in the earth, rather than a sudden release after a slow accumulation of strain.

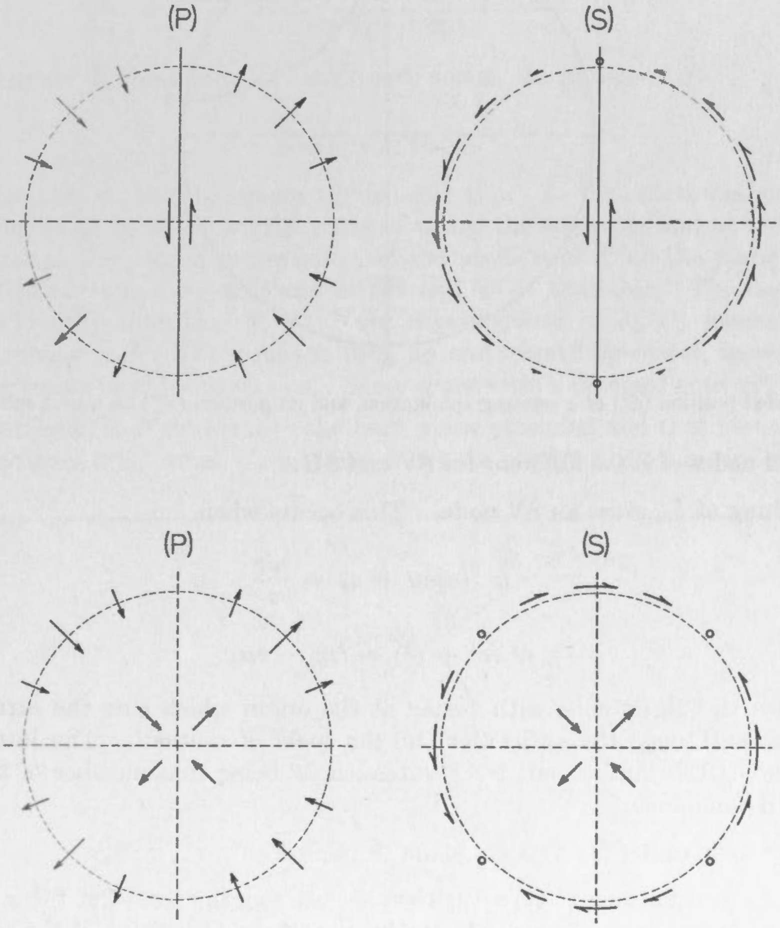

Figure 2. Distribution of first motion of P and S for a simple couple (top) as opposed to that for a pair of couples at right angles (bottom).

NON-HOMOGENEOUS EARTH

The first problem faced in applying Nakano's equations is the application of theory for an infinite homogeneous medium to the heterogeneous earth.

This is accomplished by considering the seismograph station position not at S, its location, but at S' (extended position on the earth's surface) or at S'' on a unit sphere about the focus, as in Figure 3. The first is the American method, the second that of the Soviets. Thus the equivalent seismic rays become straight lines. Also when one considers the amplitudes he must always reduce to amplitude of incident wave from observed surface motion.

We note from equation (2) that both P and S have nodes (zeros) in the fault plane

$$\lambda x + \mu y + \nu z = 0,$$

and that P has an additional node in the plane

$$lx + my + nz = 0$$

which is perpendicular to the forces of the couple. This plane has been called the auxiliary plane. The fault plane and the auxiliary plane separate regions of first compressions and first rarefactions.

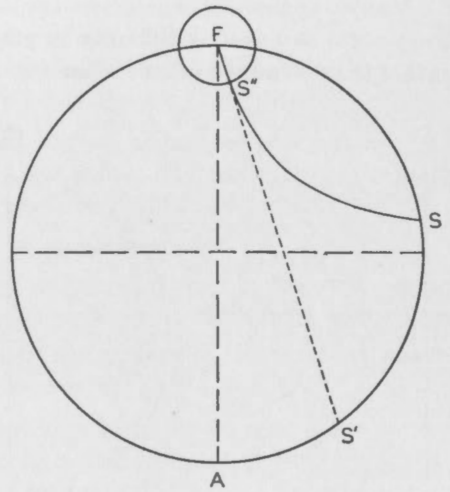

Figure 3. Extended position (S') of a seismograph station, and its position (S'') on a unit sphere about the focus.

The second nodes of S are different for SV and SH.

The vanishing of $\delta_{b\theta}$ gives an SV node. This occurs when

$$lx + my + nz = \frac{n^2 r}{z}$$

or

$$n^2 (x^2 + y^2) = lzx - mzy$$

This defines an elliptic cone with vertex at the origin which cuts the earth's surface in a circle which passes through the anticenter and the 'pole of motion'. The latter is defined as the point on the earth's surface cut by $\vec{F}$ extended, $\vec{F}$ being that member of the couple which has a downward component.

The second node of SH is a vertical plane through $\vec{F}$.

Now transform equations of type (2) to spherical coordinates. Let the x axis be directed north, the y east, the z down. The coordinates of the extended position of the station are r, φ, θ where r is distance, θ is angle of incidence and φ is azimuth of station (measured from north through east).

Equations of type (2) transform to

$$\left.\begin{aligned}
\delta_{ar} &= \frac{\Delta s}{4\pi\rho} \frac{f'''\left(t - \frac{r}{a}\right)}{a^2 r^2} (\lambda x + \mu y + \nu z)\,(l \sin\theta \cos\varphi + m \sin\theta \sin\varphi + n \cos\theta) \\
\delta_{b\varphi} &= -\frac{\Delta s}{4\pi\rho} \frac{f'''\left(t - \frac{r}{b}\right)}{b^2 r^2} (\lambda x + \mu y + \nu z)\,(l \sin\theta - m \cos\varphi) \\
\delta_{b\theta} &= \frac{\Delta s}{4\mu\rho} \frac{f'''\left(t - \frac{r}{b}\right)}{b^2 r^2} (\lambda x + \mu y + \nu z)\,[(l \cos\varphi + n \sin\varphi) \cos\theta - n \sin\theta].
\end{aligned}\right\} \quad (3)$$

We note that δ_{ar} corresponds to P motion, $\delta_{b\varphi}$ to SH motion, and $\delta_{b\theta}$ to SV motion.

We may now rotate the x (and y) axis through Φ about the vertical z axis until $\vec{F}$, that member of the couple which has a downward component, lies in the xz plane. Then in equation (3) $m = 0$ and $l = \cos\psi$, $n = \sin\psi$ where ψ is the plunge of the motion.

Then

$$\left.\begin{aligned} \frac{\delta_{ar}}{\delta_{b\varphi}} &= -\frac{b^3}{a^3}\,\frac{\sin\theta\cos(\varphi-\Phi)+\cos\theta\tan\psi}{\sin(\varphi-\Phi)} \\ \frac{\delta_{b\theta}}{\delta_{b\varphi}} &= \frac{\sin\theta\tan\psi-\cos\theta\cos(\varphi-\Phi)}{\sin(\varphi-\Phi)}\,. \end{aligned}\right\} \quad (4)$$

The unknowns are Φ, the azimuth of the trend, and ψ, the plunge of $\vec{F}$.

PROJECTIONS

In order to proceed we turn to stereographic projection. In the oldest method the extended station S' is projected on to an equatorial plane of which the epicenter and anticenter are poles, with the anticenter as the pole of projection. At the position of S' on the plane is entered the algebraic sign of the first motion of P and of SH and SV if available. The beginning of S is more difficult to identify than that of P. Note that increase in $\delta_{ar}(P)$ means motion away from epicenter, increase in $\delta_{b\theta}$(SV) means motion up and toward epicenter, increase in $\delta_{b\varphi}$(SH) is to right looking from epicenter to station. Some writers use a reversed convention for SV.

The nodal surfaces for P are planes—the fault plane extended and that plane perpendicular to it to which the forces are normal. These planes cut the earth's surface in circles and therefore

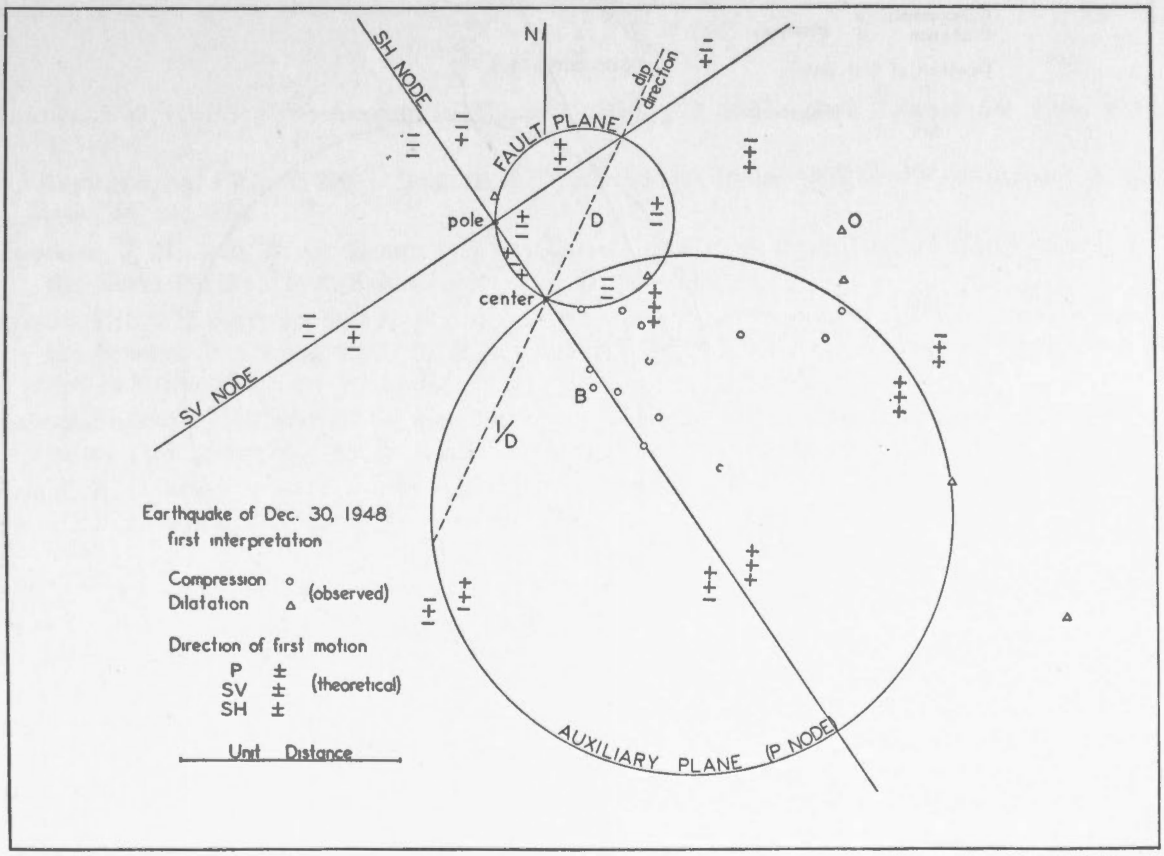

Figure 4. The fault-plane solution, after SCHEIDEGGER (1957), of the earthquake of December 30, 1948. The smaller circle is chosen as representing the fault plane. Signs of P, SV, and SH in the various domains are indicated. *O* corresponds to the position of Ottawa, *B* to Berkeley.

project as circles on the equatorial plane. Therefore on the projection two circles are to be drawn through the origin (projection of focus) such that, on crossing either, the sign of P changes. The diameters drawn through the origin have the azimuths of the dip of the fault and the dip of the auxiliary plane, respectively. The dip of the auxiliary plane is the complement of the plunge of the force $\vec{F}$. The lengths of these diameters give the magnitude of the dips.

In the drawing of the two circles there is the constraint that

$$\cos\alpha = \frac{\tan\,\psi}{\tan\,\delta}$$

where ψ is the plunge of the motion, δ the dip of the fault, and α is the angle between the traces of the fault and auxiliary plane. If one circle is well determined the above relationship determines a straight line which is the locus of the center of the second circle.

Figure 4 gives an example after Scheidegger (1957) in which he gives data for P waves of a given earthquake and then, selecting arbitrarily the smaller circle as representing the fault plane, draws the nodes of SV and SH. He gives the direction of first S motion at Ottawa only, which is that $\delta_{b\varphi}$(SH) is +. We have added to his figure the signs of $\delta_{b\varphi}$(SH) and $\delta_{b\theta}$(SV) in the various domains.

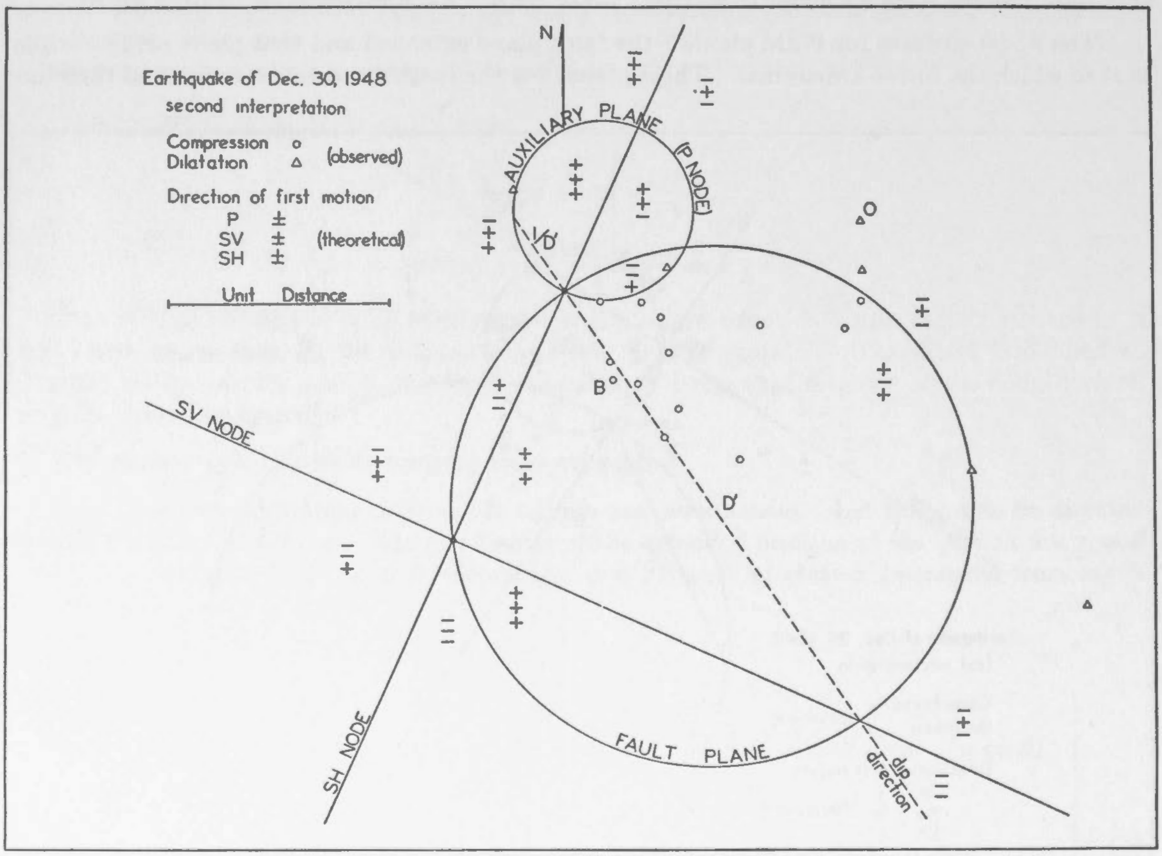

Figure 5. Fault-plane solution of the same earthquake as in Figure 5, with the larger circle assumed the fault plane.

In Figure 5 is drawn the similar figure with the larger circle assumed the fault plane. We see that the single observation at Ottawa determines that the first assumption was correct. A similar check by investigating the first motion of S at Berkeley was attempted. The test proved inconclusive, for it was impossible to determine for certain the beginning of SV and SH.

Soviet scientists plot the station at S'' in Figure 3. They have variously used the top, center, and bottom of the focal sphere as the pole of projection, according to SCHEIDEGGER. The most common practice seems to use the top of the focal sphere with the Wulff net as the basis of their stereographic projection.

Until recently the Soviet scientists have worked with data limited to observations recorded within the U.S.S.R. This limitation placed a severe restriction on their work and forced the development of other methods. In addition, then, to the ordinary methods from the observation of the first motion of the first motion of P, they have developed techniques, both analytic and graphical, for the determining of the direction of the motion vector by use of ratios such as those indicated in equation(4). KOGAN and MALINOVSKAYA (1953), for instance, have described a graphical procedure. The method is similar to that whereby in an area of metamorphic rocks one may determine the axis of folding from single observations of the dip and strike of the original bedding and of the orientation of the plane of foliation. The ratio SH/SV fixes a plane containing the motion vector, the seismic ray, and the total vector of displacement in a transverse wave. A second plane, having a similar geometric significance, is fixed by other ratios, say P/SH. The intersection of the two planes as plotted on a Wulff net determines the motion vector. Theoretically it would be possible to determine the motion from the data of a single station; a statistical average of determinations from several stations is more desirable and serves as a measure of reliability.

Methods using ratios of SH to SV imply that this ratio is constant. In the experience of the authors, this ratio varies greatly during the passage of the S group. This would render the use of ratios troublesome. Unless one can identify the first arrival of S, usually an uncertain process, it would appear that S should be used with great care.

References

ADKINS, J. D. (1940): The Alaskan Earthquake of July 22, 1937. *Bull. Seismol. Soc. Am.*, **30**, 353–376.

DE BREMAECKER, J. CL. (1956): Remark on Byerly's Fault Plane Method. *Bull. Seismol. Soc. Am.*, **46**, 215–216.

HODGSON, J. H., and W. G. MILNE (1951): Direction of Faulting in Certain Earthquakes of the North Pacific. *Bull. Seismol. Soc. Am.*, **41**, 221–242.

HONDA, H., A. MASATUKA, and K. EMURA (1956): On the Mechanism of the Earthquakes and the Stresses Producing them in Japan and its Vicinity. *Science Reports, Tôhoku Univ., Ser. 5*, **8**, 186–205.

KEYLIS-BOROK, V. I. (1956): Methods and Results of the Investigations of Earthquake Mechanisms. *Pub. Bur. Centr. Seismol. Int., Ser. A., Travaux Scientifiques*, **19**, 383–394.

KOGAN, S. D. and L. N. MALINOVSKAYA (1953): Plotting Sheets for Determining the Dynamic Parameters of Earthquake Foci. *Isvestia Akademiia Nauk SSSR, Ser. Geoph.*, No. 2, 131–147.

NAKANO, H. (1923): Notes on the Nature of the Forces which Give Rise to the Earthquake Motions. *Seismol. Bull., Centr. Met. Obs. Japan*, **1**, 92–120.

SCHEIDEGGER, A. E. (1957): The Geometrical Representation of Fault-Plane Solutions of Earthquakes. *Bull. Seismol. Soc. Am.*, **47**, 89–110.

Statistics and the Fault Plane, a Conjecture

BY R. E. INGRAM, S.J.

Rathfarnham Castle, Dublin, Eire

ABSTRACT

The paper is a note pointing to the possibility that statistics may be used to give the best position of the boundaries separating compressions from dilatations in fault-plane solutions. Tentative solutions are given for two simple cases, where separation is in terms of a single straight line, and where it is in terms of two straight lines. In each case a discriminating function is used to determine the best equation for the lines.

The success of the analysis of mechanisms of earthquakes by the fault-plane technique, using a graphical method, suggests that the same problem might be investigated with purely mathematical tools. The problem may be stated in the following way. On the surface of the earth-sphere, or in the plane of projection, the extended positions of stations form two classes of points. The first class records a compression, it is supposed that there are N^+ of such, the second class records a dilatation and it is supposed that there are N^- of these. For the sphere it will be required to find two perpendicular planes, passing through the origin—which is the epicentre—dividing the compressions from the dilatations. On the plane of projection, corresponding pair of curves must divide the plane in a similar way. If the plotting is done on the tangent plane at the epicentre, the curves are circles: if on the tangent at the antipodes they are straight lines.

Let us first consider the simplest case, which is that of a single force at the epicentre. If we use the tangent plane at the antipodes as the plane of projection, the projection of the auxiliary plane is a straight line dividing the plane into two regions. One region contains all, or as many as possible, of the N^+ points and the other contains all, or as many as possible, of the N^- points. Our data is that we are given the N^+ and N^- points in the plane and we are required to find the equation of the line. This we do by using a discriminating function (FISHER, 1950), provided the points satisfy certain conditions. It is intended to give a more detailed account of the restrictions on the distribution of the points at a later date.

Referred to suitably chosen axes in the plane (e.g. y is North and x East) the N^+ points have coordinates (x, y) and the mean value of the N^+ points is found. Let (x^+, y^+) denote this point. Likewise let (x^-, y^-) denote the mean value of the N^- points. We now relabel x and y, calling them for ease in summation x_1 and x_2.

Let $S = S(x_1, x_2) = l_1x_1 + l_2x_2 + l_3 = 0$ be the line dividing N^+ from N^-; so that, in so far as it can possibly be done, the N^+ points make $S > 0$ and the N^- points make $S < 0$ (or vice versa). It is required to find l_1, l_2, l_3.

Let (α_{ij}) be the matrix of coefficients

$$\alpha_{ij} = \Sigma x_i x_j - \Sigma x_i \, \Sigma x_j / \mathrm{N} ,$$

where the summation is taken over all the points (N) (values of x_i, x_j) and $\mathrm{N} = \mathrm{N}^+ + \mathrm{N}^-$.

Let $S^+ = S(x_i^+, y_i^+)$ and $S^- = S(x_i^-, y_i^-)$, usually called the expectation values.

Finally, let
$$W = \frac{(S^+ - S^-)^2}{l_i \, \alpha_{ij} \, l_j}$$

in which a repeated index indicates summation (Einstein convention). The lower term is thus a quadratic form but restricted to values 1, 2 of i and j.

55092-1—2

The theory (FISHER, 1950) states that l_1 and l_2 are given by maximizing W,

i.e.
$$\frac{\partial W}{\partial l_i} = 0,$$

$$2(x_i\,\alpha_{ij}\,x_j)\,(S^+ - S^-)\,(x_i^+ - x_i^-) - (S^+ - S^-)^2\,2\alpha_{ij}\,l_j = 0,$$

$$\alpha_{ij}\,l_j = \frac{(x_i\,\alpha_{ij}\,x_j)\,(x_i^+ - x_i^-)}{S^+ - S^-}\;;$$

thus l_j is proportional to $(\alpha_{ij})^{-1}\,(x_i^+ - x_i^-)$, where $(\alpha_{ij})^{-1}$ is the "information" matrix, the inverse of (α_{ij}). The third cœfficient, l_3, may be chosen to make $S^+ + S^-$ equal to zero.

Having found the equation, a standard test, e.g. SNEDECOR's F Test, may be applied to discuss the value of this discriminating function. Such tests have their value, moreover, for graphical solutions as well.

A pair of lines in the same plane of projection may be discussed in a similar way. The function S is now

$$S = (a_1x + a_2y + a_3)\,(b_1x + b_2y + b_3),$$

with the orthogonal condition*

$$a_1b_1 + a_2b_2 + a_3b_3 = 0$$

or
$$S = l_1x_1 + l_2x_2 + l_3x_3 + l_4x_4 + l_5x_5\;,$$

with
$$l_1 = a_1b_1,\quad l_2 = a_2b_2,\quad l_3 = a_1b_2 + a_2b_1,\quad l_4 = a_1b_3 + a_3b_1,\quad l_5 = a_2b_3 + a_3b_2,$$

and variables

$$x_1 = x^2 - 1,\quad x_2 = y^2 - 1,\quad x_3 = xy,\quad x_4 = x,\quad x_5 = y.$$

We calculate l_i in the same way

$$l_i \propto (\alpha_{ij})^{-1}\,(x_j^+ - x_j^-)$$

where
$$\alpha_{ij} = \Sigma x_ix_j - \Sigma x_i\,\Sigma x_j/N$$

Alternatively, we may first find one line and use it to give values to the points to obtain a second line.

At this stage it will be more profitable to work directly with points on the sphere having coordinates

$$x = D\sin i\cos i\cos\alpha\,,$$

$$y = D\sin i\cos i\sin\alpha\,,$$

$$z = D\cos^2 i\,,$$

where i is the angle of incidence of the ray leaving the focus, α is the azimuth of the station relative to the epicentre and D is the diameter of the sphere. The HODGSON tables give cot i.

The required discriminating function is then a plane

$$S = l_1x + l_2y + l_3z = 0$$

or a pair of perpendicular planes

$$S = (a_1x + a_2y + a_3z)\,(b_1x + b_2y + b_3z) = 0,$$

with
$$a_1b_1 + a_2b_2 + a_3b_3 = 0,$$

or
$$S = l_1x_1 + l_2x_2 + l_3x_3 + l_4x_4 + l_5x_5$$

$$l_1 = a_1b_1 \text{ etc.} \qquad \text{and } x_1 = x^2 - z^2 \text{ etc.}$$

when a_3b_3 is eliminated.

The coefficients may then be calculated as previously.

*This condition expresses the fact that the perpendicular from the origin on one line, multiplied by its intercept on the other, is the square of the diameter of the sphere (unity).

Finally, we must note that this type of investigation takes account of the general situation rather than the accurate drawing of a curve to pass between points. If one remembers that, to a first order of approximation, the amplitude is zero on the line and approaches zero near the line, the value of so accurate a drawing may be questioned. On the other hand, the method of discriminating functions depends on the mean values of the coordinates, x_i. Thus, to give a fair picture, we would in all probability have to take typical stations from a well marked region to avoid biasing the result. The use of amplitudes would help remedy this fault.

This note is intended to call the attention of geophysicists to the aid they may possibly obtain from the mathematical departments of the institutes in which they work. It is a tentative solution.

Example: The N^+ points are given in the (xy) plane as the points $(3,-3)$, $(4, 1)$, $(-2,-3)$, $(0,-6)$, $(0, 4)$ and the N^- points as $(2, 4)$, $(0, 6)$, $(-2, 0)$, $(-4,-2)$ and we require a line dividing the $+$ from the $-$ points. Proceeding with the calculations, we obtain

$$53l_1 + 17l_2 = 2 \qquad (x^+, y^+) = (1, -1.4)$$
$$17l_1 + 111l_2 = -3.4 \qquad (x^-, y^-) = (-1, 2)$$

which give

$$2.14l_1 + 2.80l_2 = 0,$$

and we take the approximate line

$$S = y - 1.3x - 0.3 = 0 \ ,$$

the constant term being chosen to make $S^+ + S^- = 0$.

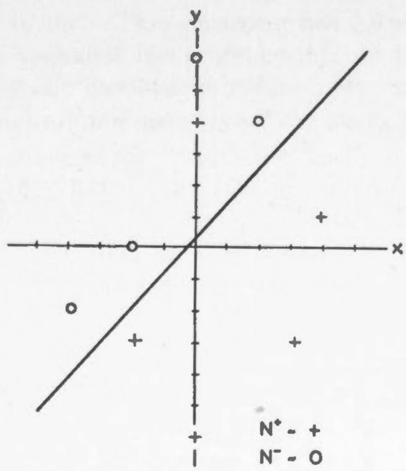

Figure 1.

From the diagram (Figure 1) we see that (0,4) is on the wrong side of this line. But no line satisfies the conditions and hence this line is acceptable. Is it the best solution?

References

Fisher, R. A. (1950): *Contributions to Mathematical Statistics.* Wiley, New York.

Moroney, M. J. (1951): *Facts from Figures, Pelican A 236.* Penguin Books. Harmondsworth.

Mechanisms of Faulting*

BY C. HEWITT DIX
California Institute of Technology, Pasadena, California, U.S.A.

ABSTRACT

The faulting picture shown by E. M. ANDERSON in his book using C. E. INGLIS' stress calculations is examined, and it appears difficult to extract energy for radiation in seismic waves from such a picture. Before and after the formation of such a crack the stress energy appears to be approximately the same.

However if there are two pre-existing 'lubricated' approximately co-planar sheet regions or sheet regions weaker than their surrounding rocks with a strong solid region between them, then this solid between may be ruptured and energy radiated. This may be modified to include the growth of a simple single lubricated crack but this later process does not seem adequate for large earthquakes.

INTRODUCTION

In a very valuable study E. M. ANDERSON (1951) has discussed faulting and dyke formation. His discussion is rich with field evidence. He seeks an understanding of the evidence in terms of basic physical principles and relationships.

The subject is one of fantastic difficulty. Geological observations mostly at the earth's surface must be interpreted. Success in this is probably in a strict sense impossible. So one must fall back on the multiple alternative process. To help push the assessment of probabilities of the alternates one tests every picture of any mechanism as severely as possible.

It is my purpose to apply a simple test to the general picture left by a reading of ANDERSON's book. The result was a surprise to me. It forced me to recast my view of the process in a way which seems quite important to me. This recasting has helped me to "understand" several field observations which have appeared incomprehensible on the basis of the view I have of ANDERSON's processes. Clearly the conclusions reached here will have to be modified. They may be of temporary service and are presented for that reason.

I acknowledge the help of many earlier students of this problem, especially the publications of BENIOFF (1949), HAFNER (1951), HUBBERT (1951), HILL and DIBBLEE (1953), MOODY and HILL (1956), ALLEN (1957), INGLIS (1913), GRIFFITH (1921, 1928), and many others. I am particularly indebted to D. F. HEWETT, C. F. RICHTER, C. R. ALLEN, ALLAN R. SANFORD, THANE MCCULLOH, PHIL BLACET, WILLIAM CHAPPLE and M. KING HUBBERT for many discussions on this subject.

Although the study can be related to the fault plane studies of this symposium it is forcing things a bit to do so. This report therefore contains only the part of the study most directly bearing on fault plane studies in the sense of this symposium. The other aspects will be presented elsewhere. This must be qualified a bit. I first learned of the viewpoint of Professor BELOUSOV at the Toronto meeting, and believe his view and mine to be in agreement. It may be that he and his associates have anticipated my studies but I have not been able to find publications to this effect. I do know, however, that Professor BENIOFF (1949), gave arguments in favor of zones of weakness some years ago.

THE CALCULATION OF STRESS ENERGY OF A FAULT

In Figures 1a and 1b are shown a situation without a fault and with a fault respectively. The stress fields at great distances away are, in the limit, the same. Both Figures represent idealized two-dimensional problems in elasticity. The lines drawn represent directions of principal stress. An orthogonal set of curves to these (not drawn) may be imagined which also represents principal stress directions.

*Publications of the Division of Geological Sciences, California Institute of Technology, Pasadena, California. Contribution No. 891.

Though I recalculated ANDERSON's curves (which were earlier calculated by C. E. INGLIS, 1913; see also MUSKHELISHVILI, 1953) (my Figure 1b, his Figure 35), I got the same results shown by ANDERSON on his page 164 but with a little more detail at greater distances. My curves are to be taken to be curves across which the principal tensile stress is a maximum.

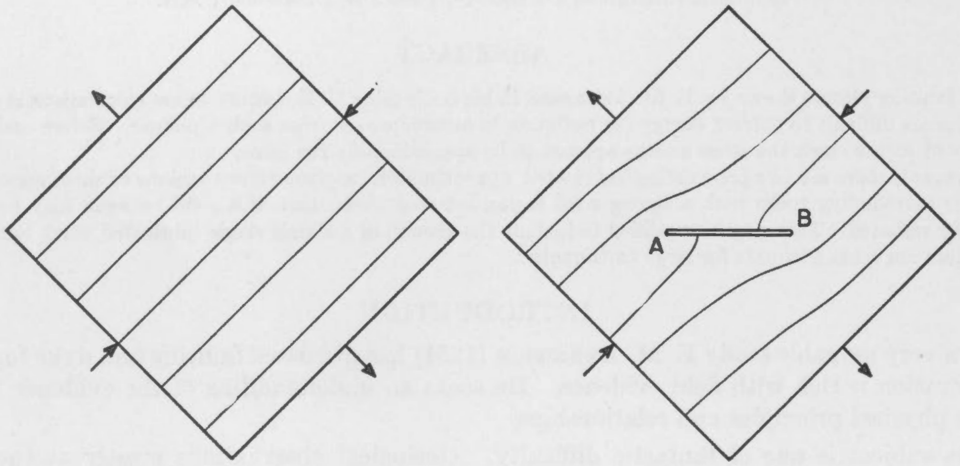

a Figure 1. b

In making the calculation a hydrostatic state of stress has been removed in both cases so that the hydrostatic pressure in the crack is taken as zero. The principal stresses at infinity are equal and opposite for both cases.

Let us now calculate the stress energy for the two cases. I did this by a numerical integration for a particular example. My idea was that I could in this way get a measure of what might be the energy available for radiation in the form of an earthquake. The two figures came out approximately the same!

Thus if we imagine the energy radiated in the form of an earthquake for a process which consists of a transition from the state represented by Figure 1a to the state represented by Figure 1b, this energy has to come from a source not yet mentioned. When thermal effects are taken into account the situation is even worse. My conclusion, stated at the meeting was that the picture presents no mechanism for making earthquakes.

A POSSIBLE MECHANISM

In what follows I shall indicate a *possible* mechanism which deviates from the picture just presented as little as possible.

Refer to Figure 2. The curves again are sketched (not yet computed in this case) to represent principal stress directions across which the orthogonal stress is a tension. The crack of Figure 1b is now sealed and its complementary extension on both sides is now open.

The situation is singular at A' and B' but let us avoid that problem by taking AA' and BB' large compared with AB. The stress applied should approach zero as one approaches A' and B'. If ones makes the stress also approach zero as D and C are approached in the proper symmetrical way, then the external applied stress will not rotate the piece considered.

Given zero stress in BB' and AA' on the crack surface, i.e., zero pressure and lubricated, for a given external applied stress, the shear stress between A and B becomes arbitrarily large as AB becomes artibrarily small. If rupture occurs motion will continue until the elastic spring has lost its energy in radiation of waves out through the elastic solid.

The above picture appears to contain some useful aspects. But it is grossly oversimplified. It shares with Figure 1 a failure to take proper account of the $r^{-\frac{1}{2}}$ singularity (GRIFFITH, 1921) at A and B. First let us hold to the mathematical hypotheses which introduce the singularity. Then we notice two cases: (a) the pressure inside the crack is zero but shear stress has an $r^{-\frac{1}{2}}$ singularity; and (b) shear stress is not applied but pressure inside the crack is not zero. In each case no real material would hold together even when the applied stress or internal pressure is arbitrarily small. So neither Figure 1b nor 2 can represent any final state nor even a static state at all.

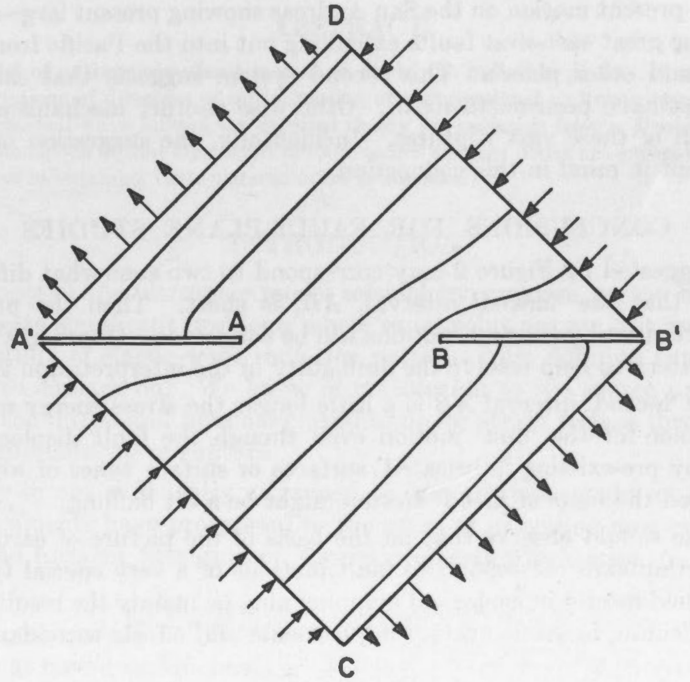

Figure 2.

As is so often the case, the villain in this scene is our forgetfulness regarding the limitations of the mathematical formulation of the physical situation—we assumed arbitrarily small strains. The neighborhoods of our singular places require a different treatment. Also the ideal sheet crack is calculated as the limit of a sequence of open rounded cavities (elliptical cylinders in Figure 1b usually). The limiting situation is selected not because it seems closer to the true case, but because of its simpler formulae. Probably one should replace the term 'crack' by 'crack with rounded ends' *and* also leave a region at each rounded end where the hypothesis of 'arbitrarily small strains' fails more or less seriously.

The above considerations do not weaken the argument about energy available for radiation. It therefore appears probable that a transition from Figure 1a to Figure 1b is ruled out. Figure 2 as an initial state and Figure 2 with AB ruptured as a final state appears to represent roughly a possible mechanism for the generation of earthquakes.

Our arguments have thus led us to the conclusion that *before* rupture can take place, cracks, sheet-like zones of weakness, sheets of melted material or the like must exist. This raises quite serious questions. I see no objection to the injection of a melt along a sheet. However the orientation of this sheet is likely to be such that its normal is the direction of maximum principal tensile stress. The reason for this orientation is that assuming isotropic cohesion (or negligible cohesion) of the rock, such an orientation corresponds to the direction of opening requiring least work for the injection process. For such an orientation however there is no shear stress in the sheet direction. It therefore appears necessary to change the stress pattern after the formation of the sheets or else guide their formation by some lack of isotropy of the materials. This latter process appears to have happened in California in the case of the San Andreas fault zone. The maximum principal stress appears to be east-west. This is the right orientation to form the clockwise lateral displacement observed on the San Andreas. However the San Andreas is slipping clockwise about 5 cm. per year indicating its 'lubrication' or weakness in some sense. Its direction seems to be influenced by the continental boundary. Local reorientation of stress to account for small dykes and faults is easy to imagine. But a great reorientation would be more difficult. There are however indications that great reorientations should not be ruled out. These are, first, the present motion on the San Andreas showing present large-scale stress orientation and, second, the great east-west faults extending out into the Pacific from Cape Mendicino, Point Conception and other places. This second system suggests that earlier the maximum principal stress must have been north-south. Otherwise another mechanism must be appealed to for the formation of these vast ruptures. Incidentally, the suggestion of VENING-MEINESZ (1947) should be kept in mind in this connection.

CONCLUSIONS FOR FAULT-PLANE STUDIES

The picture suggested by Figure 2 may correspond to two somewhat different situations.

First consider that the 'locked' interval, AB, is short. Then the principal fault-plane motion and the pattern set by the first motions will be consistent. One might even use the elongated after-shock pattern to help resolve the ambiguity in the interpretation from first P motion.

However if the 'locked' interval AB is a little longer the stress energy may not be released in this simple manner for the 'first' motion even though the fault displacement is probably ultimately guided by pre-existing 'lubricated' surfaces or surface zones of weakness. In such a case interpretation on the basis of first P motion might be a bit baffling.

Incidentally one should observe that on the basis of the picture of earthquake origin here presented, large earthquakes correspond to fault motions of a very special type. On the other hand the faults studied mostly in geological mapping may be mainly the result of slow dissipative motions, mainly reflecting isostatic gravity adjustments and effects secondary to these.

References

ALLEN, C. R. (1957): San Andreas Fault Zone in San Gorgonio Pass, Southern California. *Bull. Geol. Soc. Am.*, **68**, 315–350.

ANDERSON, E. M. (1951): *The Dynamics of Faulting.* Oliver and Boyd, Edinburgh and London.

BENIOFF, H. (1949): Seismic Evidence for the Fault Origin of Oceanic Deeps. *Bull. Geol. Soc. Am.*, **60**, 1837–1856.

GRIFFITH, A. A. (1921): The Phenomena of Rupture and Flow in Solids. *Phil. Trans. Roy. Soc. Ser. A.*, **221**, 163.

GRIFFITH, A. A. (1928): Stresses in a Plate Bounded by a Hyperbolic Cylinder. *Aeronaut. Research Comm.* (Gt. Brit.) *Reports and Memo.* No. 1152, 1–10.

HAFNER, W. (1951): Stress Distributions and Faulting. *Bull. Geol. Soc. Am.*, **62**, 373–398.

HILL, M. L., and T. W. DIBBLEE, Jr. (1953): San Andreas, Garlock and Big Pine Faults, California. *Bull. Geol. Soc. Am.*, **64**, 443–458.

HUBBERT, M. K. (1951): Mechanical Basis for Certain Familiar Geological Structures. *Bull. Geol. Soc. Am.*, **62**, 355–372.

INGLIS, C. E. (1913): Stresses in a Plate Due to the Presence of Cracks and Sharp Corners. *Trans. Inst. Naval Architects*, **55**, 219–230.

MIKHLIN, S. G., trans by A. H. ARMSTRONG (1957): *Integral Equations.* Pergamon Press, New York.

MOODY, J. D., and M. J. HILL (1956): Wrench-Fault Tectonics. *Bull. Geol. Soc. Am.*, **67**, 1207–1246.

MUSKHELISHVILI, N. I., trans. J. R. M. RADOK (1953): *Some Basic Problems of the Mathematical Theory of Elasticity.* Noordhoff, Grøningen.

VENING-MEINESZ, F. A. (1947): Shear Patterns in the Earth's Crust. *Trans. Amer. Geophys. Un.*, **28**, 1–61.

Elastic Wave Radiation from Faults in Ultrasonic Models*

BY FRANK PRESS

California Institute of Technology, Pasadena, California, U.S.A.

ABSTRACT

An ultrasonic model of an impulsive fault is used to study the radiation pattern of compressional and shear waves. Azimuthal variations of direction of initial motion of compressional and shear waves are described. The behavior of the compressional wave follows the classical theory for radiation from a dipole source. The behavior of the shear waves is anomalous in that significant motion occurs whereas nodes are expected. The relation of this work to current practices in obtaining fault-plane solution is discussed.

INTRODUCTION

The main purpose of the ultrasonic model seismology program at the Seismological Laboratory is to investigate significant problems where exact solutions are not available. From this point of view, the study of elastic wave radiation patterns from different types of sources was a natural one for us to embark on. We know of no solution to the source problem which takes into account all of the initial and boundary conditions for strain release through a fault having finite length and finite velocity of rupture.

Our technology is not sufficiently advanced to make a true model of a fault. However, we believe our experiments have progressed to the point of providing new insight into the fault solution problem and focusing attention on special problems which arise.

EXPERIMENTAL PROCEDURE

Two dimensional model techniques were employed (OLIVER *et al.*, 1954). In such models, motion is uniform over the thickness of the sheet so that sources and detectors on the face of the model occupy positions corresponding to the interior of a three-dimensional medium.

The representation of unipole and multipole sources is particularly convenient with barium titanate bimorph transducers (Figure 1). When used as detectors, these transducers offer the advantage of ready conversion from compressional to shear sensitivity by rotation of 90°.

The experimental procedure consists of observing compressional and shear wave radiation patterns at the circumference of the thin disk of plexiglas at the center of which the source is located. This corresponds to observations along the trace on the focal sphere of a plane perpendicular to the fault and auxiliary planes. Amplitudes, pulse shapes and directions of initial motion are observed.

In this paper, we report on results for impulsive singlet and dipole sources. To simulate a fault, we have introduced a slit between two elements of a dipole. Our model differs from an actual fault in that the finite velocity of rupture and locking is not taken into account.

RESULTS

SINGLET

Results for this source are depicted in Figures 2 and 3 where actual seismograms are shown for each recording position. It is important to establish (Figure 4) that the amplitude variation with azimuth follows the theoretical cosine and sine law since multipole sources will be formed by superposition of singlets.

*This research was sponsored by the Office of Ordnance Research, U.S. Army; California Institute of Technology, Division of the Geological Sciences, Contribution No. 848.

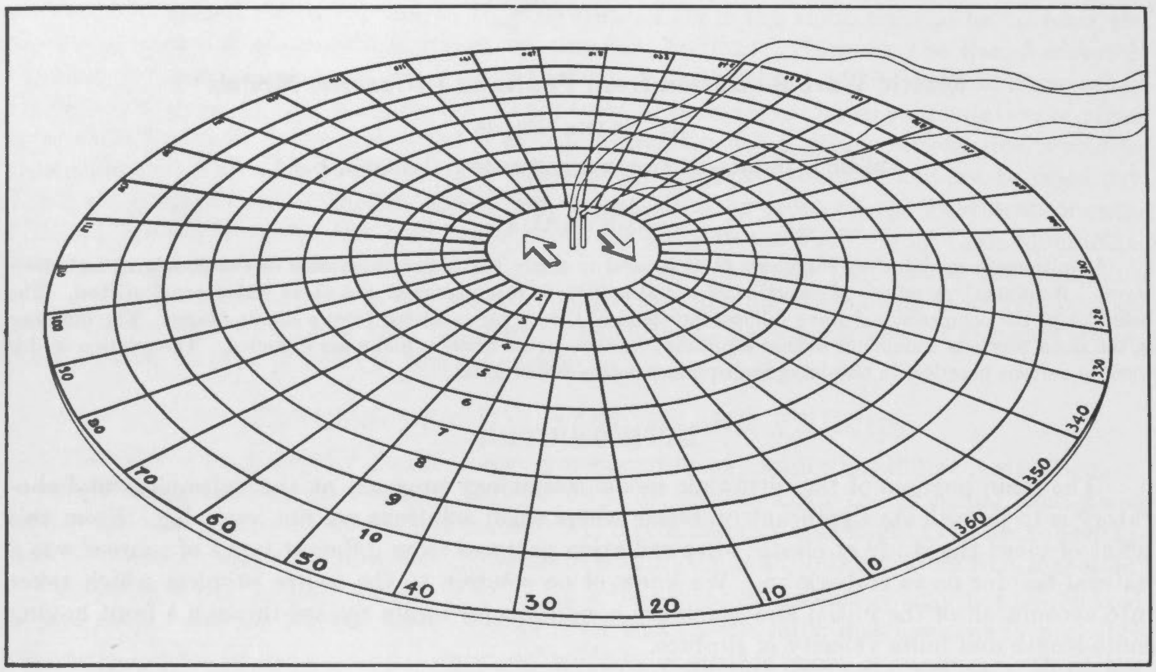

Figure 1. Two-dimensional model of dipole source.

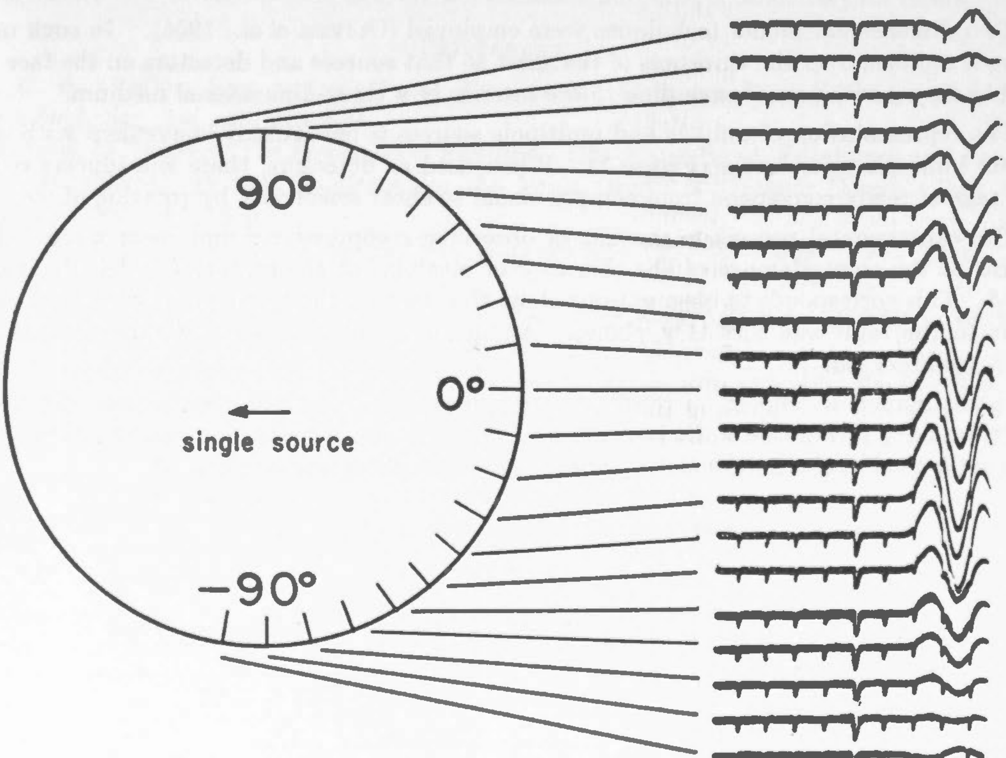

Figure 2. Compressional waves from a singlet source. Upward trace motion corresponds to inward motion on the model.

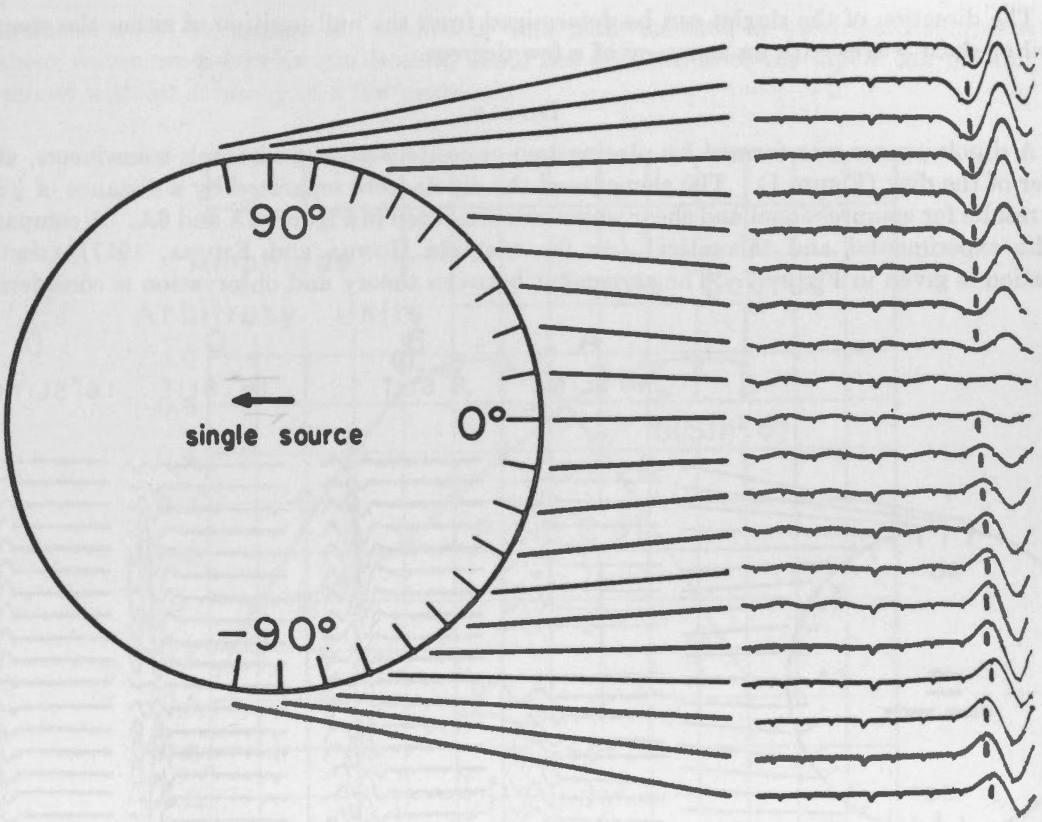

Figure 3. Shear waves from a singlet source. Downward trace motion corresponds to counterclockwise rotational motion on the model.

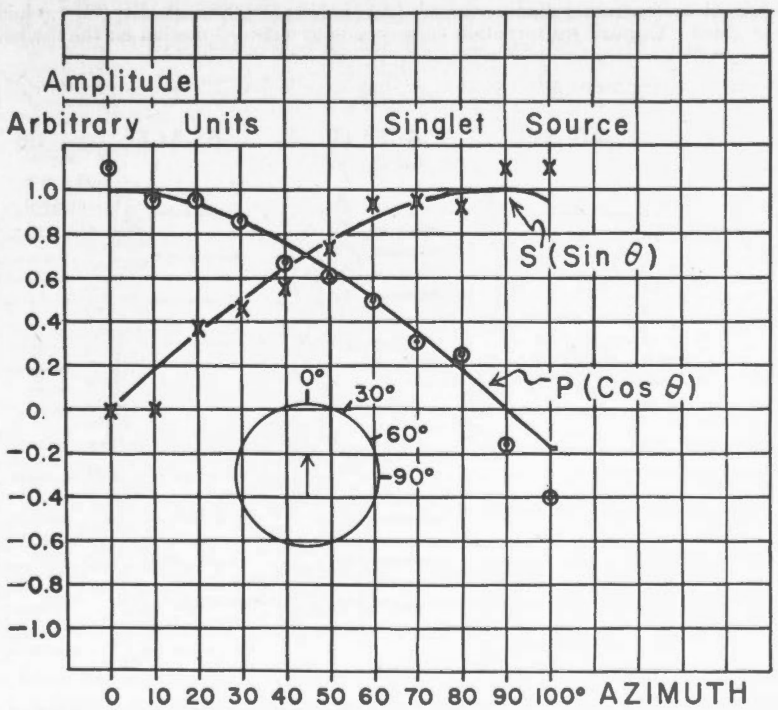

Figure 4. Observed and theoretical amplitude variation with azimuth for singlet source.

The direction of the singlet can be determined from the null position of either the compressional or shear waves with an accuracy of a few degrees.

Dipole

A dipole source was formed by placing two oppositely phased bimorph transducers, at the center of the disk (Figure 1). The elements of the dipole were separated by a distance of $\frac{1}{4}$ inch. The results for compressional and shear waves are presented in Figures 5A and 6A. A comparison of the experimental and theoretical (*see* for example HONDA and EMURA, 1957) azimuthal variation is given in Figure 7. The agreement between theory and observation is considered to

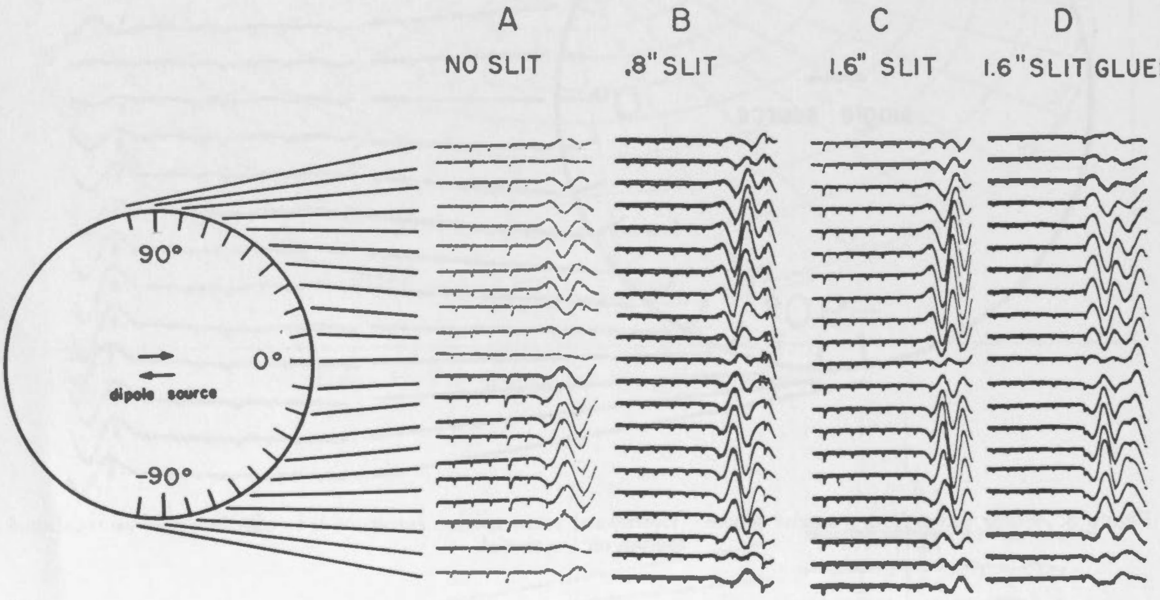

Figure 5. Compressional waves from a dipole source. (A) No slit; (B) 0.8 inch slit; (C) 1.6 inch slit; (D) 1.6 inch slit glued. Upward trace motion corresponds to outward motion on the model.

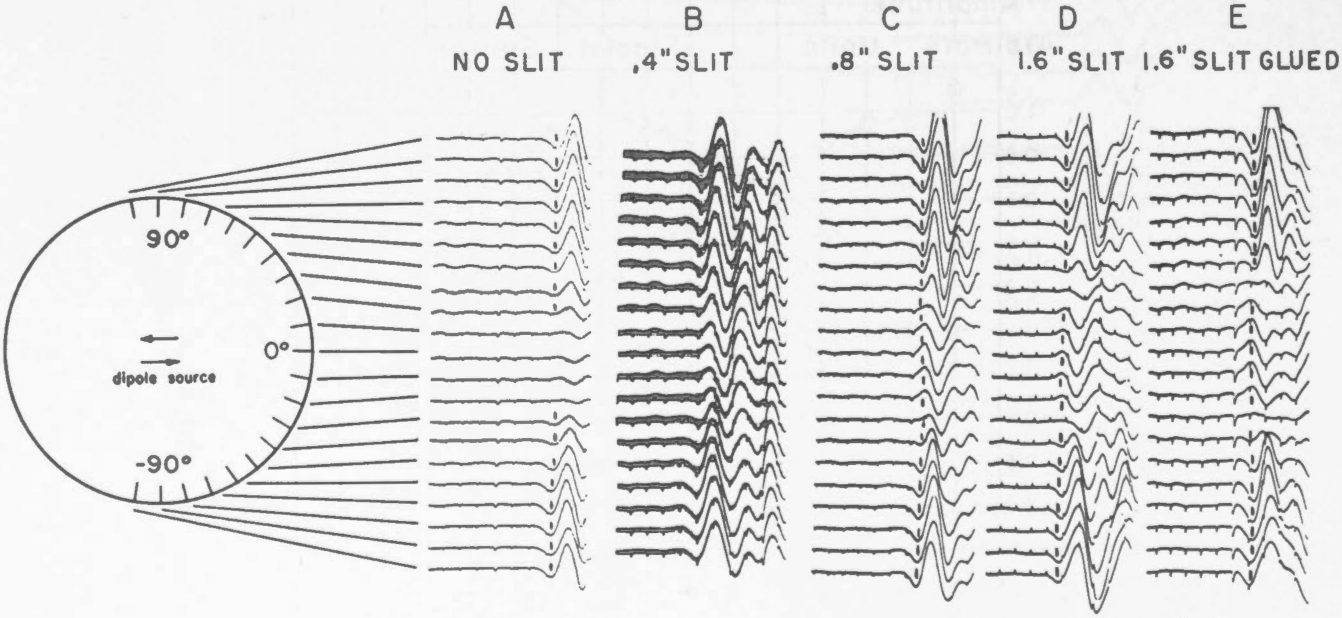

Figure 6. Shear waves from a dipole source (A) No slit; (B) 0.4 inch slit; (C) 0.8 inch slit; (D) 1.6 inch slit; (E) 1.6 inch slit glued. Downward trace motion corresponds to counterclockwise rotational motion on the model.

be satisfactory. If one applies the method of fault-plane solution in which both compressional and shear waves are used (KEYLIS-BOROK, 1956) the orientation of the dipole can be uniquely determined with an accuracy of a few degrees.

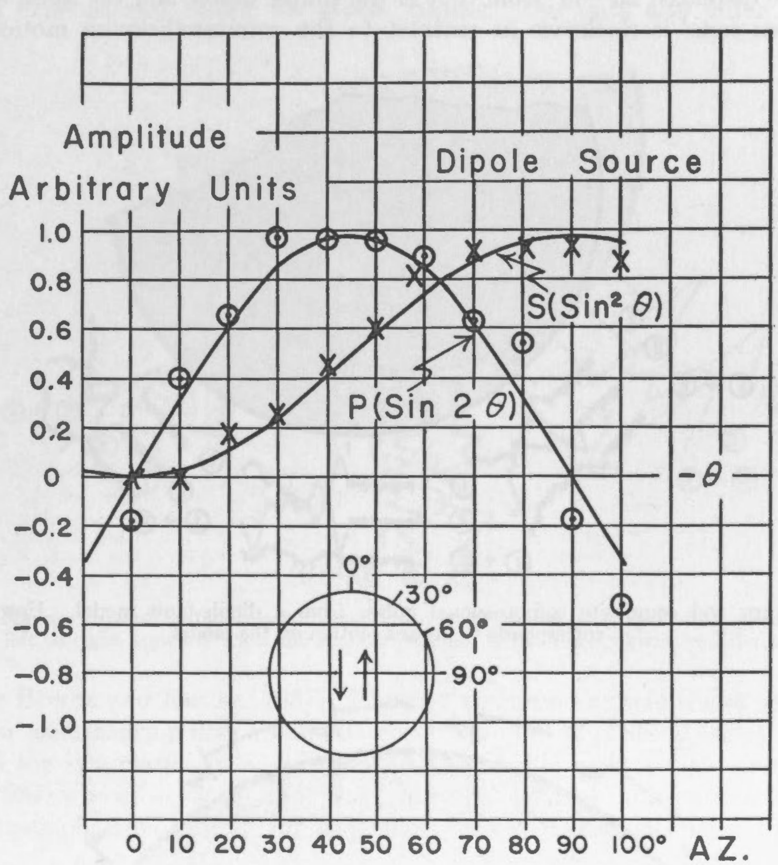

Figure 7. Observed and theoretical amplitude variation with azimuth for a dipole source.

DIPOLE-FAULT

In order to represent faulting, a narrow slit was cut between the two elements of the dipole, the void being filled with silicone. Free slipping and continuity of normal stress and displacement across the slit were provided for in this manner. The slit length was varied to study the effect of fault length on radiation pattern. In one experiment, the slit was glued to simulate a zone of reduced rigidity between the elements of the dipole.

Compressional waves observed for this model are shown in Figures 5B, C, D. The main features obtained for the dipole without slit are repeated in these seismograms. It is of some interest to see the manner in which the separate contributions from each side of a fault (elementary pulses) are superposed. In Figure 8, seismograms are presented which show elementary pulses separately and superposed as observed at three positions. The main feature in determining polarity of the composite pulse is the delay and greater attenuation of the elementary pulse which crosses the fault enroute to the point of observation. We interpret these results as a verification of the basic assumptions made for the radiation pattern of compressional waves in fault-plane solutions.

Shear waves from the dipole-fault model are presented in Figures 6B, C, D, for slits of varying lengths. These lengths correspond respectively to ½, 1, and 2 wave lengths for shear waves. Figure 6E depicts seismograms for a glued slit, i.e., a model of a fault as a zone of reduced rigidity.

A striking feature becomes apparent when the dipole-fault seismograms are compared with those of the simple dipole. Whereas shear wave amplitudes near 0° decrease to negligible values for the latter model (Figure 6A) the fault models show significant amplitudes in this zone. The null positions are displaced 25°–35° from that of the simple dipole and the sense of shear motion in the 'anomalous zone' is clockwise in contrast to the counterclockwise motion in the zones ± (30°–90°).

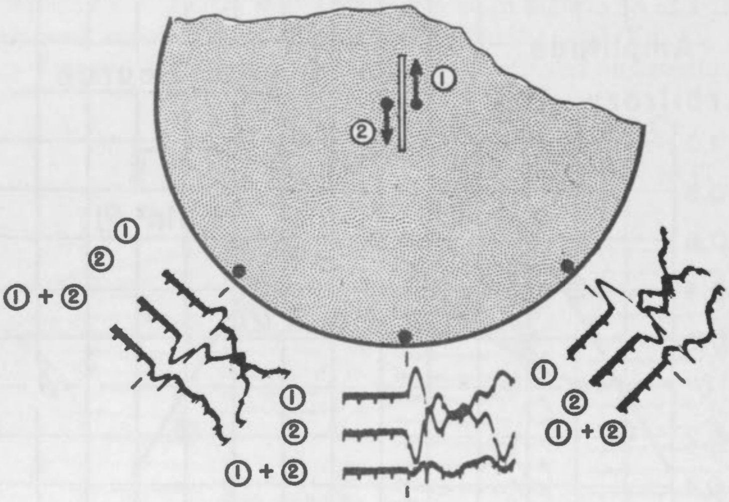

Figure 8. Elementary and composite compressional pulses from a dipole-fault model. Upward trace motion corresponds to inward motion on the model.

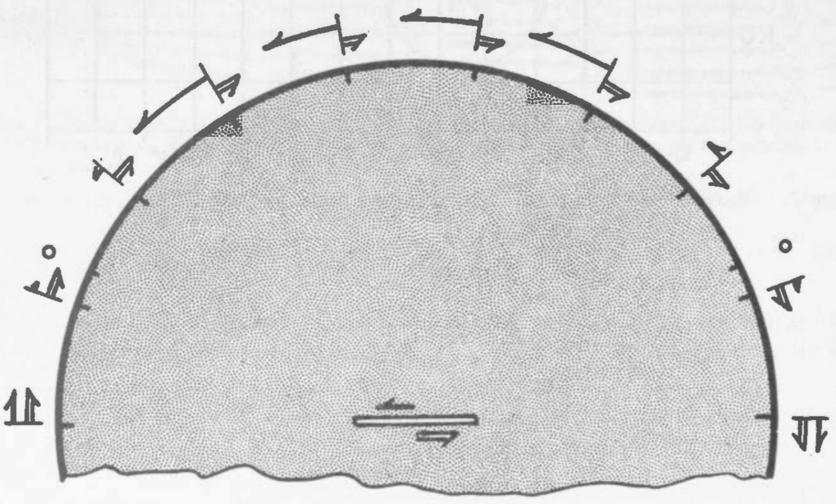

Figure 9. Sense and amplitude of elementary shear pulses in a lubricated dipole-fault model.

The anomalous shear waves may be studied further in Figure 9 where the sense and amplitude of the elementary pulses from each side of the fault are indicated separately by arrows. The near side of the fault produces waves with maximum amplitude at 90° diminishing to zero at about 25° and 155°. The sense of motion is contrary to that of the source in the range 0–25° and 155°–180°. The far side of the fault contributes waves having the same sense as the initiating impulse and showing little variation in amplitude over the range 0–180°. Figure 10 shows the corresponding seismograms for three positions together with composite pulses formed by superposition of the elementary pulses. It is seen how the two in-phase elementary pulses at 0° combine to give a resultant shear motion having the same order of magnitude as that recorded at 90°. These results were first reported in 1956 (PRESS, 1957). KATO and TAKAGI (1957) seem to have independently obtained somewhat similar results.

The shear wave radiation pattern for our dipole-fault models differs significantly from the theoretical and experimental results for dipole sources. Our data also differ with results for

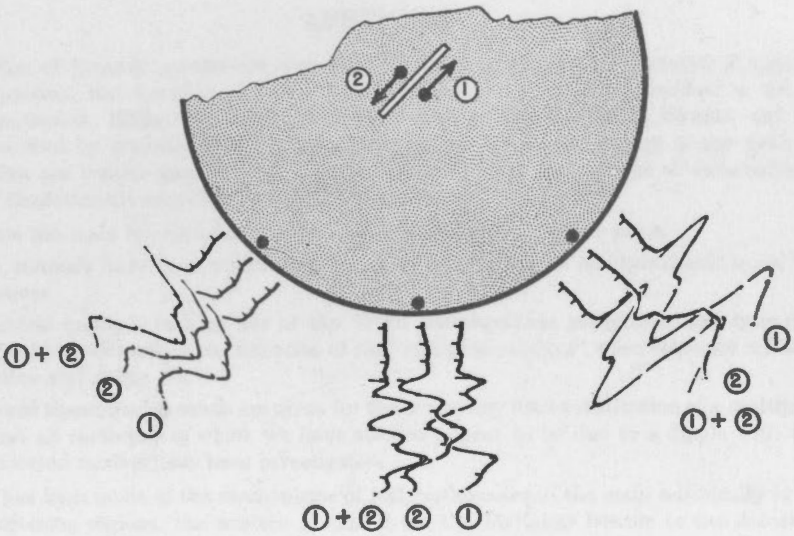

Figure 10. Seismograms showing elementary and composite shear pulses in a dipole-fault model. When reading seismograms from left to right, upward trace motion corresponds to counterclockwise rotational motion on model.

quadrupole (*see* HONDA and EMURA, 1957). The null position occurs in the range 25°–35° rather than 45° and the elementary pulses are in phase at 0° and out of phase at 90°. Thus, we cannot verify either of the two classes of assumptions usually made by investigators (KEYLIS-BOROK, 1956; HONDA, 1934) who incorporate shear wave data to determine fault-plane solutions uniquely. It is necessary to emphasize however that the validity of our fault model has not been established beyond doubt.

It is a pleasure to acknowledge the assistance of John H. Healy in the experimental program.

References

HONDA, H., (1934): On the Amplitude of P and S Waves of Deep Earthquakes. *Geophys. Mag.*, **8**, 153–164.

HONDA, H., and K. EMURA, (1957): The Production of the Two-Dimensional Elastic Waves. *Science Reports, Tôhoku Univ., Ser. 5*, **8**, 206–211.

KATO, Y., and A. TAKAGI, (1957): Seismic Studies, Part 3. *Science Reports, Tôhoku Univ., Ser.* 5, **8**, 212–224.

KEYLIS-BOROK, V. I., (1956): Methods and Results of the Investigations of Earthquake Mechanisms. *Pub. Bur. Centr. Seismol. Int., Ser. A, Travaux Scientifiques*, **19**, 383–394.

OLIVER, J., F. PRESS, and M. EWING, (1954): Two-Dimensional Model Seismology. *Geophysics*, **19**, 202–219.

PRESS, F., (1957): Elastic Wave Radiation from a Fault. *J. Acoust. Soc. Amer.*, **29**, 187.

The Study of Earthquake Mechanism

BY V. I. KEYLIS-BOROK

Geophysical Institute, U.S.S.R. Academy of Sciences, Moscow

ABSTRACT

The determination of dynamic parameters of earthquake foci (the mechanical character of rupture at the focus, the fault-plane orientation, the direction of movement) is made by the method described in the 1954 Assembly publications (KEYLIS-BOROK, 1956a). It is, in principle, similar to the method of BYERLY and of the Japanese seismologists, as described by BYERLY in the present symposium. The main feature of the method is the use of S waves, which makes the results single-valued and drastically reduces the number of observations necessary, as well as the ratios of displacement amplitudes in different waves.

The following are the main improvements in method achieved within recent years.

a. Simple methods have been worked out to exclude the influence of discontinuities on the shape of the observed waves.

b. A graphical method, making use of the Wulff stereographic projection, has been developed, which makes it possible to determine the direction of the "straightened rays" when there are refracting boundaries of any number and shape.

c. Additional theoretical grounds are given for the commonly used substitution of a multipole for the focus. While almost all earthquakes which we have studied appear to be due to a dipole with moment, several more complicated models have been investigated.

Determination has been made of the mechanisms of 300 earthquakes in the main seismically active zones of the U.S.S.R. and the adjoining regions: the western Pacific (from the Marianas Islands to the Aleutian Islands), the Hindu-Kush, the Pamirs and Tien-Shan, Kopet-Dag and Western Turkmenia, and the Caucasus. Of special interest is the Garm region (on the border of the Pamirs and Tien-Shan) where about 150 weak earthquakes, occurring within a small area, were studied.

The basic properties of dislocations in the foci of each zone have been found and compared with the general tectonics.

a. In some regions one strike direction predominates; in some instances this is parallel, in other instances transverse, to the strike of the main structures. In most regions however both systems are developed at the same time.

b. Faults with strong horizontal components of movement, and with strikes transverse to the structures are much more common in the seismic solutions than they are from geological data. However this is in line with some neotectonic data.

c. Vertical movements in the foci of some regions are characterized by the fact that during earthquakes a fault wall facing a tectonic depression is lifted up in the earthquake. This is in agreement with geological and geophysical evidence on the movements of surface foci in Japan: vertical movements during earthquakes are in the opposite sense to the secular ones.

The data obtained are of interest in deep tectonics, its relation with seismicity, etc. A great number of foci should be investigated in different tectonic regions. In this connection, international exchange of information and data is of paramount importance; this interchange is now very well established.

This report is an account of the Soviet work on earthquake mechanism (type of rupture, dip and strike of fault plane, motion direction at the source). This work is the continuation of the investigations reported by the author at the previous Assembly (KEYLIS-BOROK, 1956a).

In the first section some questions of method are considered. The second section summarizes some results of the study of nearly 300 earthquakes in the U.S.S.R. and adjacent districts.

QUESTIONS OF METHOD

As is well known, the study of earthquake mechanism is based on the displacement of various seismic waves.

We shall define as an *original wave* that wave which would be observed from a given source if the medium were a homogeneous ideally elastic one. We shall also consider the *straightened* *ray* which is the semitangent to the ray at the hypocentre. The determination of various characteristics of displacements in an original wave along the straightened ray is the first problem of an interpretation. Instead of rays we consider their stereographic projections ('virtual points of observation').*

The distribution of these characteristics is compared with the theoretical one which is calculated for the model source in a homogeneous medium. Mostly it comes to drawing nodal lines according to arrival signs of original waves. The direction of the axis of the model is then determined to obtain the earthquake mechanism as above defined.

The idea of such an interpretation procedure belongs to BYERLY.

Japanese seismologists employed an inverse procedure, calculating the theoretical field of displacements in a non-homogeneous medium and comparing it directly with observations.

The principles of BYERLY's methods and of those used in the work to be reported here seem to be alike. The main difference is that we employ the signs of transverse waves SV and SH in phases S, SS, sS, PS and so on, and ratios of displacement amplitudes P/SH, SV/SH. It makes the interpretation unambiguous and greatly lessens the quantity of observations required. We use a Wulff stereographic projection which seems to be more convenient; perhaps it is not only the matter of habit.†

A detailed account of the method we employ has already been given (BESSONOVA, *et al.*, 1957), together with related theoretical questions. A general description and a detailed discussion of interpretation procedure have also been published in English (KEYLIS-BOROK, 1957,). To avoid repetition we shall give a summary only of some questions of method investigated during recent years.

One of the main questions concerned is the excluding of the influence of intermediate boundaries on the form and direction of displacements. This is of particular importance in the study of near earthquakes and in employing reflected and head waves of different types.

THE DISTORTION OF DISPLACEMENT FORMS

To determine a displacement in an original wave we have to exclude the influence of reflections at all boundaries, including the Earth's surface, met by a real wave.

If the angle of incidence at any of these surfaces is more than critical, in which case the reflection or refraction coefficients are complex, the observed wave differs from the original wave not only in intensity but in the form of displacement as well (the number, amplitudes and periods of extrema)‡.

Similar phenomena arise when the rays focus, or when they reflect at a boundary of a non-ideal elastic medium.

However all the possible variations in the forms of reflected and refracted waves for a given primary wave form can be represented theoretically by a set of 'standard curves' (MALINOVSKAYA, 1957). Curves for two possible original waves are shown in Figure 1. The parameter φ is the argument of a complex number. This number is determined as a product of all plane wave reflection and refraction coefficients; these coefficients allow for all intersection of real rays with the boundaries. The upper curve in each column ($\varphi = 0$) coincides with the corresponding original wave forms. An observed displacement is the product of a curve in Figure 1 and some factor ρ determining the wave intensity.

The method of calculating φ and ρ is treated elsewhere (MALINOVSKAYA, 1957; PETRASHAIN, 1957a, b). As Figure 1 shows, the correlation between the original and observed waves, and the

*In previous papers I have used the less apt expression 'conventional point'.

†During recent years various interpretation procedures have been growing more and more close. For example, RITSEMA (1955) independently suggested the use of Wulff's projection and transverse wave signs. SCHEIDEGGER (1957) has examined the replacing of the Wulff projection by the projection introduced by BYERLEY. GUTENBERG (1955) used the ratio of SV/SH amplitudes to remove ambiguity.

‡*See* the author's report: "Dynamical Methods of Studying the Earth's Interior."

ratio of their amplitudes, depends greatly upon the magnitude of φ. These waves differ even in the number of extrema. For $\varphi \neq 0°$ or $180°$ usual methods do not enable us to determine either the sign or the amplitude of the original wave. The change of wave form as described above occurs more often in near earthquakes. For example it can happen for the S wave when a thin low-velocity layer exists close to the surface. In this case the angle of incidence at the base of the surface layer is, as a rule, more than critical.

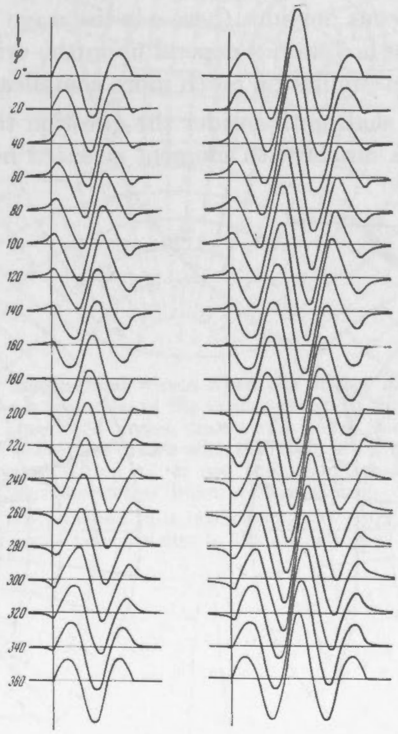

Figure 1. Variations, due to total reflection phenomena, in the displacement form for the two examples of original waves represented by the curves $\varphi = 0$.

For distant earthquakes a change in the wave form can take place when the wave is associated with a non-ideal elastic medium. This condition might obtain at the mantle-core boundary, so that some distortion of the wave form of PcP, PcS, PKP etc. is possible.

The sudden change of φ also occurs for ordinary P or S waves in cases when the front makes a caustic.

Using standard curves we can allow for the displacements form change when determining the sign or amplitude of a primary wave. In particular the influence of a surface layer upon transverse waves can be excluded by means of the diagrams given (BESSONOVA, *et al.*, 1957, *suppl.* III). In the case when total reflection has occurred at a free surface it is possible to exclude this influence, without using the standard curves, by means of the formula

$$u_b^P = \frac{1}{2 \cos i_o} \left[S_V \cos 2\, i_o - S_Z \sin 2\, i_o \right] ,$$

where u_b^P is the total displacement vector in the incident wave SV, S_Z, and S_V are the vertical and horizontal components of the surface displacement and i_o is the angle of incidence at the surface. It is interesting to note that in this case the vertical and horizontal displacement components differ in form and in phase.

Drawing of Nodal Lines when the Source is near a Boundary

The theoretical distribution of signs and nodal lines in a homogeneous medium is used to determine earthquake mechanism. The change of signs of separate waves at the boundaries, for example the sign of PP after reflection at a surface, may be allowed for in a comparatively simple way using the plane wave theory (Ingram and Hodgson, 1956).

The source itself can often be situated at a boundary or near it. If the distance between the boundary and the source is short compared with the quantity $vT/4$, the nodal lines can greatly differ from those in a homogeneous medium (here v is the wave velocity near the source and T is the first arrival period). The nodal lines depend upon the orientation of axes relative to the boundary and it makes their determination much more complicated.

Because of lack of space I shall not consider the question theoretically, but shall only give an example of nodal lines for a dipole with moment situated near a free boundary (Figure 2)

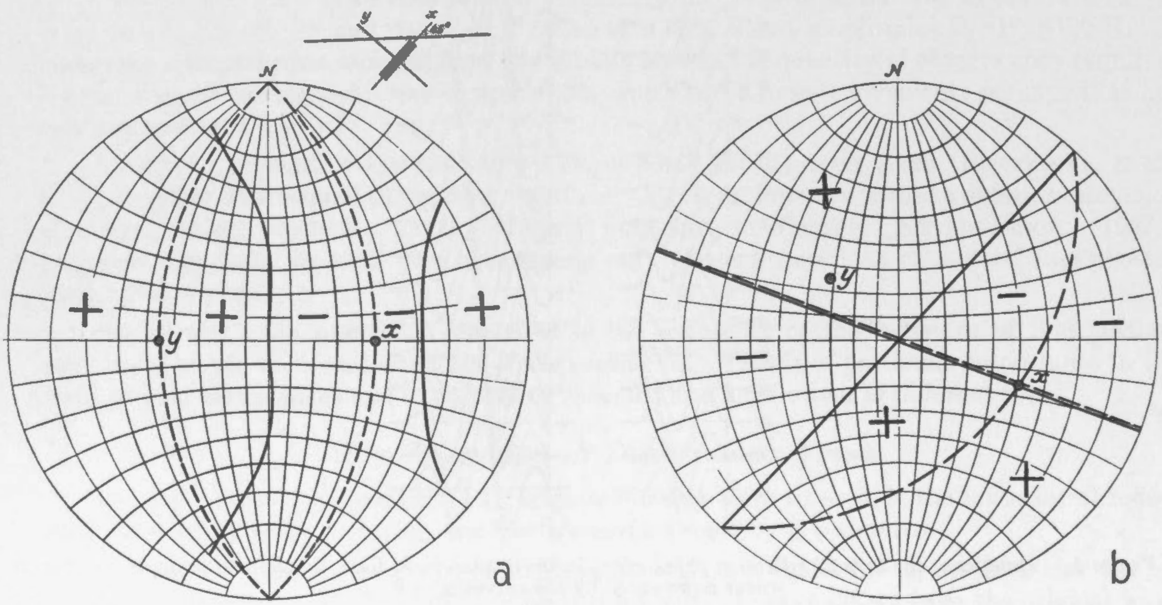

Figure 2. Examples of the nodal lines for (a) longitudinal waves and (b) SH waves, for a source near the free surface. In each case the dashed lines represent the usual nodal lines for the same source in a homogeneous medium. The nodal lines depend on the orientation of the axes x, y of the source relative to the free surface.

or an intermediate one (Figure 3). Similar calculations are carried out in cases which we considered to be typical. As is seen from Figures 2 and 3, usual methods of interpretation for such an earthquake can lead to great difficulties or to errors. One can avoid these difficulties using diagrams as shown in Figures 2 and 3 instead of the usual nodal lines. The circumstances are especially complicated for total reflection because of the above-mentioned change of displacement form. It can be seen from Figure 4 that the notion of nodal line itself looses its usual meaning.

Determination of 'Straightened Rays' in the Case of Curved or Inclined Intermediate Boundaries

The direction of straightened rays is characterized by azimuth α_h and inclination i_h. In Byerly's method instead of i_h the 'extended distance' $d = \cot i_h$ is considered; the fundamental calculations of d have been carried out by Hodgson and his colleagues and those of i_h by Ritsema.

It is usually supposed that α_h is equal to the azimuth from the epicentre to the station and that $\sin i_h = \dfrac{R_o}{R_h}\dfrac{v_h}{v_o} \sin i_o$, where v is the velocity, R the distance from the centre of the earth and where subscripts h and 0 denote the source and observation point accordingly.

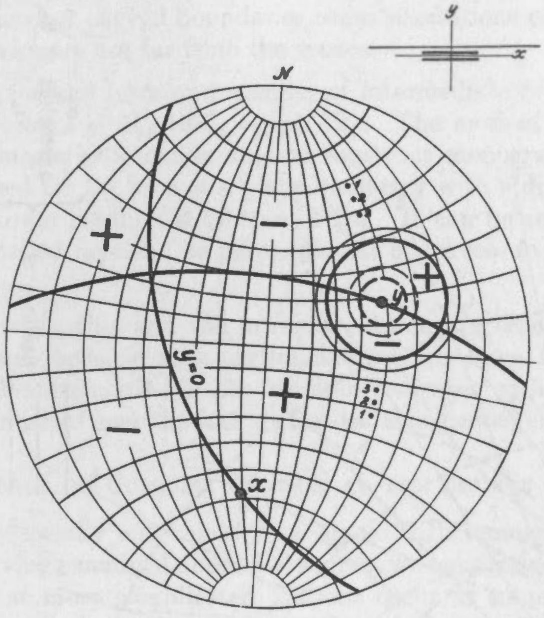

Figure 3. Additional nodal lines for longitudinal waves when the source is near an inner boundary. The fault ($y = 0$) is parallel to the boundary, the orientation of the fault relative to the free surface is arbitrary. The heavy lines represent the usual nodal lines. The closed circles, drawn with heavy lines, show the additional nodal lines in a medium with a lower velocity. The closed circles drawn with thin lines are the projection of a cone, outside of which the total reflection phenomenon occurs. Where a_i, b_i are the velocities of longitudinal and transverse waves respectively and ρ represents density, the closed circles drawn with solid lines correspond to $a_2/a_1 = 2.5$, $\rho_2/\rho_1 = 1.24$ and $a_i/b_i = \sqrt{3}$, while those drawn with dashed lines correspond to $a_2/a_1 = 4.8$, $\rho_2/\rho_1 = 1.3$ and $a_i/b_i = \sqrt{3}$. The additional nodal lines are due to the refraction at the boundary.

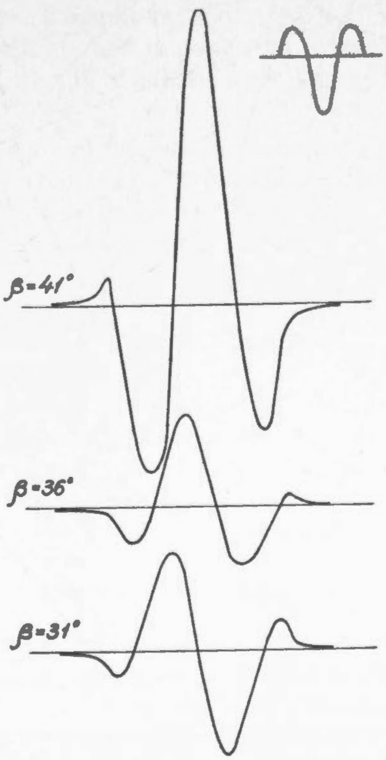

Figure 4. The Figure illustrates a change in first motion not related to the earthquake mechanism. It shows displacements in longitudinal waves along rays lying in a medium with a lower velocity (corresponding to points 1, 2, and 3 in Figure 3) and making the angle β with the y axis. The constants are the same as those corresponding to the solid circles in Figure 3. The form of the primary wave is shown in the upper right corner.

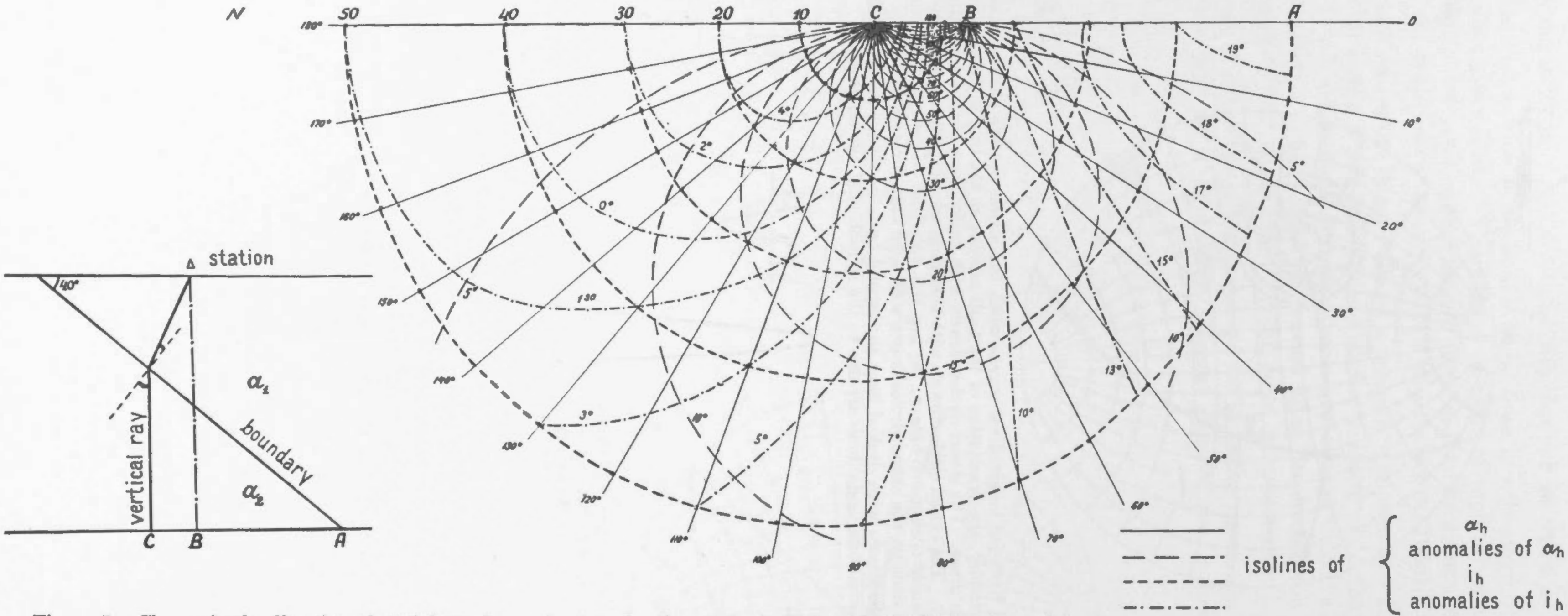

Figure 5. Change in the direction of straightened rays due to refraction at the inner boundary where $a_2/a_1 = 2.5$. A cross-section of the medium is shown in the lower left corner. All the isolines are given on a horizontal plane AC. The anomalies of i_h, α_h are, respectively, the differences $(i_h - i)$ and $(\alpha_h - \alpha)$, where i, α are the angles determined without allowance for the inner boundary. (After E. I. Galperin.)

α_h - the azimuth of the straightened ray;
i_h - its angle with the vertical.

If the wave meets inclined or curved boundaries these suggestions can lead to great errors, especially when the boundaries are not far from the source.

To determine α and i_h for any form and number of intermediate boundaries the graphical method is developed (BESSONOVA *et al.*, 1957, *suppl.* VI). The method is based upon the use of Wulff's projection. By means of it one is able to construct monograms of the type shown in Figure 5 which is composed for the case of a plane boundary with a dip of 40°. The ratio of velocities in the upper and lower medium is taken as 1:2.5. It can be seen from Figure 5 that the real direction of straightened rays can be perpendicular or reverse to that defined by means of the usual method.

The problems considered in this and the previous section are especially important when near earthquakes are studied, because near earthquake records have higher frequencies and because the influence of inhomogeneities in the medium increases with frequency. However for distant earthquakes boundaries near the foci are not to be neglected either.

MODELS OF COMPLEX MOTION AT THE SOURCE

Earthquake sources are usually equivalent to a dipole with moment (that is, to a model of a symmetrical fault). Having examined about 300 sources we have found almost no exceptions. However, the possibility that more complicated motions occur at some foci cannot be at all neglected. These motions can correspond to an asymetrical fault, a combination of a fault with a fractural opening, a fault with rotation, etc.

Point models of such motions and related nodal lines for P, SV, SH are shown in Figure 6. These models are defined (BESSONOVA, *et al.*, 1957; KEYLIS-BOROK, 1956b) by means of classical wave theory given by LOVE (1934) and STOKES.

The theoretical study of the above models and some ideas concerning the method of interpretation have been given elsewhere (BESSONOVA, *et al.*, 1957). The waves arising from various systems of multipoles have also been studied in Japan for a long time(HIRONA, 1948; HONDA *et al.*, 1952, 1957). The models are worthy of examination if there are great quantities of reliable data.

The models shown in Figures 6b and 6c seem to have the most interest; their nodal lines for P waves do not satisfy the 'orthogonality condition'. Some earthquakes discovered by HODGSON cannot be interpreted in the usual way; perhaps it would be interesting to study them using such models or to consider them in the light of the two previous sections.

THE MECHANISM OF EARTHQUAKES IN PRINCIPAL SEISMIC BELTS OF THE U.S.S.R. AND ADJACENT REGIONS

This chapter is a summary of the study of about 300 earthquakes. They are distributed in the regions in the following way (figures in brackets are the focal depths in kilometers): northwest edge of the Pacific Ocean from the Marianas Islands to the Aleutian Islands—29 (down to 580); the Hindu Kush—10 (150-240); Garm district—135 (down to 35); the Tien Shan—33 (10-20); Turkmenia—33 (down to 50); the Caucasus—57 (down to 50).

OBSERVATIONS USED

Distant earthquakes were studied mainly by use of the waves P, S, PP, SS, pP, sS, sP; for near earthquakes the waves $\overline{P}$, $\overline{S}$ and more rarely P_n and S_n (head waves) were taken. For some earthquakes we used recordings of both near and distant stations, the validity of this having been proved by correlating the forms of oscillation shown at near and distant stations. The interpretation was based mainly on arrival signs. The sign combination for P, SV, SH at each virtual point of observation has proved to be especially effective. It greatly reduces the number of observations required and enables us to study many comparatively weak earthquakes in local zones for comparison with tectonics. For example, 135 of the sources studied in the Garm district are concentrated inside a section of 70 by 140 km. This section is continually being studied by a special group of near stations. Experience shows that transverse waves are as reliable as secondary longitudinal waves (PP, pP, etc.) *if one uses seismograms rather than questionnaires.*

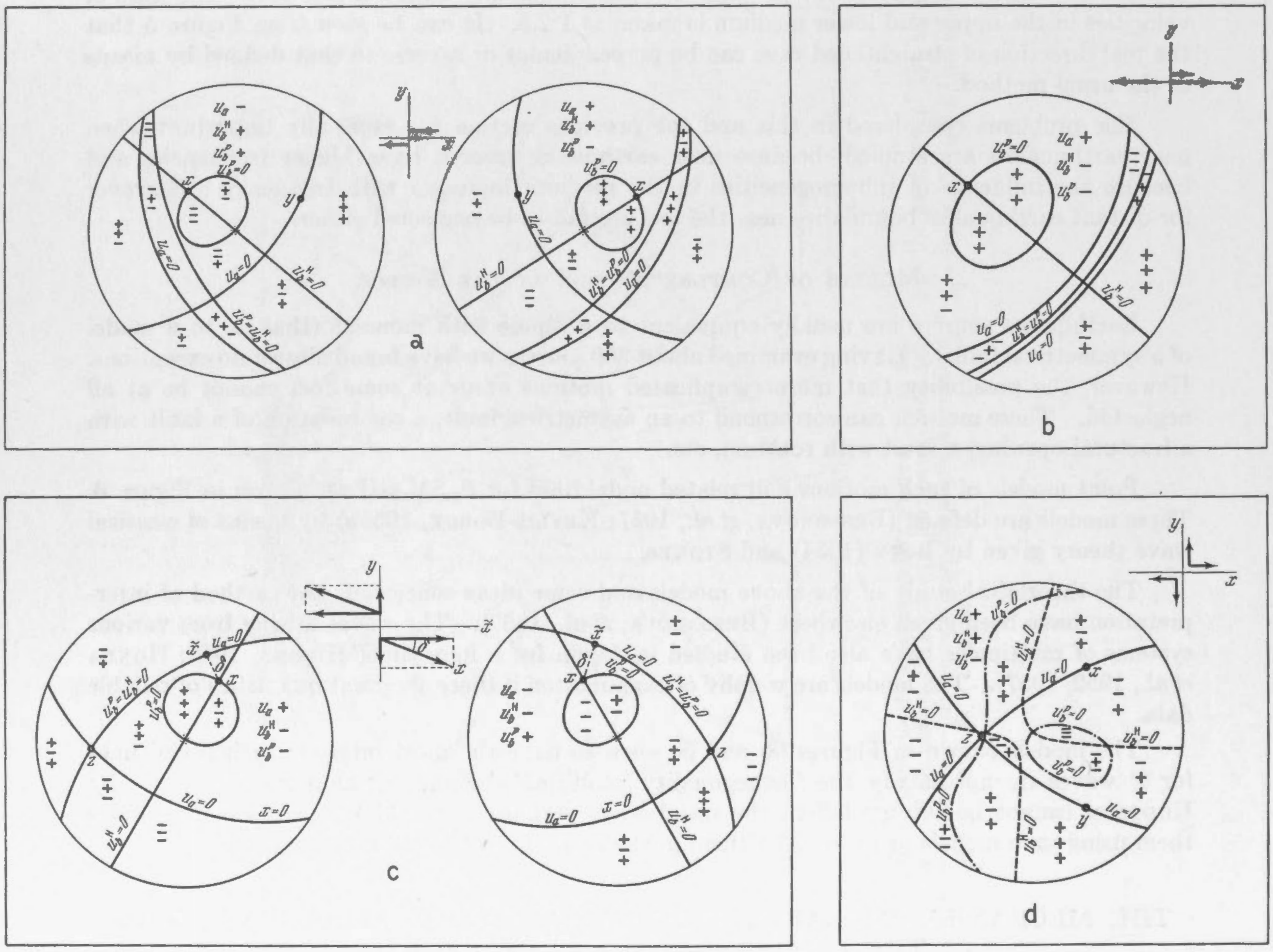

Figure 6. Nodal lines for various complex sources:
a—asymmetrical fault;
b—asymmetrical fracture openings;
c—combination of fault and fracture openings;
d—combination of the fault and rotation (or two perpendicular faults).

It can be estimated that the errors involved in determining the direction of fault-plane solutions are from 7° to 15° with the mechanism described here. To avoid errors of inaccurate drawing of the straightened rays is the most difficult problem.

Results of Interpretation

The mechanism of the earthquakes studied is shown in Figures 8 to 12; the notation used in these figures is described in Figure 7.

To make the generalization of results easier, summaries of the fault-plane stereographic projection and motion directions can conveniently be given by the method shown in Figure 13.

Such summaries for all the regions studied have been given elsewhere (BESSONOVA, *et al.*, 1957); a typical example is given in Figure 14.

A detailed description of the results of our work to date, and of its comparison with the tectonics of each region has been given in other publications (BESSONOVA *et al.*, 1957, KEYLIS-BOROK, 1956a).

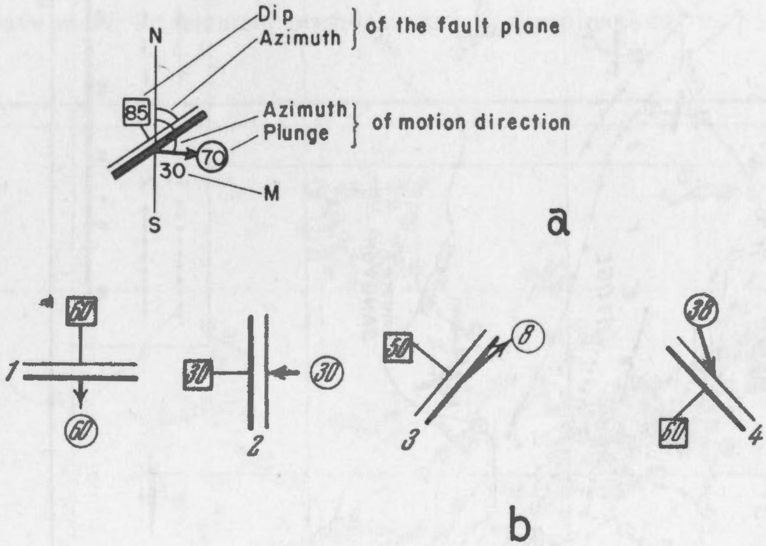

Figure 7a. The notation used in representing fault-plane solutions on maps. The heavy line represents that side of the fault that moved up. The number M is the identification number of the earthquake in the catalogue (BESSONOVA, *et al.*, 1957).

b. Some examples of the representation of fault-plane solutions.

1. Normal fault striking parallel to the latitude and dipping 60°N.
2. Thrust fault striking parallel to the meridian and dipping 30°W.
3. Strike-slip fault, dipping 50°NW. The direction of movements is NE with an inconsiderable (8°) uplift of the lower side.
4. Reverse-oblique slip fault.

In generalizing the results and comparing them with tectonic patterns one must bear certain limitations in mind.

(a) With a limited pattern of seismic stations it may not be possible to determine all possible fault systems. HODGSON, in his summary of this volume, has suggested that this may explain the difference between Soviet results and his own in the northwest Pacific. Another example is provided by the Garm district, shown in Figure 9. The special stations set out in this area were all south of the Hissar ridge, and their observations ($\overline{P}$, $\overline{S}$ waves) make it possible to determine with certainty only those faults in the Hissar ridge which strike nearly north-south and dip not more than 25° to 30°. To study all possible faults it is necessary to use additional observations from stations north of the ridge, or to use the head waves P_n, S_n at the southern stations.

Generally speaking, the system of observations will be free of this unpleasant 'selectivity' if a hypocentre is surrounded by conventional points (not necessarily by the stations themselves).

(b) The number of faults studied must be sufficiently large for the application of statistical criteria. For example, the first 30—40 faults studied in the Garm district indicated two prevailing strikes, the strikes transverse to the main structures appearing the more numerous. However, the later statistical analyses of about 150 faults showed clearly that the longitudinal faults were the more prevalent; transverse ones exist but they are not the dominant ones.

(c) Most of the earthquakes studied have been relatively weak; the general properties of their faults must be compared with tectonic features of a corresponding scale, which may be different than those corresponding to large earthquakes.

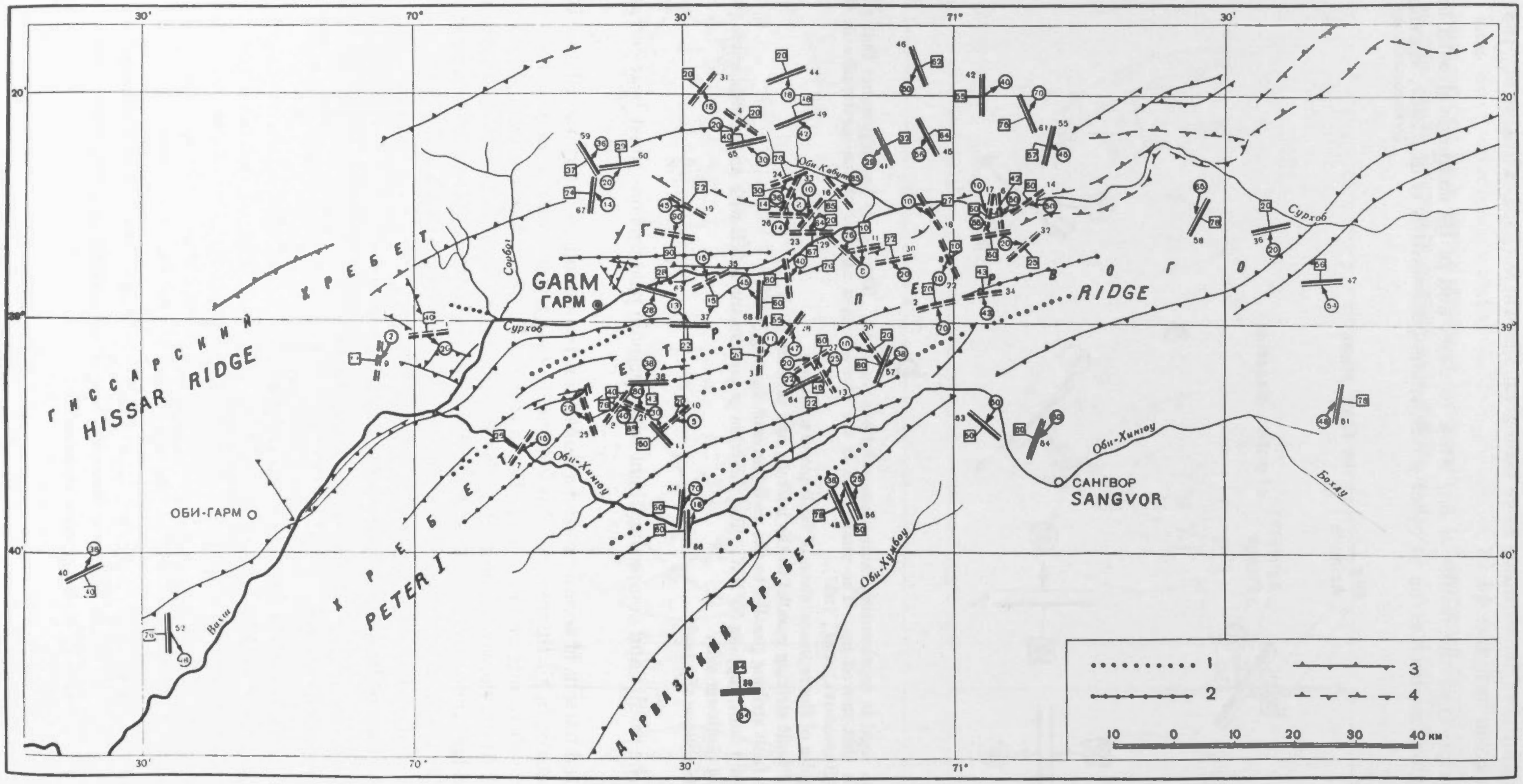

Figure 8. Fault-plane solutions for the Garm region. Legend:

1. Synclinal axes.
2. Anticlinal axes.
3. Tectonic ruptures.
4. Supposed tectonic ruptures. Solid lines represent comparatively strong earthquakes (1952-1954), recorded by local stations, dashed lines represent weaker earthquakes (1950) recorded by temporary stations.

(Interpretations made by T. I. Kukhtikova, S. D. Kogan, and L. N. Malynovskaya; tectonic data from I. E. Gubin; epicentres determined by T. I. Kukhtikova, I. L. Nersesov, and N. V. Fokina).

We shall describe here only some general patterns which seem to be sufficiently reliable.

(a) Faults of individual weak earthquakes do not usually show any correlation with local structure near the epicentre, this local structure often being so complicated that any correlation would be arbitrary. However, considering large areas, zones may usually be distinguished in which the faults have much in common, prevalent strikes, dip directions or the character of

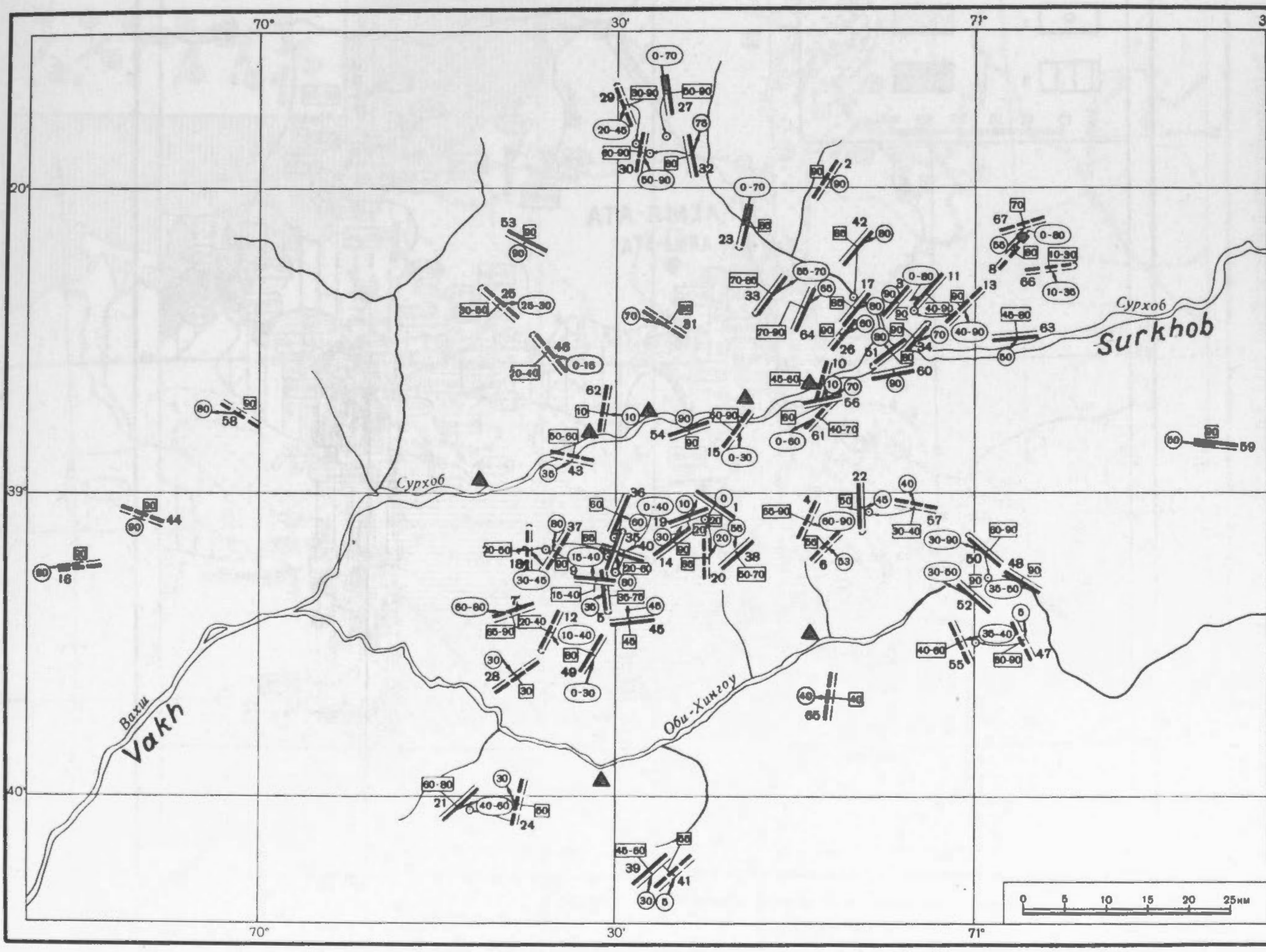

Figure 9. Fault-plane solutions for the Garm region derived from the observations of special expeditions made in 1955 and January and February of 1956. (Interpretation by L. N. Malinovskaya, G. I. Pavlova, and E. N. Bessonova; epicentres by I. L. Nersesov and T. I. Rautian).

motion being the same. Such zones coincide with large tectonic complexes, the prevailing properties of the faults being very different for different complexes. There is thus a clear correlation between earthquake faulting and tectonics, although the depth of the tectonic structures seems to be less than the focal depths of the earthquakes. This suggests that the formation of large tectonic complexes is not merely a surface phenomenon but proceeds to depth, and that earthquakes and these structures are parallel manifestations of a general process of the earth's crustal development.

(b) Eliminating, at first only qualitatively, the influence of the 'selectivity' of the stations, we can establish the fact that in the Askabad uplands and in the Garm district the prevalent fault strikes are nearly longitudinal to the main tectonic features. In many other regions two strikes can be noted, one longitudinal and the other transverse to the tectonic features. However, until the necessary statistical analysis has been applied it is not possible to say which is the more important.

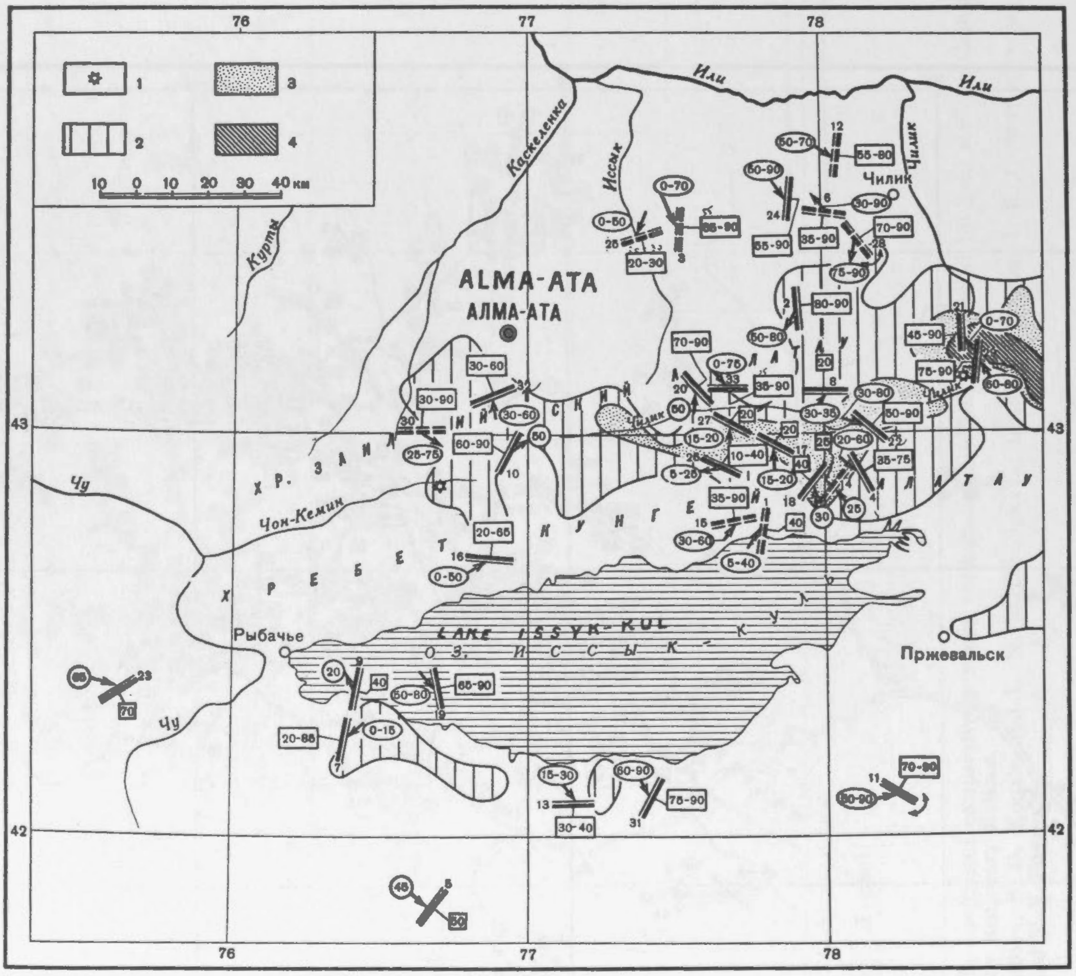

Figure 10. Fault-plane solutions for northern Tien-Shan. Legend:
1. Epicentres of strong earthquakes;
2, 3, 4. Contours giving the density of epicentres per 100 sq. km., 2 to 3, 4 to 6 and 7 to 13 respectively. (Interpretation by L. N. Malinovskaya; densities of epicentres according to N. V. Vvedenskaya; epicentres by T. M. Gorbunova, A. A. Fogel).

(c) It seems that intense horizontal motion direction components and, less definitely, transverse fault strikes are observed more often in fault-plane work than in the field. This has already been noted by Hodgson, Scheidegger, Ritsema and Byerly. This agrees with some data from geotectonics (Wegmann, 1955) concerning modern geological movements.

(d) In the foci of some districts the fault-plane strikes are parallel to the boundaries of tectonic depressions and upheavals, but that side of the fault which is nearer to the depression moves upward during the earthquake. This agrees with geological and geodetic data concerning motion direction at sources in Japan. There the vertical motion directions in the sources of earthquakes are directed opposite to the secular ones (Kobayashi, 1955), as if the earthquake were attempting to compensate for the secular change.

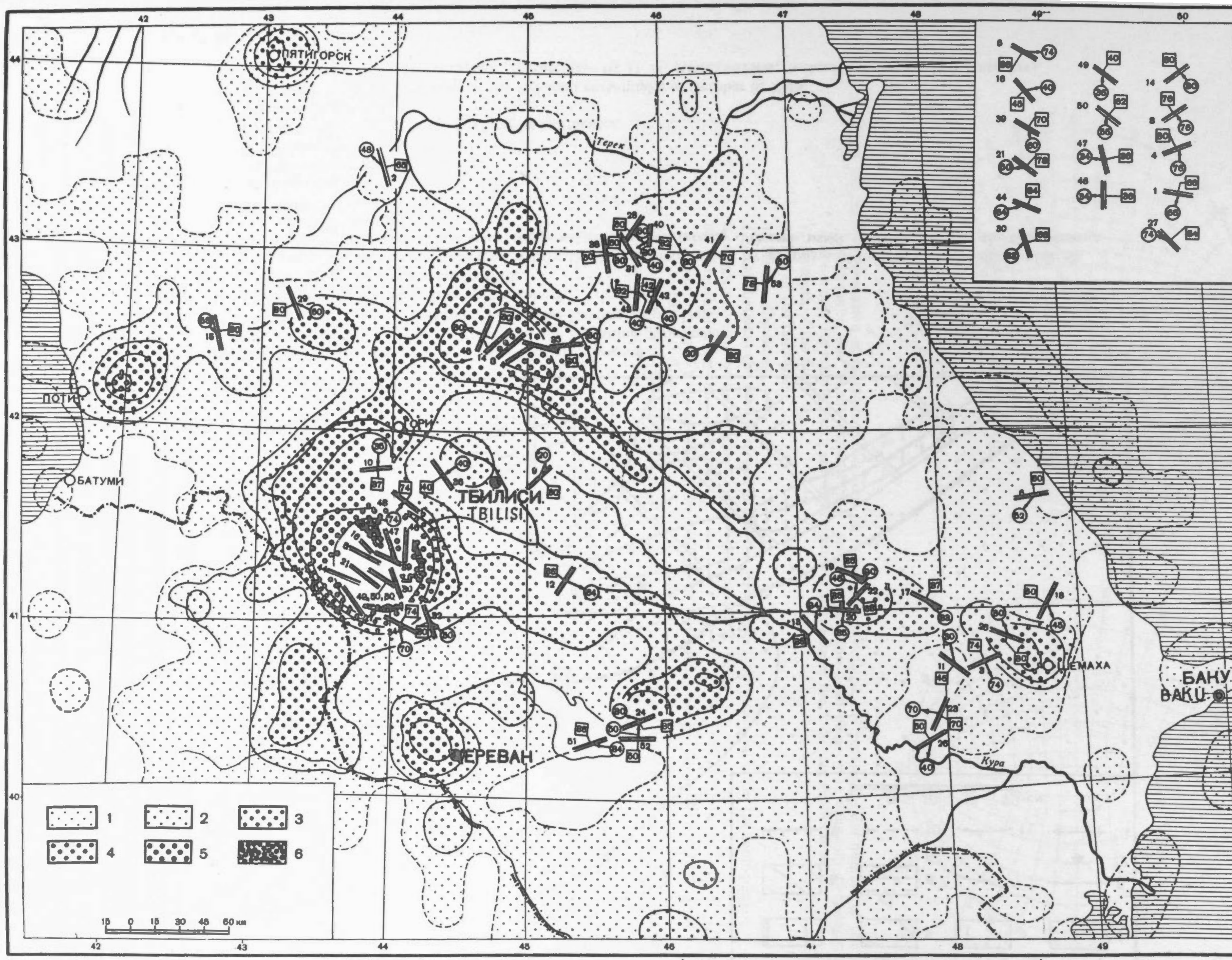

Figure 11. Fault-plane solutions for the Caucasus. For the sources of the Akhalkalaky upland, each fault is completely represented in the insert at top right. (Interpretation by O. D. Gotsadze and L. N. Malinovskaya; density of epicentres (after I. V. Kirillova), per 900 km²: 1—1 to 5; 2—6 to 10; 3—11 to 20; 4—21 to 30; 5—31 to 40; 6—40).

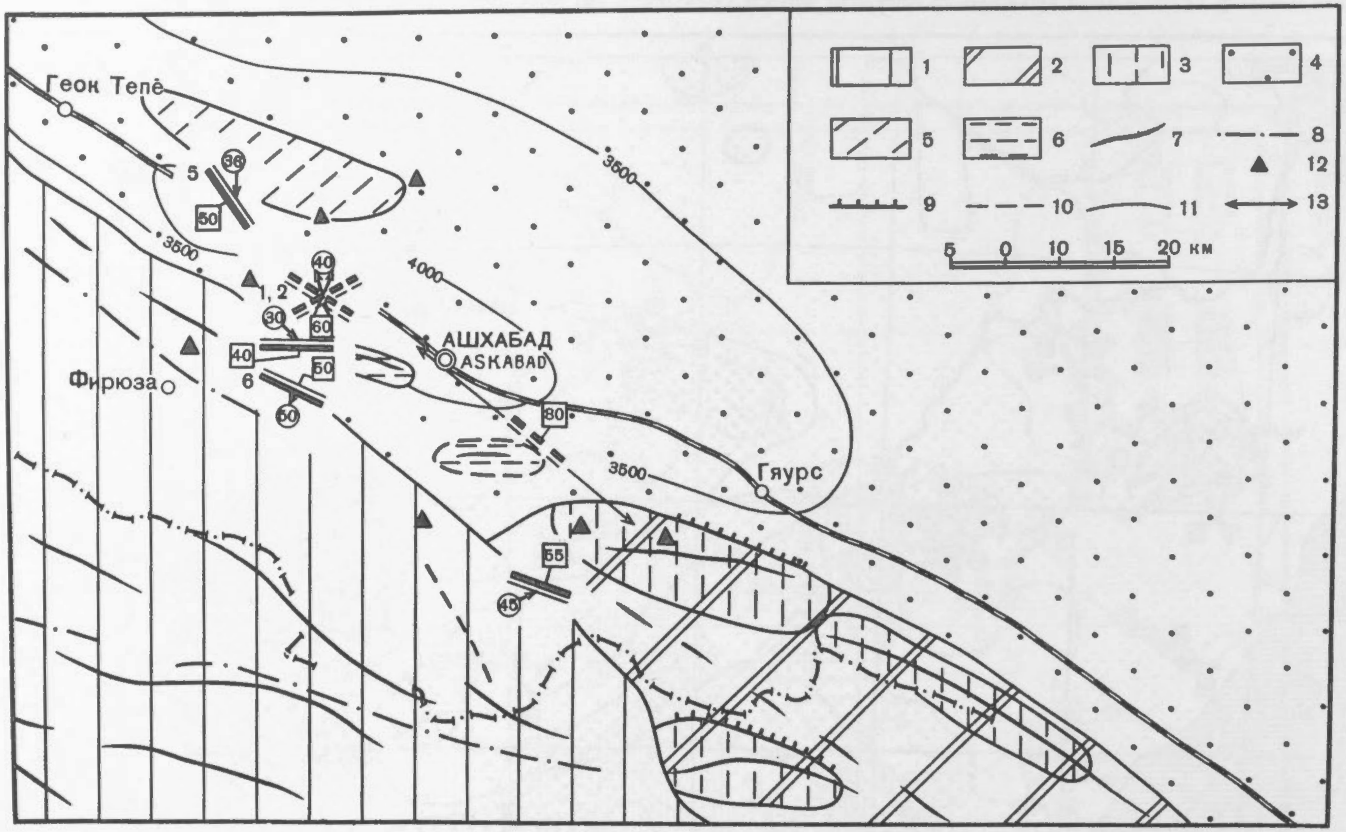

Figure 12. Fault-plane solutions for Askabad region. Legend:

1. Kopet-Dag anticlinorium (formed at the beginning of neogen).
2. Younger (the end of neogen) zone of the Eastern Kopet-Dag.
3. Large anticlinal structures within zone 2.
4. Trough in the Kopet-Dag foothills.
5. Gently sloping brachy-anticlinal within the trough determined by geophysical methods at the depth of 2—3.
6. Exposed brachy-anticlinal folds composed of the Quarternary Pliocene rocks. Formed during the Quarternary period.
7. Anticlinal axes.
8. Synclinal axes.
9. Thrusting lines.
10. Faults.
11. Isolines of the top of the Cretaceous sediments.
12. Seismic stations.
13. Axis of the epicentral zone of the Askabad earthquake of October 3, 1948.

(Interpretation by O. D. Gotzadze; hypocentres by D. N. Rustanovich; tectonic scheme by I. A.Rezanov).

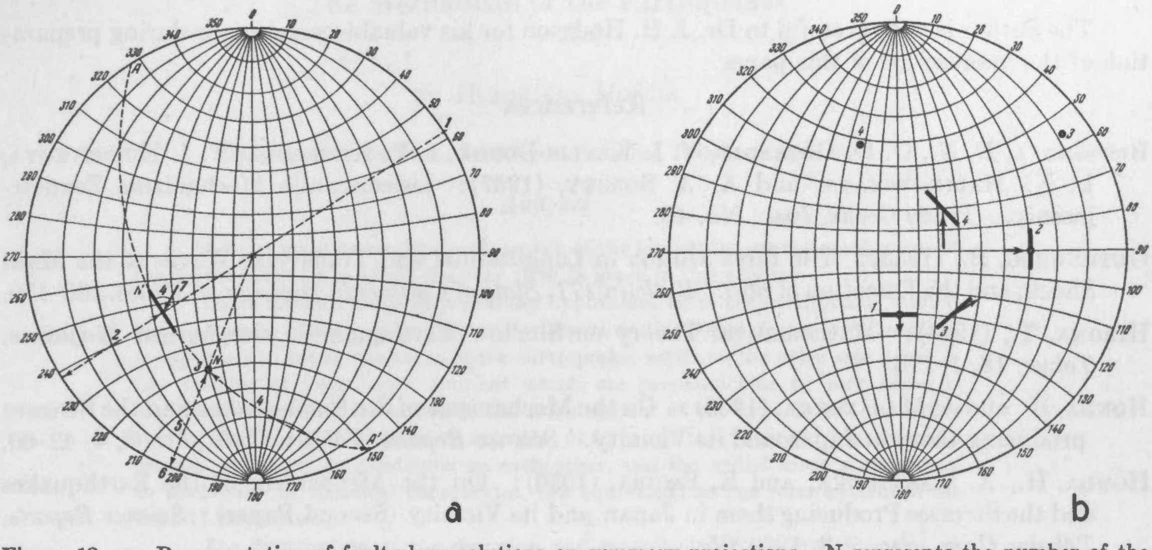

Figure 13. a. Representation of fault-plane solutions on summary projections. N represents the number of the earthquake, AA′ is the stereographic projection of the fault-plane (the summary projection shows only its middle part), and the numbered points have the following significance:

1. Azimuth of the fault dip.
2. Dip of the fault plane.
3. Motion direction.
4. Angle between the motion direction and the strike direction (measured off in the fault-plane).
5. Angle between the motion direction and the horizontal plane.
6. Azimuth of the motion direction.
7. The arrow is put near the wall of the fault moving upwards. Its projection to AA′ is directed to the motion direction.

b. Examples of fault-planes on summary projections. The numbers refer to the same fault-planes shown in Figure 7b.

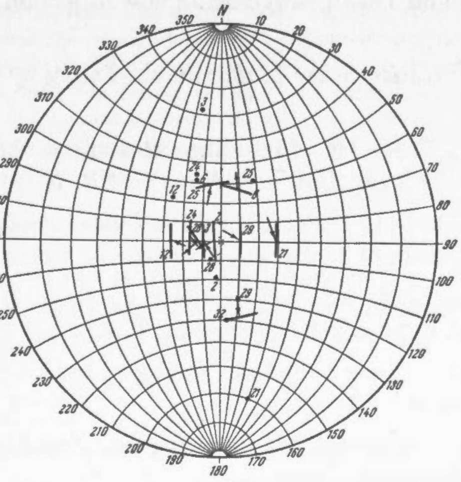

Figure 14. Summary of fault-plane solutions for northern Tien-Shan, the area to the north of the Zailiysky Ala-Tau ridge shown in Figure 10.

CONCLUSION

The main purpose of the study of earthquake mechanism is to look into the laws of the geotectonic development of the earth. One of the principal problems of further work is studying dislocation systems at foci in regions with various tectonic developments. While the different authors have their own particular methods and interests it is very encouraging for the coordination of further work that they are keeping in close touch, and that their methods are growing nearer.

The author is very grateful to Dr. J. H. Hodgson for his valuable suggestions during preparation of the manuscript of this paper.

References

BESSONOVA, E. N., O. D. GOTSADZE, V. I. KEYLIS-BOROK, I. V. KIRILLOVA, T. I. KUCHTIKOVA, L. N. MALINOVSKAYA, and A. A. SORSKY, (1957): Issledovanije Mechanizma Zemletrjaseniy. *Trudy Geofiz. Inst.*, No. 40.

GUTENBERG, B., (1955): The First Motion in Longitudinal and Transverse Waves of the Main Shock, and the Direction of Slip. *Bulletin 171, State of California Division of Mines*, 165–170.

HIRONA, T., (1948): Mathematical Theory on Shallow Earthquakes. *Geophysical Magazine, Tokyo*, **18**, 1–116.

HONDA, H., and A. MASATSUKA, (1952): On the Mechanisms of the Earthquakes and the Stresses producing them in Japan and its Vicinity. *Science Reports, Tôhoku Univ., Ser. 5*, **4**, 42–60.

HONDA, H., A. MASATSUKA, and K. EMURA, (1956): On the Mechanism of the Earthquakes and the Stresses Producing them in Japan and its Vicinity (Second Paper). *Science Reports, Tôhoku Univ., Ser. 5*, **8**, 186–205.

INGRAM, R. E., S.J., and J. H. HODGSON, (1956): Phase Change on Reflection at a Free Surface. *Bull. Seismol. Soc. Am.*, **46**, 203–213.

KEYLIS-BOROK, V. I., (1956a): Methods and Results of the Investigations of Earthquake Mechanisms. *Pub. Bur. Centr. Seismol. Int. Ser. A. Travaux Scientifiques*, **19**, 383–394.

KEYLIS-BOROK, V. I., (1956b): K Voprosu O Svjazi Totshetshnich i Objemnich Istotshnikov. *Isvestija Akadamii Nauk SSSR*, No. 4, 404–409.

KEYLIS-BOROK, V. I., (1957): The Determination of Earthquake Mechanisms Using both Longitudinal and Transverse Waves. *Annali di Geofisica*, **10**, 105-128

KOBAYASHI, T., (1955): Up and Down Movements now in Action in Japan. *Geologische Rundschau*, **43**, 233–247.

LOVE, A. E. H., (1934): *A Treatise on the Mathematical Theory of Elasticity*. Cambridge University Press, Fourth Ed.

MALINOVSKAYA, L. N., (1957a): K Metodike Rastsheta Dinamitsheskich Osobennostei Seismitsheskich Voln. *Isvestija Akademii Nauk SSSR*, No. 4, 426–439.

MALINOVSKAYA, L. N. (1957b): O Dinamitsheskich Osobennostyach Prodolnich Otrashennich Voln za Kritisheskimi Uglami. *Isvestija Akademii Nauk SSSR*, No. 5, 569–574.

NAKANO, H., (1923): Notes on the Nature of the Forces which Give Rise to the Earthquake Motions. *Seismol. Bull. Centr. Met. Obs. Japan*, **1**, 92–120.

PETRASHAIN, G. I., (1957a): *Voprosi Dinamitsheskoj Teorii Rasprostranenija Seismitsheskich Voln*. Vol. 1, Gosnebteiz-dat., Moscow.

PETRASHAIN, G. I., (1957b): *Materiali Kolitshestvennogo Isutshenija Dinamiki Seismitsheskich Voln*. Vol. 1, 2, Gosnebteiz-dat., Moscow.

RITSEMA, A. R., (1955): The Fault Plane Technique and the Mechanism in the Focus of the Hindu Kush Earthquakes. *Indian Journ. Meteor. and Geophys.*, **6**, 41–50.

SCHEIDEGGER. A. E., (1957): The Geometrical Representation of Fault-Plane Solutions of Earthquakes. *Bull. Seismol. Soc. Am.*, **47**, 89–109.

WEGMANN, E., (1955): Lebende Tektonik: Eine Ubersicht. *Geologische Rundschau*, **43**, 4–34.

The Mechanism of the Earthquakes

BY HIROKICHI HONDA

Geophysical Institute, Faculty of Science, Tôhoku University

Abstract

A brief account on the development of the knowledge on the mechanism of the earthquakes since about the year 1930, is given in this report.

There are two kinds of prevailing hypotheses as to the earthquake mechanism. In one of them, a couple of two equal and opposite forces with moment is supposed to act at the focus of the earthquake, while in the other one a set of two couples of forces with moment which are perpendicular to each other is assumed. We will call the former the force system of the type I, and the latter that of the type II. A set of two couples of forces of the nature of pressure and tension which are perpendicular to each other, and the radial force proportional to $\sin 2\theta \cos\varphi$ in spherical coordinates, are equivalent to the force system of the type II respectively.

The distribution of the direction and magnitude of the initial motion of the P, S and ScS waves of the near deep and intermediate earthquakes, observed in Japan can be explained by the theories based on the assumption that the force system of the type II acts at the origin in an infinite elastic solid. The directions of the pressure of the stresses causing the earthquakes seem to be directed perpendicularly to the trends of the deep and intermediate earthquake zones in and near Japan. For the investigation of the P, S and surface waves and the deformation of the earth's surface observed in the cases of very shallow earthquakes occurred in Japan, the theories for the force system of the nature of the type II or the radial force proportional to $\sin 2\varphi$ in cylindrical coordinates, acting at the origin on the surface of a semi-infinite elastic solid, have been applied.

The stereographic projection methods which are appropriate for the investigation of the earthquake mechanism based on the observations at the stations distributed over the world, have been proposed and developed by P. BYERLY and J. H. HODGSON, and applied to the studies of numerous earthquakes by many seismologists, the force system of the type I being assumed as the basis of the investigation. The plane bisecting the couple of forces is considered to be the fault plane. The relations between the strikes and dips of the fault planes, the motion directions along the fault planes and the geological features, are investigated.

According to the theories on the elastic waves, the patterns of the initial motions of the P waves for the force systems of the types I and II, are the same to each other. As the differences of the effects of the force systems are to be noticed in the patterns of the S waves, it is desired that the S waves observed at the distant stations may be investigated further in detail.

1 Introduction

One of the most important problems in seismology may be the investigation of the mechanism of the earthquakes or the nature of the stresses producing the earthquakes, being based on the observations of the seismic waves. After F. OMORI and

Reprinted from

The Science Reports of the Tôhoku University

Series 5, Geophysics, Vol. 9, Supplement

55092-1—4

T. SHIDA, the studies in this line have been carried out by many seismologists, and the progresses of the researches up to about 1935 were summarized for example by H. KAWASUMI (1937) in his historical sketch on the problem.

In the present paper, the author intends to state the development of knowledge concerning the problem since about 1930, the greater part of the earlier studies described in KAWASUMI'S summary being not mentioned here. The mathematical theories on the mechanism of the earthquakes are recapitulated in Chap. 2. The results of the investigations of the mechanism of the earthquakes occurred in Japan, based mainly on the seismological data obtained at near stations, are summarized in Chap. 3 An account on the development of the studies of the problem, made by P. BYERLY, J.H. HODGSON and others, based on the data obtained at the stations distributed over the world, is described in Chap. 4. And some discussions on the problem are stated in the concluding remarks, Chap. 5.

2 Mathematical Theories

Some mathematical theories which concern with the generation of the elastic waves from the source in an infinite elastic solid or on a semi-infinite elastic solid, and are related directly with the study of the mechanism of the earthquakes, are recapitulated in the present chapter.

2-1. Infinite Elastic Solid. H. NAKANO (1923) and T. MATSUZAWA (1926) investigated theoretically the propagation of the elastic waves generated by the force systems of various types applied at a point in an infinite elastic solid ; some of their results of calculation were recapitulated by HONDA *et al.*, (1956).

Let us suppose at first that two equal and opposite forces of the magnitude $K\exp(i\omega t)/\varepsilon$ act in the direction of the x-axis, at the points $y=\varepsilon/2$ and $-\varepsilon/2$ on the y-axis, as are illustrated in Fig. 1, and name the force system that of the type I. And next suppose that two couples of these force systems act simultaneously at the origin in the directions of the x- and y-axes, as are shown in Fig. 2 (a), and name the force system that of the type II. The force system of the type II is equivalent to the set of two couples of forces of the nature of pressure and tension, as are shown in Fig. 2 (b), where the x'-axis bisects the angle xoy. We take the y-axis as the polar axis of the spherical coordinates r, θ, φ (Fig. 3), and denote the r, θ, φ-components of displacement by δ_r, δ_θ, δ_φ, the motion propagated with

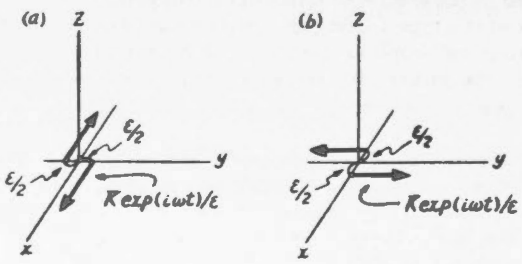

Fig. 1. The force system of the type I.

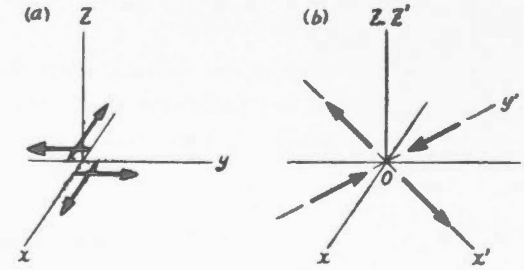

Fig. 2. The force system of the type II.

the velocity (v_p) of the P waves and that (v_s) of the S waves by p and s, the Lamé's constants by λ and μ, and the density by ρ. The displacement components of motion at large distances from the origin, produced by the force system of the type I or II are expressed as follows, in the limiting case when $\varepsilon \to 0$:

For the force system of the type I, we have,

$$\left.\begin{aligned}
\delta_{p,r} &= \frac{K}{4\pi}\frac{1}{v_p}\frac{1}{\lambda+2\mu}\frac{1}{2}\sin 2\theta\cos\varphi\frac{1}{r} \\
&\quad\times\omega\exp\left\{i\omega\left(t-\frac{r}{v_p}\right)+i\frac{\pi}{2}\right\}, \\
\delta_{s,\theta} &= \frac{K}{4\pi}\frac{1}{v_s}\frac{1}{\mu}\cos^2\theta\cos\varphi\frac{1}{r} \\
&\quad\times\omega\exp\left\{i\omega\left(t-\frac{r}{v_s}\right)+i\frac{\pi}{2}\right\}, \\
\delta_{s,\varphi} &= -\frac{K}{4\pi}\frac{1}{v_s}\frac{1}{\mu}\cos\theta\sin\varphi\frac{1}{r} \\
&\quad\times\omega\exp\left\{i\omega\left(t-\frac{r}{v_s}\right)+i\frac{\pi}{2}\right\},
\end{aligned}\right\} \quad \begin{matrix}(1)^{(65)}\\ \text{(Type I)}\end{matrix}$$

$$\delta_{p,\theta} = \delta_{p,\varphi} = \delta_{s,r} = 0\ ,$$

$$\frac{1}{v_s}\frac{1}{\mu}\Big/\frac{1}{2}\frac{1}{v_p}\frac{1}{\lambda+2\mu} \doteqdot 10.40\ , \quad (\text{for } \lambda=\mu)$$

For the force system of the type II, we have

$$\left.\begin{aligned}
\delta_{p,r} &= \frac{K}{4\pi}\frac{1}{v_p}\frac{1}{\lambda+2\mu}\sin 2\theta\cos\varphi\frac{1}{r} \\
&\quad\times\omega\exp\left\{i\omega\left(t-\frac{r}{v_p}\right)+i\frac{\pi}{2}\right\}, \\
\delta_{s,\theta} &= \frac{K}{4\pi}\frac{1}{v_s}\frac{1}{\mu}\cos 2\theta\cos\varphi\frac{1}{r} \\
&\quad\times\omega\exp\left\{i\omega\left(t-\frac{r}{v_s}\right)+i\frac{\pi}{2}\right\}, \\
\delta_{s,\varphi} &= -\frac{K}{4\pi}\frac{1}{v_s}\frac{1}{\mu}\cos\theta\sin\varphi\frac{1}{r} \\
&\quad\times\omega\exp\left\{i\omega\left(t-\frac{r}{v_s}\right)+i\frac{\pi}{2}\right\},
\end{aligned}\right\} \quad \begin{matrix}(2)^{(65)}\\ \text{(Type II)}\end{matrix}$$

$$\delta_{p,\theta} = \delta_{p,\varphi} = \delta_{s,r} = 0\ ,$$

$$\frac{1}{v_s}\frac{1}{\mu}\Big/\frac{1}{v_p}\frac{1}{\lambda+2\mu} \doteqdot 5.20\ , \quad (\text{for } \lambda=\mu)\ .$$

When we suppose that the radial force $F_r = F\sin 2\theta\cos\varphi\exp(i\omega t)$, Fig. 4, acts on the surface of the small spherical cavity of the radius a or the *model sphere* constructed around the origin, the displacement components at large distances from the origin in the limiting case when $a\to 0$, are given by

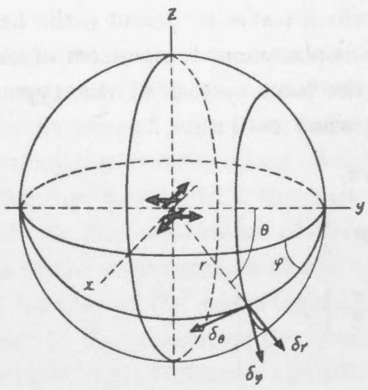

Fig. 3. The spherical coordinates.

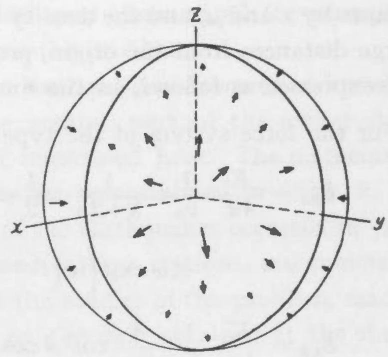

Fig. 4. $F_r/\exp(i\omega t) = F\sin 2\theta \cos\varphi$.[65]

$$
\left.
\begin{aligned}
\delta_{p,r} &= D \sin 2\theta \cos\varphi \frac{1}{r} \\
&\qquad \times \exp\left\{ i\omega\left(t - \frac{r}{v_p}\right) + i\frac{\pi}{2}\right\}, \\
\delta_{s,\theta} &= \left(\frac{k}{h}\right)^3 D \cos 2\theta \cos\varphi \frac{1}{r} \\
&\qquad \times \exp\left\{ i\omega\left(t - \frac{r}{v_s}\right) + i\frac{\pi}{2}\right\}, \\
\delta_{s,\varphi} &= -\left(\frac{k}{h}\right)^3 D \cos\theta \sin\varphi \frac{1}{r} \\
&\qquad \times \exp\left\{ i\omega\left(t - \frac{r}{v_s}\right) + i\frac{\pi}{2}\right\},
\end{aligned}
\right\} \quad (3)^{(65)}
$$

$$
D = a^3 F \frac{h^3}{6\mu k^2 + 3\lambda h^2 - 2\mu h^2}, \quad h = \frac{\omega}{v_p}, \quad k = \frac{\omega}{v_s}.
$$

For $\lambda = \mu$, (3) can be expressed as follows ;

$$
\left.
\begin{aligned}
\delta_{p,r} &= A_1 \sin 2\theta \cos\varphi \frac{1}{r} \\
&\qquad \times \omega \exp\left\{ i\omega\left(t - \frac{r}{v_p}\right) + i\frac{\pi}{2}\right\}, \\
\delta_{s,\theta} &= 5.20\, A_1 \cos 2\theta \cos\varphi \frac{1}{r} \\
&\qquad \times \omega \exp\left\{ i\omega\left(t - \frac{r}{v_s}\right) + i\frac{\pi}{2}\right\} \\
\delta_{s,\varphi} &= -5.20\, A_1 \cos\theta \sin\varphi \frac{1}{r} \\
&\qquad \times \omega \exp\left\{ i\omega\left(t - \frac{r}{v_s}\right) + i\frac{\pi}{2}\right\},
\end{aligned}
\right\} \quad (3')^{(65)}
$$

$$
A_1 = \frac{1}{19\sqrt{3}} \frac{1}{\mu^{3/2}} \rho^{1/2} a^3 F, \quad \left(\frac{k}{h}\right)^3 \doteq 5.20 .
$$

The expressions (3′) are quite similar to (2). The force system illustrated in Fig. 4 is essentially equivalent to that of the type II shown in Fig. 2 (a) or (b), in the effects of producing the P as well as S waves. The direction of the maximum tension ($\theta=\pi/4$, $\varphi=0$ — $\theta=3\pi/4$, $\varphi=\pi$) and that of the maximum pressure ($\theta=3\pi/4$, $\varphi=0$ — $\theta=\pi/4$, $\varphi=\pi$) in the force system shown in Fig. 4, correspond to the directions of the forces of the nature of tension and pressure illustrated in Fig. 2 (b).

The rates of the energies e_p and e_s of the P and S waves expressed by (3′), which are propagated outward across a large spherical surface constructed around the origin, are expressed as follows (HONDA, 1951);

$$e_p = \frac{32\pi^3}{15}\frac{\rho v_p}{T^2}A_1^2\,, \qquad e_s = \frac{48\pi^3}{15}\frac{\rho v_s}{T^2}(5.20\,A_1)^2\,, \qquad T = \frac{2\pi}{\omega}\,. \qquad (4)^{(59)}$$

When the force is not periodic but of shock type and is assumed to vary with time according to the expression $f(t)=1/(t^2+c^2)$, c being a positive constant, Fig. 5 (a), the corresponding displacement components are obtained by performing the operation

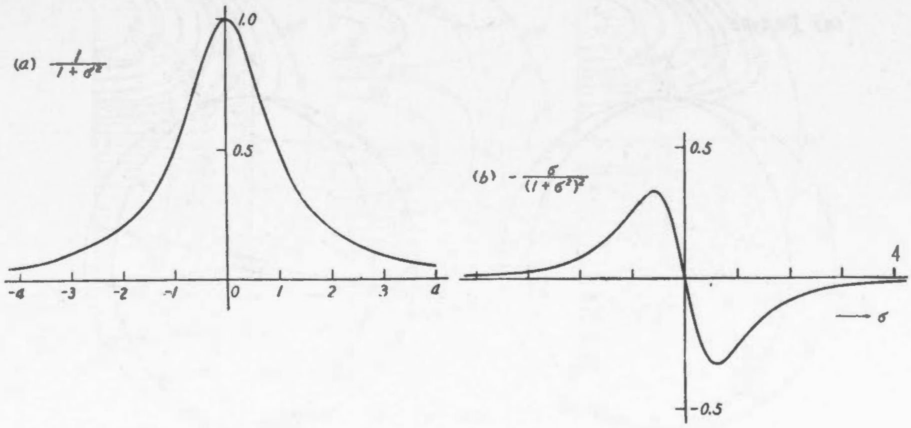

Fig. 5. $1/(1+\sigma^2)$ and $-\sigma/(1+\sigma^2)^2$.[65]

$$\frac{1}{\pi}\,Re\int_0^\infty d\omega\int_{-\infty}^{\infty} f(\alpha)\exp(-i\,\omega\,\alpha)\,d\alpha$$

to the expressions of δ obtained for the periodic forces. All the expressions (1), (2) and (3′) contain the same factor $\omega\exp\{i\omega(t-r/v)+i\pi/2\}$ as to ω, v being v_p or v_s according to the terms concerned, and we have

$$\frac{1}{\pi}\,Re\int_0^\infty \omega\,d\,\omega\int_{-\infty}^{\infty}\frac{1}{\alpha^2+c^2}\exp\Big[-i\omega\Big\{\alpha-\Big(t-\frac{r}{v}\Big)+i\,\frac{\pi}{2}\Big\}\Big]\,d\alpha$$

$$= -\frac{2}{c^3}\,\frac{\sigma}{(1+\sigma^2)^2}\,, \qquad \sigma=\frac{1}{c}\Big(t-\frac{r}{v}\Big). \qquad (5)^{(65)}$$

The variation of $-\sigma/(1+\sigma^2)^2$ with σ, Fig. 5 (b), shows that the motions propagated with the velocities v_p and v_s for the aperiodic case, consist of a single to and fro movement respectively. The patterns of the distribution with respect to θ and φ of the direction and magnitude of the initial motion of the P and S waves for the impulsive force systems of the types I and II, are expressed by following formulae,

$$\left.\begin{aligned} &(\delta_{p,r})_{\rm I} \cdots\cdots\cdots \tfrac{1}{2}\sin 2\theta\cos\varphi\,, \\ &(\delta_{s,\theta})_{\rm I} \cdots\cdots\cdots \cos^2\theta\cos\varphi\,, \\ &(\delta_{s,\varphi})_{\rm I} \cdots\cdots\cdots -\cos\theta\sin\varphi\,, \end{aligned}\right\} \quad \begin{aligned} &(6) \\ &(\text{Type I}) \end{aligned}$$

for the force system of the type I, and

$$\left.\begin{aligned} &(\delta_{p,r})_{\rm II} \cdots\cdots\cdots \sin 2\theta\cos\varphi\,, \\ &(\delta_{s,\theta})_{\rm II} \cdots\cdots\cdots \cos 2\theta\cos\varphi\,, \\ &(\delta_{s,\varphi})_{\rm II} \cdots\cdots\cdots -\cos\theta\sin\varphi\,, \end{aligned}\right\} \quad \begin{aligned} &(7) \\ &(\text{Type II}) \end{aligned}$$

for the force system of the type II, and are illustrated in Fig. 6 (a) and (b). The initial motion of the P waves is condensational and rarefactional in alternate zones bounded by two planes which are perpendicular to each other, in both cases I and II. The

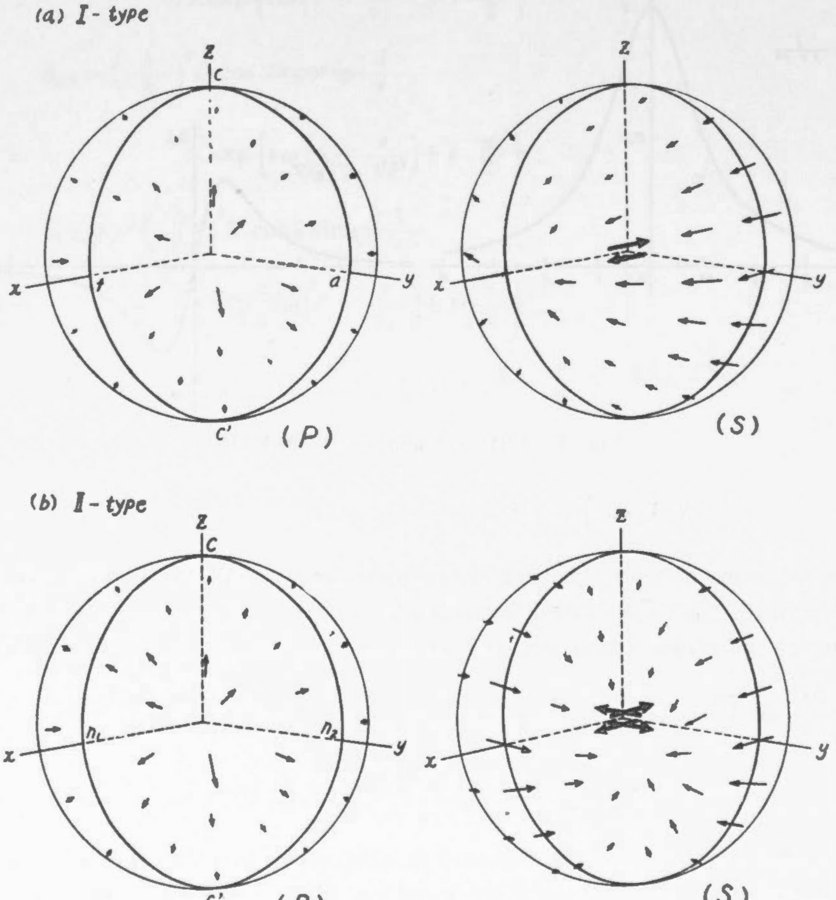

Fig. 6. The initial motion of the P and S waves; (a) for the force system of the type I, and (b) for that of II [65]

plane cfc' in Fig. 6 (a) is called 'the fault plane' and the plane cac' 'the auxiliary plane', and the direction of the forces 'the motion direction'. No distinction between the planes cfc' and cac' can be found, as far as only the initial motion of the P waves are concerned. The planes cn_1c' and cn_2c' in Fig. 6 (b) are the nodal planes for the P waves. The magnitude of the S waves is maximum in the auxiliary plane and minimum in the fault plane in the case I, whereas it is maximum in both nodal planes in the case II. The difference between the cases I and II, can be noticed in the distribution of the direction and magnitude of the initial motion of the S waves.

In order to illustrate the distribution with respect to θ and φ of the magnitude of the P and S waves emitted from the source for the case II, the values of $[P]=\sin 2\theta \cos \varphi$, $[S]=5.20\sqrt{(\cos 2\theta \cos \varphi)^2+(\cos \theta \sin \varphi)^2}$ and $[S]/[P]$ are shown in Fig. 7. The amplitude of the S waves is in general larger than that of the P waves except

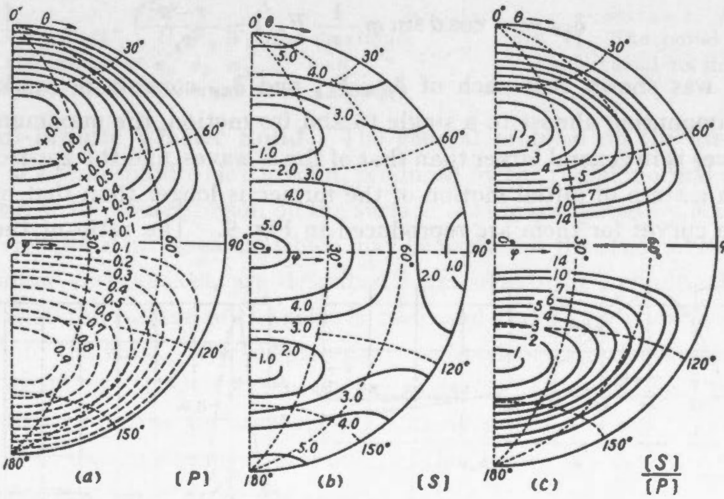

Fig. 7. $[P]$, $[S]$ and $[S]/[P]$.[51]

near the azimuths ($\theta=\pi/4, \varphi=0$; $\theta=3\pi/4, \varphi=0$; ......), where $[P]$ is maximum and $[S]$ is minimum (HONDA, 1934).

When the radius of the model sphere, whose surface is assumed to be subjected to the radial force $F_r=F \sin 2\theta \cos \varphi \exp(i\omega t)$, is not very small compared with the wave length l_p of the P waves, the ratio of the coefficients of the amplitude of the S waves to that of the P waves in (3') is not 5.20, but $5.20R$ for $\lambda=\mu$. The values of R for various values of a/l_p are shown in Fig. 8. (HONDA and T. MIURA, 1938). The amplitude of the S waves becomes even smaller than that of the P waves, when a/l_p is larger than a certain value. The general cases in which the radius of the model sphere is not very small and the force is impulsive instead of

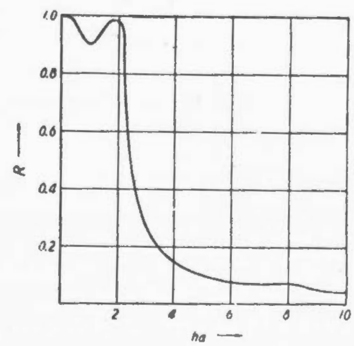

Fig. 8. R and $hc=2\pi a/l_p$.[56]

periodic, were treated by G. NISHIMURA and T. TAKAYAMA (1938) When the conditions at the surface of a spherical cavity of the radius a are given as follows,

$$\widehat{(rr)}_{r=a} = -P f(t) \sin 2\theta \cos \varphi\,, \quad \widehat{(r\theta)}_{r=a} = \widehat{(r\varphi)}_{r=a} = 0\,,$$

$$\begin{aligned} f(t) &= t/t_m \cdot \exp(1 - t/t_m)\,, \quad \text{for } t \geqq 0\,, \quad t_m : \text{a positive constant,} \\ &= 0 \qquad\qquad\qquad\quad\;\;, \quad \text{for } t < 0\,, \end{aligned}$$

the displacement components are expressed as following;

$$\left.\begin{aligned} \delta_{p,r} &= \sin 2\theta \cos \varphi \frac{1}{r} F_1\left(t - \frac{r-a}{v_p}\right)\,, \\ \delta_{s,\theta} &= \cos 2\theta \cos \varphi \frac{1}{r} F_2\left(t - \frac{r-a}{v_s}\right)\,, \\ \delta_{s,\varphi} &= -\cos \theta \sin \varphi \frac{1}{r} F_2\left(t - \frac{r-a}{v_s}\right)\,. \end{aligned}\right\} \tag{8}$$

And it was shown that each of $\delta_{p,r}$, $\delta_{s,\theta}$ and $\delta_{s,\varphi}$ consists of marked damped oscillation amounting almost to a single to and fro motion, the maximum amplitude of the S waves is in general larger than that of the P waves, and the apparent period of vibration in a state of initial motion of the former is longer than that of the latter. Some of the curves for them are reproduced in Fig. 9. The ratio of the maximum

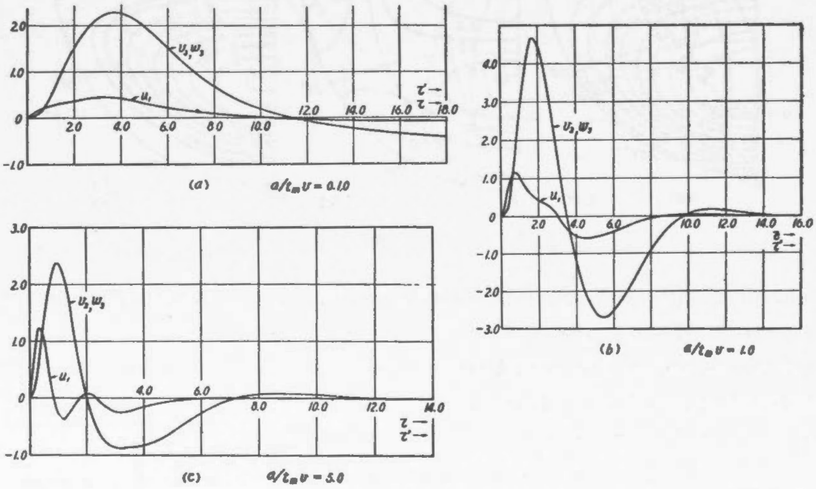

Fig. 9. $u_1 = F_1(\tau)$ and v_3, $w_3 = F_2(\tau')$. $\tau = t-(r-a)/v_p$, $\tau' = t-(r-a)/v_s$, $v = v_p$. (After NISHIMURA *et al.*, 1938.)

amplitude of $\delta_{s,\theta}$ or $\delta_{s,\varphi}$ to that of $\delta_{p,r}$ is shown in Fig. 10; the ratio is maximum amounting to about 5.4 when $a/t_m v_p$ is small being less than unity, and it becomes very small especially when $a/t_m v_p$ exceeds 15.

The problems on the generation of the elastic waves in an infinite elastic solid from the source subjected to various prescribed forces have been investigated also by M. HASEGAWA (1930), H. JEFFREYS (1931), K. SEZAWA and K. KANAI (1932, 36, 41,42), KAWASUMI and R. YOSIYAMA (1935), SEZAWA (1935), G. NISHIMURA (1937),

W. INOUYE (1936,37,38), J.A. SHARPE (1942), BYERLY, A.I. MEI and C. ROMNEY (1949), Y. SATÔ (1949.50), S. HOMMA (1952), J. VANĚK (1953), P.A. HEELAN (1953), T. USAMI and T. HIRONO (1956), Z. DROSTE (1956), and R. TEISSEYRE (1956).

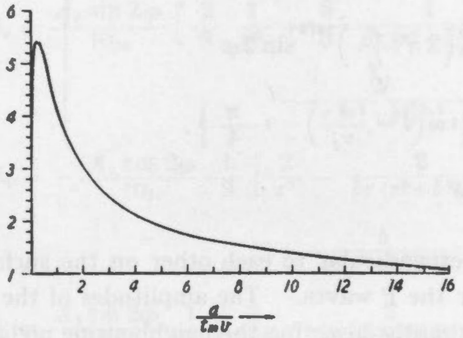

Fig. 10. $V_3, W_3/U_1$. U_1, V_3, W_3; the maximum amplitudes of u_1, v_3, w_3. $v=v_p$. (After NISHIMURA *et al.*, 1938.)

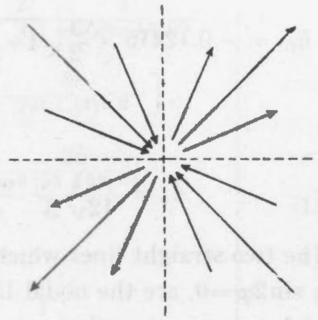

Fig. 11. The radial force proportional to $\sin 2\varphi$.

2-2. Semi-infinite Elastic Solid. The general problem on the disturbances at the surface of a semi-infinite elastic solid, produced by the radial, normal or transverse forces applied at the source region on the surface, was investigated by NAKANO (1,930). Some of the results of his research, which may be useful for the study of the mechanism of very shallow earthquakes, are described here. Take the cylindrical coordinates (r, φ, z) so that the surface of the solid is $z=0$, and the z-axis is directed vertically downward into the solid. The displacement components are denoted by δ_r, δ_φ and δ_z. The periodic radial force $Ar^3 \sin 2\varphi \exp(i\omega t)$, Fig. 11, is assumed to be applied in the domain $r<\bar{r}$ on the surface, where $\bar{r}$ is smaller than the wave length l_p of the P waves. Then the displacement of motion of the surface is represented by the sum of three kinds of displacements which consist of δ_p, δ_s and δ_3 propagated with the velocities v_p, v_s and v_3 (v_3; the velocity of the Rayleigh waves) respectively. For the case $\lambda=\mu$, we have

$$\left.\begin{aligned}
\delta_{p,r} &= 6.9282\, A_1\left(2\pi\frac{r}{l_p}\right)^{-2}\sin 2\varphi \exp\left\{i\omega\left(t-\frac{r}{v_p}\right)\right\},\\
\delta_{p,\varphi} &= O\left(2\pi\frac{r}{l_p}\right)^{-3},\\
\delta_{p,z} &= -2.4494\, A_1\left(2\pi\frac{r}{l_p}\right)^{-2}\sin 2\varphi \exp\left\{i\omega\left(t-\frac{r}{v_p}\right)\right\},
\end{aligned}\right\} \qquad (9)$$

$$\left.\begin{aligned}
\delta_{s,r} &= O\left(2\pi\frac{r}{l_p}\right)^{-2},\\
\delta_{s,\varphi} &= -0.2887\times 3^{1/2} A_1\left(2\pi\frac{r}{l_p}\right)^{-1}\cos 2\varphi \exp\left\{i\omega\left(t-\frac{r}{v_s}\right)-i\frac{\pi}{2}\right\},\\
\delta_{s,z} &= O\left(2\pi\frac{r}{l_p}\right)^{-2},
\end{aligned}\right\} \qquad (10)$$

$$\delta_{3,r} = 0.08459\times\frac{3}{2}\sqrt{1+\frac{1}{\sqrt{3}}}\, A_1\left(2\pi\frac{r}{l_p}\right)^{-1/2}\sin 2\varphi\times$$

$$\times \exp\left\{i\omega\left(t-\frac{r}{v_s}\right)+i\frac{\pi}{4}\right\},$$

$$\delta_{s,\varphi}=O\left(2\pi\frac{r}{l_p}\right)^{-3/2}, \tag{11}$$

$$\delta_{s,z}=-0.12415\times\frac{3}{2}\sqrt{1+\frac{1}{\sqrt{3}}}A_1\left(2\pi\frac{r}{l_p}\right)^{-1/2}\sin 2\varphi$$

$$\times \exp\left\{i\omega\left(t-\frac{r}{v_s}\right)-i\frac{\pi}{4}\right\},$$

$$A_1=\frac{1}{12\sqrt{3}}\frac{\omega^2\rho}{\mu^2}A\bar{r}^6.$$

The two straight lines which are perpendicular to each other on the surface for which $\sin 2\varphi=0$, are the nodal lines for the P waves. The amplitudes of the P and Rayleigh waves are maximum in the azimuths bisecting the neighbouring nodal lines, whereas that of the S waves is maximum in the azimuths along the nodal lines.

HIRONO (1948, 49) investigated theoretically the propagation of the elastic waves in a semi-infinite elastic solid, which are produced from the source on the surface of the solid. When the radial force $\Pi_2(r)\cos 2\varphi\exp(i\omega t)$ is assumed to act in the region within a small circle of radius r_0 ($r_0 \ll l_p$) on the surface, the displacement component δ_R along the direction of R ($R=\sqrt{r^2+z^2}$), δ_θ along that of θ ($\tan\theta=r/z$), and δ_φ are given as following;

$$\delta_{p,R}=-2A_2\frac{\cos\theta\sin^2\theta\sqrt{n^2-\sin^2\theta}}{D(\cos\theta)}\cos 2\varphi$$

$$\times\frac{1}{kR}\exp\left\{i\omega\left(t-\frac{R}{v_p}\right)\right\},$$

$$\delta_{s,\theta}=-n^2A_2\frac{\cos\theta\sin\theta(2\cos^2\theta-1)}{E(\cos\theta)}\cos 2\varphi \tag{12}$$

$$\times\frac{1}{kR}\exp\left\{i\omega\left(t-\frac{R}{v_s}\right)\right\},$$

$$\delta_{s,\varphi}=n^2A_2\sin\theta\sin 2\varphi\frac{1}{kR}\exp\left\{i\omega\left(t-\frac{R}{v_s}\right)\right\},$$

$$D(\cos\theta)=(n^2-2\sin^2\theta)^2+4\cos\theta\sin^2\theta\sqrt{n^2-\sin^2\theta},$$

$$E(\cos\theta)=(2\sin^2\theta-1)^2+4\cos\theta\sin^2\theta\sqrt{1/n^2-\sin^2\theta},$$

$$A_2=-\frac{h^2}{\mu}\frac{i}{4}\int_0^{r_0}\Pi_2(r)r^2dr, \quad n=\sqrt{\frac{\lambda+2\mu}{\mu}}.$$

The dip angular distribution of $P=\delta_{p,r}$, $S_1=-\delta_{s,\theta}$ and $S_2=\delta_{s,\varphi}$, Fig. 12, are shown in Fig. 13 for the case $\lambda=\mu$. The cases in which the applied forces are not periodic but aperiodic of shock type, were studied also by HIRONO.

The deformation of a semi-infinite elastic solid by the statical force applied at the surface of it, was investigated by HONDA and MIURA (1935). The problem may be related to the study of the deformation of the earth's surface which is sometimes observed in severe very shallow earthquakes. When the radial statical force $F_r=$

$A_2\{r^3/(r^2+b^2)^{7/2}\}\sin 2\varphi$ is assumed to act on the surface, the displacement components δ_r, δ_φ and δ_z of the statical deformation at the surface, are expressed as following for the case $\lambda=\mu$;

$$\left.\begin{aligned}
\delta_r &= \frac{A_2 \sin 2\varphi}{10\mu}\Big[\frac{2}{3}\frac{1}{r^2}+\frac{5}{3}\frac{1}{br\,(r^2+b^2)^{1/2}}-\frac{2}{3}\frac{1}{r^2\,(r^2+b^2)^{1/2}} \\
&\qquad -\frac{2b}{r\,(r^2+b^2)^{3/2}}-\frac{3}{2}\frac{br}{(r^2+b^2)^{5/2}}\Big], \\
\delta_\varphi &= -\frac{A_2 \cos 2\varphi}{10\mu}\frac{1}{3}\Big[\frac{2}{r^2}-\frac{2}{br\,(r^2+b^2)^{1/2}}-\frac{2b}{r^2\,(r^2+b^2)^{1/2}} \\
&\qquad +\frac{b}{r\,(r^2+b^2)^{3/2}}\Big], \\
\delta_z &= \frac{A_2 \sin 2\varphi}{10\mu}\frac{1}{3}\Big[\frac{2}{br^2}-\frac{2}{r^2\,(r^2+b^2)^{1/2}}-\frac{1}{(r^2+b^2)^{3/2}} \\
&\qquad -\frac{3}{2}\frac{r^2}{(r^2+b^2)^{5/2}}\Big].
\end{aligned}\right\} \quad (13)$$

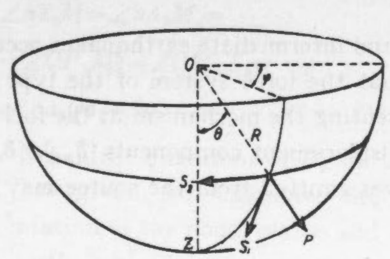

Fig. 12. The direction of motion of $P=\delta_{p,r}$, $S_1=-\delta_{s,\theta}$ and $S_2=\delta_{s,\varphi}$. (After HIRONO, 1948.)

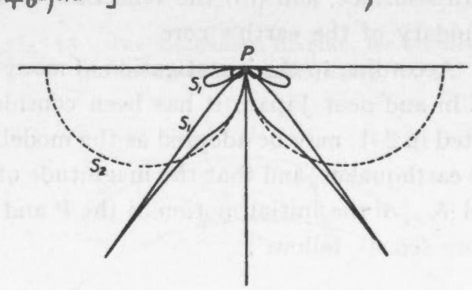

Fig. 13. The dip angular distribution of the body waves P, S_1 and S_2. (After HIRONO, 1948.)

The horizontal displacements at the surface are shown by the arrows in Fig. 14, b being assumed to be 10, where the shaded area means that the region is elevated slightly.

The problem on the deformation of the surface of a semi-infinite elastic solid, produced by a statical source lying beneath the surface of the solid, was investigated by F. J. W. WHIPPLE (1936), K. SOEDA (1944), and N. YAMAKAWA (1955).

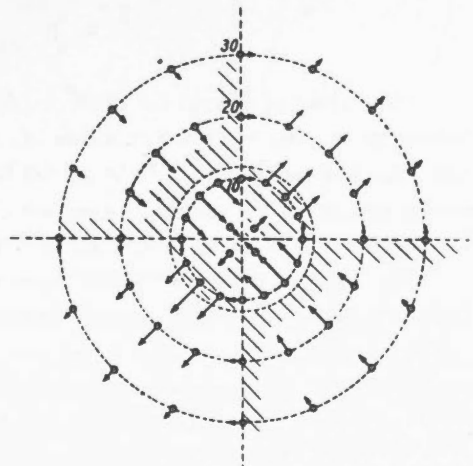

Fig. 14. Statical deformation of the surface.[55]

3 Investigation of Earthquake Mechanism based on the Observations at Near Stations

3-1. Mechanism of Deep and Intermediate Earthquakes.

3–1a. *Theories.* The investigation of the mechanism of the earthquakes in Japan, has been much facilitated by the use of the observations made at the seismological stations, which are equipped with the seismographs of the same type and distributed very closely. Some of the results of the studies on the mechanism of the deep and intermediate earthquakes, carried out in this country, are described in the present chapter.

In order to compute theoretically the motion at the earth's surface which are caused by the incident direct waves or the waves, reflected once at the earth's surface or the outer boundary of the earth's core, such as P, S, pP and ScS, we must take into account, (i) the mechanism of the generation of the seismic waves at the focus of the earthquake, (ii) the variation of the velocity of the waves with the depth from the earth's surface, and (iii) the reflection of the waves at the earth's surface or at the boundary of the earth's core

According to the investigation of many deep and intermediate earthquakes occurred in and near Japan, it has been considered that the force system of the type II stated in 2–1, may be adopted as the model representing the mechanism at the foci of the earthquakes, and that the magnitude of the displacement components $[\delta_{p,r}]$, $[\delta_{s,\theta}]$ and $[\delta_{s,\varphi}]$ of the initial motion of the P and S waves emitted from the source may be expressed as follows ;

$$\left.\begin{aligned} [\delta_{p,r}] &= A_p \frac{1}{r} \sin 2\theta \cos\varphi , \\ [\delta_{s,\theta}] &= A_s \frac{1}{r} \cos 2\theta \cos\varphi , \\ [\delta_{s,\varphi}] &= -A_s \frac{1}{r} \cos\theta \sin\varphi .. \end{aligned}\right\} \quad (14)$$

The values of A_p and the ratio A_s/A_p depend on the magnitude of the earthquake. When the values of the constants A_p and A_s and the orientation of the axes of the spherical coordinates of the model sphere are given, then the amplitudes of the initial motion of the seismic waves which are emitted in any direction θ, φ from the focus can be calculated by the use of the formulae (14).

Fig. 15 illustrates the model sphere of the earthquake mechanism, when it is viewed from the vertically upward direction u. We will call the projected figure the *mechanism diagram*. P_1 and T_1 on the sphere represent the directions of the maximum pressure and tension. Great circles n_1Qn_1' and n_2Qn_2' are the nodal planes for the P waves, and the hatched part and the blank part correspond to the directions in which the initial motions of the P waves are condensational and rarefactional respectively. The points of intersection of the great circle passing through P_1 and T_1, with n_1Qn_1' and n_2Qn_2' are denoted by M_1 and M_2. M_1 corresponds to the y-axis, M_2 to the x-axis, and Q to the z-axis in Fig. 4. If ua_1 and ua_2 are the arcs of the great circles which are perpendicular to n_1Qn_1' and n_2Qn_2' respectively, the directions of ua_1 and ua_2 are the dip directions, and ua_1 and ua_2 are the inclinations, and $90°-ua_1$ and $90°-ua_2$ are the dips of the nodal planes. The directions of n_1n_1' and n_2n_2' are the strikes of the planes. Obviously there hold following relations;

$P_1M_1=M_1T_1=T_1M_2=\cdots=45°,$

$QP_1=QM_1=QT_1=QM_2=\cdot=90°,$

$\angle a_1uM_2=\angle a_2uM_1=\cdots=180°,$

$a_2M_1=a_1M_2=\cdots\cdots\cdots=90°,$

$\angle ua_1M=\angle ua_2M_2=\cdots\cdots$

$=\angle QP_1M_1=\angle QM_1T_1=\cdots$

$=\angle a_1Qa_2=90°.$

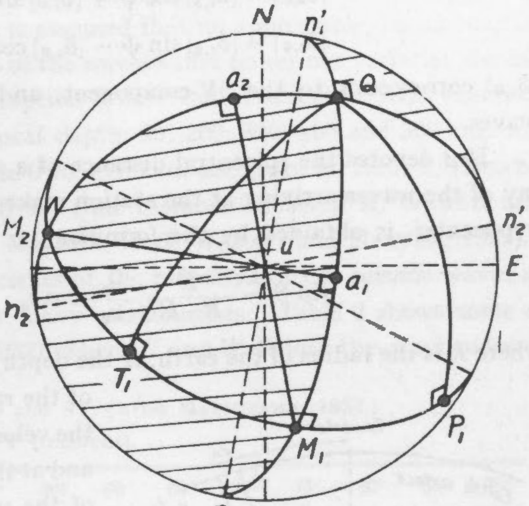

Fig. 15. The mechanism diagram for the deep and intermediate earthquakes.[65]

When the directions of P_1 and T_1 are given for example, the orientation of the nodal planes and so forth, are obtained by the use of the formulae of spherical trigonometry.

We denote by B a point on the mechanism diagram, corresponding to the direction of the seismic ray which makes the angle Θ with the vertical drawn upward at the hypocenter, and lies in the vertical plane directed in the azimuth Φ, being measured from the vertical plane passing through uM_1 (Fig. 16). Let $\alpha=uM_1$, $\beta=\angle uM_1a_1$, then from the formulae

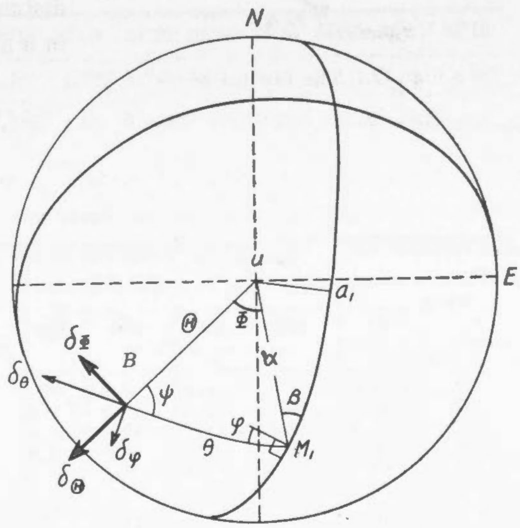

Fig. 16. Illustration of the direction of motion on the mechanism diagram.

$$\left.\begin{aligned}\cos\theta &= \cos\Theta\cos\alpha+\sin\Theta\sin\alpha\cos\Phi\,,\\ \frac{\sin\Phi}{\sin\beta} &= \frac{\sin\left(\frac{\pi}{2}-\beta+\varphi\right)}{\sin\Theta}=\frac{\sin\psi}{\sin\alpha}\,,\quad \psi=\angle uBM_1,\end{aligned}\right\} \qquad (15)$$

we can obtain the relations between (Θ,Φ) and (θ,φ,ψ). The Θ, Φ-components of displacement of the initial motion of the S waves, are

$$\left.\begin{aligned} [\delta_{s,\Theta}] &= [\delta_{s,\theta}] \cos \psi + [\delta_{s,\varphi}] \sin \psi \,, \\ [\delta_{s,\Phi}] &= [\delta_{s,\theta}] \sin \psi - [\delta_{s,\varphi}] \cos \psi \,. \end{aligned}\right\} \tag{16}$$

$[\delta_{s,\Theta}]$ corresponds to the SV-component, and $[\delta_{s,\Phi}]$ to the SH-component of the S waves.

If Δ denotes the epicentral distance of a station, the angle Θ which the seismic ray of the waves arriving at the station makes with the vertical drawn upward at the hypocenter, is obtained by the formulae ;

$$\sin \Theta = \frac{R}{R-H} \frac{v_h}{v_0} \cos e_0 \,; \qquad \cos e_0 = v_0 \frac{dT}{d\Delta} \,, \tag{17}$$

where R is the radius of the earth, H the depth of the focus, e_0 the angle of emergence of the ray at the earth's surface, and v_0 and v_h the velocities of the waves at the earth's surface and at the focus (Fig. 17). T is the travel time of the waves which arrive at the station.

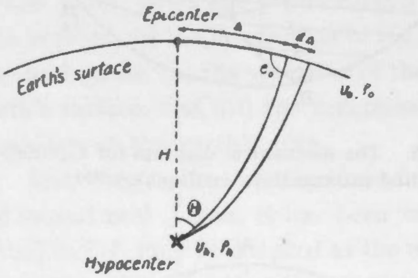

Fig. 17. The ray for P.

The distance factor f which represents the diminution of the amplitude of the seismic waves traveling along curved path with the distance from the hypocenter, instead of $1/r$ in a homogeneous medium, can be expressed as

$$f = \sqrt{\frac{\rho_h v_h}{\rho_0 v_0}} \sqrt{\frac{\sin \Theta}{R \sin \frac{\Delta}{R} \sin e_0} \frac{d\Theta}{d\Delta}} \,, \tag{18}$$

Table 1. Θ and f.

	$\Theta°$ (63)						f (10^{-3}km^{-1}) (60)				
Hkm / Δkm	80	200	320	400	500	Hkm / Δkm	80	200	320	400	500
20	17.0	7.4	4.6	3.8	3.2	20	1.98	0.934	0.836	0.541	0.458
50	36.2	16.6	10.8	9.0	7.5	50	1.62	842	702	497	432
100	60.0	29.0	19.8	16.9	14.3	100	1.23	678	580	455	405
200	78.0	48.5	34.9	30.0	26.0	200	0.426	448	425	390	361
300	86.0	61.5	47.1	41.3	36.4	300	293	343	347	338	325
400	90.6	70.0	57.0	50.8	45.6	400	219	276	287	294	293
500	94.9	75.7	64.5	59.4	54.1	500	162	225	243	259	263
600	96.2	80.8	71.1	66.6	61.7	600	121	193	211	224	237
700	97.7	83.2	77.0	72.3	68.6	700	92	170	187	175	212
800	98.7	89.0	82.1	77.1	74.4	800	75	152	160	141	189
900	99.6	92.7	86.8	81.2	79.2	900	68	137	155	134	165
1000	100.7	96.1	90.0	84.8	82.9	1000	78	126	144	144	128
1200	104.5	102.4	98.0	94.8	89.0	1200	93	109	128	152	143
1400	109.7	108.6	106.3	103.9	98.5	1400	90	101	117	112	123
1600	114.8	114.4	113.0	110.6	104.9	1600	82	85	93	89	95
1800	119.9	119.5	118.7	115.4	109.7	1800	76	73	77	75	79
2000	124.8	123.9	123.0	119.3	113.5	2000	69	62	62	62	64
2400	132.8	130.6	128.8	125.0	118.7	2400	46	46	44	46	47
2800	137.4	135.2	133.0	129.1	122.4	2800	34	36	34	37	38
3200	140.6	139.0	136.1	132.2	125.5	3200	23	27	28	29	32
3600	142.2	141.4	138.4	134.5	127.9	3600	16	20	23	24	26
4000	144.0	142.8	139.8	136.1	129.8	4000	12	14	18	17	24

where ρ_0 and ρ_h are the densities of the earth's crust at the earth's surface and at the focus respectively. In deriving (18), it is assumed that no appreciable discontinuities exist in the earth, and that the periods of the waves suffer no serious variation during the propagation, and the effect of absorption is left out of account. The values of f calculated for the P waves, for the focal depth; 80, 200, 320, 400 and 500 km, and for the epicentral distance varying from 0 to 4,000 km are given in Table 1, (HONDA and H. ITÔ, 1951), which are based on the time distance tables of K. WADATI and others (WADATI, K. SAGISAKA, and K. MASUDA, 1933, WADATI and MASUDA, 1933).

The numerical values of the coefficients of the reflection of the seismic waves at the earth's surface have been given by many seismologists. Table 2 shows some of the results obtained by MATSUZAWA (1932), where U and W denote the amplitudes of

Table 2. Reflection of P and SV. (After MATSUZAWA, 1932,)

(a) P (incident).

i	0°	5°	10°	20°	30°	40°	50°	60°	65°	70°	75°	80°	85°	90°
U_p	0	.201	.400	.780	1.120	1.382	1.617	1.732	1.743	1.717	1.608	1.405	.971	0
W_p	2	1.990	1.963	1.858	1.692	1.479	1.241	1.00	.885	.771	.658	.530	.349	0

(b) SV (incident).

i	0°	2°35′	5°45′	11°23′	16°43′	21°47′	26°15′	30°00′	31°33′	32°52′	33°54′	34°40′	35°07′	35°16′
U_s	2	1.9965	1.981	1.937	1.869	1.789	1.730	1.732	1.787	1.901	2.12	2.511	3.28	4.899
W_s	0	.1160	.2302	.4503	.6443	.8124	.9325	1.00	1.0065	.9883	.9316	.8110	.5620	0

the horizontal and vertical components of displacement of the earth's surface, when the P or SV waves of unit amplitude of displacement are incident, the angle of incidence being i. The Poisson's ratio of the medium is assumed to be 1/4. The relative am-

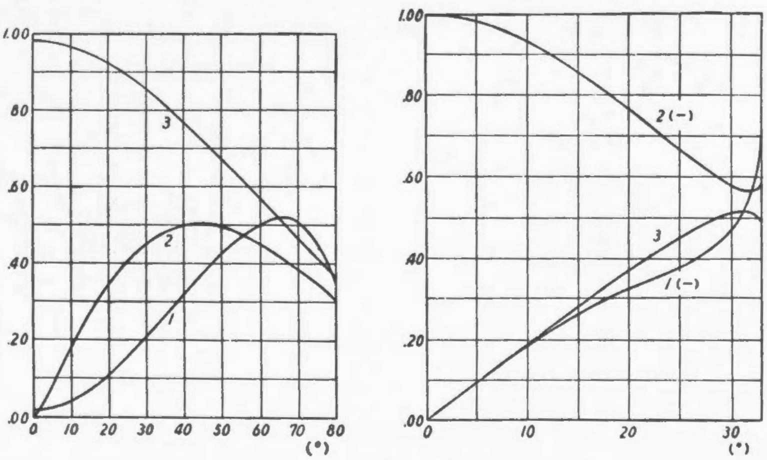

(a) P (incident). (b) SV (incident).

Fig. 18. The relative amplitudes of the reflected P (1), reflected SV (2) and refracted P (3), when P (a) or SV (b) in the mantle is incident against the core.[60]

plitudes of the waves reflected or refracted at the surface of the earth's core, to those of P and S waves incident from the mantle, are illustrated in Fig. 18 (HONDA and ITÔ, 1951). The density of the mantle outside the core is taken as 6.0 g/c.c. and that of the core just within the boundary as 9.5 g/c.c. The velocities of the P and S waves in the mantle are taken as 13.0 and 7.25 km/sec respectively. The velocity of the P waves within the boundary of the core is taken as 8.5 km/sec, and that of the S waves as zero or the core is assumed to be liquid.

The initial motions of the P and S waves to be observed at the earth's surface can be calculated theoretically, being based on the theories and relations stated above. As an example of very simple cases, we will consider at first the case in which the polar axis of the model sphere representing the mechanism of the earthquake, is directed vertically upward. One of the nodal planes for the P waves is directed vertically and the other horizontally. Let us assume that the ray emitted in the direction (θ,φ) from the focus, arrives at the point of the earth's surface whose epicentral distance is Δ, and the azimuth to the epicenter is Φ. We can take $\Theta=\theta$ and $\Phi=\varphi$ in this case. The amplitude $[P]$ of the initial motion of the P waves at the earth's surface is expressed by

$$[P] = 2 f A_p \sin 2\theta \cos\varphi \,, \tag{19}$$

as it is practically twice that of the incident P waves.

The Δ and Φ-components, $[S]_\Delta$ and $[S]_\Phi$, of the horizontal motion of the earth's surface due to the incident S waves, are

$$\left.\begin{aligned} [S]_\Delta &= U_s f A_s \cos 2\theta \cos\varphi \,, \\ [S]_\Phi &= -2 f A_s \cos\theta \sin\varphi \,. \end{aligned}\right\} \tag{20}$$

The amplitude of the horizontal motion of the earth's surface due to the incident SH waves is just twice that of the incident ones. In Fig. 19 (a), are shown the

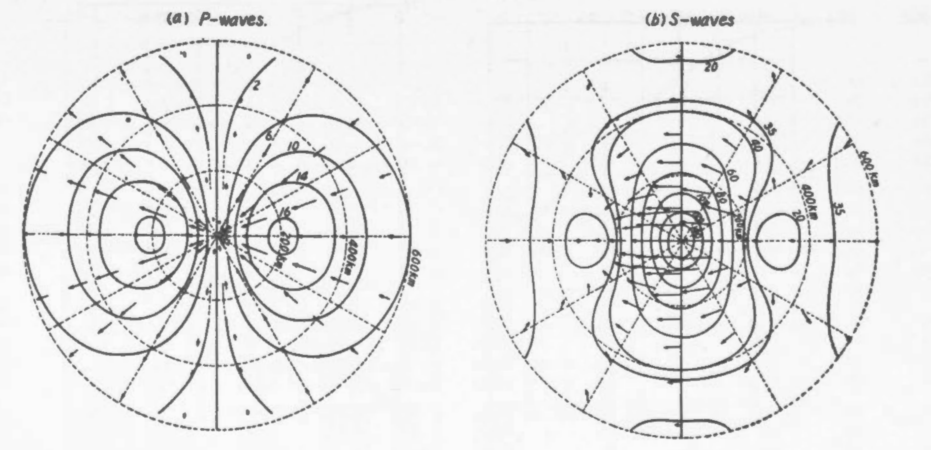

Fig. 19. The initial motions of P and S at the earth's surface for a special case.[51]

direction and magnitude of the initial motion of the P waves at the earth's surface, and in Fig. 19 (b) those of the horizontal components of the initial motion of the S waves, in the region within 600 km from the epicenter for the earthquake whose focal depth is 300 km. The ratio A_s/A_p is assumed to be 5.20 in the example.

Next, we will treat the general case in which the polar axis of the model sphere is directed in any direction. Let Φ be the azimuth of a point of the earth's surface to the epicenter measured from a certain direction, and Θ and Δ be the same as in foregoing example. The amplitude of the intial motion of the P waves at the earth's surface can be calculated by the use of apparently the same formula as (19). The horizontal components of the initial motion of the S waves are given by

$$\left.\begin{aligned} [S]_\Delta &= U_s f[\delta_{s,\Theta}] , \\ [S]_\Phi &= 2f\,[\delta_{s,\Phi}] . \end{aligned}\right\} \qquad (21)$$

The initial motion of the ScS waves at the earth's surface near the epicenter, can be also calculated theoretically. If the ray of the S waves emitted almost vertically downward from the hypocenter makes the angle e_c with the surface of the earth's core, and r_c is the radius of the core,

$$\cos e_c = \frac{R}{r_c}\frac{v_c}{v_0}\cos e_0 , \qquad (22)$$

where v_0 and v_c are the velocities of the S waves at the earth's surface and just outside the core (Fig. 20). The angles $i_h=180° -\Theta'$ and $i_c=90°-e_c$ as are shown in the figure, and the distance factor f_{ScS} for the ScS waves are calculated (e.g. HONDA and ITÔ, 1951) by the use of the time-distance tables of WADATI and MASUDA (1934). When we assume that the earth's core is liquid, the δ_Φ component of the S waves is reflected totally at the core, and the ratio q of the amplitude of the reflected S waves to that of $\delta_{s,\Theta}'$ (SV waves) incident at the core can be obtained from Fig. 18(b). The radial and transverse components $[ScS]_\Delta$ and $[ScS]_\Phi$ of the horizontal components of the initial motion of the ScS waves to be observed at the earth's surface near the epicenter, are given by

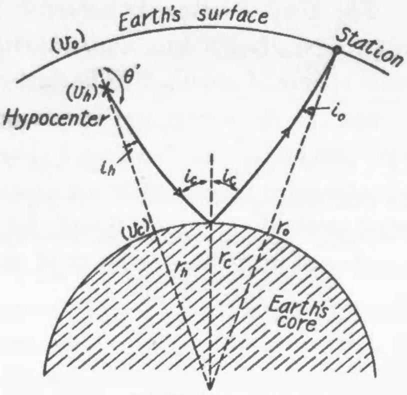

Fig. 20. The ray for ScS.

$$\left.\begin{aligned} [ScS]_\Delta &= -\,U_s\, q f_{ScS}[\delta_{s,\Theta'}] , \\ [ScS]_\Phi &= 2f_{ScS}[\delta_{s,\Phi}] . \end{aligned}\right\} \qquad (23)$$

3–1b. *Examples.* Some examples of the results of the investigation of the mechanism of the deep earthquakes occurred in Japan, are given below.

The Deep Earthquake occurred on June 2, 1929, *near Shima Peninsula.* The epicenter lies at $\lambda=137°.2$E, $\varphi=34°.3$N, and the focal depth $H=320$ km. The polar axis of the nodal sphere representing the mechanism of the earthquake, is considered to be inclined by 13° in the direction N98°E from the epicenter, and one of the nodal planes for the P waves strikes to N 8°E. The direction and magnitude of the initial motion of the P waves and those of the horizontal components of the S waves, are illustrated in Fig. 21, where the observed values are shown by the arrows of thick lines, and the

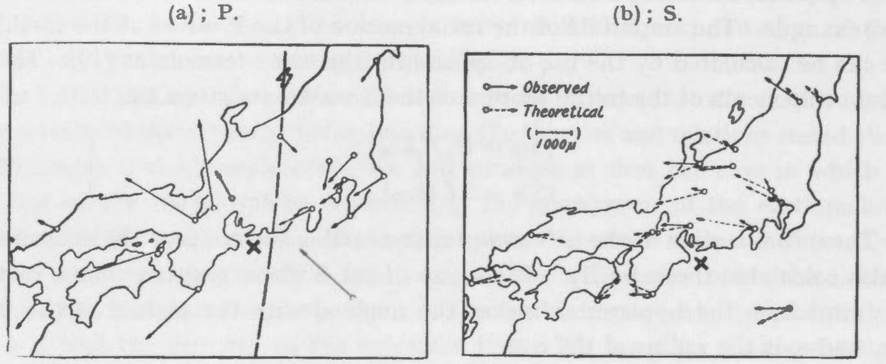

Fig. 21. The deep earthquake occurred on June 2, 1929, near Shima Peninsula.[51].
(a) The initial motion of P. (b) The horizontal component of the initial motion of S.

theoretically expected values by the arrows of dotted lines. A_p and A_s are assumed to be $A_p=4.94\times 10^5$ cm², $A_s=14.1\times 10^5$ cm². (HONDA, 1934. HONDA *et al.*, 1938.)

The Deep Earthquake occurred on Feb. 20, 1931, *near Vladivostok.* $\lambda=135.°7$ E, $\varphi=44°.5$ N, $H=320$ km, $A_p=18\times 10^5$ cm², $A_s=14\times 10^5$ cm². The polar axis of the model sphere is assumed to be inclined by 50° in the vertical plane N79° E passing through the epicenter, and the same vertical plane is considered to be one of the nodal planes for the P waves. The initial motions of the P and S waves observed and calculated theoretically are given in Fig. 22. The direction and magnitude of the initial motions of P, pP, S and ScS calculated theoretically for Stuttgart ($\Delta=76°$), being based on the assumption of the mechanism of the earthquake, are illustrated

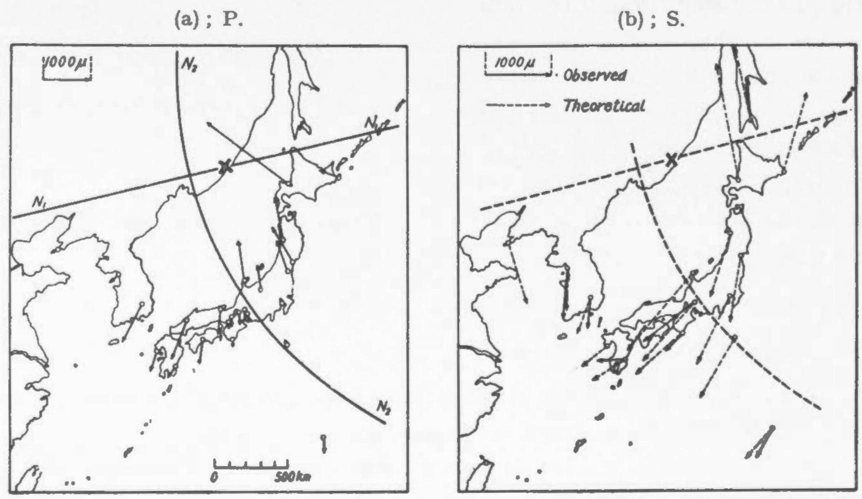

Fig. 22. The horizontal component of the initial motion of P (a) and S (b) for the deep earthquake occurred on Feb. 20, 1931, near Vladivostok.[60]

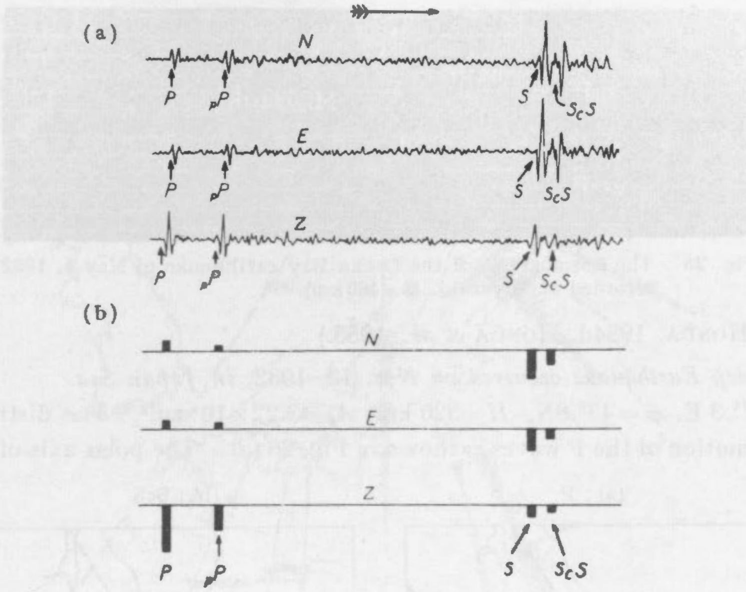

Fig. 23. The seismograms recorded at Stuttgart (a), and the initial motions of P, pP, S and ScS calculated theoretically (b), for the earthquake of Feb. 20, 1931.[60]

schematically together with the seismograms of these waves recorded at Stuttgart, in Fig. 23. (HONDA and ITÔ, 1951.)

The Deep Earthquake occurred on May 5, 1932, in Osaka Bay.

$\lambda=135°.4$ E, $\varphi=34°.6$ N, $H=360$ km, $A_p=5.92\times10^4$ cm,[2] ($A_s=5.20\times A_p$). The polar axis of the model sphere is considered to be directed vertically upward, and one of the nodal planes to be the vertical plane directed to N 35° W through the epicenter. The pattern of the condensation and rarefaction of the initial motion of the P waves, and the direction and magnitude of the horizontal component of the initial motion of the S waves observed and calculated theoretically, are illustrated in Fig. 24. The seismograms of the earthquake recorded at Miyazaki ($\Delta=480$ km) are shown in

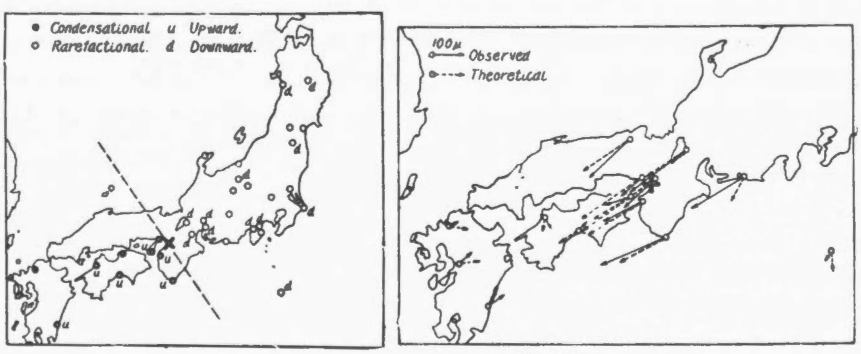

Fig. 24. The deep earthquake occurred on May 5, 1932, in Osaka Bay.[54],[64] (a); The initial motion of P. (b); The horizontal component of the initial motion of S.

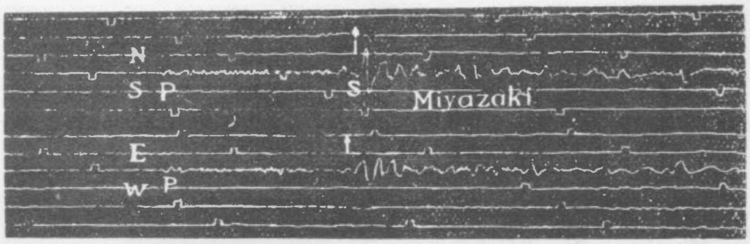

Fig. 25. The seismograms of the Osaka Bay earthquake of May 5, 1932, recorded at Miyazaki. (Δ=480 km).(54)

Fig. 25. (HONDA, 1934d. HONDA *et al.*, 1955.)

The Deep Earthquake occurred on Nov. 13, 1932, *in Japan Sea.*

$\lambda=137°.3$ E, $\varphi=43°.6$N, $H=320$ km, $A_p=3.22\times10^6$ cm^2. The distribution of the initial motion of the P waves is shown in Fig. 26 (a). The polar axis of the model

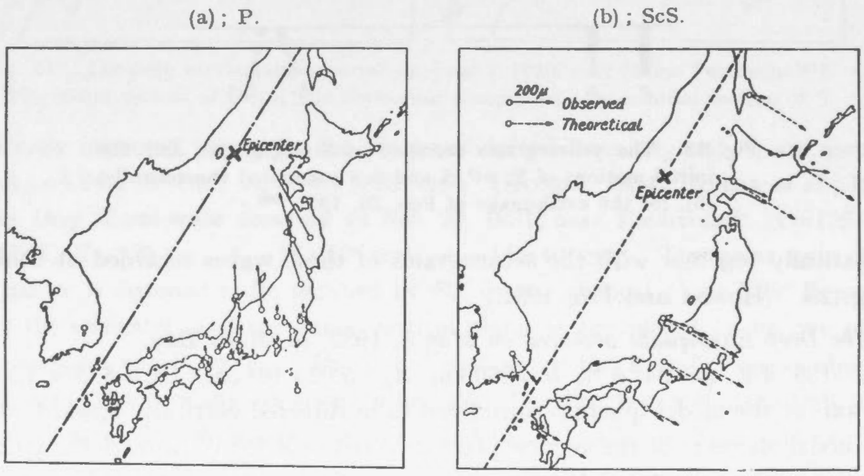

Fig. 26. The deep earthquake occurred on Nov. 13, 1932, in Japan Sea.(52),(64) (a); The initial motion of P. (b); The horizontal component of the initial motion of ScS.

sphere is considered to be directed vertically upward, and one of the nodal planes to be vertical plane directed to N 35°E passing through the epicenter. The observed horizontal components of the initial motion of the ScS waves, and those calculated theoretically from the assumption that the core is liquid and $A_s=5.20\times A_p$ provisionally, are illustrated in Fig 26 (b). As the observed amplitudes of the ScS waves are about half of those expected theoretically, A_s should be supposed to be about 2.6 A_p instead of 5.20 A_p. The seismograms recorded at some stations in this country are shown on a map in Fig. 27, to illustrate the regular distribution of the various types of the seismograms especially as to the relative amplitudes of the P and S waves, which is consistent with that expected theoretically. The seismograms including the ScS waves recorded at Siomisaki is shown in Fig. 28. (HONDA, 1933, 34b, HONDA *et al.*, 1955.)

The Deep Earthquake occurred on Dec. 1, 1936, *near the Island Yaku.*

$\lambda=129°.0$E, $\varphi=30°.7$ N, $H=270$ Km, $A_p=2.6\times10^5$ cm^2. The initial motions of the P waves are shown in Fig. 29 (a). The polar axis of the model sphere is con-

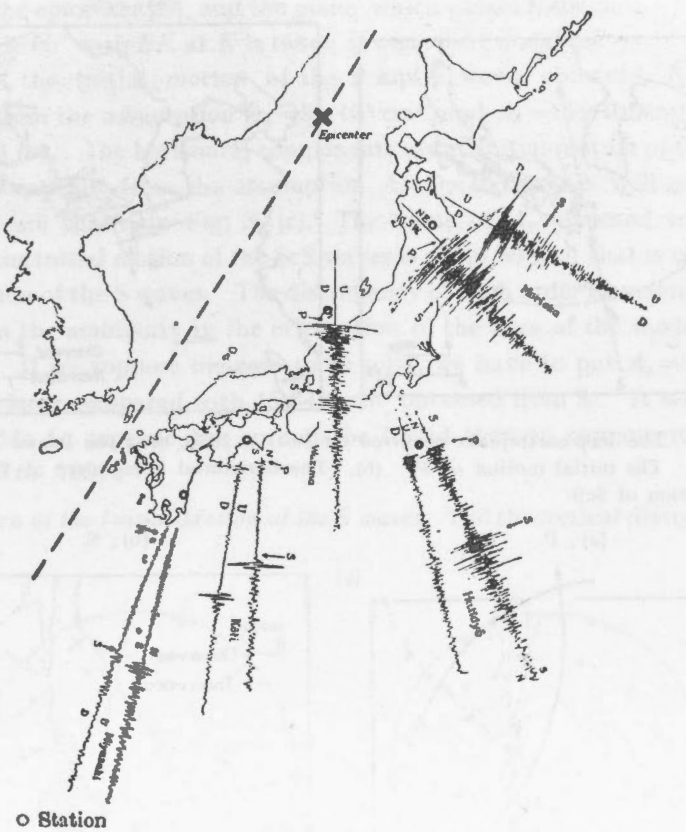

Fig. 27. The seismograms of the Japan Sea earthquake of Nov 13, 1932, recorded at some stations in Japan.[50]

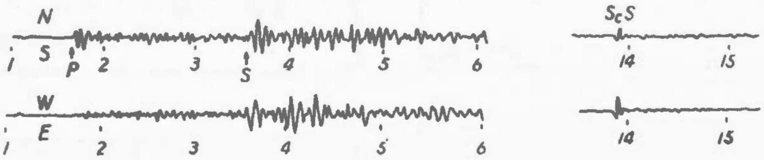

Fig. 28. The seismograms of the Japan Sea earthquake of Nov. 13, 1932, recorded at Siomisaki. (Δ=1,124 km).[52]

sidered to be inclined by 30° in the vertical plane striking N 10°E from the epicenter, which is taken to be one of the nodal planes. The horizontal components of the initial motion of the ScS waves observed, and those calculated theoretically based on the assumption that the core is liquid and $A_s=3.5\times10^5$ cm², are illustrated in Fig. 29 (b). (HONDA and Y. HASAYA, 1940.)

The Deep Earthquake occurred on Apr. 21, 1939, *in Japan Sea.*

$\lambda=140°.2$E, $\varphi=47°.6$N, $H=530$ km, $A_p=5\times10^5$ cm², $A_s=15\times10^5$ cm². The polar axis (K) of the model sphere is considered to be inclined by 60° in the direction

(a) ; P. (b) ; ScS.

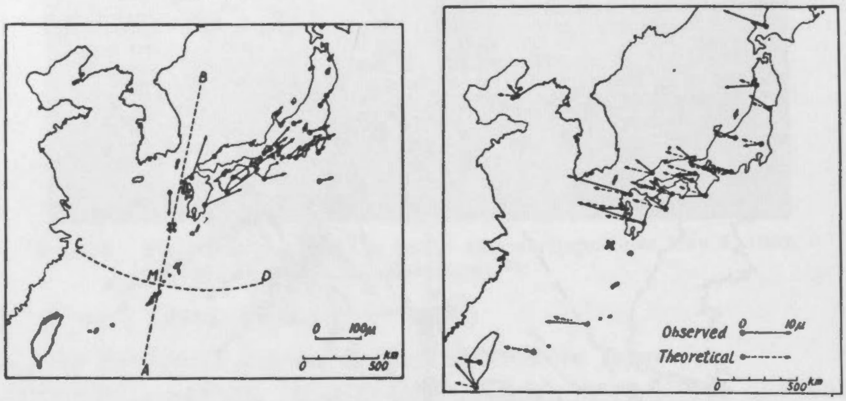

Fig. 29. The deep earthquake occurred on Dec. 1, 1936, near the Island Yaku.[58] (a). The initial motion of P. (b). The horizontal component of the initial motion of ScS.

(a) ; P.

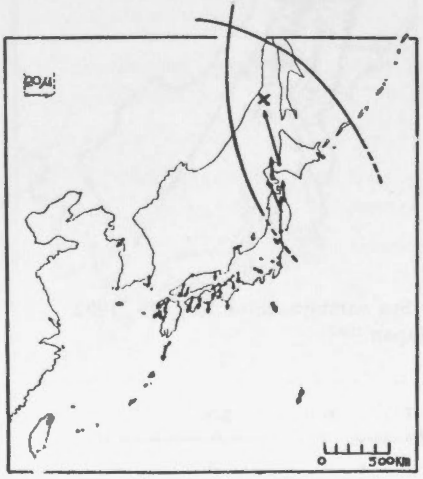

(b) ; S.

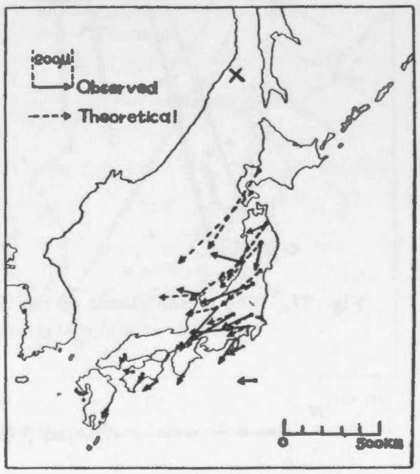

(c) ; ScS.

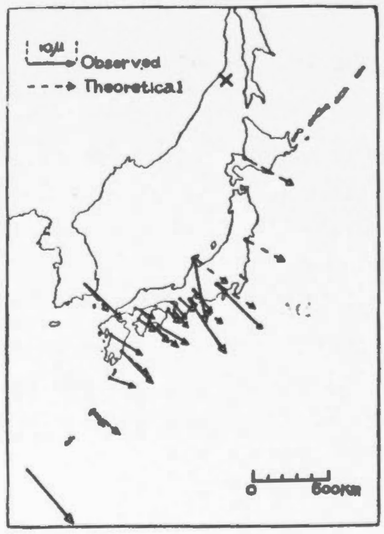

Fig. 30. The horizontal components of the initial motion of P (a), S (b) and ScS (c), of the deep earthquake occurred on Apr. 21, 1939, in Japan Sea.[60]

N 88°E from the epicenter (E), and the plane which passes through the polar axis and makes the angle 60° with EK at K is taken as one of the nodal planes. The horizontal components of the initial motion of the P and S waves observed, and calculated theoretically from the assumption $A_p=5\times10^5$ cm^2, and $A_s=15\times10^5$ cm^2 are shown in Fig. 30 (a) and (b). The horizontal components of the initial motion of the ScS waves calculated theoretically from the assumption $A_s=9\times10^5$ cm^2, as well as those actually observed are shown in Fig. 30 (c). The value of A_s supposed to explain the amplitude of the initial motion of the ScS waves is about 60% of that is obtained from the investigation of the S waves. The discrepancy of such order of magnitude may be produced from the ambiguity in the orientation of the axes of the model sphere and other causes. If we suppose the core to be solid, we have to put $A_s=180\times10^5$ cm^2, which is very large compared with 15×10^5 cm^2 obtained from S. It seems to be far more reasonable to suppose the core to be liquid than to suppose it to be solid. (HONDA and ITÔ, 1951.)

Illustration of the Initial Motion of the S waves. The theoretical distribution of the

(a)

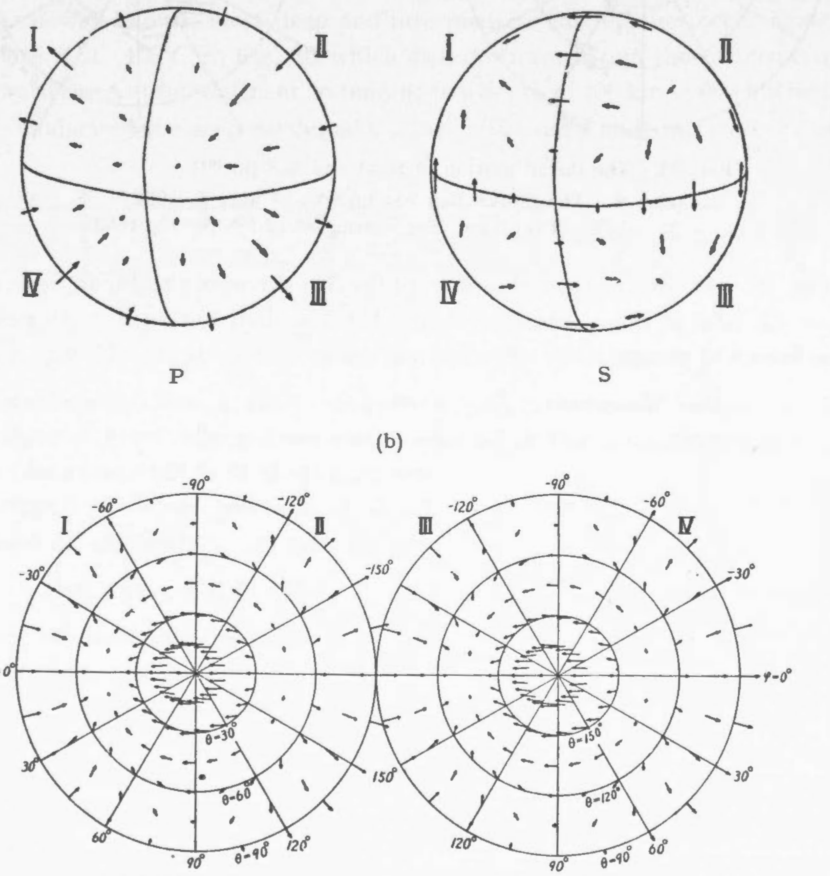

(b)

Fig. 31. (a). The initial motions of P and S on a sphere constructed around the focus.[64]
(b). The illustration of the initial motion of S.[64]

direction and magnitude of the initial motion of the P and S waves on a sphere which is constructed around the hypocenter and includes the model sphere in it, is illustrated schematically also in Fig. 31 (a). If the sphere is divided into two parts by one of the nodal planes for the P waves and are represented on one plane as is shown in Fig. 31 (b,) the distribution of the initial motion of the S waves can be represented by the arrows in the figure. I,II,III and IV show the corresponding quadrants in Fig. 31 (a) and (b) to each other. Fig. 32 (a) shows the direction of the initial motion of the S waves of the Osaka Bay earthquake of May 5, 1932 in the quadrants I and II,

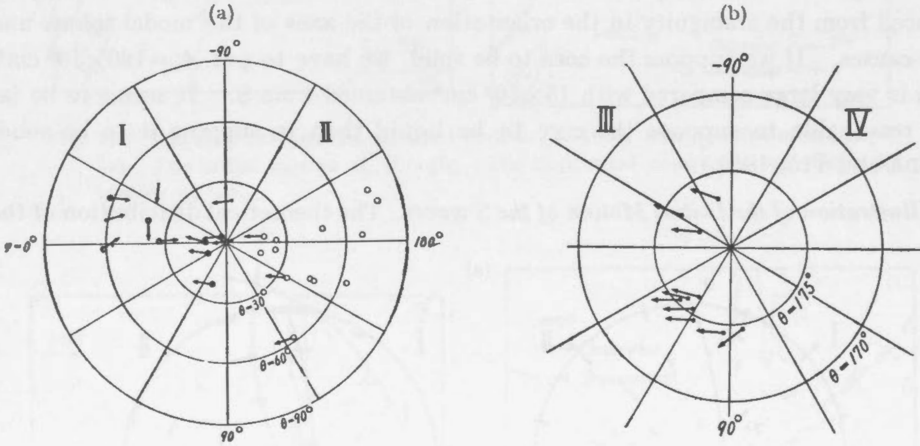

Fig. 32. The initial motion of S (a) and ScS (b).[64]
(a); S. The Osaka Bay earthquake of May 5, 1932.
(b); ScS. The Japan Sea earthquake of Nov. 13, 1932.

and Fig. 32 (b) shows the initial motion of the ScS waves of the Japan Sea earthquake of Nov. 13, 1932 in the quadrants III and IV. The distribution in both cases is consistent with the theoretically expected one shown in Fig. 31 (b). (HONDA *et al.*, 1955.)

3–1c. ***A_p, A_s and Magnitude of Deep Earthquake.*** Both A_p and A_s have been evaluated for 11 deep earthquakes, and A_p for more 5 deep earthquakes. log A_p is proportional to the magnitude M of the earthquake estimated by B. GUTENBERG and C. F. RICHTER (1949), Fig. 33, and the relation can be expressed by

$$M = 0.74 \log A_p + 2.61 \ .$$

log A_s is also proportional to M.

The relation between the ratio $[R] = A_s/5.20A_p$ and A_p is shown in Fig. 34. $[R]$ is nearly unity when A_p is very small, whereas it is very small for large A_p. That A_p is large means that the magnitude and hence the radius of the focal region may be large. The relation obtained here will probably be consistent with the theoretical relation illustrated in Fig. 8.

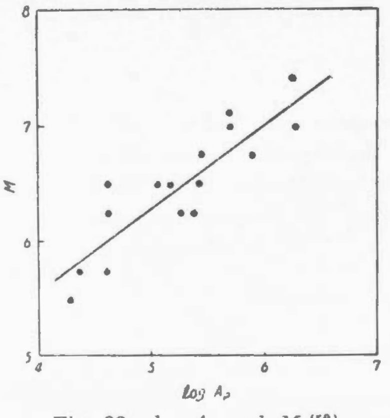

Fig. 33. log A_p and M.[59]

(HONDA, 1951, 54.)

The apparent periods of the initial motion of the deep earthquakes also become large with the magnitude of the earthquakes. (HONDA and ITÔ, 1940.)

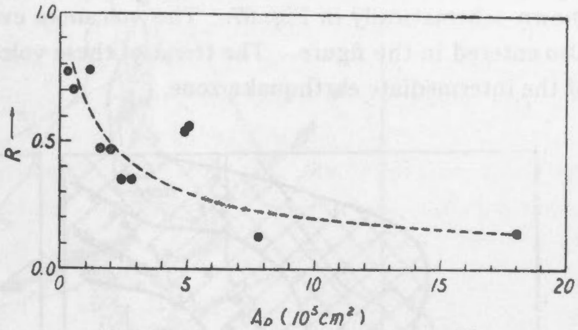

Fig. 34. A_p and $[R]=A_s/5.20\,A_p$.[63]

3-1d. *Statistical Investigation of the Mechanism of Deep and Intermediate Earthquakes.* The earthquakes are classed here as shallow when the focal depth does not exceed 100 km, intermediate when it is from 100 km to 250 km, and deep when it exceeds 250 km. There occurred 87 deep earthquakes, 58 intermediate earthquakes and 841 shallow earthquakes during the period 1927 to 1949 in and near Japan; all the earthquakes being classed as remarkable and moderate in this country. The geographical distribution of the deep and intermediate earthquakes is shown in Fig. 35. As is well known, most deep and intermediate earthquakes occur along the curved surface *ABC-A'B'C'* in Fig. 36, which dips downward from the eastern coast of Honsyû toward the Asiatic continent, extending to a depth of 400 km to 600 km beneath the outer boundary of the deep earthquake zone. The deep and intermediate earth-

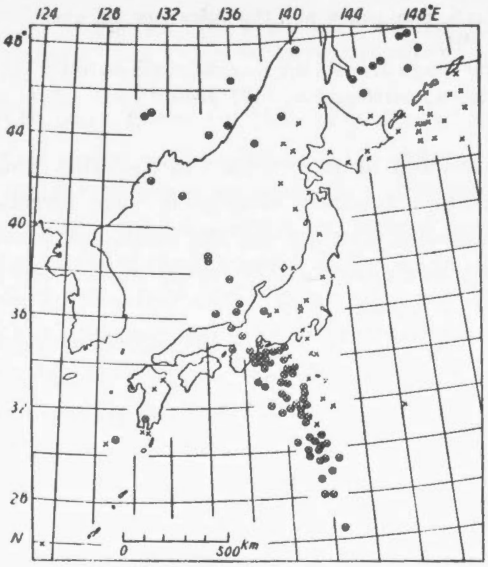

Fig. 35.

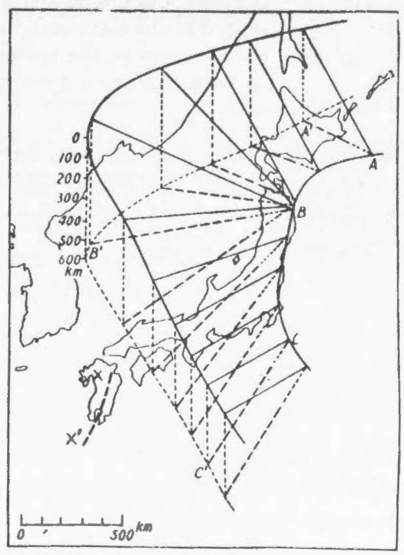

Fig. 36.

Fig. 35. The deep and intermediate earthquakes, 1927–1949.[61]
⊗ : deep earthquake, $H \geqq 250$ km.
× : intermediate earthquake, $250 > H \geqq 100$ km.

Fig. 36. The inclined surface (ABC-A'B'C') along which the deep and intermediate earthquakes occur.[61]

quake zones and the region in which shallow earthquakes occur most frequently are shown schematically in Fig. 37. The volcanoes ever erupted in the historical time are also entered in the figure. The trend of these volcanoes is nearly coincident with that of the intermediate earthquake zone.

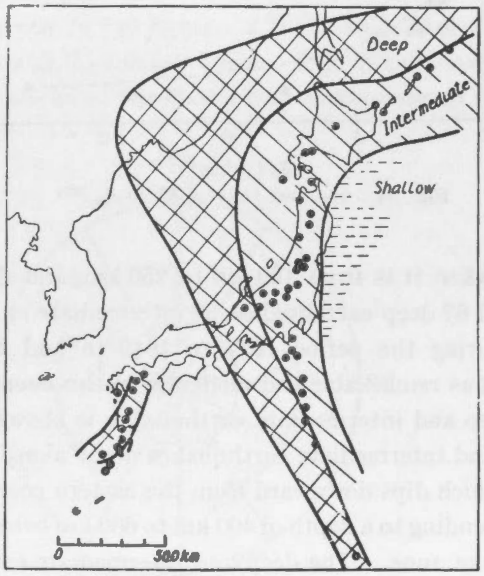

Fig. 37.

Fig. 38.

Fig. 37. The deep and intermediate earthquake zones, and the volcanoes (◎) ever erupted in the historical time.[61]

Fig. 38. The direction of the horizontal component of the maximum pressure for the deep (⊗) and intermediate (×) earthquakes, 1927-1949.[61]

The mechanisms of 34 deep earthquakes and 10 intermediate earthquakes, among the earthquakes occurred during the period, have been elucidated. The directions of the horizontal components of the maximum pressure for the earthquakes as are illustrated in Fig. 38, are directed nearly perpendicularly to the trends of the deep and intermediate earthquake zones and the active volcanic zone.

Let the deep and intermediate earthquake zones be divided provisionally into five regions (*ab*), (*c*), (*de*), (*fg*) and (*hi*) as are shown in Fig. 39, and consider a virtual earthquake corresponding to the mean state of the stresses causing the earthquakes in each region. Now it is assumed that one of the nodal planes of the P waves corresponds to the fault plane when faulting motion occurrs at the focus, whereas the earthquake is produced by the large scale stress of the nature of the force system of the type II acting in the vast region including the focal domain in it. And so, one of the nodal planes for each virtual earthquake being supposed to be a fault plane, the directions of the relative motion of the Pacific side to the Asiatic side are illustrated by arrows in Fig. 39. For the virtual earthquake in the region (*c*) for example, the dip direction of the fault plane is S34°E, the strike N56°E, the dip 73° and the slip angle 50°. The faulting motions are nearly reverse for the regions (*ab*), (*c*) and (*fg*), nearly transcurrent

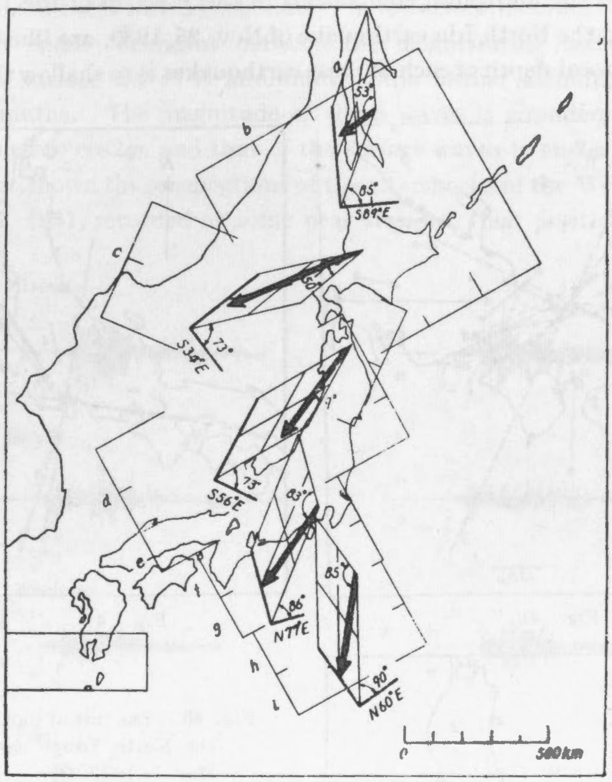

Fig. 39. The hypothetical direction of the relative motion of the Pacific side to the Asiatic side.[65]

for (*de*) and vertical for (*hi*). The directions of these relative motions do not lie in general in the surface *ABC-A'B'C'*. Anyhow, it seems to exists the general tendency for the Pacific side to be relatively forced downward and toward the Asiatic continental side, which is forced upward and toward the eastern offing of Honsyû. Of course, the choice of one of the two nodal planes as the fault plane is arbitrary, and the statement denoted here is only one of the various possible ways of explanation as to the causes of the deep and intermediate earthquakes in and near Japan. (Honda *et al.*, 1952, 56).

3-1e. Various hypotheses concerning the tectonic activity of the circum-Pacific earthquake zones have been proposed by J. Coulomb (1945), H. Benioff (1949, 54, 55), H.H. Hess (1951), Vening Meinesz (1954), J.T. Wilson (1954), H.Stille (1955), and A.E. Scheidegger (1955, 56). Some of them seem to be consistent with a possible explanation of our statistical investigation, that the Pacific side is overthrusted by the Asiatic side. Gutenberg and Richter (1951) stated that, 'possibly over a long period of geological time the uppermost layers surrounding the Pacific basin have been displaced toward its center relative to the lower layers'.

3-2. Mechanism of Very Shallow Earthquakes.

3-2 a. *Mechanism of Very Shallow Earthquakes.* The distribution of the direction and magnitude of the initial motion of the P waves of the North Tango earthquake of Mar. 7, 1927, and those of the horizontal components of the P waves of the Itô earthquake of Mar. 22, 1930, and the North Idu earthquake of Nov. 25, 1930, are illustrated in Fig. 40, 41 and 42. The focal depth of each of these earthquakes is so shallow that the focus can

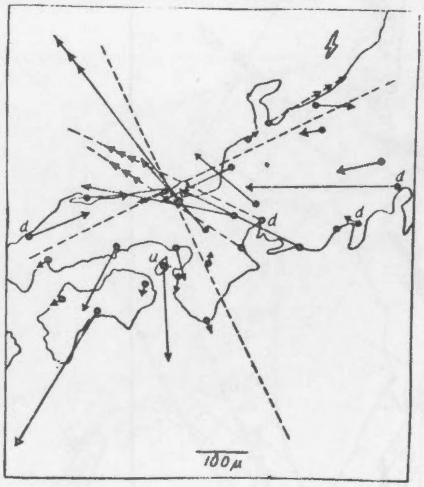

Fig. 40.

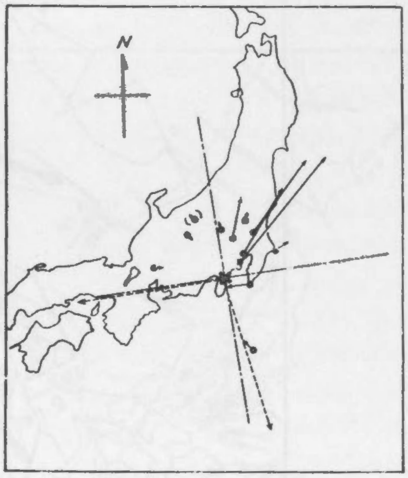

Fig. 41.

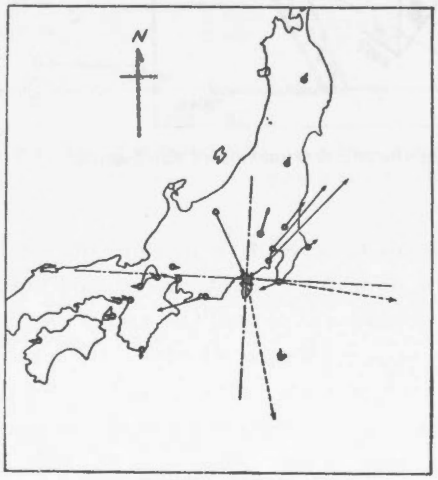

Fig. 42.

Fig. 40. The initial motion of P for the North Tango earthquake of Mar. 7, 1927.[48]

Fig. 41. The horizontal component of the initial motion of P for the Itô earthquake of Mar. 22, 1930.[47]

Fig. 42. The horizontal component of the initial motion of P for the North Idu earthquake of Nov. 25, 1930.[47]

be considered to lie in the earth's surface or within 10 or 15 km from the earth's surface at most. The initial motions of the P waves are condensational in the two quadrants lying opposite to each other, and rarefactional in the other two quadrants, when the earth's surface is divided into four quadrants by two straight nodal lines crossing orthogonally at the epicenter. The magnitude of the initial motion of the P waves is minimum in the azimuths along the nodal lines and maximum in the middle azimuths between the neighbouring nodal lines, and its distribution can be approximately represented by the expression $(1/\Delta^2)\sin 2\varphi$; where Δ is the epicentral distance and φ is the azimuth of the station to the epicenter measured from one of the nodal lines.

Inspecting the seismograms of these and other very shallow earthquakes, it was found that the amplitude of the S waves is maximum in the azimuths along the nodal lines and minimum in the middle azimuths between the neighbouring nodal lines, and the amplitude of the surface waves is minimum in the former azimuths and maximum in the latter azimuths. The magnitude of the S waves is considered to be approximately proportional to $\cos 2\varphi$, and that of the surface waves to $\sin 2\varphi$.

In Fig. 43, are shown the seismograms of the aftershocks of the West Saitama earthquake of Sept. 21, 1931, recorded at some near stations, their positions relative to the

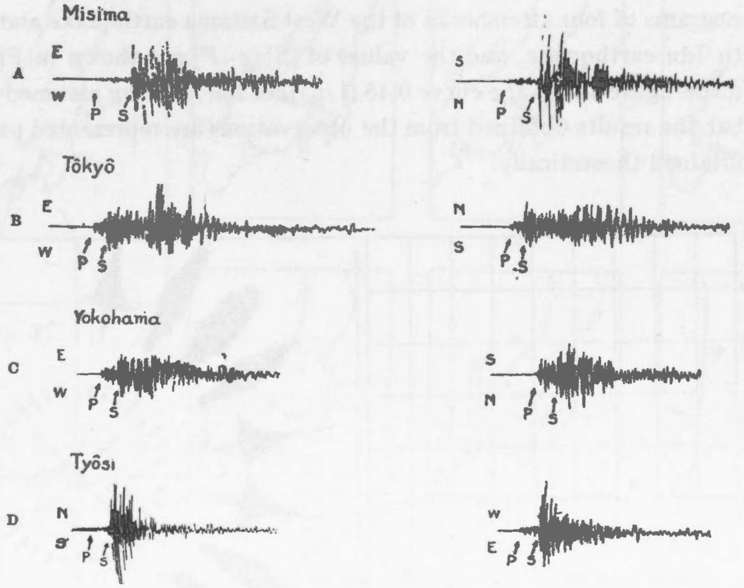

Fig. 43. The seismograms of the aftershocks of the West Saitama earthquake of Sept. 21, 1931.[48] (A),(B),(C) ; 1h22m Sept. 24, 1931. (D); 2h36m Oct. 3, 1931.

nodal lines being illustrated in Fig. 44. The focal depths of these earthquakes are also very shallow. The amplitudes of the P and surface waves are very small and those of the S waves are large at Misima and Tyôsi which are situated near the nodal line, whereas the amplitudes of P and surface waves are large and those of the S waves are small at Tôkyô and Yokohama situated in the middle azimuths between the neighbouring nodal lines.

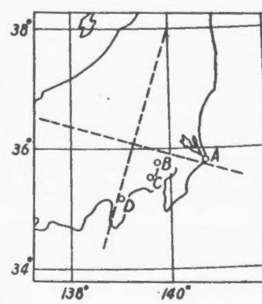

Fig. 44. The nodal lines for the aftershocks of the West Saitama earthquake.[48] A : Tyôsi, B : Tôkyô, C : Yokohama, D : Mishima.

When the radial force of the magnitude $Ar^3 \sin 2\varphi \times \exp(i\omega t)$, is assumed to be applied in the small circular area around the origin on the surface of a semi-infinite elastic solid, the amplitude of the P waves at a point on the surface is expected theoretically to be proportional to $(1/r^2) \sin 2\varphi$, (9), after NAKANO (1930), and the relation seems to be consistent with that obtained from the study of the observations of the initial motion of the P waves for very shallow earthquakes. The amplitudes of the S and surface waves should be theoretically proportional to $\cos 2\varphi$, (10), and $\sin 2\varphi$, (11), respectively, and these relations also are consistent with those obtained from the observations. The ratio of the amplitude $[\delta_{s,\varphi}]$ of the S waves to the amplitude $[\delta_{p,r}]$ of the P waves at the station (r, φ) on the surface, can be expressed theoretically by the formula, by making use of (9) and (10),

$$\frac{1}{r}\,\frac{[\delta_{s,\varphi}]}{[\delta_{p,r}]} = 0.45 \cdot \frac{1}{l_p}\,|\cot 2\varphi|\,, \quad l_p\text{; the wave length of the P waves.}$$

The largest amplitudes $[P]$ and $[S]$ of the P and S waves respectively, were measured on the seismograms of four aftershocks of the West Saitama earthquake and a foreshock of the North Idu earthquake, and the values of $[S]/\Delta \cdot [P]$ are shown in Fig. 45. The thick line in the figure shows the curve $0.45\,(1/l_p)\,|\cot 2\phi|$, l_p being assumed to be 10km. It is seen that the results obtained from the observations are represented pretty well by the curve obtained theoretically.

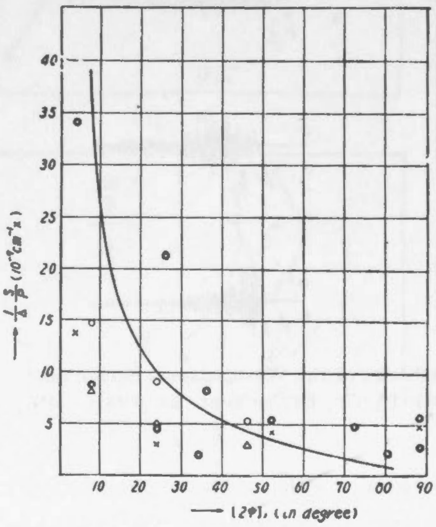

Fig. 45.

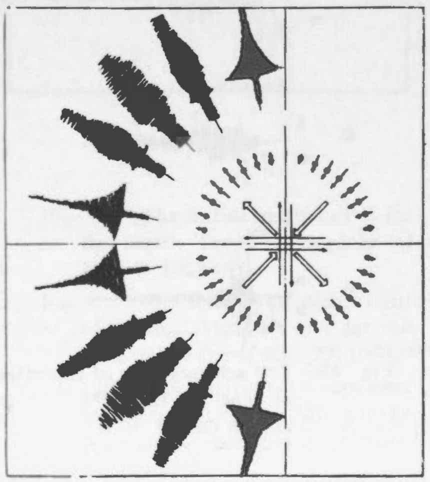

Fig. 46.

Fig 45. $[S]/\Delta \cdot [P]$ and $2|\varphi|$. Aftershocks of the West Saitama earthquake and a foreshock of the North Idu earthquake.[48]

Aftershocks of the West Saitama earthquake.

×; 21h46m Sept. 23, 1931. ◉; 1h22m Sept. 24, 1931.

△; 13h54m Sept. 28, 1931. ○; 2h36m Oct. 3, 1931.

Foreshock of the North Idu earthquake.

◎; 16h05m Nov. 25, 1930.

Fig 46. The mechanism and the types of the seismograms for very shallow earthquake.[48]

←: The initial motion of P.

The relations between the mechanism at the focus, the initial motion of the P waves and the types of the seismograms, are illustrated schematically in Fig. 46. (Honda, 1931, 32a.)

Kawasumi (1934a), and Honda and H. Watanabe (1952) tried to take the effects of the increase of the velocity of the seismic waves from the earth's surface into account in the investigation of the magnitude of the P waves of the very shallow earthquakes, instead of treating the crust as homogeneous. The latter authors employed the results of HIRONO's theoretical studies (Sect. 2–2) on the P and S waves, emitted from the surface source into the interior of a semi infinite elastic solid.

3–2 b. *Mechanism of Aftershocks and Swarm Earthquakes.* The patterns of the condensation and rarefaction of the initial motion of the P waves of the West Saitama

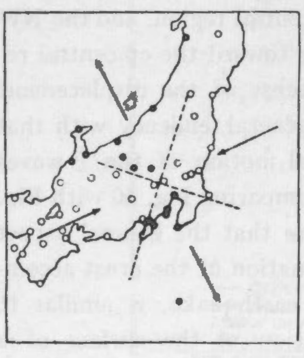

Fig. 47.

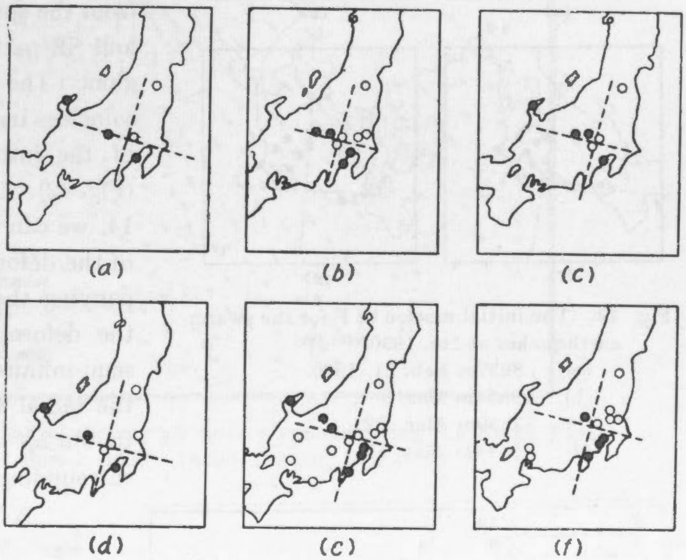

Fig. 48.

Fig. 47. The initial motion of P for the West Saitama earthquake of Sept. 21, 1931.[48]
●: Condensation. ○: Rarefaction.

Fig. 48. The initial motion of P for the aftershocks of the West Saitama earthquake.[48],[63]
●: Condensation. ○: Rarefaction.

(a) 15h49m Sept. 21, 1931
(b) 21h46m Sept. 23.
(c) 1h22m Sept. 24.
(d) 21h11m Sept. 24.
(e) 13h54m Sept. 28.
(f) 2h36m Oct. 3.

earthquake of Sept. 21, 1931, and of six rather conspicuous aftershocks of the main shock, are shown in Fig. 47 and 48. The mechanisms of the main earthquake and its aftershocks seem to be quite similar to each other.

For about four months from February to May in 1930, there occurred numerous very shallow earthquakes, swarm earthquakes, at Itô. The pattern of the condensation and rarefaction of the initial motion of the P waves of rather conspicuous earthquakes out of the swarm, are illustrated in Fig. 49. The mechanisms of these earthquakes seem also to be similar to each other. (HONDA, 1932a).

3–2 c. *Deformation of the Earth Crust Accompanying Very Shallow Earthquake.* A remarkable fault directed north and south, was observed in the North Idu earthquake of Nov. 25, 1930. The strike of the fault was nearly coincident with one of the nodal lines of the P waves. But the deformation of the crust accompanying the earthquake is not confined to the simple faulting motion. By the precise surveying performed after

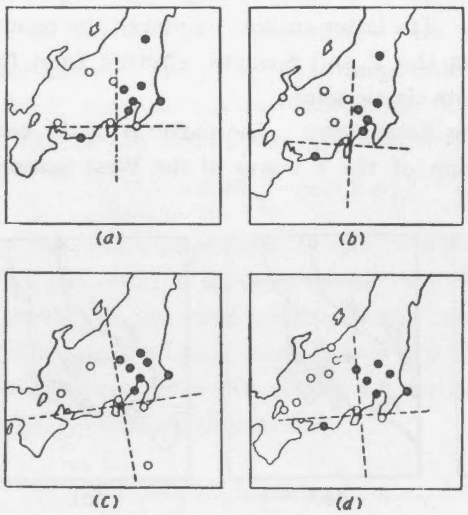

Fig. 49. The initial motion of P for the swarm earthquakes at Itô, 1930.[(48),(63)]
(a); 8h37m Feb. 21, 1930.
(b); 19h54m Mar. 9.
(c); 17h50m Mar. 22.
(d); 5h14m May 17.

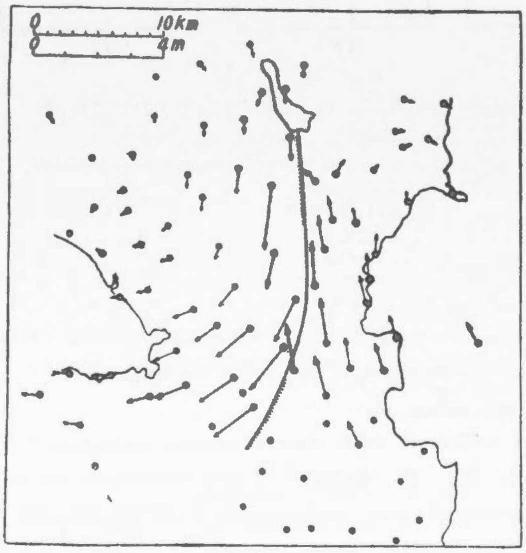

Fig. 50. The deformation of the earth's surface accompanying the North Idu earthquake of Nov. 25, 1930. (After TSUBOI, 1939.)

the earthquake, it was found that a large area surrounding the epicentral region was deformed at the earthquake. The horizontal dislocation of the earth's surface is shown by arrows in Fig. 50 (C. TSUBOI, 1939). The NE and SW parts of the region are displaced away from the epicentral region, and the NW and SE parts toward the epicentral region. The sense of the displacement coincides in general tendency with that of the initial motion of the P waves (Fig. 42). Comparing Fig. 50 with Fig. 14, we can see that the general aspect of the deformation of the crust accompanying the earthquake, is similar to the deformation of the surface of a semi-infinite elastic solid produced by the radial force which is proportional to $\sin 2\varphi$ and applied at the region surrounding the origin on the surface.

A large fault directed NW-SE, was observed at the time of the North Tango earthquake of Mar. 7, 1927. The strike of the fault coincides nearly with that of one of the nodal lines of the P waves (Fig. 40). Accompanying the earthquake, there occurred a remarkable deformation of the earth crust in the epicentral region (Fig. 51, after TSUBOI, 1939). The NE side of the fault is displaced toward NW, and the SW part toward SW. The pattern of deformation is similar to that in the lower half of Fig. 14, and the sense of dislocation is also nearly consistent with that of the initial motion of the P waves (Fig. 40). (HONDA and MIURA, 1935).

It is especially to be noticed that not only the distribution of the direction and magnitude of the seismic waves but also the general feature of the deformation of the earth crust accompanying very shallow earthquake, are explained theoretically by the hypothesis of the force system of the type II, even in the cases when distinct faults are observed at the earth's surface, except in the region very close to the fault. According to

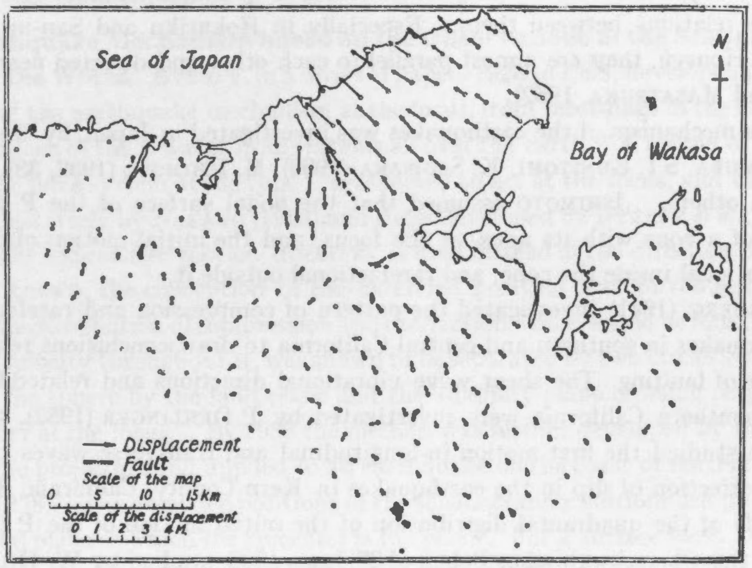

Fig. 51. The deformation of the earth's surface accompanying the North Tango earthquake of Mar. 7, 1927. (After TSUBOI, 1939.)

the theory of elasticity expressed e.g. by the equations such as $X_y = Y_x$ ...., it may be considered to be natural to suppose that the vast region in the earth is subjected to the large scale stresses corresponding to the force system of the type II, that the earthquakes occur when some faults or sudden collapses are generated by the stress, and yet that the general features of the seismic waves and the deformation of the earth crust surrounding the focal region are governed by the large scale stresses.

3–2 d. *Statistical Investigation of the Mechanism of Very Shallow Earthquakes.* The number of very shallow earthquakes occurred in or near Japan, and caused damage more or less during the period

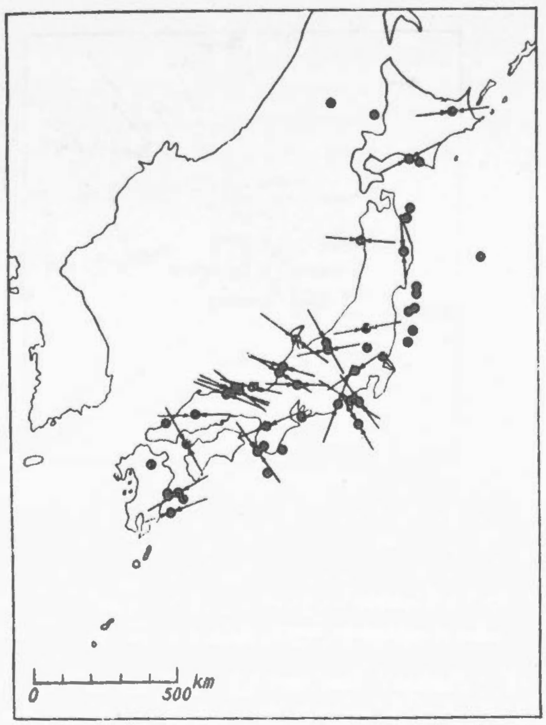

Fig. 52. The direction of the horizontal maximum pressure for the very shallow earthquakes, 1927-1949.[61]

1927 to 1949, amounted to 62. The mechanisms of 27 earthquakes out of them have been elucidated. When the directions of the horizontal maximum pressure for these 27 earthquakes are shown by arrows on a map (Fig. 52), it is seen that there exist some relations between them. Especially in Hokuriku and San-in, the Japan Sea side of Honsyû, they are almost parallel to each other and directed nearly NW-SE. (HONDA and MASATSUKA, 1952).

3-2 e. The mechanism of the earthquakes was investigated in Japan, by OMORI, SHIDA, S.T. NAKAMURA, S.I. KUNITOMI, K. SAGISAKA (1930), M. ISHIMOTO (1932, 33), H. TAKAGI (1950) and others. ISHIMOTO assumed that the nodal surface of the P waves is in the shape of a cone with its apex at the focus, and the initial motion of the P waves is condensational inside the cone, and rarefactional outside it.

GUTENBERG (1941) investigated the pattern of compression and rarefaction in the local earthquakes in southern and central California to draw conclusions respecting the mechanism of faulting. The shear wave vibrational directions and related fault movements in southern California were investigated by P. DEHLINGER (1952). GUTENBERG (1955) also studied the first motion in longitudinal and transverse waves of the main shock and direction of slip in the earthquakes in Kern County, California, during 1952. An example of the quadrantal distribution of the initial motion of the P (P_g and P_n) waves for the Oberschwäbisches Beben of 27 June, 1935, studied by W. HILLER (1953), is shown in Fig. 53. DI FILIPPO *et al.* (1949, 50) and P. CALOI *et al.* (1952, 55, 56) investigated the mechanism of the earthquakes occurred in Italy.

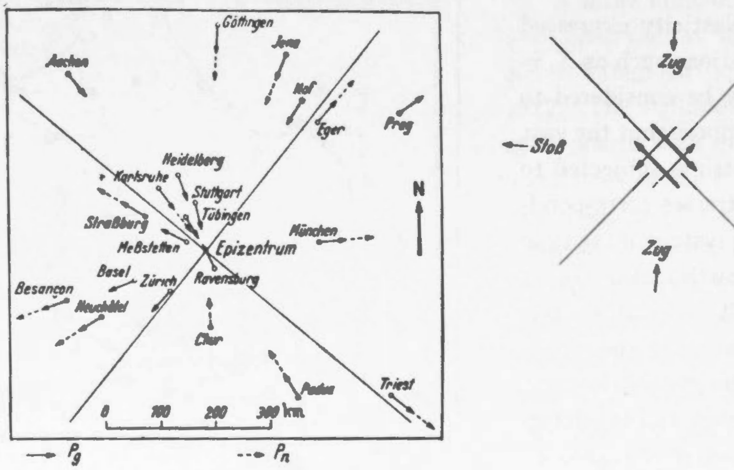

Fig. 53. The initial motion of P_g and P_n and the mechanism for the Oberschwäbisches Beben of June 27, 1935. (After HILLER, 1953.)

4 Investigation of Earthquake Mechanism based on the Observations at the Stations distributed over the World

4-1. Distant Earthquakes recorded at Individual Stations. P. E. GHERZI, O. SOMVILLE and others showed that the initial motions of the P waves recorded at individual station are condensational for distant earthquakes occurring in certain regions and rarefactional for those in other regions. BYERLY and J. F. EVERNDEN (1950) published a map for circum-Pacific epicnters, showing the nature of the initial motions of the P waves recorded at Berkeley. M. BÅTH (1952) made a similar investigation for Pasadena and Huancayo, and J.W. JONES (1952) for Seattle.

4-2. Earthquake Mechanism based on the Observations at the Stations distributed over the World. BYERLY, in a series of papers 1926 to 1955, developed the methods for studying the earthquake mechanism at the focus, from recordings of the compressions and rarefactions of the P waves from stations all over the earth. A couple of forces with moment, the force system of the type I, is assumed to act at the focus, and the results of the theoretical study by NAKANO (1923) and those developed by BYERLY *et al.*, (1949) were adopted. The expression 'motion direction' is used instead of the direction of the forces. As is well known, the conception of the extended position was introduced by him in 1928, and the distribution of compression and rarefaction which would be found on a sphere of uniform velocity throughout it, was shown to be separated by two circles, which are the sections of the sphere by the fault plane and the auxiliary plane crossing perpendicularly to each other at the focus. 'By 1938 the method was further developed by the use of the stereographic projection and applied to an earthquake on the coast of northern California (BYERLY, 1938). The extended positions of the seismographic stations are projected onto an equatorial plane of which the epicenter is the pole'*. For a surface focus, the extended distance is equal to $R \tan e$, where R is the radius of the earth and e the angle of emergence of the seismic ray arriving at the station (Fig. 54). 'These projected points are marked as to whether the first P wave was a compression or a rarefaction. The problem is then to draw

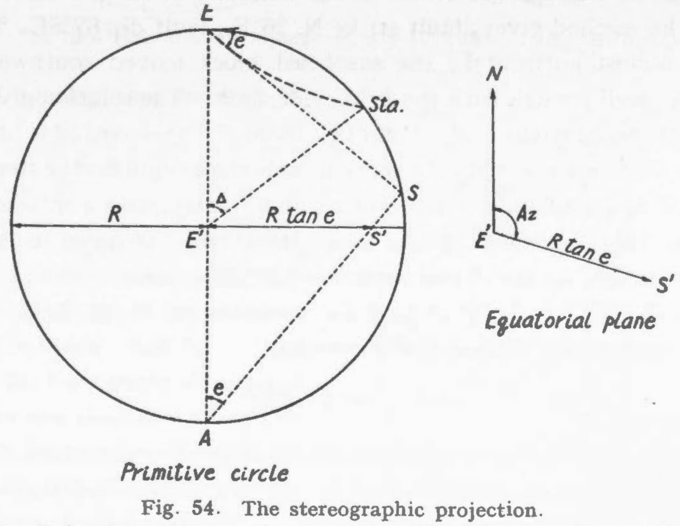

Fig. 54. The stereographic projection.
E: Epicenter. A: Anticenter. Sta: Station. S: Extended position of station. e: Angle of emergence. S': Stereographic projection of S. ---- : Seismic ray. Az: Azimuth of station from epicenter. (After BYERLY, 1955.)

two circles on this equatorial plane which pass through the focus and which separate regions of compression and rarefaction'*, as the circles on the sphere project into circles on the map. The stereographic projection method was applied to the Montana earthquake of

June 28, 1925; the projection for the earthquake is shown in Fig. 55. (BYERLY, 1955). 'The strike of the fault is given by the direction of a tangent drawn at the projection of the epicenter to the fault plane circle. The auxiliary plane is described by the second

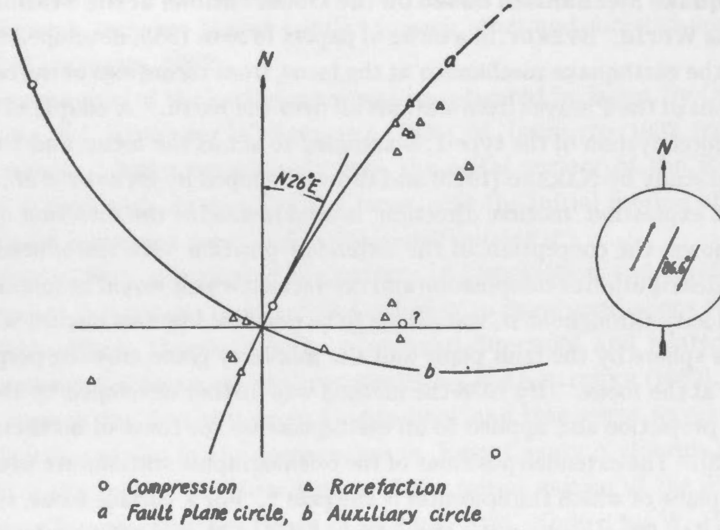

Fig. 55. The Montana earthquake of June 28, 1925. (After BYERLY, 1955)

circle on the projection. The plunge of the line of motion of the fault is given by the direction of the line through the center of the auxiliary circle and the epicenter. For the example the method gives: fault strike N. 26°E., fault dip 87°SE. The motion on the fault was almost horizontal; the southeast block moved southwest. Thus the direction agrees well enough with the field evidence'*. The solution given here is one of the two possible solutions. (* ; BYERLY, 1955)

HODGSON *et al.* have developed remarkably the technique for the stereographic projection method and applied the method to many earthquakes, in a series of papers published since 1951. For non-surface foucs, the earth is stripped to the focal depth, and the method is used for the virtual surface focus. The tables of the extended distances for the phases P, PKP, PcP, PP and pP for various focal depths have been produced. There holds a relationship, orthogonality criterion,

$$\cos\theta = \tan\beta / \tan\delta$$

between the angle of intersection of the two circles θ, the dip of the fault δ, and the plunge of the line of movement on the fault β. (J.D. ADKINS, 1940, HODGSON *et al.*, 1951).

A fault plane solution for the New Hebrides earthquake of May 17, 1950, is shown in Fig. 56. 'The circles represent two planes, one striking approximately NS and dipping 79° to the W, the other striking approximately EW and dipping 71° to the N. There is no way of recognizing which of these planes is the fault plane and which the auxiliary plane, but the fact that the circles are almost orthogonal indicates that the movement must be almost strike-slip or *transcurrent*. For example, suppose that the NS striking plane is the fault. Then the EW plane is the auxiliary plane, which is by definition perpendicular to the direction of slipping. It follows that this direction must be approximately NS, parallel to the strike of the fault. Strike-slip faulting is therefore indicated. On the other hand, if the circles had been tangential a similar argu-

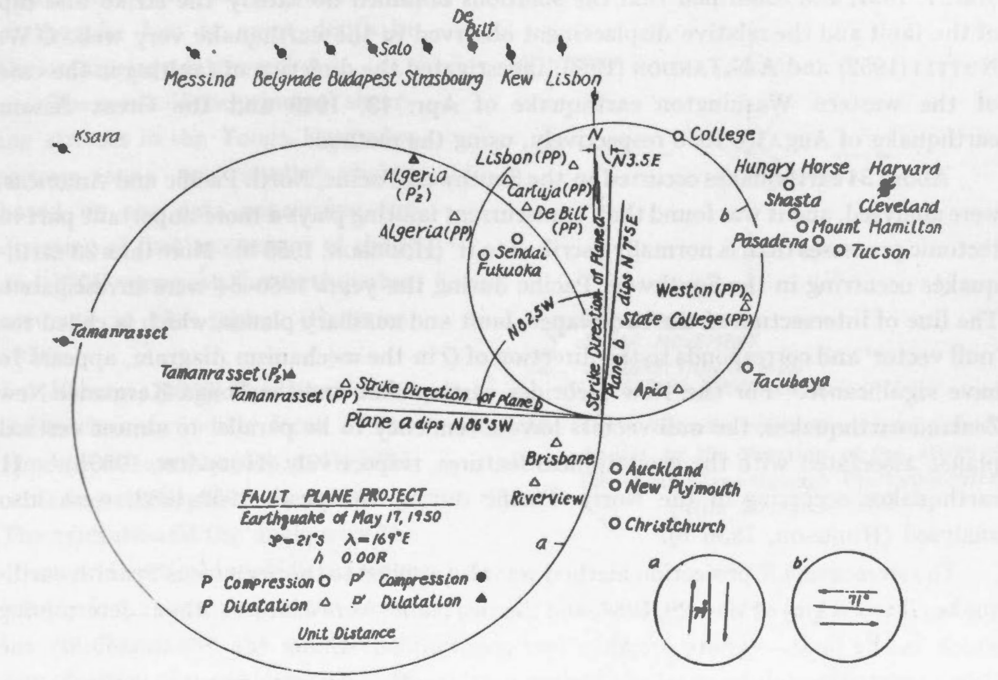

Fig. 56. The New Hebrides earthquake of May 17, 1950. (After HODGSON, 1955)

ment would show that motion must be perpendicular to the strike. In the small circular diagrams labelled *a* and *b* the two possibilities have been illustrated, the arrows representing the horizontal projection of the motion vector slightly displaced from the center of the diagram for clarity' (HODGSON, 1955 b). The mechanism of the earthquake illustrated by the small circular diagrams *a* and *b* in Fig. 56, can be shown schematically by the mechanism diagram which is explained in Sect. 3-1. Assuming that one of the nodal planes strikes approximately N4°E and dips 79° to the W, and the other one strikes N83°W and dips 71° to the N, we can obtain the directions of P_1, T_1, M_1, M_2 and Q. The mechanism diagram basing on these data is shown in

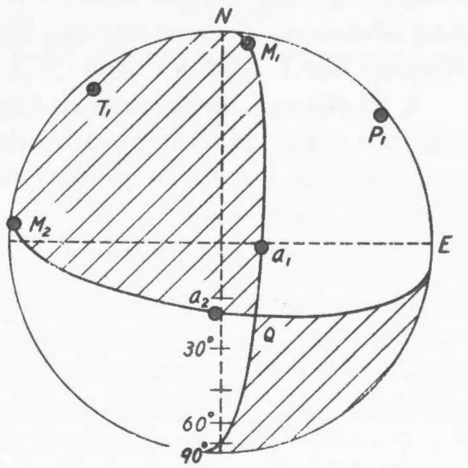

Fig. 57. The mechanism diagram for the New Hebrides earthquake of May 17, 1950.
P_1; N51°E (85°). T_1; N41°W (68°).
M_1; N 7°E (71°). M_2; N87°W (79°).
a_1; S87°E (11°). a_2; S 7°W (19°).
Q; S26°E (22°). (Slip angle)$_{1,2}$=20°,12°

Fig. 57. The directions of M_1 and M_2 correspond to the supposed directions of motion illustrated by arrows in *a* and *b* of Fig. 56, respectively.

HODGSON (1955a), applied his method of analysis to the Tango earthquake, Japan, of Mar. 7, 1927, and confirmed that the solutions obtained do satisfy the strike and dip of the fault and the relative displacement observed in the earthquake very well. O.W. NUTTLI (1952) and A.N.TANDON (1955) investigated the direction of faulting in the case of the western Washington earthquake of Apr. 13, 1949 and the Great Assam earthquake of Aug. 15, 1950 respectively, using the method.

About 34 earthquakes occurred in the Southwest Pacific, North Pacific and Americas, were analysed, and it was found that 'transcurrent faulting plays a more important part in tectonic processes than is normally ascribed to it' (HODGSON, 1955 b). More than 23 earthquakes occurring in the Southwest Pacific during the years 1950–54 were investigated. The line of intersection of the two planes, fault and auxiliary planes, which is called the 'null vector' and corresponds to the direction of Q in the mechanism diagram, appears to have significance. For the New Hebrides earthquakes and the Tonga-Kermadec-New Zealand earthquakes, the null vectors have a tendency to lie parallel to almost vertical planes associated with the geographical features, respectively (HODGSON, 1956 a). 11 earthquakes occurring in the North Pacific during the years 1950–1953, were also analysed (HODGSON, 1956 b).

The stereographic projection method was also applied to the deep focus Spanish earthquake (H=650 km) of Mar. 29, 1954, and the two planes were defined without determining which is the fault. 'There are thus two possibilities. Under the first possibility the fault is approximately vertical and strikes north-south. The movement is vertical, such that the eastern side of the fault rises with respect to the western side. Under the second possibility the fault is approximately horizontal, and the movement is also horizontal, the material above the focus moving due east with respect to the material below the focus' (HODGSON and J. I. COCK, 1956).

S. Mühlhäuser (1957) determined the mechanisms for 11 earthquakes in the years 1931–1950 in the Pacific area. 'It results that there is no general rule for the mechanisms, although the strikes of the fault planes in general coincide with the circum-Pacific structural lines.'

L.P.G. KONING (1942) investigated the mechanism of the deep earthquake of June 29, 1934 occurred in the Flores Sea at a depth of 720 km. Two other deep earthquakes in the Indonesian Archipelago, one with epicenter in the Java Sea (Aug. 11, 1937. H; 610km), the other with epicenter in Mindanao (Sept. 22, 1940. H; 660 km), were investigated by A.R. RITSEMA (1953)*. 'In all these cases it has been determined that the earthquake originated by a sudden shear movement along a flat plane in the focus"* and it is 'not certain, however, about the dip of the actual shear plane because we get two possible planes of shear movement perpendicular to each other for each single earthquake'.* Fig. 58 'shows a schematic section perpendicular to the strike of the shear plane through the focus of one of the earthquakes. Only a normal dip-slip movement along one of the possible planes of shear movement can explain the distribution of the + (condensation) and - (rarefaction) areas at the earth's surface. That means the existence of a tension force in horizontal sense, or a compression force in vertical sense at the depth of the focus'.* And it is expected 'that this type of movement in earthquake foci at great depth in the archipelago is general'.*

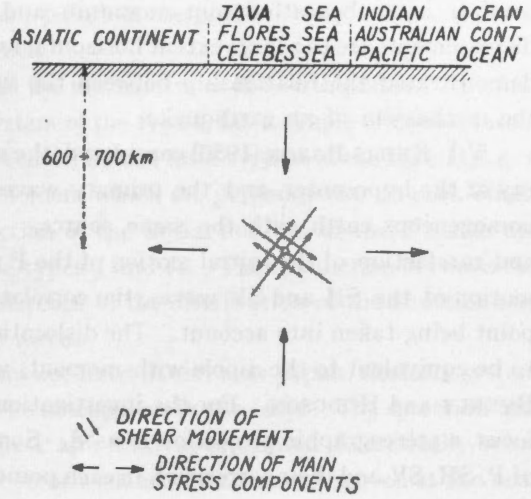

Fig. 58. The schematic vertical section perpendicular to the direction of the strike of the shear plane through the hypocenter. (After RITSEMA, 1953.)

The sense of the principal shearing stresses in the Tonga-Kermadec seismic zone was studied, being based on the data concerning the direction of first movement of the P and PKP waves of the earthquakes occurred in the region (RITSEMA, 1954).

RITSEMA (1955) investigated also the mechanism in the focus of the Hindu Kush earthquakes, 1917–1952, centering at a depth of about 220 km. The azimuth and the angle with the downward vertical in which the wave left the focus were used as the variables in illustrating the mechanism. Compression and dilatation data of the P and PKP waves were the bases of the study. It was found 'that the earthquakes are caused by a thrust fault movement in the focus. The principal stress component (greatest compression) acts about horizontal in the NW-SE azimuth, the smallest stress component (greatest stretching) about vertical somewhat inclined towards SW. The derived stress system is not in contradiction with the about NE-SW tending Hindu Kush mountain system'. Fig. 59 shows the vertical section through the focus in the NW-SE azimuth. It is noticed that the sense of the first motion of the S waves illustrated in the figure seems to be in accordance with that shown schematically in Fig. 6 (b) for the force system of the type II.

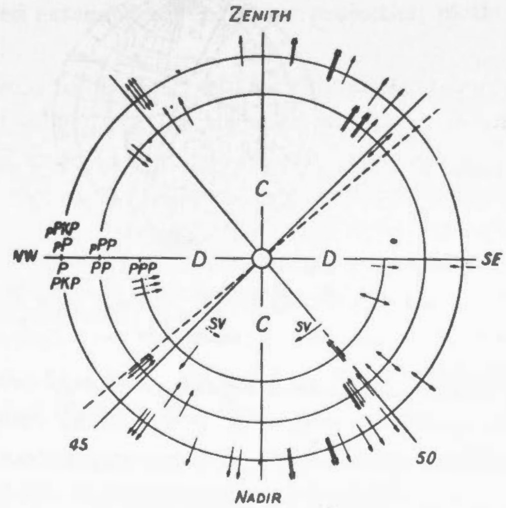

Fig. 59. The vertical section through the Hindu Kush earthquake center in the NW-SE azimuth. (After RITSEMA, 1955.)

A.E. SCHEIDEGGER (1955) collected the results of the studies of the displacements which are considered to be taking place during the occurrence of an earthquake in its focus, published by various authors, and analysed their bearing upon the physics of orogenesis.

He found that the earthquakes are localized in almost planar zones dipping at some intermediate angle beneath recent mountain and island belts, and that the differential displacements are to a large extent horizontal i.e. transcurrent. SCHEIDEGGER (1957) also demonstrated the relationship between the various methods devised for representing the mechanism of an earthquake.

V.I. KEILIS-BOROK (1956) considered 'the straight ray', semi-tangent to the seismic ray at the hypocenter, and 'the primary waves' which would be observed in a virtual homogeneous earth with the same source. He treated not only the condensation and rarefaction of the initial motion of the P waves, but also the senses of the initial motion of the SH and SV waves, the correlation of the signs of these phases for every point being taken into account. The dislocations in the source are considered as a rule to be equivalent to the dipole with moment, which is the same one as that adopted by BYERLY and HODGSON. For the investigation and illustration of the mechanism at the focus, a stereographic projection is used. Some examples of interpretation using signs of P, SH, SV and their correlation in each point, given from top to bottom, are illustrated in Fig. 60, where the points (directions of the seismic rays in the hypocenter) are plotted in a stereographic projection. The mechanisms of many earthquakes occurred in the

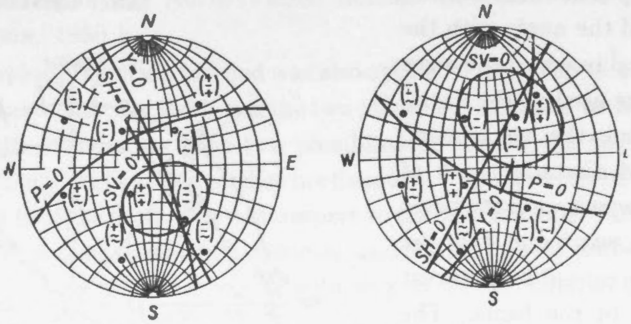

Fig. 60. Some examples of interpretation using the signs of P, SH and SV. (After KEILIS-BOROK, 1956.)

southern and eastern regions of Russia were investigated, and it was confirmed that the geological 'structures as well as the earthquakes seem to be the parallel results of general seismotectonic strains acting in vast regions.'

4-3. S and Other Waves. The initial motions of the S waves as well as other waves, have been studied by F. NEUMANN (1930), R. STONELEY (1951), K. ERGIN (1952), R.R. HEINRICH and H.K. HAILL (1952), and R.E. INGRAM (1953). INGRAM and HODGSON (1956) investigated theoretically the phase changes of PP and pP on reflection at the earth's surface, and the results are expressed for various focal depths, in terms of epicentral distances for PP and for pP between which there is no phase change on reflection.

5 Concluding Remarks

Some of the results of the investigations on the mechanism of the earthquakes by many seismologists since about 1930, have been described in foregoing chapters of the present paper. Now let us state about some points of the problem which are considered to necessitate especially further researches.

There are two kinds of assumptions on the mechanism of the earthquakes. The first one of them is represented by the force system of the type I, i.e. a couple of double forces with moment, and the second one is represented by the force system of the type II, i.e. a set of two couples of double forces with moment which are perpendicular to each other. The patterns of condensation and rarefaction of the initial motions of the P waves are similar to each other for the systems of the types I and II. The distinction between the two force systems is recognized in the difference of the distribution of the direction and magnitude of the initial motions of the S waves.

In the investigation of the earthquakes occurred in and near Japan, the force system of the type II is considered to represent the mechanism in the focus. The direction and the magnitude of the initial motions of the P and S waves calculated theoretically being based on the assumption, are shown to be in accordance with those observed at the near stations in Japan.

On the other hand, it is considered by many seismologists that the force system of the type I represents the mechanism of the earthquakes. The patterns of compressions and rarefactions of the P waves observed at the stations over the world, are explained being based on the assumption and the so-called extended stereographic projection method being used.

The force system of the type I may seem to be consistent with the elastic rebound theory. But it is to be noticed that not only the distribution of the direction and magnitude of the initial motions of the P and the S waves of deep as well as very shallow earthquakes, but also the deformation of the earth's surface accompanying some very shallow earthquakes in Japan, can be explained by the dynamical and statical force systems of the type II respectively, even when conspicuous faults are observed on the earth's surface. Further and minute investigations of the initial motion of the S waves observed at the stations over the world are desired, to be able to see which of the two assumed force systems of the types I and II, may be preferred as that representing the mechanism in the foci of the earthquakes.

Acknowledgement. The author expresses his sincere thanks to Messrs. H. SIMA, K. NAKAMURA and K. EMURA, who helped him in preparing the manuscript.

References

1. ADKINS, J. D. (1940): The Alaskan Earthquake of July 22, 1937. *Bull. Seismol. Soc. Am.*, **30**, 353-376.
2. BÅTH, M. (1952): Initial Motion of the First Longitudinal Earthquake Wave recorded at Pasadena and Huancayo. *Bull. Seismol. Soc. Am.*, **42**, 175-195.
3. BENIOFF, H. (1949): Seismic Evidence for the Fault Origin of Oceanic Deeps. *Bull. Geol. Soc. Am.*, **60**, 1837-1856.
4. BENIOFF, H. (1954): Orogenesis and Deep Crustal Structure — Additional Evidence from Seismology. *Bull. Geol. Soc. Am.*, **65**, 385-400.
5. BENIOFF, H. (1955): Seismic Evidence for Crustal Structure and Tectonic Activity. *'Crust of the Earth'* edited by A. POLDERVAART, 61-73.

6. Byerly, P. (1926) : The Montana Earthquake of June 28, 1925, G.M.C.T. *Bull. Seismol. Soc. Am.*, **16**, 209–265.

7. Byerly, P. (1928) : The Nature of the First Motion in the Chilean Earthquake of November 11, 1922. *Am. Journ. Sci. 5th Ser.*, **16**, 232-236.

8. Byerly, P. (1930) : Love Waves and the Nature of the Origin of the Chilean Earthquake of November 11, 1922. *Am. Journ. Sci. 5th Ser.*, **19**, 274-282.

9. Byerly, P. (1934) : The Texas Earthquake of August 16, 1931. *Bull. Seismol. Soc. Am.*, **24**, 81–99.

10. Byerly, P. (1935) : The First Preliminary Waves of the Nevada Earthquake of Dec. 20, 1932. *Bull. Seismol. Soc. Am.*, **25**, 62–80.

11. Byerly, P. (1938) : The Earthquake of July 6, 1934 : Amplitudes and First Motion. *Bull. Seismol. Soc. Am.*, **28**, 1-13.

12. Byerly, P., A. I. Mei, and C. Romney (1949) : Dependence on Azimuth of the Amplitudes of P and PP. *Bull. Seismol. Soc. Am.*, **39**, 269-284.

13. Byerly, P. and J. F. Evernden (1950) : First Motion in Earthquakes recorded at Berkeley. *Bull. Seismol. Soc. Am.*, **40**, 291-298.

14. Byerly, P. (1955) : Nature of Faulting as deduced from Seismograms. *'Crust of the Earth'*, 75–85.

15. Caloi, P. (1952) : Struttura Geologico-Sismico Dell' Europa Centro-Meridionale, Dell' Italia E Dell' Mediterraneo Centro-Occidentale, Quole Résulta Da Recenti Ricerche Cempiute in Italia. *Annali di Geofisica*, **5**, 507-518.

16. Caloi, P., D. Di Filippo, and M. C. Spadea (1955) : Onde Sismiche Guidate Dagli Strati Sedimentari. *Annali di Geofisica*, **8**, 9–21.

17. Caloi, P., M. De Panfilis, D. Di Filippo, L. Marcelli, and M. C. Spadae (1956) : Terremoti Della Val Padana Del 15-16 Maggio 1951. *Annali di Geofisica*, **9**, 63-105.

18. Coulomb, J. (1945) : Seismes Profonds et Grandes Anomalies Negatives de la Pesanteur peuvent-ils etrê attribués à une Extension Plastique ? *Annales de Géophysique*, **3**, 244–255.

19. Dehlinger, P. (1952) : Shear-Wave Vibrational Directions and Related Fault Movements in Southern California Earthquakes. *Bull. Seismol. Soc. Am.*, **42**, 155-173.

20. Di Filippo, D., and L. Marcelli (1949) : Sur Movimento Iniziale delle Onde Sismiche registrate a Roma durante in Periodo 1938-1943. *Annali di Geofisica*, **2**, 589-606.

21. Di Filippo, D. (1950) : Sulla Rappresentazione in Superficie della Natura Dinamica di Una Scossa All'ipocentro. *Annali di Geofisica*, **3**, 263-279, 379-391.

22. Droste, Z. (1956) : The Angular Distribution of the Energy Density in Seismic Waves. *Acta Geophysica Polonica*, **4**, 215–225.

23. Ergin, K. (1952) : Observations on the Recorded Ground Motion due to P, PcP, S and ScS. *Bull. Seismol. Soc. Am.*, **42**, 263–270.

24. Ergin, K. (1953) : Amplitude of PcP, PcS, ScS and ScP in Deep-Focus Earthquakes. *Bull. Seismol. Soc. Am.*, **43**, 63–83.

25. Gutenberg, B. (1941) : Mechanism of Faulting in Southern California indicated by Seismograms. *Bull. Seismol. Soc. Am.*, **31**, 263-302.

26. Gutenberg, B., and C.F. Richter (1951) : Evidence from Deep-Focus Earthquakes. *'Internal Constitution of the Earth'* edited by B. Gutenberg, 305–313.

27. Gutenberg, B. (1955) : The First Motion in Longitudinal and Transverse Waves of the Main Shock and the Direction of Slip. *'Earthquakes in Kern County during* 1952.' Bulletin. **171**, 165–170, Division of Mines, Sate of California.

28. Hasegawa, M. (1930) : Die Erste Bewegung bei Einem Erdbeben. *Beitr. z. Geophys.*, **27**, 102–125.

29. Heelan, P.A. (1953) : Radiation from a Cylindrical Source of Finite Length. *Geophysics*, **18**, 685–696.

30. Heinrich, R.R., and H.K. Haill (1952) : On the Recorded Motion of the S Phase at Florissant. *Bull. Seismol. Soc. Am.*, **42**, 145-154.

31. Hess, H.H. (1951) : Comment on Mountain Building. *Trans. Am Geophys. Union*, **32**, 428–531.

32. Hiller, W. (1953) : "Oberschwäbisches Beben von 27, Juni 1935......" *'Kleine Erdbebenkunde'* by K. Jung, 51.

33. HIRONO, T. (1948, 49): Mathematical Theory on Shallow Earthquake. *Geophys. Mag.*, **18**, 1–116, **21**, 1–97.

34. HODGSON, J.H., and W.G. MILNE (1951): Direction of Faulting in Certain Earthquakes of the North Pacific. *Bull. Seismol. Soc. Am.*, **41**, 221–242.

35. HODGSON, J.H., and R.S. STOREY (1953): Tables extending BYERLY's Fault-Plane Techniques to Earthquakes of Any Focal Depth. *Bull. Seismol. Soc. Am.*, **43**, 49–61.

36. HODGSON, J.H., and P.C. BREMMER (1953): Direction of Faulting in the Ancash, Peru, Earthquake of November 10, 1946, from Teleseismic Evidence. *Bull. Seismol. Soc. Am.*, **43**, 121–125.

37. HODGSON, J.H., and R.S. STOREY (1954): Direction of Faulting in Some of the Larger Earthquakes of 1949. *Bull. Seismol. Soc. Am.*, **44**, 57–83.

38. HODGSON, J.H., and J.F.J. ALLEN (1954, a): Tables of Extended Distances for PKP and PcP. *Pub. Dominion Obs. Ottawa*, **16**, 329–348.

39. HODGSON, J.H., and J.F.J. ALLEN (1954, b): Tables of Extended Distances for PP and pP, *Pub. Dominion Obs. Ottawa*, **16**, 349–362.

40. HODGSON, J.H. (1955, a): Fault Plane Solution for the Tango, Japan, Earthquake of March 7, 1927. *Bull. Seismol. Soc. Am.*, **45**, 37–41.

41. HODGSON, J.H. (1955, b): Direction of Faulting in Pacific Earthquakes. *Geofisica Pura e Applicata*, **32**, 31–42.

42. HODGSON, J.H., J.F.J. ALLEN, and J.I. COCK (1956): Tables of Extended Distances for PPP, pPP, pPKP and for P at Very Short Distances. *Pub. Dominion Obs. Ottawa*, **18**, 85–100.

43. HODGSON, J.H. (1956, a): Direction of Faulting in Some of the Larger Earthquakes of the Southwest Pacific, 1950–1954. *Pub. Dominion Obs. Ottawa*, **18**, 171–216.

44. HODGSON, J.H. (1956, b): Direction of Faulting in Some of the Larger Earthquakes of the North Pacific, 1950–1953. *Pub. Dominion Obs. Ottawa*, **18**, 219–252.

45. HODGSON, J.H., and J.I. COCK (1956): Direction of Faulting in the Deep-Focus Spanish Earthquake of March 29, 1954. *Tellus*, **8**, 321–328.

46. Homma, S. (1952): Initial Value Problem in the Theory of Elastic Waves. *Geophys. Mag.*, **23**, 145–182.

47. HONDA, H. (1931): On the Initial Motion and the Types of the Seismograms of the North Idu and the Itô Earthquakes. *Geophys. Mag.*, **4**, 185–213.

48. HONDA, H. (1932, a): On the Mechanism and the Types of the Seismograms of Shallow Earthquakes. *Geophys. Mag.*, **5**, 69–88.

49. HONDA, H. (1932, b): On the Types of the Seismograms and the Mechanism of Deep Earthquakes. *Geophys. Mag.*, **5**, 301–326.

50. HONDA, H. (1933): Notes on the Mechanism of Deep Earthquakes. *Geophys. Mag.*, **7**, 257–267.

51. HONDA, H. (1934, a): On the Amplitude of the P and the S Waves of Deep Earthquakes. *Geophys. Mag.*, **8**, 153–164.

52. HONDA, H, (1934, b): On the ScS Waves and the Rigidity of the Earth's Core. *Geophys. Mag.*, **8**, 165–177

53. HONDA, H. (1934, c): On the Mechanism of Deep Earthquakes and the Stress in the Deep Layer of the Earth Crust. *Geophys. Mag.*, **8**, 179–185.

54. HONDA, H. (1934, d): On the Amplitude of the P and the S Waves of Deep Earthquakes (Second Paper). *Geophys. Mag.*, **8**, 327–332.

55. HONDA, H., and T. MIURA (1935): On the Strain produced in a Semi-infinite Elastic Solid by Statical Surface Force, with Some Applications to Seismology. *Geophys Mag.*, **9**, 61–81.

56. HONDA, H., and T. MIURA (1938): On the Amplitude of the P and the S Waves of Deep Earthquakes (Third Paper). *Geophys. Mag.*, **11**. 299–305.

57. HONDA, H., and H, ITÔ (1940): On the Period of the P Waves and the Magnitude of the Earthquake. *Geophys. Mag.*, **13**, 155–161.

58. HONDA, H., and Y. HASAYA (1940): On the ScS Waves and the Rigidity of the Earth's Core (Second Paper). *Geophys. Mag.*, **13**, 219–230.

59. HONDA, H. (1951): Amplitudes of P and S, Magnitude and Energy of Deep Earthquakes. *Science Reports, Tôhoku Univ. Ser.* **5**, *Gepohys.*, **3**, 138–143.

60. Honda, H., and H. Itô (1951) : On the Reflected Waves from Deep Focus Earthquakes. *Science Reports, Tôhoku Univ. Ser.* 5, *Gepohys.*, **3**, 144 155.

61. Honda, H., and A. Masatsuka (1952) : On the Mechanisms of the Earthquakes and the Stresses producing Them in Japan and Its Vicinity. *Science Reports, Tôhoku Univ. Ser.* 5, *Geophys.*, **4**, 42–60.

62. Honda, H., and H. Watanabe (1952) : A Remark on the Amplitude of the Initial Motion of Very Shallow Earthququkes. *Science Reports, Tôhoku Univ. Ser.* 5, *Geophys.*, **4**, 94–97.

63. Honda, H. (1954) : *'The Seismic Waves,'* 1-230, (In Japanese).

64. Honda, H., H Sima, and K. Nakamura (1955) : The ScS Wave, the Mechanism of Deep Earthquake and the Rigidity of the Earth's Core. *Science Reports, Tôhoku Univ. Ser.* 5, *Geophys.*, **7**, 169–179.

65. Honda, H., A. Masatsuka, and K. Emura (1956) : On the Mechanism of the Earthquakes and the Stresses producing Them in Japan and Its Vicinity (Second Paper). *Science Reports, Tôhoku Univ. Ser.* 5, *Geophys.*, **8**, 186–205.

66. Ingram, R.E., (1953) : Vibration Angle of S Wave. *Bull. Seismol. Soc. Am.*, **43**, 145-151.

67. Ingram, R.E. and J.H. Hodgson (1956) : Phase Change of PP and pP on Reflection at a Free Surface. *Bull. Seismol. Soc. Am.*, **46**, 203–213.

68. Inouye, W. (1936,37,38) : Notes on the Origins of Earthquakes. *Bull. Earthquake Res. Inst.*, **14**, 582–598, **15**, 90–101, 674–685, 686–696, 956-964, **16**, 125 130, 597–631.

69. Ishimoto, M. (1932) : Existence d'une Source Quadruple au Foyer Sismique d'aprés l'étude de la Distribution des Mouvements Initiaux des Secousses Sismiques. *Bull. Earthquake Res. Inst.*, **10**, 449-471.

70. Ishimoto, M. (1933) : La Déformation de la Croûte Terrestre et la Production des Ondes Sismique au Foyer. *Bull. Earthquake Res. Inst.*, **11**, 254–274.

71. Jeffreys, H. (1931) : On the Cause of Oscillatory Movements in Seismograms. *Monthly Notices. Roy. Astr. Soc. Geophys. Suppl.*, **2**, 407-416.

72. Jones, J.W. (1952) : Seismogram Types and Initial Motion at Seattle. *Pub. Bur. Centr. Seismol. Int. Ser. A. Travaux Scientifiques*, **18**, 221-236.

73. Kanai, K. (1951) : Possibility of the Period of P-Waves becoming Smaller than Those of S-Waves. *Bull. Earthquake Res. Inst.*, **29**, 529-537.

74. Kanai, K. (1952) : Examinations of the Assumption concerning Mechanism of Earthquake Origin through Seismograms. *Bull. Earthquake Res. Inst.*, **30**, 39–51.

75. Kanai, K., K. Osada, and S. Yoshizawa, (1953) : The Relation between the Amplitude and the Period of Earthquake Motion. *Bull. Earthquake Res. Inst.*, **31**, 45–55.

76. Kawasumi, H. (1933,34a,34b) : Sudy on the Propagation of Seismic Waves. *Bull. Earthquake Res. Inst.*, **11**, 403 453, **12**, 660-705, 854-856.

77. Kawasumi, H., and R. Yosiyama (1934) : On the Mechanism of a Deep-Seated Earthquake as revealed by the Distribution of the Initial Motions at Stations throughout the World. *Proc. Imp. Acad. Japan*, **10**, 345–348.

78. Kawasumi, H., and R. Yosiyama (1935) : On the Elastic Wave animated by the Potential Energy of Initial Strain. *Bull. Earthquake Res. Inst.*, **13**, 496-503.

79. Kawasumi, H. (1937) : An Historical Sketch of the Development of Knowledge concerning the Initial Motion of an Earthquake. *Pub. Bur. Centr. Seismol. Int. Ser. A. Travaux Scientifiques*, **15**, 1 76.

80. Keilis-Borok, V.I. (1956) : Methods and Results of the Investigations of Earthquake Mechanism (A Brief Information). *Pub. Bur. Centr. Seismol. Int. Ser. A. Travaux Scientifiques*, **19**, 383 394.

81. Konig, L.P.G. (1942) : On the Mechanism of Deep Focus Earthquakes. *Beitr. z. Geophys.*, **58**, 159–197.

82. Matsuzawa, T. (1926) : On the Relative Magnitude of the Preliminary and the Principal Portion of Earthquake Motions. *Jap. Journ. Astro. and Geophys.*, **4**, 1–33.

83. Matsuzawa, T. (1932) : An Example of the Surface Reflection of the Plane Waves. *Zishin*, **4**, 125-139. (In Japanese).

84. Mühlhäuser, S. (1957) : Herdmechanische Vorgänge bei Einigen Zirkumpazifischen Erdbeben. *Tellus*, **9**, 104–117.

85. Nakano, H. (1923) : Notes on the Nature of the Forces which give Rise to the Earthquake Motions. *Seismol. Bull. Centr. Met. Obs. Japan*, **1**, 92-120.

86. NAKANO, H. (1930) : Some Problems concerning the Propagation of the Disturbances in and on Semi-infinite Elastic Solid. *Geophys. Mag.*, **2**, 189–348.

87. NEUMANN, F. (1930) : An Analysis of the S-Wave. *Bull. Seismol. Soc. Am.*, **20**, 15–32.

88. NISHIMURA, G. (1937) : On the Elastic Waves due to Pressure Variation on the Inner Surface of a Spherical Cavity in an Elastic Solid. *Bull. Earthquake Res. Inst.*, **15**, 614-635.

89. NISHIMURA, G., and T. TAKAYAMA (1938) : Seismic Waves due to Tractions applied to the Inner Surface of a Spherical Cavity in an Elastic Earth. *Bull. Earthquake Res. Inst.*, **16**, 317–354.

90. NUTTLI, O.W. (1952) : The Western Washington Earthquake of April 13, 1949. *Bull. Seismol. Soc. Am.*, **42**, 21–28.

91. RITSEMA, A.R. (1953) : Some New Data about Earthquake Movements at Great Depth in the Indonesian Archipelago. *Indonesian Journal for Natural Science*, **1-3**, 34–40.

92. RITSEMA, A.R. (1954) : The Sense of the Principal Shearing Stresses in the Tonga-Kermadec Seismic Zone. *Indonesian Journal of Science*, **5**, 161–175.

93. RITSEMA, A.R. (1955) : The Fault Plane Technique and the Mechanism in the Focus of the Hindu Kush Earthquakes. *Indian Journal of Meteorol. and Geophys.*, **6**, 41-50.

94. SAGISAKA, K. (1930) : A Relation between the Motion at a Hypocenter and the Types of Seismograms. *Geophys. Mag.*, **3**, 165–176.

95. SATÔ, Y. (1949) : Boundary Conditions in the Problem of Generation of Elastic Waves. *Bull. Earthquake Res. Inst.*, **27**, 1–9.

96. SATÔ, Y. (1950) : Transformations of Wave-functions related to the Transformations of Coordinate Systems. *Bull. Earthquake Res. Inst.*, **28**, 1–22, 175-217.

97. SCHEIDEGGER, A.E. (1955) : The Physics of Orogenesis in the Light of New Seismological Evidence. *Trans. Roy. Soc. Canada*, Sec. **4**, **49**, 65-93.

98. SCHEIDEGGER, A. E. (1956) : Forces in the Earth's Curst. *'Handb. d. Phys.* edited by S. FLÜGGE, *Geophys. I'*, 258-287.

99. SCHEIDEGGER, A.E. (1957) : The Geometrical Representation of Fault-Plane Solutions of Earthquakes. *Bull. Seismol. Soc. Am.*, **47**, 89-110.

100. SEZAWA, K. and K.KANAI (1932) : Amplitudes of P-and S-Waves at Different Focal Distances. *Bull. Earthquake Res. Inst.*, **10**, 299–334.

101. SEZAWA, K. (1935) : Elastic Waves produced by Applying Statical Force to a Body or by Releasing It from a Body. *Bull. Earthquake Res. Inst.*, **13**, 740–749.

102. SEZAWA, K., and K. KANAI (1936) : Elastic Waves formed by Local Stress Changes of Different Rapidities. *Bull. Earthquake Res. Inst.*, **14**, 10–17.

103. SEZAWA, K., and K. KANAI (1941,42) : Transmission of Arbitrary Elastic Waves from a Spherical Source, solved with Operational Calculus. *Bull. Earthquake Res. Inst.*, **19**, 151-161, 417-442, **20**, 1-19.

104. SHARPE, J.A. (1942) : The Production of Elastic Waves by Explosion Pressures. I. Theory and Empirical Field Observations. *Geophysics*, **7**, 144–154.

105. SOEDA, K. (1944) : On the Deformation produced in a Semi-infinite Elastic Solid by an Internal Source of Stress. *Kenshin Zihô*, **13**, 263–291. (In Japanese).

106. STILLE, H. (1955) : Recent Deformations of the Earth's Crust in the Light of Those of Earlier Epochs. *'Crust of the Earth'*, 171-191.

107. STONELEY, R. (1951) : Polarisation of the S-Phase of Seismograms. *Annali di Geofisica*, **4**, 3-8.

108. TAKAGI, H. (1950) : On the Distribution of Initial Motion of Seismic Waves (Summary). *Mem. Kôbe Marine Obs.*, **8**, 50-68.

109. TANDON, A.N. (1955) : Direction of Faulting in the Great Assam Earthquake of 15 August, 1950. *Indian Journ. Meteorol. and Geophys.*, **6**, 61-64.

110. TEISSEYRE, R. (1956) : Non-Local Models of Seismic Foci. *Acta Geophysica Polonica*, **4**, 226-236.

111. TSUBOI, C. (1939) : Deformations of the Earth's Crust as disclosed by Geodetic Measurements. *Beitr. z. Geophys. Ergeb. d. Kosmischen Physik*, **4**, 106-168.

112. USAMI, T., and T. HIRONO (1956) : Elastic Waves generated from a Spheroidal Cavity whose Wall is subjected to Normal Stress of Harmonic Type. *Papers in Meteorol. and Geophys.*, Meteorol. Res. Inst. Tôkyô, **7**, 288-321.

113. VANĚK, J. (1953) : A Contribution to the Theory of Elastic Waves produced by Shock.

Chechosl. Journ. Phys., **3**, 97-119.

114. Vening Meinesz, F.A. (1954) : Indonesian Archipelago : A Geophysical Study. *Bull. Geol. Soc. Am.*, **65**, 143-164.

115. Wadati, K., K. Sagisaka, and K. Masuda (1933) : On the Travel Time of Earthquake Waves (Part I). *Geophys. Mag.*, **7**, 87-99.

116. Wadati, K., and K. Masuda (1933, 34) : On the Travel Time of Earthquake Waves (Part V, VI). *Geophys. Mag.*, **7**, 269-290, **8**, 187-194.

117. Whipple, F.J.W. (1936) : On the Theory of the Strains in an Elastic Solid bounded by a Plane when there is a Nucleus of Strain at an Internal Point, and on the Relation of the Theory to Seismology. *Monthly Notices Roy. Astr. Soc. Geophys. Suppl.*, **3**, 380-388.

118. Willmore, P.L., and J.H. Hodgson (1955) : Charts for Measuring Azimuth and Distance for Tracing Seismic Rays through the Earth. *Pub. Dominion Obs. Ottawa*, **16**, 405-414.

119. Wilson, J.T. (1954) : The Development and Structure of the Crust. *'The Earth as a Planet'* edited by G.P. Kuiper, 138-214.

120. Yamakawa, N. (1955) : On the Strain produced in a Semi-infinite Elastic Solid by an Interior Source of Stress. *Zishin*, **8**, 84-98. (In Japanese).

(Added in proof.)

Hodgson, J.H. (1957) : Nature of Faulting in Large Earthquakes. *Bull. Geol. Soc. Am.*, **68**, 611-644.

Kogan, S. D. (1955) : Dynamical Parameters for Origin of Deep Earthquakes. *Publ. Geophys. Inst. Acad. Sci. U.S.S.R.* **30**, 30-81. (In Russian).

On the Focal Mechanism of Southeast Asian Earthquakes

by A. R. RITSEMA,

Meteorological and Geophysical Institute, Djakarta, Indonesia.

ABSTRACT

The mechanism in the focus of about 60 southeast Asian earthquakes has been determined. BYERLY's method (1938) in the form developed by the present writer is used. With the help of seismogram readings of the position of the line of polarization of S waves it was determined that in at least twelve of the shocks a single couple of forces acting along the line of fault movement was the cause of the earthquakes (KEYLIS-BOROK, 1956). In about half of the total material, however, no conclusive evidence could be found for a choice between this type of mechanism in the focus and that of two opposite couples of forces of equal magnitude acting along lines perpendicular to each other (HONDA, 1957). In the following it is assumed that these shocks also are caused by the first mentioned force system in the focus. Following and amplifying HODGSON's statement (1958), it is concluded that sufficiently reliable data for earthquake mechanism studies can be expected only from P, PKP and S waves. According to the fault movements in the focus different earthquake types are distinguished (transcurrent, clockwise and counterclockwise, normal and reversed).

In the section dealing with southeast Asian earthquake mechanism it is seen that transcurrent fault movements are about three times more common than they should be in case of a chance distribution of earthquake types. Evidence is given for small differences of earthquake mechanisms in depth and region. It is concluded that most of the fault displacements are directed perpendicular to the steeply dipping zones of seismic activity in the region. Also in the shocks in which these directions do not coincide, the plane of action still stands more or less perpendicular to this zone. This coincidence for the great majority of the earthquakes can only mean that the distribution of earthquakes in space and the fault displacements of the same probably are expressions of one and the same causal fact.

From the earthquake mechanisms shown to exist in the New Guinea-Solomons arcs it should follow that in these areas the seismic activity is concentrated in a zone steeply dipping under the Pacific Ocean side and not under the continental (i.e. Australian) side as is the case in the Sunda and the Celebes-Philippines arcs.

GENERAL PRINCIPLES OF THE METHOD

INTRODUCTION

Focal mechanism studies of earthquakes of the Sunda arc, the Celebes-Philippines arc, and the New Guinea-Solomons arcs were executed at the Seismological Department of the Meteorological and Geophysical Institute, Djakarta. Table I comprises the solutions reached. The data on which the solutions are based can be found in the publication series of the Djakarta Institute. One solution reached by HODGSON (1956) for an earthquake of the Solomon Islands group is included in the Table as earthquake number 43. The tentative determination of the direction of fault displacement of this shock is based on the S waves observed at the Indonesian stations.

The solutions reached by VELDKAMP (1957) for Sumatran shocks are not included in the list. The complete solutions of these shocks will appear in the near future in the publication series of the Royal Netherlands Meteorological Institute, De Bilt.

The principle on which the study of earthquake mechanisms is based is the assumption that the initial character of the seismic waves remains the same from a small sphere around the focus to the observing stations. A compressional (or dilatational) P wave in a station means that the wave started from the focal region as a compression (or dilatation).. At the same time it is assumed that the angle α between the line of polarization of an S wave and the plane of incidence remains constant. This means that the proportion SH/SV as determined in the station is the same as that in the focal region.

Table I. The earthquake mechanisms of southeast Asia.

No.	Date G.M.T.	Epicenter	Depth Magnitude	I	II	III	IV	V	VI	Type	Evidence
1	1930 June 4 09h 50m 29s	6 1/2° S 128 1/2 E	0.06 R 6 3/4	53° 14	160° 50	52°	313° 36	205° 22	91° 46	P (R)	poor
2	1931 Mar. 28 12.38.37	7 S 129 1/2 E	0.01 R 7.3	50 7	144 29	30	307 60	190 15	93 26	R (P)	poor
3	1934 June 29 08.25.17	6 3/4 S 123 3/4 E	0.11 R 6.9	98 38	340 31	41	223 36	35 54	180 4	T (R)	poor
4	1935 Oct. 4 05.15.36	6 N 125 E	0.07 R 6 1/2	50 70	290 10	31	197 16	309 52	96 33	T (R)	poor
5	1936 Jan. 20 16.56.19	6 N 127 E	0.01 R 7.1	175 4	85 6	6	300 82 1/2	40 1	130 7	L (P)	fair
6	1936 Apr. 28 13.35.45	6 1/2 S 129 E	0.03 R 6 1/2	300 35	47 23	29	163 46	358 43	261 7	L (T)	poor
7	1936 May 8 09.11.34	5 3/4 S 112 3/4 E	0.09 R 6 1/2	235 9	143 15	15	355 72	98 4	190 17	L (P)	poor
8	1936 June 10 08.23.21	5 1/2 S 147 E	0.02 R 6.9	97 23	196 20	22	323 58	56 2	147 32	R (P)	fair
9	1937 Apr. 5 06.56.41	1 S 133 E	0.01 R 6.9	215 7	123 18	19	326 70	171 18	78 8	R (T)	fair
10	1937 Aug. 11 00.55.52	6 1/2 S 116 1/2 E	0.09 R 7.2	347 66	191 22	67	98 8	208 66	4 22	T (R)	poor
11	1938 Aug. 18 09.30.04	3 3/4 S 102 3/4 E	0.01 R 6.9	330 63	150 27	90	60 0	330 18	150 72	P (?)	poor
12	1938 Aug. 31 17.45.13	4 S 151 1/2 E	0.05 R 6 3/4	106 13	200 18	19	342 68	244 3	152 22	R (P)	poor
13	1938 Oct. 20 02.19.29	9 1/4 S 123 E	0.01 R 7.3	264 42	156 19	26	49 42	200 44	305 14	T (R)	fair
14	1939 Dec. 21 21.00.40	0 123 E	0.02 R 8.0	150 57	357 30	67	260 12	166 14	30 71	P (L)	fair
15	1940 June 18 13.52.33	5 1/2 N 123 E	0.08 R 6 1/2	120 50	315 39	79	218 7	224 76	122 3	T (R)	poor
16	1940 June 22 11.36.46	0 122 1/2 E	0.03 R 6 3/4	148 36	25 37	48	266 33	357 1	87 57	P (L)	fair
17	1940 Sept. 22 22.51.58	7 1/2 N 123 1/2 E	0.10 R 6 3/4	302 52	55 17	28	157 33	17 50	261 21	T (L)	fair
18	1940 Oct. 7 06.43.04	5 N 126 E	0.01 R 7.0	322 26	72 35	40	203 44	13 46	108 5	T (L)	poor
19	1941 Jan. 31 02.38.40	6 1/2 S 128 1/2 E	0.03 R 6 3/4	174 9	77 36	37	276 53	132 32	30 18	R (T)	fair
20	1941 Feb. 4 14.03.12	9 N 124 E	0.09 R 6.9	321 44	105 40	63	212 19	35 70	303 2	T (L)	fair
21	1941 Feb. 25 05.37.45	9° S 125 E	0.02 R 6.9	135 42	38 7	10	300 47	184 23	67 34	L (P)	fair
22	1941 Sept. 4 10.21.44	4 1/2 S 154 E	0.01 R 7.1	208 25	103 28	32	332 50	65 2	156 40	L (P)	fair
23	1941 Sept. 17 06.48.04	1/4 N 122 3/4 E	0.03 R 7.1	91 23	344 34	38	208 47	43 42	306 8	R (T)	fair
24	1941 Nov. 27 08.37.34	6 1/2 S 121 E	0.07 R 6 3/4	137 17	23 53	57	238 32	342 21	100 51	P (L)	fair
25	1942 May 28 01.01.48	0 124 E	0.01 R 7.5	120 15	212 8	8	329 73	167 16	75 5	L (T)	fair
26	1942 July 25 06.22.35	11 1/2 N 124 1/2 E	0.01 R 6 3/4	200 12	293 13	14	68 72	247 18	337 1/2	L (T)	fair
27	1943 June 30 10.49.02	7 S 122 E	0.11 R 6 3/4	278 20	180 20	22	49 61	318 0	228 29	L (P)	poor
28	1943 Dec. 1 06.04.55	4 1/2 S 144 E	0.01 R 7.2	171 6 1/2	80 12	12	290 76	126 13	35 3	R (T)	fair
29	1944 Mar. 22 00.43.18	8 1/2 S 123 1/2 E	0.03 R 7.5	110 25	12 16	18	252 60	152 6	59 30	L (P)	fair
30	1945 Apr. 22 09.51.18	5 N 123 E	0.10 R 6 3/4	240 10	133 60	61	335 28	211 47	83 29	T (R)	poor

Table I. The earthquake mechanismes of southeast Asia—*Concluded.*

No.	Date G.M.T.	Epicenter	Depth Magnitude	I	II	III	IV	V	VI	Type	Evidence
31	1945 May 9 03.31.13	7 1/2° S 124 E	0.08 R 6.3/4	107° 45	355° 20	30°	249° 38	40° 48	147° 15	T (R)	poor
32	1946 June 15 18.29.16	3 S 128 E	0.01 R 6 1/4	128 17	34 13	14	268 68	80 22	172 3	R (T)	poor
33	1948 Jan. 28 03.47.21	1 1/2 N 126 1/2 E	0.01 R 7.2	304 30	187 37	44	61 38	249 52	154 4	T (R)	fair
34	1949 Apr. 23 11.15.39	8 S 121 E	0.01 R 7.1	76 20	185 40	44	327 43	225 13	122 44	P (R)	poor
35	1949 Apr. 30 01.23.37	7 N 125 E	0.02 R 7.4	157 21	257 23	26	30 58	297 2	206 32	R (P)	fair
36	1950 Aug. 7 02.44.45	7 1/2 N 124 1/2 E	0.01 R 6 3/4	141 23	240 20	23	7 58	100 2	191 32	R (P)	fair
37	1950 Sept. 14 09.05.50	1/2 N 127 E	0.03 R 6 1/2	51 4	321 4	4	186 84	6 6	276 0	R (T)	poor
38	1950 Dec. 4 16.28.01	5 S 153 1/2 E	0.01 R 7	113 30	221 28	33	345 47	76 1	167 43	R (P)	fair
39	1951 Feb. 17 21.07.09	7 S 146 E	0.03 R 7 1/4	158 55	56 8	14	320 34	88 42	208 29	T (R)	fair
40	1952 Feb. 11 07.01.06	5 1/2 S 109 3/4 E	0.10 R 6.9	94 26	198 26	30	326 51	146 39	56 0	L (T)	fair
41	1952 Feb. 14 03.38.15	7 3/4 S 126 1/2 E	0.00 R 7 1/4	217 3	126 16	16	317 74	173 13	81 10	R (T)	fair
42	1952 Mar. 19 10.57.09	9 1/2 N 126 E	0.00 R 7 1/2	228 37	102 38	50	344 31	165 59	75 1	T (R)	fair
43	1952 May 9 17.47.40	6 1/2 S 155 E	0.01 R 7	308 34	206 18	22	93 50	350 10	253 38	L (P)	poor
44	1952 July 13 17.34.30	3 S 127 1/2 E	0.00 R 6 1/2	121 64	263 18	45	349 19	87 25	227 59	P (R)	fair
45	1953 Jan. 20 17.33.07	1 1/2 N 126 E	0.00 R 6 1/2	65 10	155 1	1	252 80	111 8	19 6	L (T)	fair
46	1953 Apr. 6 00.36.16	7 1/4 S 131 E	0.00 R 7	217 31	112 23	28	352 50	162 40	256 5	R (T)	fair
47	1953 June 25 10.44.57	8 1/2 S 123 1/2 E	0.00 R 7 1/4	114 3	204 2 1/2	3	330 86	69 0	159 4	R (P)	fair
48	1953 July 7 04.07.48	1 N 100 E	0.03 R 6 1/2	320 53	95 28	52	197 22	293 14	52 64	P (R)	fair
49	1953 Nov. 13 16.17.05	3 1/2 N 96 E	0.00 R 6 1/4	288 1	18 2	2	168 88	63 1/2	333 2	R (P)	poor
50	1953 Dec. 2 04.24.51	2 3/4 S 141 1/2 E	0.00 R 6 1/2	130 1	40 2	2	245 88	355 1/2	85 2	L (P)	fair
51	1954 Jan. 1 13.04.19	9 S 123 1/2 E	0.01 R 6 1/2	236 26	327 1	1	58 64	188 17	285 19	R (P)	fair
52	1954 Feb. 20 18.35.07	7 S 124 1/2 E	0.09 R 6 3/4	340 62	89 10	22	184 26	61 47	291 31	T (L)	fair
53	1954 Mar. 3 06.02.55	5 1/2 S 142 1/2 E	0.00 R 7	282 14	191 5	5	83 75	236 14	327 6	R (T)	fair
54	1954 June 6 16.50.40	3 S 135 1/2 E	0.00 R 7	249 2	346 75	75	158 15	55 41	264 44	P (R)	fair
55	1954 June 7 10.15.33	3 1/2 S 152 1/2 E	0.07 R 6 3/4	191 2	99 43	43	283 47	154 31	46 27	R (T)	fair
56	1954 July 3 22.31.25	6 1/2 S 105 1/2 E	0.01 R 6 3/4	37 24	165 54	63	295 25	198 16	78 60	P (R)	fair
57	1954 Sept. 20 00.39.28	1 1/2 S 120 1/2 E	0.00 R 6	145 52	254 14	24	354 35	100 23	217 47	P (R)	fair
58	1954 Oct. 3 23.21.35	1 1/2 S 127 1/2 E	0.00 R 6 1/4	201 3	110 10	10	307 80	65 5	155 9	L (P)	fair
59	1954 Nov. 2 08.24.10	8 S 119 E	0.00 R 6 1/2	91 3	182 16	16	352 74	228 9	135 13	R (P)	fair

Methods

After gathering the initial motion data of P, PKP and S waves of many stations all over the world, the following procedure is pursued to arrive at a solution.

1. Determine the azimuth of the station from the epicenter, the epicentral distance, and the azimuth of the epicenter from the station. This is done using a chart published by the Dominion Observatory (Willmore and Hodgson, 1955).

2. Determine the angle i at which the wave left the focus to emerge at the station. This is done with the help of a set of graphs showing for any depth of fucus (with intervals of 0.01R) the (i, Δ)-functions. The graphs are based on the Seismological Tables of Jeffreys and Bullen, and are calculated in the usual way (Byerly, 1955; Ritsema, 1952; Hodgson and Storey, 1953). An example of such a graph is shown in Figure 1.

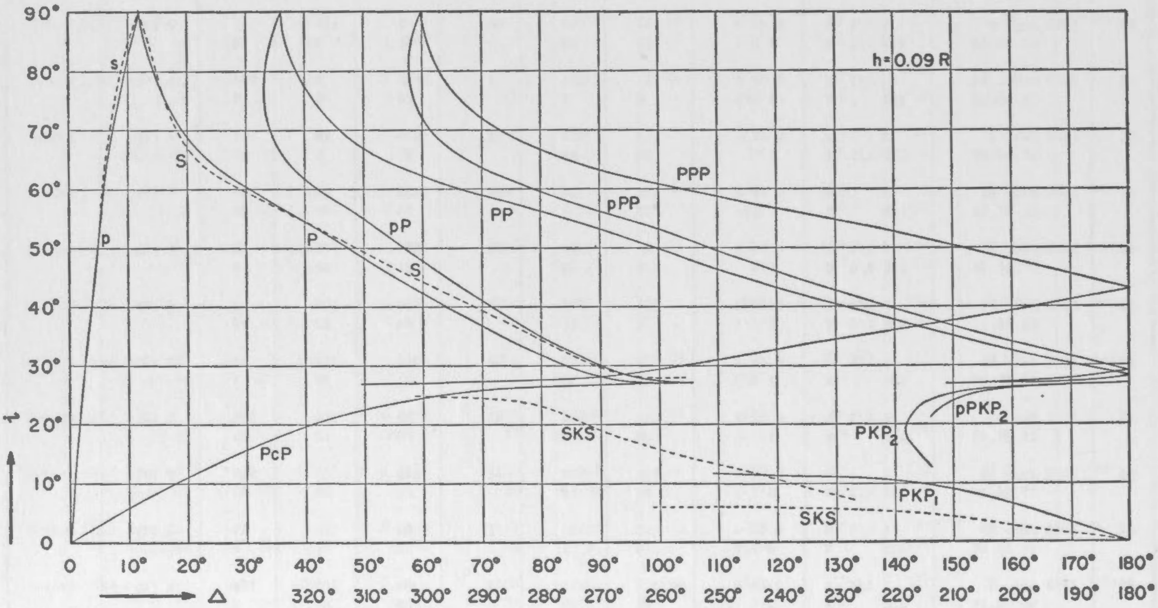

Figure 1. (i,Δ) curves for a focal depth of 0.09 R.

3. Plot the compressions and dilatations of the P and PKP waves in a diagram in the appropriate azimuth and at a distance of tan $i/2$ from the centre (*see* Figure 2).

4. Separate the compressions and dilatations by two nodal lines perpendicular to each other These lines must follow the course of a meridional line of Wulff's stereographic projection net (Figure 3). They represent the nodal planes in the focus in which no P wave is propagated.

5. Resolve S wave amplitudes in the SH and SV components with the help of the azimuth of the epicenter from the station. The angle α is determined, of which the tangent equals SH/SV.

6. Plot a vector in the diagram from the proper place of observation in a direction that makes an angle of α with the radial direction between the centre of the diagram and the station's projection. Note the sign of the initial motions, for SH either to left (L) or to right (R), and for SV either upward (U) or downward (D), (*see* Figure 4).

7. Determine which of the two types of initial S-wave motions was the actual one. In type I (*see* Keylis-Brook, 1956) with a single couple of forces in the focus acting along the line of fault movement, all S-wave vectors in the diagram must follow meridional lines that come together in the point representing the direction of fault movement (*see* Figure 5). In type II (*see* Honda, 1957) with two couples of forces of equal magnitude but opposed direction acting along the lines perpendicular to the two nodal planes for longitudinal waves in the focus, the

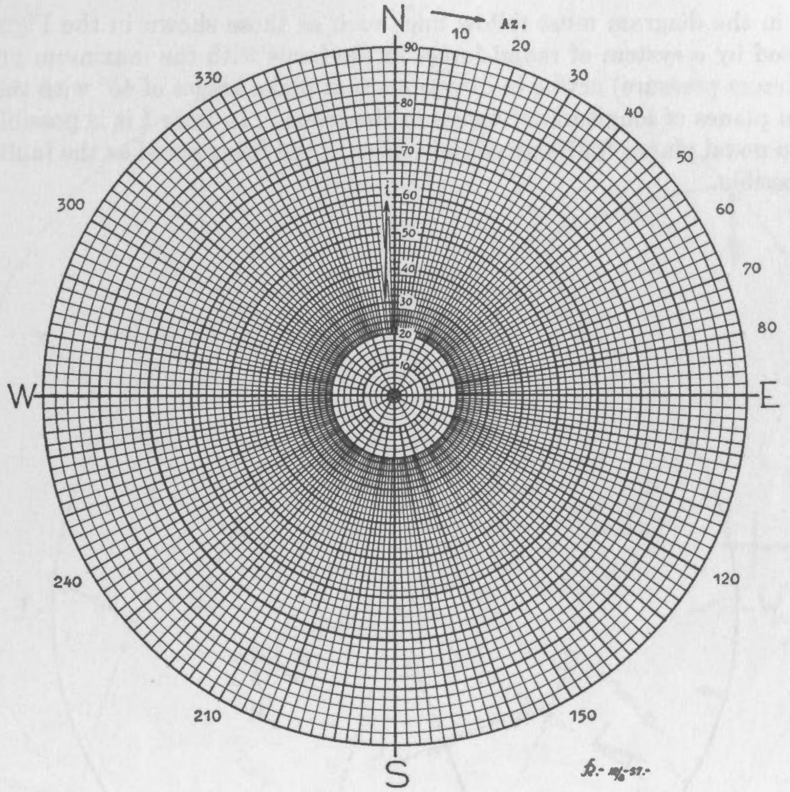

Figure 2. (*i,Az*) diagram used for the plotting of the data.

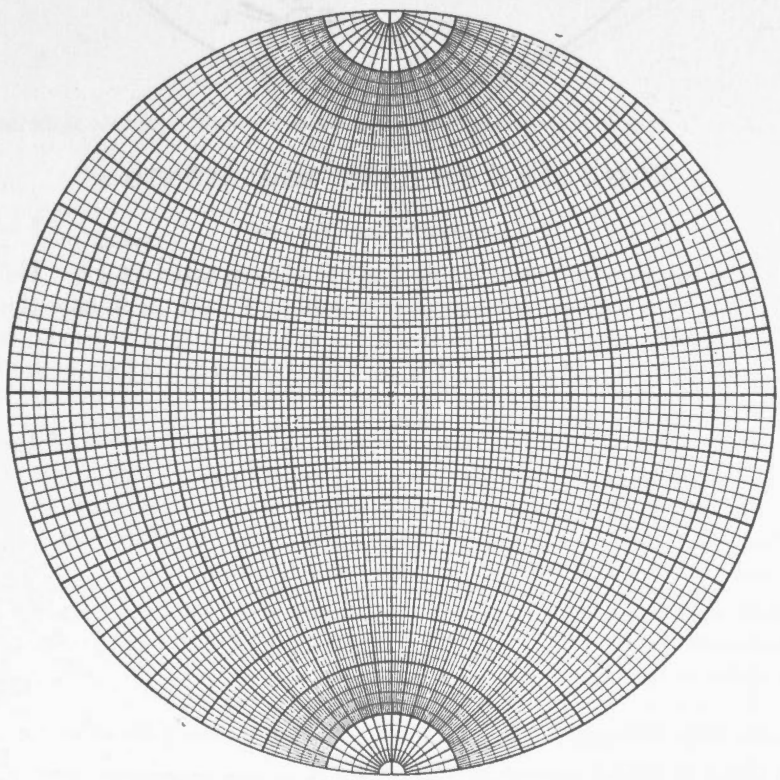

Figure 3. Wulff's stereographic projection net used for the determination of the course of the nodal lines and the direction of fault movement.

S-wave vectors in the diagram must follow lines such as those shown in the Figure 6. Case II also can be caused by a system of radial forces in the focus with the maximum pressure and the tension (or minimum pressure) acting in directions that make angles of 45° with those of the poles of the two nodal planes of longitudinal waves in the focus. In type I it is possible to determine which of the two nodal planes for longitudinal waves in the focus acted as the fault plane, in type II this is not possible.

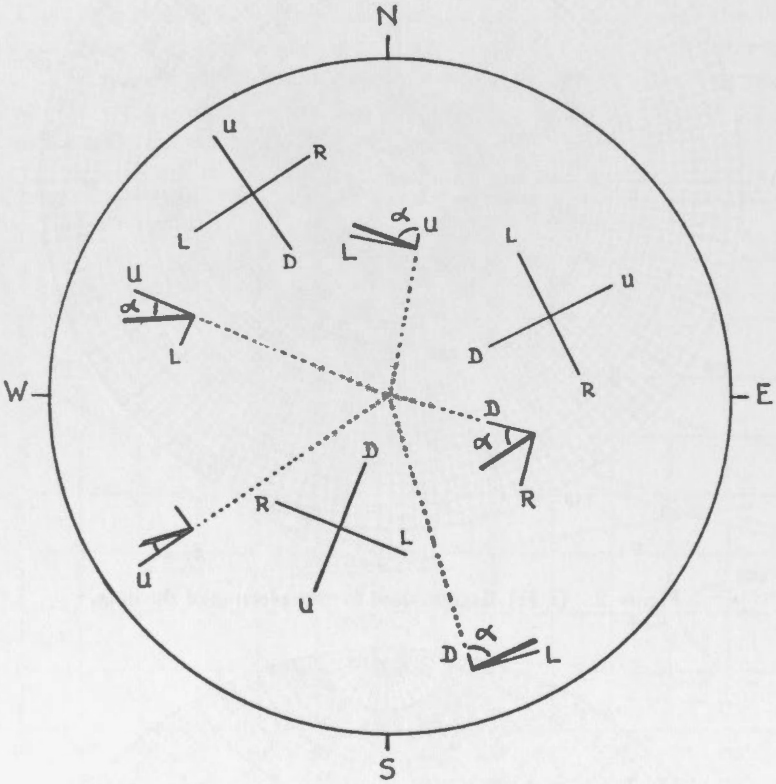

Figure 4. The plotting of S-wave data in the diagram.

Longitudinal Waves

Evidence for the solutions given in Table I is not always satisfactory. This can be caused by a scarcity of data, by a high percentage of contradictory data, or in case the position of the two nodal planes for longitudinal waves in the focus is fairly well established, by a lack of sufficiently reliable S-wave data. In Table II the earthquakes are listed for which no solution could be reached.

Numbers of consistent and inconsistent data of longitudinal waves of the earthquake of Table I are listed in Table III. These figures partly reflect the reliability of the solution, but a high number of consistent data do not implicitly mean that the solution is 'fair'. That also depends upon the distribution of the data in the diagram, and therefore it is not possible, solely on the basis of these numbers, to give the shock a classification.

It is seen from the Table that on the average 8 out of 9 P-wave data are consistent, and 7 out of 9 PKP-wave data. The percentage of the consistent data of reflected longitudinal waves is always of the order of about 2 out of 3.

S Waves and the Determination of the Type of Force System in the Focus

The actual sense of initial motion of the S wave is not implicitly needed for the choice between the two force types I and II; the position of the line of polarization is sufficient for the

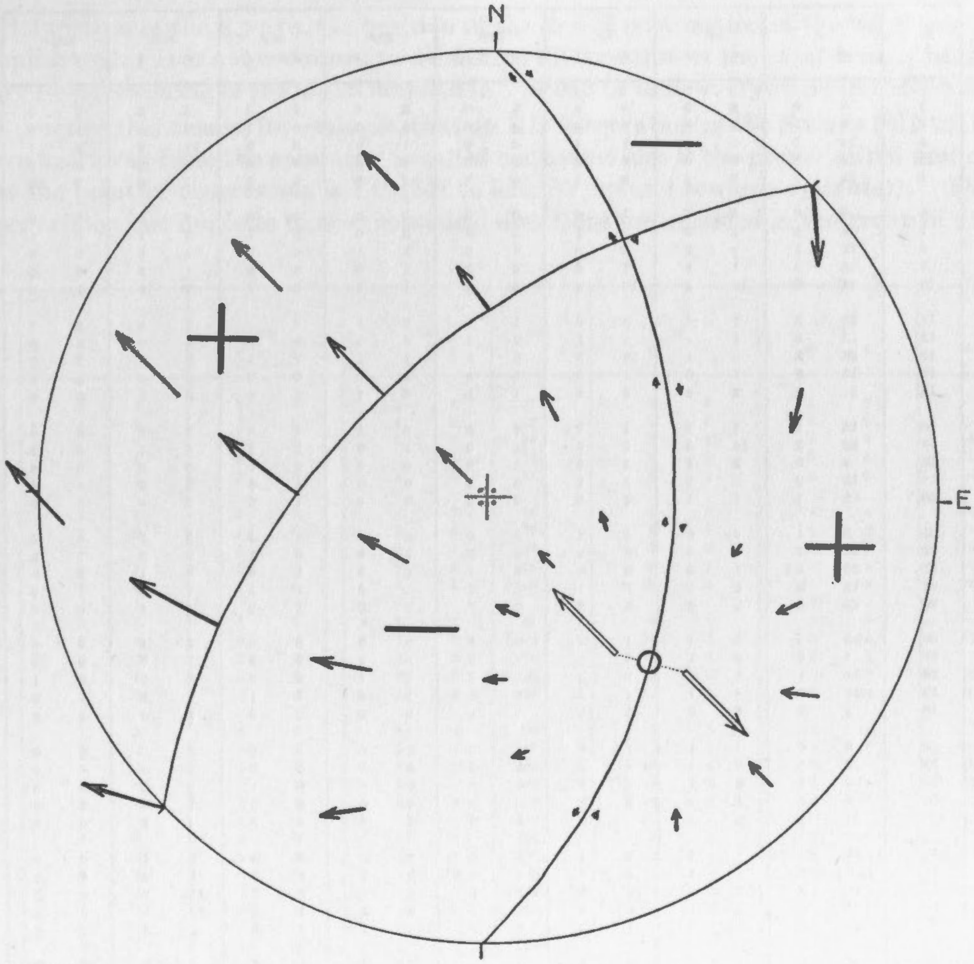

Figure 5. Theoretical course of S-wave vectors caused by force system of type I in the earthquake focus.

Table II. Earthquakes for which no solution could be reached.

Year and Date	H Time	Epicenter	Focal Depth	Magnitude
1934 October 26	14^h 44^m 29^s	6°S 124°E	0.11 R	6 3/4
1935 July 11	13 03 42	4 S 111 E	0.09 R	6
1936 February 12	09 34 30	6 S 116 E	0.09 R	6 1/2
February 27	10 04 08	7 S 127 E	0.02 R	6 3/4
May 19	07 22 26	5 1/2 S 112 1/2 E	0.09 R	6 1/2
1937 May 12	02 44 55	4 1/2 S 144 E	0.02 R	6 3/4
1938 January 18	04 20 04	4 S 101 1/2 E	0.01 R	6 1/2
April 4	21 09 03	7 S 127 E	0.06 R	6
May 8	14 40 35	6 S 124 E	0.10 R	5 3/4
1939 June 13	20 39 55	3/4 N 125 3/4 E	0.02 R	6.9
December 20	13 04 06	7 S 120 E	0.10 R	6
1941 January 2	16 49 38	3 N 122 1/2 E	0.07 R	6 1/4
March 14	16 08 18	7 S 120 E	0.08 R	6
1947 December 4	14 46 40	7 1/2 N 124 1/2 E	0.07 R	6

No.	P c	P i	pP c	pP i	ṗP c	ṗP i	pPP c	pPP i	PPP c	PPP i	PcP c	PcP i	PKP c	PKP i	pPKP c	pPKP i
1	5	0	0	0	0	0	0	0	0	0	0	0	2	0	0	0
2	9	1	0	4	4	0	0	0	0	0	0	1	3	1	1	0
3	14	2	1	3	1	5	2	2	1	0	0	0	11	0	0	1
4	8	0	0	0	0	0	0	0	0	0	0	0	0	0	0	0
5	13	3	0	1	0	1	0	0	1	0	0	0	2	0	0	0
6	8	0	2	0	1	0	0	0	0	0	0	0	0	0	0	0
7	6	0	4	3	2	1	2	0	0	0	0	1	3	1	0	1
8	17	1	2	2	4	0	2	0	1	1	0	0	4	0	0	0
9	15	3	1	0	7	4	0	0	1	0	0	0	1	0	0	0
10	36	6	18	4	10	8	5	8	1	3	0	2	7	0	1	0
11	22	2	7	1	8	0	1	1	0	1	0	0	6	0	1	0
12	12	0	1	1	1	3	0	0	0	0	0	1	4	0	0	0
13	25	3	8	1	13	3	6	0	2	1	2	1	8	1	0	0
14	17	6	1	0	1	0	0	0	0	0	0	0	2	0	0	0
15	21	2	9	3	2	5	1	1	0	1	0	0	0	1	0	0
16	18	2	2	2	1	2	0	0	0	1	0	0	3	2	0	0
17	33	2	14	3	9	6	14	0	1	0	3	1	6	1	0	2
18	9	0	2	1	2	0	0	0	0	0	0	0	0	0	0	0
19	13	0	2	0	3	1	0	0	0	0	1	0	2	0	0	0
20	19	2	1	1	2	0	0	0	0	0	1	0	2	0	0	0
21	8	1	0	0	0	1	0	0	0	0	1	0	2	1	0	0
22	16	2	4	0	6	2	0	0	1	0	0	1	9	3	1	0
23	29	0	7	9	9	6	5	4	4	0	1	0	5	1	1	0
24	15	0	6	0	7	1	1	1	1	0	1	1	7	0	1	0
25	22	3	0	2	6	2	0	0	2	0	0	0	4	2	0	0
26	14	2	0	1	1	2	0	0	0	0	0	0	2	1	0	0
27	5	0	0	1	0	2	1	0	0	0	0	0	2	0	0	0
28	11	1	1	2	5	3	0	0	0	1	0	0	6	3	0	1
29	11	0	4	1	4	3	0	0	0	0	0	1	9	2	0	0
30	3	0	0	0	0	0	0	0	0	0	0	0	1	0	0	0
31	6	0	1	1	1	0	0	0	0	0	0	0	3	2	0	0
32	7	0	2	1	1	5	0	0	0	0	0	0	2	0	0	0
33	9	1	0	1	1	2	0	0	0	0	0	1	2	1	0	0
34	8	0	1	2	5	2	0	0	0	0	0	0	1	0	0	0
35	24	5	2	1	4	3	0	0	1	0	0	0	4	2	0	0
36	21	4	1	1	5	4	1	0	0	0	0	0	6	1	0	0
37	6	0	0	1	4	0	0	0	0	1	0	0	1	0	0	0
38	21	3	2	2	3	6	1	0	0	0	0	0	11	6	0	2
39	24	5	4	1	6	5	0	0	0	0	1	0	12	3	0	2
40	39	6	8	0	6	3	0	0	3	2	1	0	17	4	3	4
41	24	6	1	0	19	5	0	0	2	1	0	0	14	3	0	0
42	55	10	0	0	15	6	0	0	5	1	0	0	7	4	0	0
43	24	5	1	0	6	1	0	0	0	0	0	0	22	7	1	3
44	17	3	0	0	10	3	0	0	1	0	0	0	7	4	1	0
45	22	3	0	0	10	2	0	0	4	1	1	0	12	3	0	0
46	31	2	0	0	16	7	0	0	1	0	2	1	19	6	0	0
47	30	5	0	0	13	9	0	0	1	1	0	0	22	5	0	0
48	28	5	2	2	6	1	3	0	0	0	0	0	9	5	0	0
49	24	4	0	0	4	2	0	0	0	0	0	0	12	3	0	0
50	25	6	1	0	9	4	0	0	1	0	0	0	9	3	1	0
51	15	1	3	0	7	3	1	0	0	0	2	0	11	7	1	1
52	39	4	5	4	5	2	3	0	4	0	2	0	19	7	1	1
53	35	7	0	0	22	8	0	0	7	1	0	0	28	5	0	0
54	33	7	0	0	20	7	0	0	2	1	0	0	23	4	0	0
55	42	1	8	6	9	9	0	0	1	0	1	0	14	7	0	2
56	66	3	2	0	16	12	0	0	3	1	2	0	27	8	0	0
57	17	1	0	0	10	2	0	0	0	0	2	1	7	3	0	0
58	19	1	0	0	5	2	0	0	0	0	2	0	3	1	0	0
59	22	3	0	0	12	3	0	0	2	1	1	0	11	4	0	0
Total	1187	145	141	69	359	179	49	17	54	20	27	13	448	128	14	20

Table III. Numbers of consistent (c) and inconsistent (i) data of longitudinal waves of the single earthquakes.

purpose. This position differs enough in types I and II to be able to determine which of the two was the actual one (*see* Figures 5 and 6).

This consideration is rather important, as it has been shown by Hodgson and Adams (1958) and also during this study that the reliability of the reading of any impulse that arrives later than P or PKP is considerably decreased. But in spite of the impossibility of a reliable reading of the initial motion of the S wave, the position of the line of polarization of the wave can be determined quite well. It is not necessary to determine this position at the exact time of beginning of the wave by a measuring of the initial amplitude. It can be done everywhere in the S-wave train.

In practice this means, for example, that an RD observation of the S wave (SH to the right, SV down and away from the epicenter) is called consistent also if the proper initial motion of the wave at the point of observation is LU (SH to left, SV up and towards epicenter). Thus, only the observations just opposite to the theoretical directions are included in the group of consistent data.

No.	Ia		Ib		II		No.	Ia		Ib		II	
	c	i	c	i	c	i		c	i	c	i	c	i
1	3	0	1	2	2	1	31	5	0	1	4	3	2
2	4	0	1	3	2	2	32	3	1	1	3	1	3
3	1	0	0	1	1	0	33	7	1	4	4	4	4
4	4	1	2	3	2	3	34	2	1	1	2	1	2
5	7	1	3	5	4	4	35	7	2	3	6	5	4
6	3	1	2	2	2	2	36	6	2	4	4	2	6
7	7	0	1	6	3	4	37	2	1	1	2	2	1
8	2	1	2	1	2	1	38	7	4	5	6	5	6
9	6	1	1	6	5	2	39	8	1	3	6	6	3
10	5	0	1	4	4	1	40	16	4	11	9	11	9
11	2	1	1	2	1	2	41	9	4	5	8	8	5
12	2	0	0	2	1	1	42	16	5	8	13	15	6
13	4	0	2	2	4	0	43	1	0	0	1	1	0
14	2	0	1	1	2	0	44	14	3	4	13	13	4
15	5	0	3	2	3	2	45	14	5	5	14	10	9
16	8	2	4	6	6	4	46	18	5	8	15	13	10
17	2	2	1	3	2	2	47	13	0	1	12	9	4
18	4	1	1	4	3	2	48	17	4	14	7	15	6
19	3	0	0	3	2	1	49	8	5	7	6	6	7
20	9	3	7	5	8	4	50	18	0	2	16	12	6
21	5	1	3	3	2	4	51	7	3	3	7	6	4
22	6	2	3	5	4	4	52	24	8	20	12	23	9
23	9	2	2	9	2	9	53	13	5	5	13	11	7
24	4	1	1	4	4	1	54	19	2	12	9	12	9
25	6	2	3	5	4	4	55	13	2	8	7	8	7
26	2	1	1	2	0	3	56	20	4	10	14	17	7
27	5	0	1	4	4	1	57	9	2	3	8	7	4
28	3	0	1	2	3	0	58	9	4	4	9	7	6
29	4	2	2	4	2	4	59	9	3	3	9	8	4
30	3	0	2	1	2	1							
							TOTAL	444	106	209	341	329	221

Table IV. Numbers of consistent (c) and inconsistent (i) S-wave data in the case of three different force systems in the focus.

In Table IV the number of consistent and inconsistent observations of S polarization are listed for each earthquake under three different assumptions. In column Ia it is assumed that a single couple acts in the focus, (type I of HONDA, 1957) and that nodal plane *a* is the fault. In column Ib it is again assumed that a single couple acts at the focus but that plane *b* represents the fault. In each case we have designated as *a* that plane giving the higher percentage of consistent data. In column II it has been assumed that two equal couples acted at right angles to each other in the focus (type II of HONDA, 1957).

Because the designation *a* has been given to that plane having the fewer inconsistencies, there is no significance in the difference between columns Ia and Ib. It is a difference between Ia and II which we must seek.

It is not always clear that there is such a difference; in nearly half of the earthquakes there is no appreciable difference between the numbers of consistent and inconsistent data. These shocks do not give sufficient evidence for the choice between the focal force systems I and II.

However it is worth noting that none of the earthquakes shows clearly better percentages for force type II than for force type Ia, whereas there are quite a few earthquakes with clearly

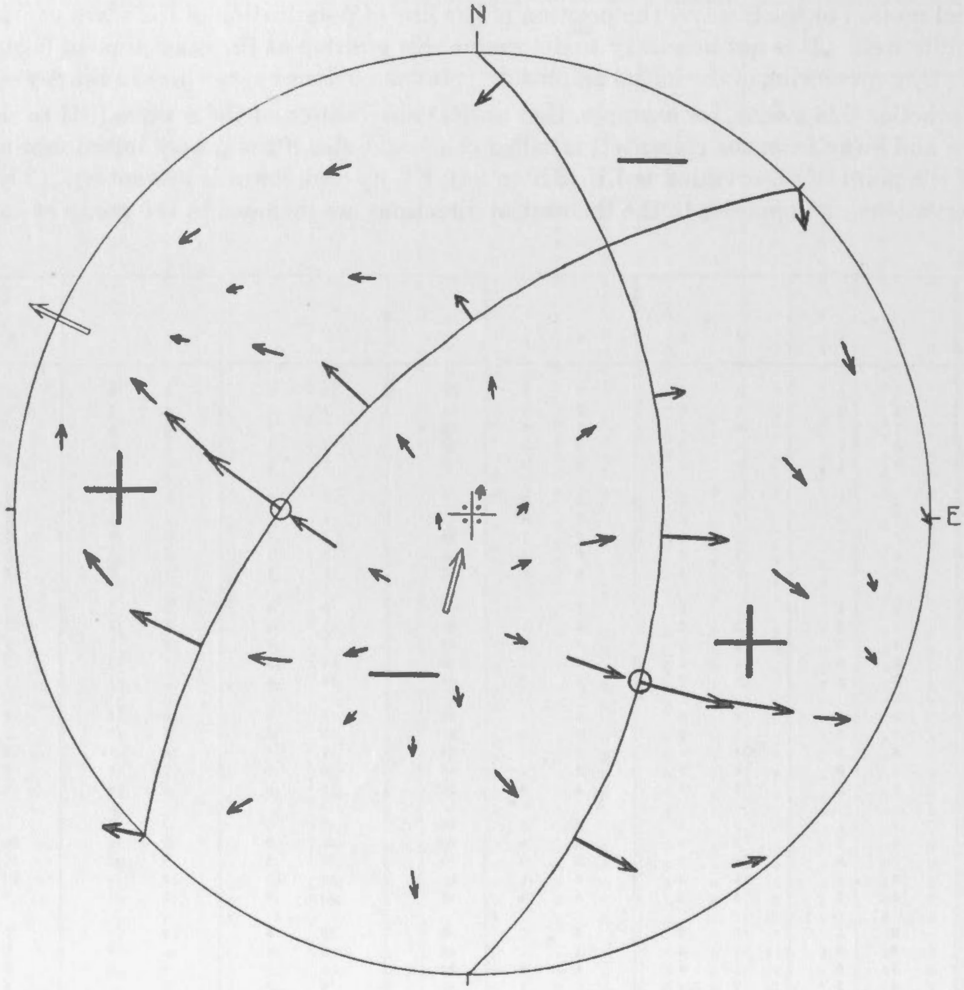

Figure 6. Theoretical course of S-wave vectors caused by force system of type II in the earthquake focus.

higher percentages of consistent data in case Ia than in case II (for example the numbers 5, 7, 21, 23, 29, 33, 36, 40, 46, 50, 54, and 55). It is clear then that a single couple of forces in the focus acting in a plane perpendicular to the fault plane and including the direction of fault movement is most likely the cause for at least part of the earthquakes of Table I.

There is no preference shown by the earthquakes, either of group Ia or II, for a particular depth level or region. The earthquakes of which the S-wave data are not conclusive are distributed at random at all depth levels and through all seismic zones.

For a unification of the material it has been assumed that all the earthquakes have been caused by a single couple acting in the focus. This procedure is possible because it is usually not very difficult to make a choice between the force types Ia and Ib.

For the total material then, the consistent and inconsistent data appear in the following percentages:

Ia-4:1; Ib-2:3; II-3:2

Thus, on the average it seems that there are 4 consistent S data out of a total of 5 if we assume that force type I is the cause of all earthquakes. If we do not include the S-wave readings that are opposite to the theoretical motions in the group of consistent data, it seems that there is a chance of only 50 per cent of a reading being consistent. This means that the data as such are useless.

It should be mentioned that the S-wave data of other stations were reported to the Djakarta Institute in the form of a motion to the N and W, or to S, E and Up, etc. In most cases no amplitude figures were included. That means that the position of the line of polarization of the wave could only be determined with an accuracy of 45° in the plane perpendicular to the direction of propagation of the wave. With this consideration in mind it was determined which observation was consistent and which inconsistent. Possibly this procedure is a cause for errors in the solutions given, but it is not likely that serious errors in the determination of the type of force system in the focus can be the result of this simplification.

Nevertheless in the next questionnaire concerning southeast Asian earthquakes that is now in preparation, special attention will be drawn to this point.

Other Waves

For SKS waves the considerations that make it possible to use S-wave data for studies concerning earthquake mechanism, are not valid. This is because SKS waves are always polarized in the plane of incidence after refraction through the earth's core, and therefore only consist of SV components. This is clearly demonstrated by the SKS data that were gathered and that show about equal percentages of consistent and inconsistent data.

It is clear from this that it is very unlikely indeed that reflected transverse waves could be of any use either. The complications caused by a reflection of a transverse wave of which only the position of the line of polarization in the station can be determined are such that it seems nearly impossible to expect reasonably reliable data for the polarization direction of the wave in the focal region.

The conclusion is that sufficiently reliable data for earthquake mechanism studies only can be expected from P, PKP and S waves (*see* also Hodgson and Adams, 1958).

This is the reason that the older solutions have been reviewed, and that some of the solutions of Table I differ somewhat from those given in the earlier publications. The solutions presented here are based on direct P, PKP and S waves only.

The Solutions

The solutions are given in the form of the figures in six columns of Table I. These columns represent respectively:

I—The direction of the pole of the fault plane (azimuth N through E, and inclination),

II—The direction of the fault displacement (azimuth and inclination),

III—The slip angle (measured between the direction of fault movement and the strike of the fault plane),

IV—The direction of the pole of the plane of action. The plane of action is that plane standing perpendicular to both nodal planes for longitudinal waves in the focus. This is the plane in which the direction of fault movement and also the principal stresses are situated. The pole of the plane of action is the null vector of Hodgson (1957),

V and VI—The azimuth and inclination of the two lines that make angles of 45° with the directions I and II. Along these lines the maximum and minimum pressure components respectively should act in case the force system II were the cause of the earthquake

It is clear that not all directions given in the table are independent of each other. In fact, only two of these directions plus the type description are sufficient for a determination of the other four factors. Figure 7 shows how the six factors of Table I are measured in Wulff's stereographic projection net in which the data were plotted. The diagram of earthquake No. 29 is used as an example.

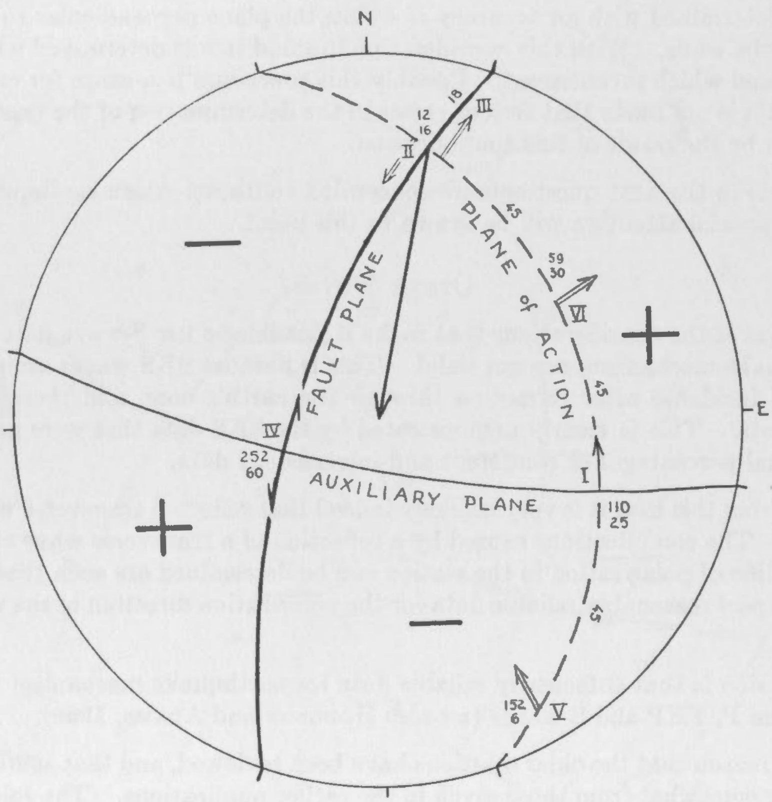

Figure 7. Example of a solution obtained with the method described in the text. Earthquake 29 has been used.

Earthquake Types

According to the following fault movements, eight different types of earthquakes are distinguished:

right lateral, partly normal	R(T)
right lateral, partly reverse	R(P)
left lateral, partly normal	L(T)
left lateral, partly reverse	L(P)
normal, partly right lateral	T(R)
normal, partly left lateral	T(L)
reverse, partly right lateral	P(R)
reverse, partly left lateral	P(L)

A right lateral, clockwise or dextral transcurrent fault movement is indicated by an R for *right*; a left lateral, counterclockwise or sinistral transcurrent fault movement by an L for *left*. A normal fault movement is indicated by a T for the *tension* (or minimum pressure) component that is the more horizontal of the two forces in case mechanism II is acting in the focus. A reverse fault movement is indicated by a P for the maximal *pressure* component that is the more horizontal of the two forces in case mechanism II is acting in the focus.

A random distribution of the different types should result in 8.3 per cent for the first four types, the mainly transcurrent fault movements, and 16.7 per cent for each of the latter four types, the normal and reverse fault movements (*see* also Ritsema, 1957c).

Distribution of Earthquake Types in Depth

Table V gives the total numbers of T, of P, of R and of L shocks at different depth levels. It is seen that at shallow and intermediate depths, clockwise transcurrent fault movements are in the majority, and normal faults at great depths.

TABLE V

Earthquake type distribution in depth

	T	P	R	L
0.00 R	1	3	6	3
0.01	3	3	7	5
0.02	.	1	2	1
0.03	1	2	3	2
0.04	.	.	.	.
0.05	.	.	1	.
0.06	.	1	.	.
0.07	1	1	1	.
0.08	2	.	.	.
0.09	3	.	.	1
0.10	2	.	.	1
0.11 R	1	.	.	1
Total	14	11	20	14

In Table VI the same numbers for shallow, intermediate and deep earthquakes are gathered for the separate regions of the Sunda arc, the Celebes-Philippines arc and the New Guinea-Solomons arcs. The groups are divided such that the earthquakes of the north and central

TABLE VI

Regional distribution of earthquake types in depth

Sunda	T	P	R	L
0.00 R	.	.	5	.
0.01–0.04 R	1	4	3	3
0.04–0.11 R	4	2	.	3
Celebes-Philippines				
0.00 R	1	2	.	2
0.01–0.04 R	2	2	5	3
0.04–0.10 R	5	.	.	.
New Guinea-Solomons				
0.00 R	.	1	1	1
0.01–0.04 R	1	.	4	2
0.04–0.07 R	.	.	2	.
Total				
0.00 R	1	3	6	3
0.01–0.04R	4	6	12	8
0.04–0.11 R	9	2	2	3

Moluccas are included in the Celebes-Philippines arc. The percentage distribution of the different types is shown in the Figure 8.

From the table and Figure 8 it seems that there are regional differences. In the Sunda and Celebes-Philippines arcs the percentage of transcurrent fault movements decreases from shallow to deep levels; in the New Guinea-Solomons arcs this seems to be reversed (*see* also RITSEMA, 1957c).

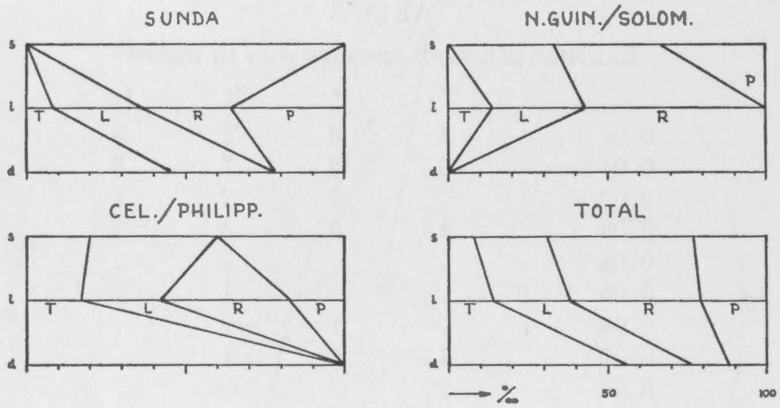

Figure 8. Earthquake type distribution in depth and in regions.

In all regions, however, transcurrent fault movements prevail in shallow and intermediate depth levels. In the Sunda arc there is a clear change from right lateral fault movements at shallow depths to left lateral at great depths. In the New Guinea-Solomon Islands arcs this seems to be reversed.

It is understood that for statistical purposes the total number of shocks investigated is still somewhat small, therefore it is possible that the percentage figures will undergo some change with the increase of data. It is remarkable, however, to note that the total figures for the 'fair' solutions only, neglecting the 'poor' ones, produce percentage figures that are almost the same as those of the total material.

DISTRIBUTION OF EARTHQUAKE TYPES IN DIFFERENT MAGNITUDE RANGES

From Table VII it is clear that none of the special earthquake types is exclusively confined to the greater or to the smaller magnitude ranges. The distribution of the earthquake types is about the same in all magnitude ranges represented in the table. The excess of the transcurrent fault movements over the other types of fault movement is varying from two to four times in the different magnitude ranges.

TABLE VII

DISTRIBUTION OF EARTHQUAKE TYPES IN DIFFERENT MAGNITUDE RANGES

	T	P	R	L
7½–8	1	1	.	2
7–7.4	6	2	9	3
6¾–6.9	6	4	6	4
6–6.7	2	3	5	5

Direction of the Pole of the Fault Plane

The mean dip of the fault plane calculated for every depth level with an interval of 0.01 R shows a rather irregular distribution. There is a tendency, however, for steeper dips at more shallow depths. The mean values for shallow, intermediate and deep earthquakes are 73°, 64° and 56° respectively. That for the total material is 64°.

Using only the 'fair' solutions, excluding the 'poor' ones, the last figure changes to 65°. There is thus no material influence of the classification of the solutions on the average figures.

There are only 12 shocks of the 59 in which the dip of the fault plane was smaller than or equal to 45°. Six of these are deep shocks, 4 are intermediate and 2 shallow. The same tendency that is valid for the mean figures shows itself in these numbers.

The average angle of inclination of the pole of the fault plane for shallow, intermediate and deep shocks thus is respectively 17°, 26° and 34°.

Diagrams were constructed that show for each of the three seismic regions the direction of the pole of the fault plane of the earthquakes with epicenter in these regions. Wulff's stereographic projection net has been used here and also for the construction of the diagrams to follow. It seems that there is no systematical distribution of these directions that are represented by the points in Figures 9, 10 and 11. The only tendency that does exist, is that most of the fault planes seem to have a strike more or less perpendicular to the general trend of the seismic zones, although there are a number of exceptions.

The arrows that are shown in the figures give for each of the earthquakes the direction in which the lower of the two fault blocks moved. (Compare the direction of earthquake 29 in Figure 9 with that indicated in point I of Figure 7).

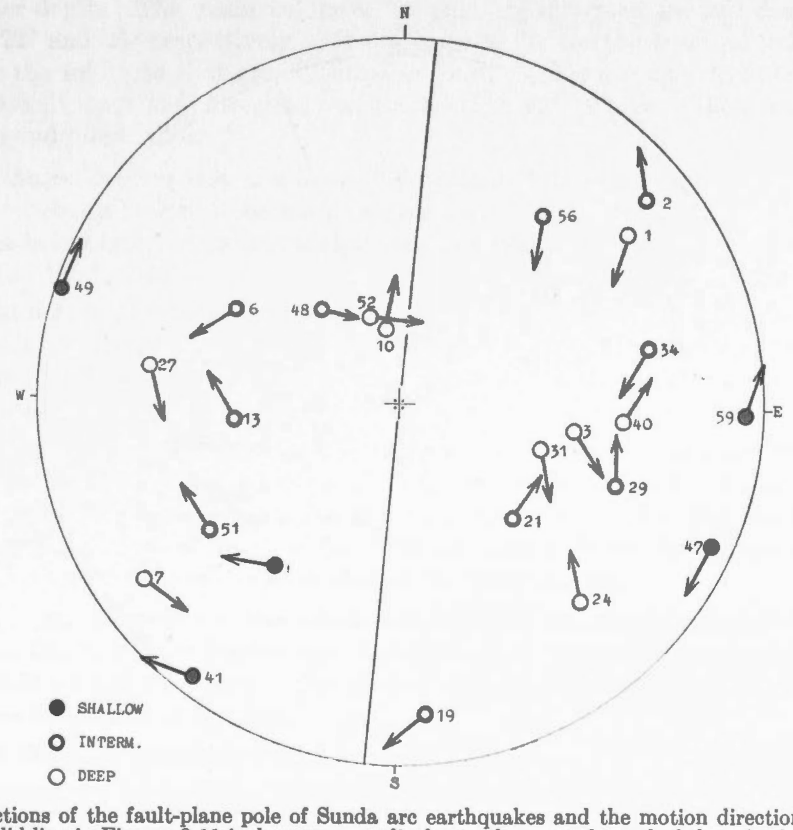

Figure 9. Directions of the fault-plane pole of Sunda arc earthquakes and the motion directions of the footwall. The solid line in Figures 9-11 is drawn perpendicular to the general trend of the seismic zone.

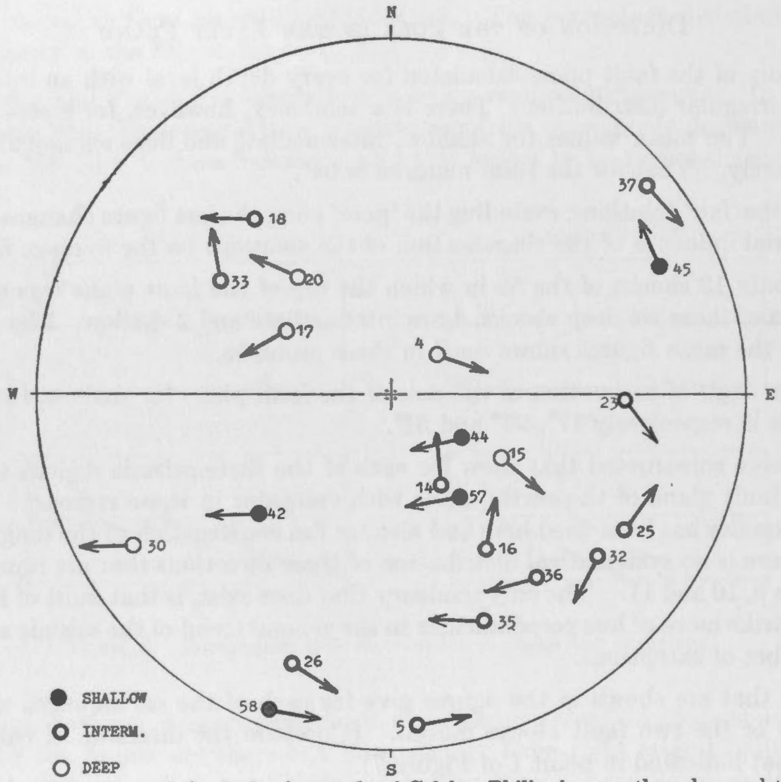

Figure 10. Directions of the fault-plane pole of Celebes-Philippines earthquakes and the motion directions of the footwall.

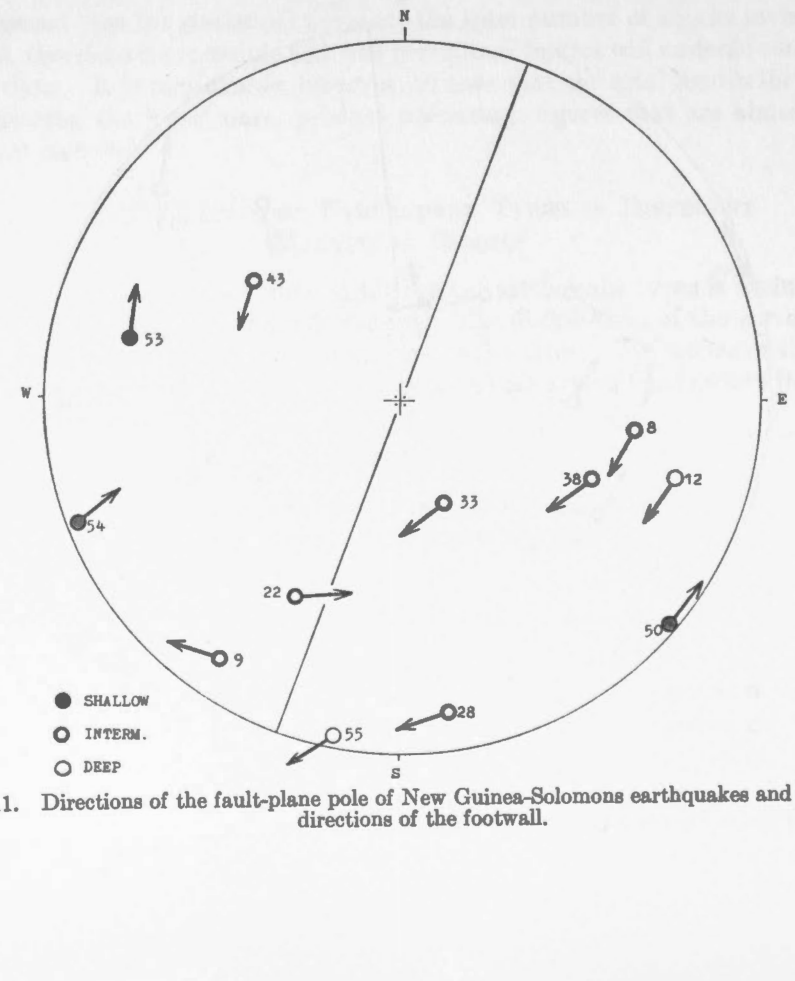

Figure 11. Directions of the fault-plane pole of New Guinea-Solomons earthquakes and the motion directions of the footwall.

In general the arrows follow meridional lines that converge in directions about perpendicular to the general trend of the zone and inclined somewhat to the S in the Sunda arc, to the E in the Celebes-Philippines arc, and to the SSW in the third region under consideration. That means that these block movements nearly always take place in a plane standing perpendicular to the zone of seismic activity that is dipping under the Asian continent for the first two regions. For the third region (Figure 11) the convergence of the arrows at the SSW side of the seismic zone could then be interpreted to mean that here the zone is dipping under the Pacific side and not under the continental (here Australian) side such as in the other two regions.

No system can be found in the distribution of the sense of the block movements. In no part of the diagrams are all arrows pointing in a single direction; always there are those pointing in the opposite direction. Not even for the earthquakes of a particular depth interval can a regular system be found.

Earthquakes with exceptional block movement directions in Figure 9 are numbers 48 (of the Sumatra salient, where the general trend of the zone is changed from about E-W to SE-NW), 3, 6, 52, and in a lesser degree also numbers 24 and 31. Of these only number 52, classified as 'fair', is rather serious.

In Figure 10 the outstanding exceptions are numbers 33, 14, 16 and 23. Of these the first one is in the Moluccas, and the other three from the N arm of Celebes where the general trend is changed from about N-S to E-W. Therefore none of these is serious.

In Figure 11 the only rather serious exception is earthquake 54, classified as 'fair'.

Azimuth and Plunge of the Fault Movement Direction

The single values of the plunge of the fault displacement direction for each depth interval of 0.01 R are rather irregular, but on the average the tendency exists for somewhat greater plunges at greater depth. The mean values of the shallow, intermediate and deep earthquake groups are 17°, 22° and 30° respectively. The average value for the total material is 23°, the same as that for the solutions that are classified as 'fair'. There are only five shocks in which the plunge of the fault movement direction was greater than 45°. Three of these are deep shocks, one intermediate and one shallow.

Except for the tendencies just mentioned no evident differences exist between the earthquakes of different depth levels of the same seismic zone. Therefore in Figures 12, 13 and 14 no distinction has been made for earthquakes of certain depth intervals. Instead the earthquake type is indicated in the figures.

It is seen that here is a tendency for a concentration of fault movement directions in azimuths about perpendicular to the seismic zone. This seems to be especially true for the earthquakes with a mainly and partly reverse fault character. Those with a mainly and partly normal fault character are distributed more at random.

In Figure 12, the diagram for the earthquakes of the Sunda arc, the most deviating fault movement directions of P and (P) earthquakes are those of numbers 51, 2 and 7. The first has a slip angle of only 1° and therefore the (P) character is very faint, and the other two are classified as 'poor'. Earthquake 48 is in the Sumatra salient of the Sunda arc and therefore its position is not directly comparable with that of the other shocks.

In Figure 13, the diagram for the Celebes-Philippines arc, earthquakes 14 and 16 have epicenters near to the N arm of Celebes and therefore are in line with the approximately E-W trend of the seismic zone at that place. The other P and (P) shocks are in line with the general N-S trend of the greater part of the zone.

In Figure 14 the only exception is earthquake number 22.

No clear system can be found in the distribution of R and L fault movement directions. Therefore diagrams of these have not been reproduced here.

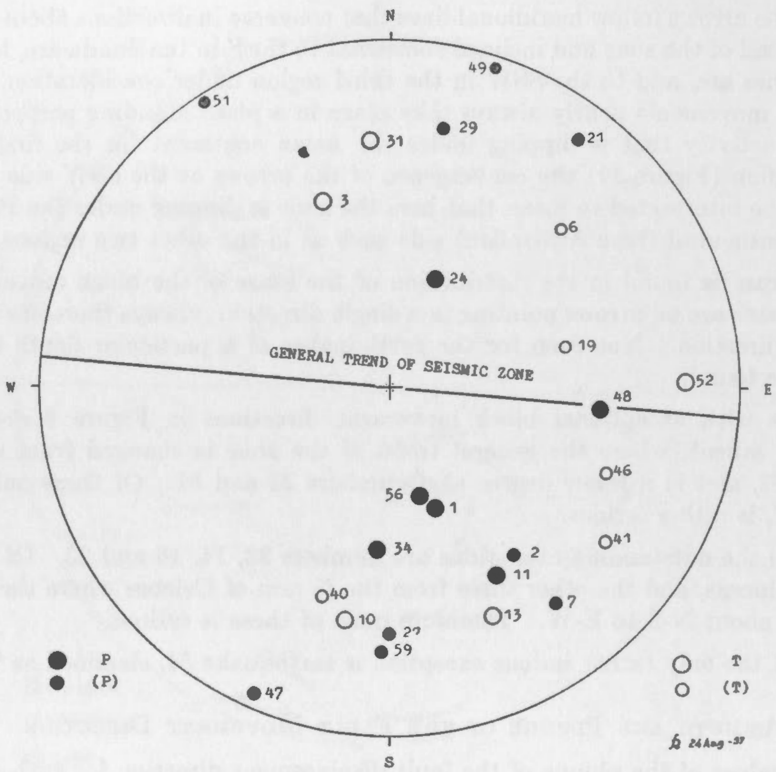

Figure 12. Fault movement directions in Sunda arc earthquakes. The solid line in Figures 12-14 represents the general trend of the seismic zone.

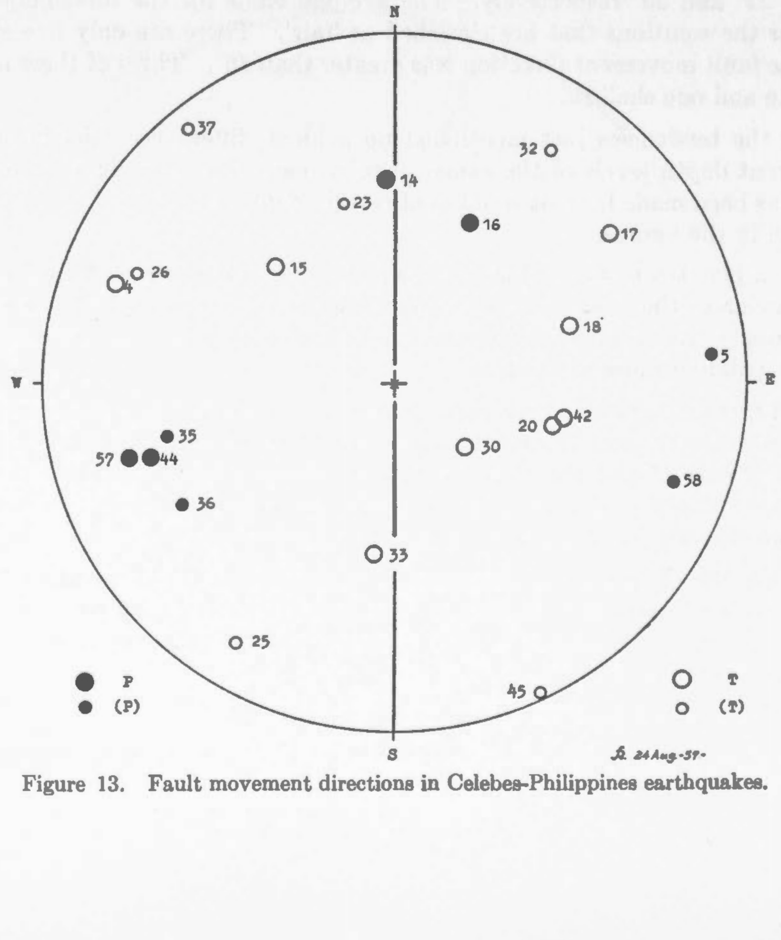

Figure 13. Fault movement directions in Celebes-Philippines earthquakes.

A remarkable tendency, however, does exist in the form of a concentration of the fault movement directions of R(T) and L(P) shocks in certain azimuths, and those of R(P) and L(T) shocks in the opposite directions. These azimuths seem to be related to the direction of the

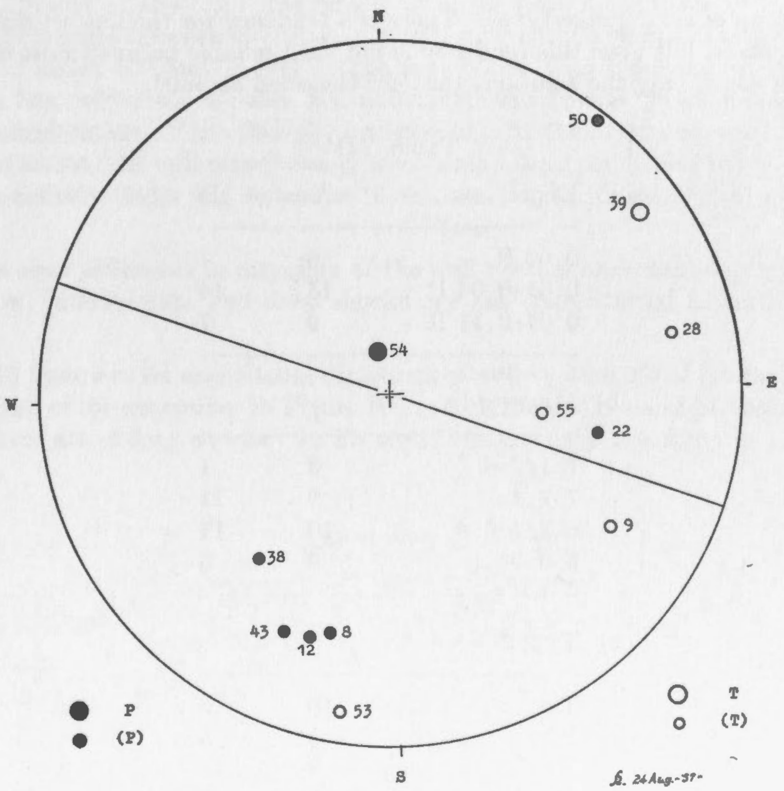

Figure 14. Fault movement directions in New Guinea-Solomons earthquakes.

seismic zone. R(T) and L(P) fault movements are directed in easterly azimuths in the approximately W-E trending Sunda arc, in northerly azimuths in the approximately S-N trending Celebes-Philippines arc, and in ESE azimuths in the New Guinea-Solomons arcs of which the greatest elongation lies in this direction. R(P) and L(T) fault movements are directed just in the opposite azimuths in the length direction of the zones.

Clear exceptions to this latter rule are numbers 2, 6 and 49 of the Sunda arc; number 49 belonging to the Sumatra salient, and both others classified as 'poor'. Number 58 of the Celebes-Philippines arc also is not in line with this rule, but this earthquake is situated in the Moluccas archipelago with its intricate structural lines. The only other exception is number 45 of the Solomons Islands arc, classified as 'poor'.

The transcurrent parts of the mainly normal and mainly reverse fault movements in general are not in accordance with the rule outlined above. Thus, until more data are available on these seismic zones, the rule should not be considered as definite.

The Plunge of the Fault Displacement and that of the Pole of the Fault Plane

The study of the initial motion of P and PKP waves results in two nodal planes, either of which may be the fault plane. The choice of the actual fault plane seems to be independent of the difference in plunge between the two poles of the nodal planes.

Table VIII shows the numbers of earthquakes for which the actual fault displacement plunges steeper, B, and less steep, A, than the direction of the pole of the fault plane. Table VIII shows that there is no preference for a fault displacement in the steepest or in the less steep nodal plane at any depth level. Table VIIIb shows that there is no preference either for one of the two possible fault planes in some special magnitude range. Finally Table VIIIc shows that the numbers of steepest and less steep possible fault movement directions are nearly the same in each group of earthquake types. There is a tendency for the flattest direction in the T group of earthquakes, but even this tendency is not very reliable because most of the difference disappears if we count only the solutions that are classified as 'fair'.

Table VIII

a)

Depth	A	B
0.00 R	6	7
0.01–0.04 R	15	14
0.04–0.11 R	9	7

b)

Magnitude		
7 1/2–8	3	1
7–7.4	8	11
6 3/4–6.9	10	11
6–6.7	9	5

c)

Type		
T	10	5
P	5	5
R	8	11
L	7	7

Thus, it can be concluded that neither in depth, nor in magnitude or type does there exist a preference for the steepest or for the less steep possible direction of fault movement to be the actual one.

The Slip Angle at Different Depths

Although the divergencies of the mean figures are considerable, a clear tendency exists for greater slip angles at increasing depths. The mean values for shallow, intermediate and deep earthquakes are 21°, 30°, and 41° respectively. This confirms that at great depth a more important percentage of the earthquakes is normal or reversed than at shallow depths, where a far greater percentage is of the transcurrent fault type.

There are 13 slip angles greater than 45°, 6 of deep shocks, 5 of intermediate and 2 of shallow ones. The average slip angle of the total material is 31°, that of the 'fair' solutions only, 29°.

Direction of the Pole of the Plane of Action—the "Null Vector"

We recall that the plane of action has been defined as that plane perpendicular to both the nodal planes, and that the pole of this plane is the null vector of Hodgson. Although the values of the dip of the plane of action for the single depth intervals of 0.01 R are somewhat confused, on the average there is a clear increase of dip with increasing depth of focus. The mean figures for shallow, intermediate and deep shocks are respectively 29°, 39° and 54°. The average of the total material is 41°, and 40° for the 'fair' solutions only. From these figures it is clear that most shallow earthquakes are transcurrent, and most of the deep shocks are normal or reverse.

In 11 out of 16 deep shocks the plane of action had a dip greater than 45°, and in 9 out of 13 shallow shocks the dip was smaller than 45°. There is a clear gradual change in dip between the depth ranges.

Figures 15, 16 and 17 show that the directions of the pole of the plane of action are almost confined to the solid angle between two planes, with a strike in the length direction of the seismic zone, and dips of about 50° and 75°–85°. The first plane, with the smallest inclination, dips under the Java Sea, under the Celebes Sea and under the Pacific Ocean in the three seismic regions under consideration. The other plane always dips in the opposite direction. This means that the plane of action (the null plane) nearly always stands perpendicular to the steeply dipping zone of seismic activity under the Asian continent, and for the third region under the Pacific Ocean.

There is no clear difference in direction of the null vectors of certain depth intervals. The points of shallow, intermediate and deep shocks are not concentrated in certain parts of the diagram.

In Figure 15 there are six exceptional directions of null vectors, all of intermediate and deep earthquakes. Half of the exceptions in Figure 16 are of north Celebes and Moluccas earthquakes, and the other three are of deep shocks. In Figure 17 there is only one exception, earthquake 54.

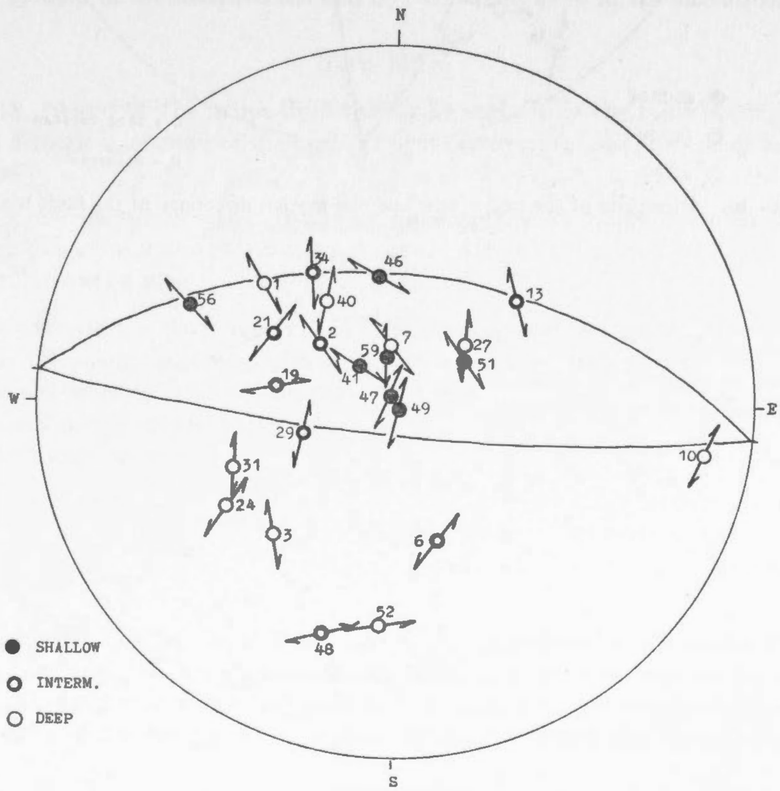

Figure 15. Directions of the null vector and the motion directions of the fault blocks in Sunda arc earthquakes.

The confinement of the directions of the null vectors to the solid angle between the planes that have been drawn in the figures for each seismic region, is not as perfect as that shown by HODGSON (1956) to exist in the Tonga-Kermadec and New Hebrides seismic zones. These latter zones, however, are very simple and straight, whereas in all of the seismic zones that are under consideration here there are bends that easily may complicate the general lines and make the diagrams less clear.

55092-1—8½

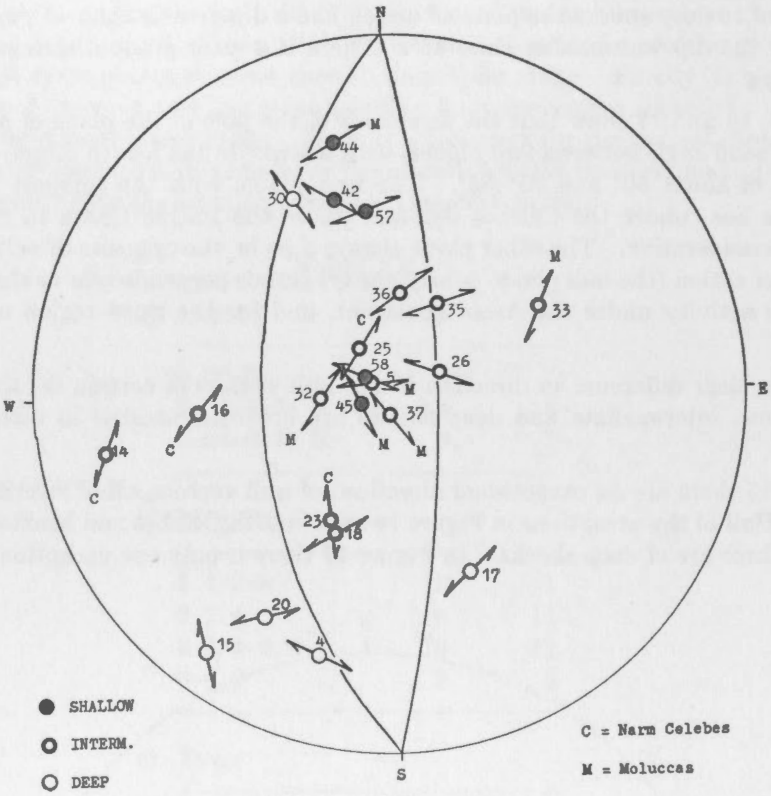

Figure 16. Directions of the null vector and the motion directions of the fault blocks in Celebes-Philippines earthquakes.

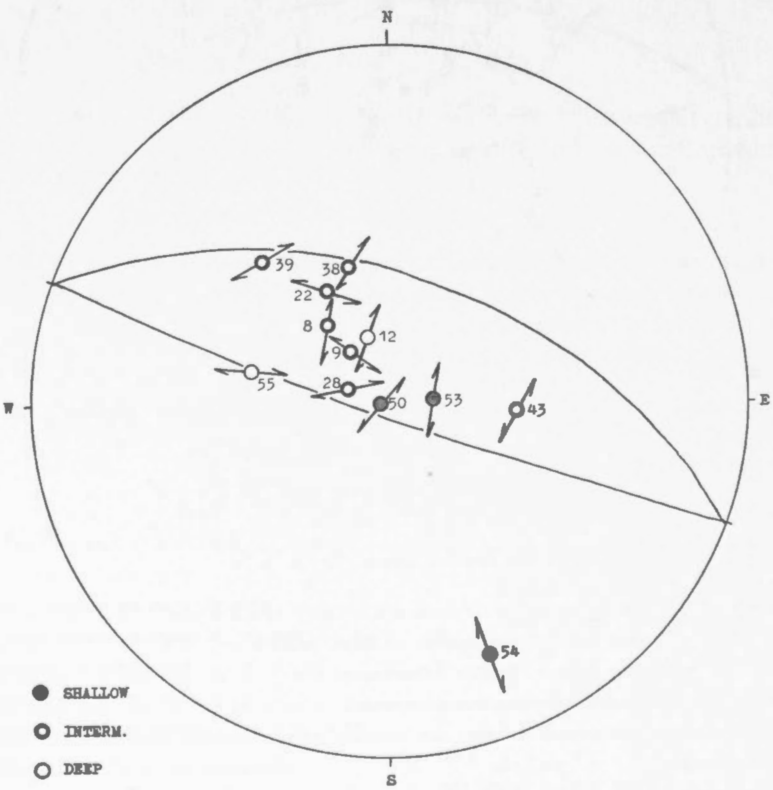

Figure 17. Directions of the null vector and the motion directions of the fault blocks in New Guinea-Solomons earthquakes.

The two half-arrows drawn through each point of observation represent the motion directions of the two adjacent fault blocks with respect to each other. (Compare the direction and the sense of the half-arrows of earthquake number 29 in Figure 15 with the same in point IV of Figure 7).

It is seen that most of the half-arrows are directed almost perpendicular to the meridional lines that come together in the direction of the general trend of the seismic zones.

More or less clear exceptions to this rule in the Sunda arc are numbers 48 (of the Sumatra salient), 52, 19, 41 and 46. The last three, however, are of the extreme eastern part of the Sunda arc where the general trend of the zone is changing from W-E to WSW-ENE. In Figure 16 more or less clear exceptions are numbers 14, 16, 23 and 25 (all of the northern arm of Celebes with its approximate E-W trend), and 32, 33, 37 and 45 (all of the Moluccas archipelago with its intricate structural lines) and numbers 4 and 15 both classified as 'poor'. Numbers 9, 22, 28 and 55 are exceptions in Figure 17, all of which are classified as 'fair'.

There is no clear indication that the distribution of the clockwise and counterclockwise motion vectors is subject to a certain rule; this in contrast to the opinion expressed earlier on the earthquakes of the Sunda arc when the solutions of only a part of the earthquakes used here were known (Ritsema, 1957b). Although several tendencies can be found to exist in the figures, no clear system in the distribution can be found, not even in the earthquakes of a certain depth interval.

The Maps

In Figures 18, 19 and 20 the azimuth of the strike and dip of the fault plane, and that of the fault movement direction, of each of the earthquakes is shown for shallow, intermediate and deep shocks respectively.

The maps stress once more the intimate connection that exists between the direction of fault displacement and the trend of the seismic zone. Almost all fault displacements are directed about perpendicular to the zone.

Clear exceptions are the deep shocks 7, 17, 52 and 55, and the intermediate shocks 6, 9, 11, 19 and 22. But all other fault displacements are almost perfectly in line with the direction perpendicular to the seismic zone at the place of the epicenter. Note for example the shift in the direction of fault displacement to SE azimuths in the extreme east of the Sunda arc (12, 41, 46) and near the north extremity of the north arm of Celebes (37, 45).

It is clear from these instances that the direction of fault displacement is neither uniform in the whole area, nor in the single regions in which the area has been divided. The directions follow more or less closely all bends and curves in the seismic zones, nearly always standing perpendicular to these.

It is apparent that for regions with intricate structural lines the direction of fault displacements as concluded to exist from earthquake mechanism studies, can be an important help in distinguishing the major structural directions. If more data are available this procedure can be used for the area of the central and northern Moluccas, where the three seismic zones come together.

APPENDIX

It is understood that the S-wave data used in the investigations are not perfect, and in the second place that in about half of all shocks these imperfect S data do not give conclusive evidence for a choice between the two types of force systems. In fact, there are only 12 earthquakes that clearly point to force type I, and about 20 shocks with a smaller preference for the same force system in the focus.

So, the evidence on which the assumption is based that all earthquakes were caused by force type I in the focus is only faint. Therefore the consequences have also been considered for

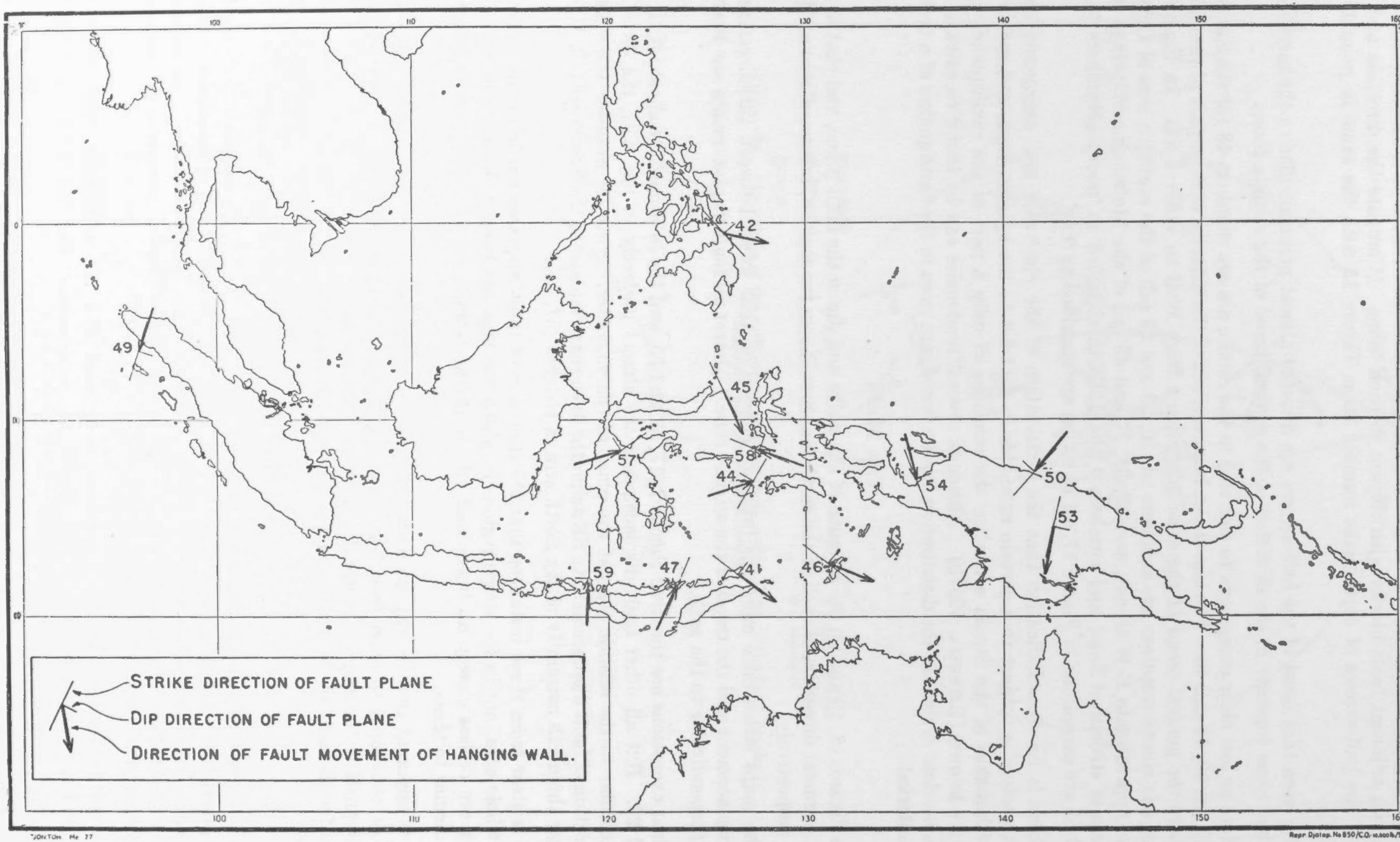

Figure 18. Epicenter map of shallow earthquakes with the azimuth of the fault movement directions and of the strike and dip of the fault planes.

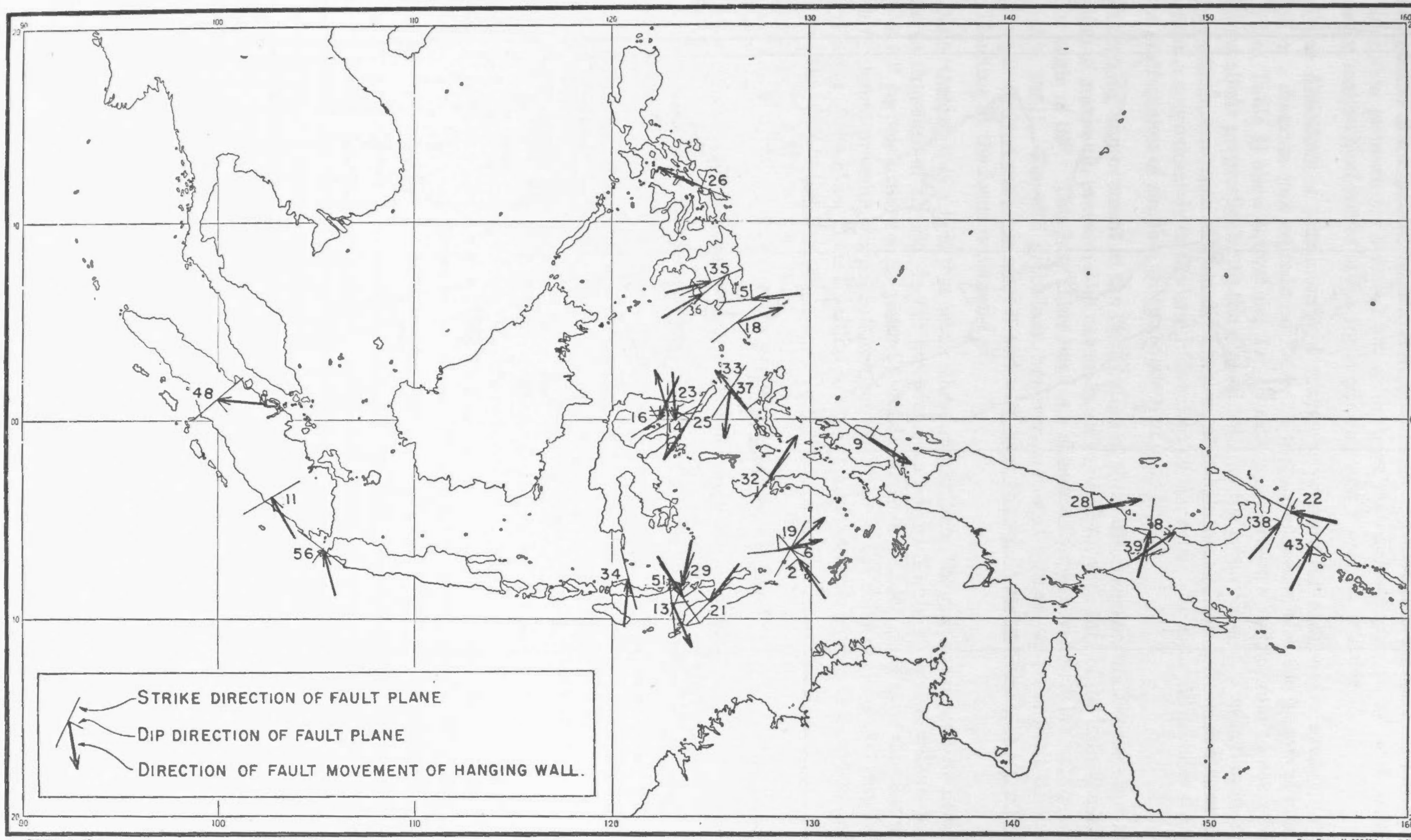

Figure 19. Epicenter map of intermediate earthquakes with the azimuth of the fault movements and of the strike and dip of the fault planes.

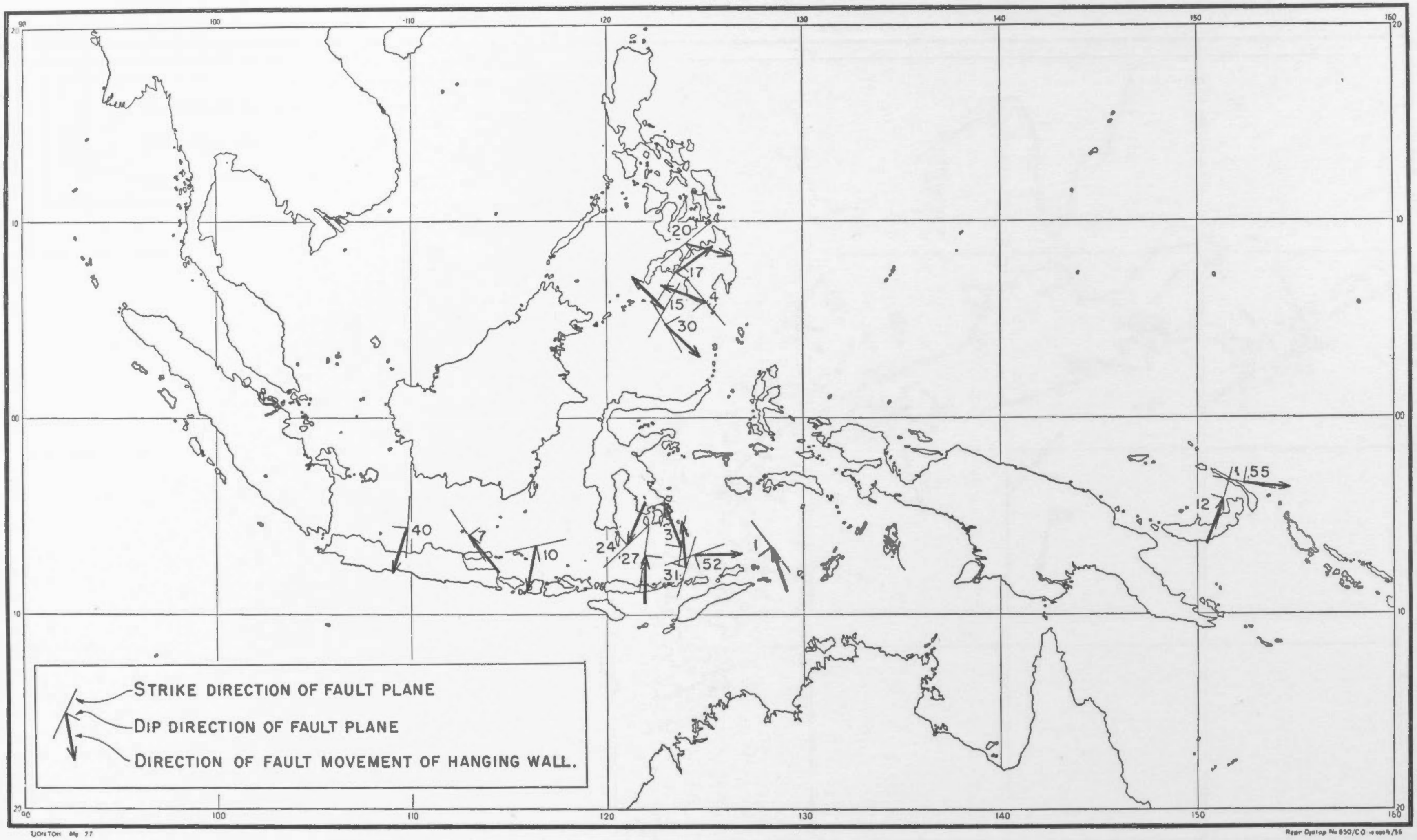

Figure 20. Epicenter map of deep earthquakes with the azimuth of the fault movement directions and of the strike and dip of the fault planes.

all earthquakes of a supposed force system of type II. In that case the directions of maximum and minimum pressure (or tension) act along lines that make angles of 45° with both nodal planes for longitudinal waves in the focus (*see* columns V and VI in Table I).

These directions of maximum and minimum pressure for each single seismic zone were plotted in a diagram (not reproduced here). The diagrams (and also the figures of columns V and VI of Table I) show a tendency for all maximum pressure components to concentrate in directions about perpendicular to the general trend of the seismic zone. The minimum pressure components show a more random distribution, although most of these components are directed in azimuths approximately in the length direction of the zone. No clear differences are evident for the earthquakes of shallow, intermediate and deep levels.

A striking improvement in the distribution of these directions occurs if we assume that the direction of maximum pressure does not make an angle of 45° with that of the fault displacement, but an angle of 30°. This last value has been chosen as a mean value of laboratory data (*see* HUBBERT, 1951). For this procedure, however, we must assume that the fault displacement direction as derived earlier is correct and with that the whole assumption of a force system of type II acting in the focus is disposed of.

Nevertheless, it is a fact that under these suppositions the maximum pressure components of the earthquakes of the Sunda arc are concentrated, with only a few exceptions, in a solid angle of 60° perpendicular to the general trend of the zone. At the same time the vast majority of the minimum pressure components are concentrated in the solid angle of 60° parallel to the general trend of the zone. It is true that in the other two seismic regions the tendencies are the same but the distribution less perfect.

CONCLUSIONS AND SUMMARY

From these considerations the following conclusions can be drawn:

1. It is most likely that force type I, a single couple of forces in the focus, is the origin of the earthquakes of the region.

2. In all magnitude ranges, and in all of the seismic zones in the region, transcurrent fault movements are about three times as frequent as they should be in case of a chance distribution. The fault movements of this type therefore are definitely the most dominating and important.

3. There are indications of small differences in the earthquake mechanisms of different depth levels and seismic zones, (for example greater percentages of normal fault type earthquakes at great depth; gradual changes in dip of the fault plane, plunge of the fault displacement direction, slip angle, and dip of the plane of action at different depth levels; greater frequency of transcurrent fault movements in Pacific regions than in Sunda and Celebes-Philippines arcs).

4. In general the fault displacements are directed perpendicular to the steeply dipping zones of seismic activity in the region. Also when this is not the case the plane of action (null plane) in which the fault movement takes place and in which the forces causing the earthquake are acting, stands about perpendicular to the seismic zone. It is clear therefore that the distribution of earthquakes in space and the mechanisms of the same are clearly related to each other, and that it is most likely that both are expressions of one and the same cause.

5. No clear system can be found in the sense of the fault displacements. The sense of the arrows in Figures 9–11 and 15–17 is not uniform, not even in part of the diagrams or for earthquakes of a certain depth level.

ACKNOWLEDGMENTS

Our special thanks go to the numerous seismologists all over the world who furnished the data on which this study is based.

References

BYERLY, P. (1938): The Earthquake of July 6, 1934: Amplitudes and First Motion. *Bull. Seismol. Soc. Am.*, **28**, 1–13.

BYERLY, P. (1955): Nature of Faulting as Deduced from Seismograms. p. 75–85 *in* Poldervaart, Arie, *Editor*, Crust of the Earth: *Geol. Soc. Am.*, Special Paper 62.

HODGSON, J. H. (1956): Direction of Faulting in Some of the Larger Earthquakes of the South-west Pacific, 1950-1954. *Publications of the Dominion Observatory, Ottawa*, **18**, 169–216.

HODGSON, J. H. (1957): Nature of Faulting in Large Earthquakes. *Bull. Geol. Soc. Am.*, **68**, 611–643.

HODGSON, J. H., and W. M. ADAMS (1958): A Study of the Inconsistent Observations in the Fault-Plane Project. *Bull. Seismol. Soc. Am.*, **48**, 17–31.

HODGSON, J. H., and R. S. STOREY, (1953): Tables Extending Byerly's Fault-Plane Techniques to Earthquakes of any Focal Depth. *Bull. Seismol. Soc. Am.*, **43**, 49–61.

HONDA, H. (1957): The Mechanism of the Earthquakes. *Science Reports, Tôhoku Univ., Ser. 5*, **9**, Supplement 1–46.

HONDA, H., and A. MASATSUKA (1952): On the Mechanism of the Earthquakes and the Stresses Producing them in Japan and its Vicinity. *Science Reports, Tôhoku Univ., Ser. 5*, **4**, 42–60.

HONDA, H., A. MASATSUKA, and K. EMURA (1956): On the Mechanism of the Earthquakes and the Stresses Producing them in Japan and its Vicinity (Second Paper). *Science Reports, Tôhoku Univ., Ser. 5*, **8**, 186–205.

HUBBERT, King (1951): Mechanical Basis for Certain Familiar Geological Structures. *Bull. Geol. Soc. Am.*, **62**, 355–372.

JEFFREYS, H., and K. E. BULLEN (1940): *Seismological Tables.* British Association for the Advancement of Science.

KEYLIS-BOROK, V. I. (1956): Methods and Results of the Investigation of Earthquake Mechanisms. *Publ. Bur. Centr. Seismol. Int., Ser. A, Travaux Scientifiques*, **19**, 383–394.

RITSEMA, A. R. (1952): *Over Diepe Aardbevingen in de Indische Archipel.* Doctoral Dissertation, University of Utrecht.

RITSEMA, A. R. (1956): The Mechanism in the Focus of 28 South-East Asian Earthquakes. *Verhandelingen 50, Meteor. and Geophys. Institute, Djakarta.*

RITSEMA, A. R. (1957a): On the Use of Transverse Waves in Earthquake Mechanism Studies and The Direction of Fault Displacement in SE Asian Earthquakes. *Verhandelingen 52, Meteor. and Geophys. Institute, Djakarta.*

RITSEMA, A. R. (1957b): Earthquake-Generating Stress Systems in Southeast Asia. *Bull. Seismol. Soc. Am.*, **47**, 267–279.

RITSEMA, A. R. (1957c): Pacific and 'Mediterranean' Earthquake Mechanisms. *Trans. Amer. Geophys. Union*, **38**, 349–353.

RITSEMA, A. R. (1957d): Fault Plane Solutions for Southeast Asian Earthquakes. *Verhandelingen 54, Meteor. and Geophys. Institute, Djakarta.*

SCHEIDEGGER, A. E. (1955): The Physics of Orogenesis in the Light of New Seismological Evidence. *Trans. Royal Society, Canada, Sec. 4*, **49**, 65–93.

SCHEIDEGGER, A. E. (1957): The Geometrical Representation of Fault-Plane Solutions of Earthquakes. *Bull. Seismol. Soc. Am.*, **47**, 89–110.

VELDKAMP, J. (1957): Mechanism of Shallow and Intermediate Earthquakes in Sumatra. *Verhand. Kon. Ned. Geol. Mijnbk. Gen., Geol. Ser.*, **18**, 295–303.

WILLMORE, P. L., and J. H. HODGSON (1955): Charts for Measuring Azimuth and Distance and for Tracing Seismic Rays Through the Earth. *Publications of the Dominion Observatory, Ottawa*, **16**, 405–414.

The Null Vector as a Guide to Regional Tectonic Patterns

BY JOHN H. HODGSON

Dominion Observatory, Ottawa, Canada.

ABSTRACT

The paper is a sequel to one published earlier (HODGSON, 1957) in which 75 solutions were summarized and discussed. Here 86 additional solutions are given, from various authors, making a total of 161 solutions available for discussion.

Two new areas, southeast Asia and the zone from the Marianas to Japan, have been added to the two already known in which faulting is not exclusively strike-slip. While there can be no doubt of the extreme importance of strike-slip faulting, it appears possible that a disproportionate number of solutions have come from areas in which faulting is exclusively strike-slip, and that the importance of strike-slip faulting has thereby been overemphasized in earlier papers.

Analysis of the direction of dip-slip gives no support to the contraction hypothesis, either in limited areas or in the world as a whole.

The null vectors for tectonically simple areas show simple patterns related to the geographic features. This inspires some confidence in the null vector as a diagnostic tool. So used, it suggests that in both the northeast Pacific and the northwest Pacific a double system of failures is going on, while the Aleutians, central Asia and the Mediterranean are so tectonically complex that only limited areas of them can be considered at the same time.

INTRODUCTION

In a recent paper (HODGSON, 1957) the fault-plane project of the Dominion Observatory was reviewed, a summary was provided of all the solutions by BYERLY's method then available, and the implications of these solutions to geology were discussed. The present paper is a sequel to that earlier one; it will review recent advances in theory and technique in the work of this Observatory, summarize the additional solutions which have become available, and discuss these solutions from the same point of view as that used in the earlier paper.

REVIEW OF RECENT DOMINION OBSERVATORY CONTRIBUTIONS

Comparison of Projections

Because the fault-plane work has grown up independently in several countries, different projections have been used by various investigators, and intercomparison of techniques has been made difficult by the several languages in which the papers are written. SCHEIDEGGER (1957) has gone into the question of projections very thoroughly, and has shown that the projections used in the Soviet Union, in Holland and Indonesia, and by the followers of BYERLY, are all equivalent, and that no other projection is likely to have any additional merit.

Study of Inconsistent Observations

A statistical study has been made (HODGSON and ADAMS, 1958) of the inconsistent observations in the fault-plane solutions summarized in the earlier paper. This work showed that a small number of stations were contributing a relatively high percentage of the inconsistent observations. When these stations were eliminated, the proportion of inconsistencies in P and PKP was just under 14 per cent. The percentage of inconsistencies in the reflected phases, however, was so high as to suggest that these phases were producing random observations. This matter has been investigated in two subsequent papers (HODGSON and COCK, 1957; HODGSON and STEVENS, 1958) by basing solutions solely on direct phases and then testing the data on the reflected phases by comparison with the completed solutions. It has been proven conclusively that, as reported in questionnaires, observations of reflected phases are random.

Solution Confirmed by Field Observation

In the earlier paper ten examples were given of fault-plane solutions which had received some measure of confirmation from field observations; an additional solution may now be added to this list. This is for the Baja California earthquake of February 9, 1956.

The fault-plane solution (Hodgson and Stevens, 1958) shows plane *b* striking N72°W and dipping 72° northeast. Regarding this plane as the fault, the movement is right-lateral strike-slip, with the northeast hangingwall rising slightly.

Shor and Roberts (1958) report a zone of *en echelon* faulting, the mean direction of the zone being N60°W. The fault was apparently very steep. Movement was right-lateral strike-slip with the northeast side rising. The correlation between the seismic solution and the field observations is very satisfactory.

SUMMARY AND DISCUSSION OF NEW SOLUTIONS

Summary of the Solutions

In preparing the summary of new solutions shown in Table I, the findings of Scheidegger (1957) that the various projections are all equivalent has permitted the inclusion of a large number of solutions from Ritsema. However, solutions such as those of the Japanese, which are based on observations at near stations only, have not been included because the dips of the planes are not sufficiently well defined for the purpose of the analysis to follow. In view of the doubts which surround the use of S, solutions which have been based even in part on S have been excluded from the summary. Solutions which, in the opinion of the author, have been based on inadequate data have been excluded from the summary without explanation.

Within these limits 86 additional solutions have become available, 26 of them from Ritsema (1956), 9 from Mühlhäuser (1957), 38 from this Observatory (Hodgson and Cock, 1957; Hodgson and Stevens, 1958) and 13 from various other authors as indicated in the table. The form of the table, and the significance of the various notations employed in it, are identical to those used in the equivalent table of the earlier paper (Hodgson, 1957).

Nature of the Faulting

In the earlier paper it was found that all but 8 of the 75 earthquakes there summarized were the result of strike-slip faulting. In the present listing there are 24 earthquakes in which the dip component is larger than the strike component. This is a much higher percentage than in the earlier paper, but not so large as to vitiate the conclusion that strike-slip faulting is of paramount importance in large earthquakes. Thirteen of the earthquakes in which dip-slip predominates lie in the New Guinea-Indonesia-Sumatra sector and have already been discussed by Ritsema (1956). Nine others are from the zone between the Marianas and Japan. Combining the results of the earlier paper with this one, there have been 17 earthquakes analysed for this area, in 9 of which dip-slip has predominated. In the earlier paper it was shown that in Alaska and in the Pacific coast of British Columbia and Washington the faulting was not exclusively strike-slip. It appears that Japan and Indonesia are two other such areas.

Most of the earthquakes studied have been the result of strike-slip faulting, but even in these it is possible to define the dip component as thrust or tensional. Table II examines the results of such an analysis, for various geographical areas and focal depths; the table combines results from the two papers. It seems clear that the sense of the dip components give no support to the contraction hypothesis, which would demand thrusts near the surface and tensions at depth. There is actually a slight tendency in the reverse direction. There seems again a suggestion that thrusts predominate (31 to 12) in the south Pacific and tensions in the north Pacific (16 to 9). The data are still much too scanty to allow a final conclusion in the matter.

Table I. Summary of additional fault-plane solutions.

EARTHQUAKE				PLANE a					PLANE b					Null Vector		DEXTRAL Solution	SINISTRAL Solution	REFERENCE
Date	φ	λ	Focal Depth-km.	Strike Direction	Dip Direction	Dip	Strike Component	Dip Component	Strike Direction	Dip Direction	Dip	Strike Component	Dip Component	Trend	Plunge			
New Zealand - Kermadecs - Tonga - Fiji																		
February 19, 1954	30° S	177.7° W	Normal	N 29.5° E	S 60.5° E	87°	0.985	+0.175	N 60° W	N 30° E	80°	0.999	+0.053	N 48° E	79.5°	b	a	Hodgson and Cock, 1957.
- alternative solution -				N 78.5° E	N 11.5° W	73°	0.889	+0.459	N 21° W	S 69° W	64°	0.946	+0.325	N 72° W	58°	b	a	Hodgson and Cock, 1957.
December 10, 1950	28.7°S	179° W	300	N 85° E	N 5° W	88°	0.707	+0.707	N 7° W	S 83° W	45°	0.999	+0.049	S 87° W	45°	b	a	Mühlhäuser, 1957.
January 10, 1956	25° S	176° W	Normal	N 25° E	S 65° E	82°	0.981	-0.193	N 67° W	N 23° E	79°	0.990	-0.142	N 60° E	76.4°	a	b	Hodgson and Stevens, 1958.
August 18, 1954	21.5°S	176° W	150	N 27° E	S 63° E	81°	0.932	-0.363	N 67° W	N 23° E	69°	0.986	-0.168	N 50° E	66.8°	a	b	Hodgson and Cock, 1957.
September 13, 1954	21° S	175.5° W	150	N 17° E	S 73° E	84°	0.939	-0.345	N 75° W	N 15° E	70°	0.994	-0.112	N 32° E	69.6°	a	b	Hodgson and Cock, 1957.
September 15, 1954	18° S	178.5° W	600	N 51.5° E	N 38.5° W	83°	0.864	-0.504	N 34.5° W	N 55.5°E	60°	0.990	-0.141	N 39.5°E	59.4°	b	a	Hodgson and Cock, 1957.
November 10, 1955	15° S	174° W	100	←	Not defined		→	+ →	N 80° W	N 10° E	87°	←	+	Not defined	→	a	b	Hodgson and Stevens, 1958.
New Hebrides - Solomons																		
January 5, 1955	16°S	167.5° E	Normal	N 56.5° E	S 33.5° E	56°	0.999	-0.022	N 33.5° W	N 56.5°E	89°	0.820	-0.572	S 35.5°E	55.9°	a	b	Hodgson and Cock, 1957.
October 13, 1955	9.5°S	161° E	Normal	←	Not defined		→	+1.	←	Not defined		→	+1.		→	Thrust		Hodgson and Stevens, 1958.
August 16, 1955	6° S	155° E	200	N 49° E	N 41° W	81°	0.944	+0.330	N 38° W	N 52° E	71°	0.986	+0.166	N 26° E	68.9°	a	b	Hodgson and Stevens, 1958.
Marianas - Bonins - Japan - Kuriles - Kamchatka																		
February 1, 1956	19° N	145.5° E	350	←	Not defined			-1. →	←	Not defined			-1.		→	Normal		Hodgson and Stevens, 1958.
May 30, 1955	24.5°N	142.5° E	600	N 70° E	N 20° W	35°	1.000	-0.000	N 20° W	S 70° W	90°	0.574	-0.819	N 21° W	35.4°	a	b	Hodgson and Cock, 1957.
February 18, 1956	30° N	137.5° E	450	N 29° E	S 61° E	56°	0.892	-0.452	N 76° W	N 14° E	68°	0.798	-0.603	N 78° E	47.7°	a	b	Hodgson and Stevens, 1958.
April 17, 1948	33° N	135.5° E	Normal	N 43° E	S 47° E	86°	0.000	+1.00	N 43° E	N 47° W	4°	0.000	+1.00	N 43° E	0°	Thrust		Mühlhäuser, 1957.
July 18, 1952	34.4°N	135.8° E	70	N 74° E	S 16° E	71°	0.918	-0.396	N 14° W	N 76° E	68°	0.936	-0.351	S 65° E	62.4°	a	b	Ichikawa, 1955.
May 14, 1954	36° N	137° E	250	N 56° E	N 34° W	68°	0.991	+0.132	N 31° W	N 59° E	83°	0.926	+0.378	N 14.5° W	66.9°	a	b	Hodgson and Cock, 1957.
May 23, 1938	36.5°N	141.6° E	Normal	N 31° W	N 59° E	84°	0.000	+1.00	N 31° W	S 59° W	6°	0.000	+1.00	N 31° W	0°	Thrust		Mühlhäuser, 1957.
November 2, 1936	38.3°N	141.9° E	Normal	N 37° E	S 53° E	75°	0.000	+1.00	N 37° E	N 53° W	15°	0.000	+1.00	N 37° E	0°	Thrust		Mühlhäuser, 1957.
March 4, 1952	42.1°N	143.9° E	40	N 16° E	N 74° W	85°	0.0	-1.0	N 16° E	S 74° E	5°	0.0	-1.0	N 16° E	0°	Normal		Ichikawa, 1955.
November 13, 1932	43.4°N	137° E	330	N 32° E	N 58° W	70°	0.628	+0.778	N 82° W	S 8° W	43°	0.865	+0.502	S 47.5°W	35.1°	b	a	Mühlhäuser, 1957.
September 11, 1935	43.6°N	146° E	Normal	←	Not defined			+1. →	←	Not defined			+1.		→	Thrust		Muhlhäuser, 1957.
February 28, 1950	46.2°N	143.5° E	320	N 5° E	N 85° W	69°	0.997	-0.075	N 84° W	N 6° E	86°	0.933	-0.350	N 73° W	67.7°	b	a	Ichikawa, 1955.
July 6, 1954	46.5°N	153.5° E	100	←	Not defined			+ →	N 22° W	N 68° E	62°	←	+	Not defined			→	Hodgson and Cock, 1957.
June 30, 1936	51° N	161.1° E	Normal	N 55° E	N 35° W	66°	←	+		Not defined			+				→	Mühlhäuser, 1957.
May 3, 1954	51.5°N	159.5° E	Normal	N 9° E	N 81° W	70°	0.938	-0.346	N 74° W	N 16° E	71°	0.988	-0.362	N 34° W	62.2°	b	a	Hodgson and Cock, 1957.
April 17, 1955	52° N	159.2°	Normal	N 51° E	N 39° W	84°	0.978	-0.210	N 38° W	N 52° E	78°	0.994	-0.107	N 25° E	76.9°	b	a	Hodgson and Cock, 1957.
Aleutians																		
June 2, 1955	51.5°N	180°	Normal	N 86° E	←	90°				Not defined				N 86° E			→	Hodgson and Cock, 1957.
June 20, 1955	51.5°N	180°	Normal	N 38° E	N 52° W	58°	0.752	-0.660	N 27° W	N 63° E	56°	0.769	-0.639	N 7.5° E	39.7°	b	a	Hodgson and Cock, 1957.
April 17, 1954	51.5°N	179° W	Normal	N 87.5°E	N 2.5° W	82°	0.994	-0.106	N 3° W	S 87° W	84°	0.990	-0.140	N 40° W	80.0°	a	b	Hodgson and Cock, 1957.
-alternative solution -				N 45° E	S 45° E	84°	0.965	-0.261	N 46° W	N 44° E	75°	0.994	-0.108	N 66° E	74.3°	a	b	Hodgson and Cock, 1957.
March 14, 1955	52.5°N	173.5° W	100	N 19° E	N 71° W	70°	0.979	-0.203	N 67° W	N 23° E	79°	0.938	-0.348	N 39° W	66.3°	b	a	Hodgson and Cock, 1957.
January 13, 1955	53° N	167.5° W	Normal	N 52° E	S 38° E	89°	0.961	+0.275	N 39° W	N 51° E	74°	0.999	+0.018	N 66° E	73.3°	b	a	Hodgson and Cock, 1957.
Alaska - United States - Central America - Caribbean																		
October 3, 1954	60.5°N	151° W	100	N 36° E	S 54° E	52°	0.958	-0.285	N 45.5° W	S 44.5°W	77°	0.775	-0.632	S 31° E	49.3°	b	a	Hodgson and Cock, 1957.
July 6, 1954	39.5°N	118.5°W	Normal	N 56° E	N 34° W	51°	0.963	-0.268	N 24° W	N 66° E	78°	0.765	-0.643	N 10° W	48°	b	a	Tocher, 1955.

Table I. Summary of additional fault-plane solutions—*Continued*

EARTHQUAKE				PLANE a					PLANE b					Null Vector		DEXTRAL Solution	SINISTRAL Solution	REFERENCE
Date	φ	λ	Focal Depth-km.	Strike Direction	Dip Direction	Dip	Strike Component	Dip Component	Strike Direction	Dip Direction	Dip	Strike Component	Dip Component	Trend	Plunge			
Alaska - United States - Central America - Caribbean (Cont'd)																		
August 24, 1954	39.5°N	118.5° W	Normal	N 45° E	N 45° W	51°	0.587	-0.810	N 5° W	N 85° E	51°	0.587	-0.810	N 20° E	27.7°	b	a	Tocher, 1955.
December 16, 1954	39.5°N	118° W	Normal	N 66° E	N 24° W	66°	0.858	-0.514	N 11° W	N 79° E	62°	0.887	-0.461	N 31° E	52.0	b	a	Romney, 1957.
February 9, 1956	31.5°N	116° W	Normal	N 19° E	S 71° E	85°	0.951	+0.311	N 72° W	N 18° E	72°	0.996	+0.092	N 35° E	70.9°	b	a	Hodgson and Stevens, 1958.
April 29 A, 1954.	28.5°N	113° W	Normal	N 46° E	S 44° E	88°	0.925	+0.379	N 45° W	N 45° E	68°	0.999	+0.038	N 50° E	68°	b	a	Hodgson and Cock, 1957.
April 29 B, 1954	28.5°N	113° W	Normal	N 46° E	S 44° E	88°	0.925	+0.379	N 45° W	N 45° E	68°	0.999	+0.038	N 50° E	68°	b	a	Hodgson and Cock, 1957.
July 9, 1956	20° N	73° W	100	N 13° E	S 77° E	64°	0.977	+0.213	N 82° W	N 8° E	79°	0.894	+0.447	N 77° E	61.6°	b	a	Hodgson and Stevens, 1958.
January 15, 1931	16.4°N	96.3° W	Normal	N 2° E	S 88° E	74°	0.987	+0.162	N 87° E	N 3° W	81°	0.960	+0.279	N 60° E	70.7°	b	a	Mühlhäuser, 1957.
August 28, 1955	14° N	91° W	60	N 7° E	S 83° E	73°	0.789	+0.615	N 85° E	N 5° W	54°	0.932	+0.361	N 27° E	48.6°	b	a	Hodgson and Stevens, 1958.
February 19 B, 1954	12.5°N	87.5°W	Normal	N 28.5° E	N 61.5° W	55°	0.985	-0.170	N 55° W	N 35° E	82°	0.815	-0.579	N 44° W	53.3°	b	a	Hodgson and Cock, 1957
July 18, 1934	8.2°N	82.6° W	Normal	N 79° E	N 11° W	84°	0.890	-0.456	N	E	63°	0.993	-0.117	N 69.3°E	61.4°	b	a	Mühlhäuser, 1957.
April 27, 1954	6° N	82.5° W	Normal	N 6.5° E	S 83.5° E	85°	0.970	-0.243	N 85° W	N 5° E	76°	0.996	-0.090	N 27° E	75.2°	a	b	Hodgson and Cock, 1957.
South America																		
January 8, 1956	19° S	70° W	Normal	N 18° E	N 72° W	83°	0.919	-0.393	N 69° W	N 21° E	67°	0.991	-0.132	N 2° E	65.8°	b	a	Hodgson and Stevens, 1958.
December 7, 1953	22° S	68.5° W	100	N 32° E	S 58° E	79°	0.812	-0.584	N 66° W	N 24° E	55°	0.973	-0.233	N 46° E	53.5°	a	b	Ingram, 1957.
April 19, 1955	30° S	72° W	Normal	N 35° E	N 55° W	72°	0.946	-0.325	N 49° W	N 41° E	72°	0.946	-0.325	N 6° W	64.4°	b	a	Hodgson and Cock, 1957.
December 17, 1949	53.6°S	69.9° W	Normal	← Not defined →					N 51.5° W	N 38.5° E	83°	←	→	S 65° E	← Not defined →			Rascher, 1952
South Pacific																		
November 22, 1955	24.5°S	123° W	Normal	N 2° E	N 88° W	89°	0.981	+0.197	N 88° W	N 2° E	79°	0.999	+0.018	N 1° W	78.5°	a	b	Hodgson and Stevens, 1958.
New Guinea - Indonesia - Philippines - Sumatra																		
January 31, 1956	4° S	152° E	400	← Not defined				-1.	Not defined				-1. →			Normal		Hodgson and Stevens, 1958.
March 3, 1954	5.5°S	142.5° E	Normal	N 12° E	S 78° E	76°	0.996	-0.090	N 79° W	N 11° E	85°	0.970	-0.243	N 82° E	75°	a	b	Ritsema, 1956.
December 2, 1953	2.7°S	141.5° E	Normal	N 40° E	N 50° W	89°	0.999	+0.034	N 50° W	S 40° W	88°	0.999	+0.017	S 67° W	87.7°	b	a	Ritsema, 1956.
August 21, 1955	3° S	137.5° E	Normal	N 74° E	S 16° E	60°	0.934	+0.357	N 26° W	N 64° E	72°	0.851	+0.526	S 53° E	54.0°	b	a	Hodgson and Stevens, 1958.
June 6, 1954	3° S	135.5° E	Normal	N 21° W	N 69° E	88°	0.000	+1.00	N 21° W	S 69° W	2°	0.000	+1.00	N 21° W	0°	Thrust		Ritsema, 1956.
April 6, 1953	7.3°S	131.0° E	Normal	N 22° E	N 68° W	67°	0.829	-0.560	N 53° W	N 37° E	59°	0.890	-0.456	N 8° W	49.5°	b	a	Ritsema, 1956.
January 31, 1941	6.5°S	128.5° E	200	N 78° E	N 12° W	81°	0.111	-0.994	N 40° E	S 50° E	11°	0.573	-0.820	N 77° E	8°	b	a	Ritsema, 1956.
October 3, 1954	1.5°S	127.5° E	Normal	N 20° E	N 70° W	80°	0.999	+0.053	N 70° W	N 20° E	87°	0.985	+0.175	N 52° W	79.4°	a	b	Ritsema, 1956.
July 13, 1952	3.1°S	127.4° E	Normal	N 31° E	N 59° W	26°	0.709	+0.705	N 17° W	N 73° E	72°	0.327	+0.945	N 12° W	19°	Thrust		Ritsema, 1956.
February 14, 1952	7.7°S	126.5° E	Normal	N 36° E	N 54° W	74°	0.999	-0.055	N 53° W	N 37° E	87°	0.961	-0.277	N 43° W	73.3°	b	a	Ritsema, 1956.
January 20, 1953	1.5°N	126° E	Normal	N 65° E	N 25° W	89°	0.984	-0.181	N 25° W	S 65° W	80°	0.999	-0.018	S 70° W	80°	a	b	Ritsema, 1956.
March 19, 1952	9.5°N	126° E	Normal	N 12° E	N 78° W	52°	0.645	-0.764	N 42° W	N 48° E	53°	0.637	-0.771	N 16° W	30.3°	b	a	Ritsema, 1956.
February 20, 1954	6.9°S	124.5° E	600	N 70° E	S 20° E	28°	0.929	-0.370	N 1° W	S 89° W	80°	0.443	-0.897	S 4° W	27°	b	a	Ritsema, 1956.
- alternative solution -				N 15° W	S 75° W	79°	0.535	-0.845	N 88° W	N 2° E	34°	0.940	-0.341	N 24 W	32°	b	a	Ritsema, 1956.
January 1, 1954	9.0°S	123.5° E	100	N 57° E	S 33° E	89°	0.901	+0.434	N 34° W	N 56° E	64°	0.999	+0.019	N 62° E	65°	b	a	Ritsema, 1956.
June 25, 1953	8.5°S	123.5° E	Normal	N 24° E	N 66° W	87°	0.999	+0.033	N 66° W	N 24° E	88°	0.999	+0.049	N 26° W	86.1°	a	b	Ritsema, 1956.
September 22, 1940	7.5°N	123.5° E	650	N 32° E	S 58° E	38°	0.880	-0.475	N 35° W	S 55° W	73°	0.567	-0.824	S 24° E	33°	b	a	Ritsema, 1956.
October 20, 1938	9.2°S	123.0° E	100	N 66° E	N 24° W	71°	0.706	-0.708	N 6° W	N 84° E	48°	0.899	-0.438	N 48° E	42.4°	b	a	Ritsema, 1956.
June 18, 1940	5.4°N	123.0° E	550	N 45° E	N 45° W	43°	0.000	-1.00	N 45° E	S 45° E	47°	0.000	-1.00	N 45° E	0°	Normal		Ritsema, 1956.
September 17, 1941	0.1°N	122.7° E	200	N 0° E	N 90° W	66°	0.837	-0.548	N 75° E	S 15° E	60°	0.883	-0.470	S 32° W	50°	a	b	Ritsema, 1956.
November 27, 1941	6.6°S	121.1° E	500	N 47° E	N 43° W	73°	0.550	+0.835	N 67° W	S 23° W	37°	0.874	+0.486	S 58° W	31°	b	a	Ritsema, 1956.
September 20, 1954	1.5°S	120.5° E	Normal	N 55° E	N 35° W	38°	0.919	-0.393	N 16° W	N 74° E	76°	0.583	-0.812	N 6° W	34°	a	b	Ritsema, 1956.
November 2, 1954	8.0°S	119.0° E	Normal	N 1° E	N 89° W	87°	0.961	+0.277	N 88° W	N 2° E	74°	0.999	+0.055	N 10° W	74°	a	b	Ritsema, 1956.

Table I. Summary of additional fault-plane solutions—*Concluded*

EARTHQUAKE				PLANE a					PLANE b					Null Vector		DEXTRAL Solution	SINISTRAL Solution	REFERENCE
Date	φ	λ	Focal Depth-km.	Strike Direction	Dip Direction	Dip	Strike Component	Dip Component	Strike Direction	Dip Direction	Dip	Strike Component	Dip Component	Trend	Plunge			
New Guinea - Indonesia - Philippines - Sumatra (Cont'd)																		
August 11, 1937	6.5°S	116.5°E	600	N 79° W	N 11° E	68°	0.000	-1.00	N 79° W	S 11° W	22°	0.000	-1.00	S 79° E	0°	Normal		Ritsema, 1956.
February 11, 1952	5.5°S	109.8°E	650	N 4° E	N 86° W	64°	0.873	-0.488	N 72° W	N 18° E	64°	0.873	-0.488	N 34° W	51.4°	b	a	Ritsema, 1956.
July 3, 1954	6.5°S	105.5° E	100	N 53° W	S 37° W	66°	0.000	+1.00	N 53° W	N 37° E	24°	0.000	+1.00	N 52° W	0°	Thrust		Ritsema, 1956.
August 18, 1938	3.8°S	102.8° E	100	N 60° E	N 30° W	63°	0.000	+1.00	N 60° E	S 30° E	27°	0.000	+1.00	N 60° E	0°	Thrust		Ritsema, 1956.
July 7, 1953	1.0°N	100° E	200	N 5° E	N 85° W	62°	0.426	+0.905	N 50° E	S 40° E	37°	0.626	+0.780	S 18° W	21.8°	b	a	Ritsemu, 1956.
November 13, 1953	3.5°N	96° E	Normal	N 18° E	S 72° E	89°	0.999	+0.034	N 72° W	S 18° W	88°	0.999	+0.017	S 9° E	87.8°	a	b	Ritsema, 1956.
Central Asia																		
August 15, 1950	28.5°N	98.7° E	Normal	E W	N	75°	0.000	-1.00	E W	S	15°	0.000	-1.00	E W	0°	Pure Normal		Tandon, 1954.
March 21, 1954	24.4°N	95.2° E	180	N 50° E	N 40° W	60°	0.829	+0.560	N 56° W	S 34° W	61°	0.820	+0.572	S 88° W	46.4°	b	a	Tandon and Mukherjee, 1956.
July 21, 1956	23.5°N	70.2° E	Normal	N 57° E	N 33° W	65°	0.985	-0.173	N 29° W	N 61° E	81°	0.904	-0.428	N 11° W	64°	b	a	Tandon, 1957.
Mediterranean and Azores																		
September 12, 1955	32.5°N	30° E	Normal	N 33° E	N 57° W	64°	0.783	+0.623	N 38° W	N 52° E	56°	0.849	+0.529	N 4° E	44.2°	a	b	Hodgson and Stevens, 1958
July 16, 1955	37.5°N	27° E	Normal	N 40° E	N 50° W	84°	0.995	+0.105	N 50° W	N 40° E	84°	0.995	+0.105	N 6° W	81°	a	b	Hodgson and Cock, 1957.
July 9 A, 1956	37°N	26° E	Normal	N 43° E	N 47° W	72°	0.798	-0.603	N 62° W	S 28° W	55°	0.926	-0.377	S 65° W	48.1°	a	b	Hodgson and Stevens, 1958
April 30, 1954	39°N	22° E	Normal	N 86° E	N 4° W	18°	0.998	-0.069	N 46° W	S 44° W	78°	0.954	-0.301	N 49° W	13°	a	b	Hodgson and Cock, 1957.
March 16, 1941	38.5°N	12.0° E	85	N 68° E	N 22° W	59°	1.00	0.000	N 22° W		90°	1.00	0.000	N 68° E	59°	b	a	Di Filippo, 1950 a.
November 25, 1941	37.3°N	19.0° W	Normal	N 87° E	N 3° W	90°	1.00	0.000	N 3° W	N 87° E	70°	1.00	0.000	N 87° E	70°	a	b	Di Filippo, 1950 b.

Table II. Relationship of Thrust (+) and Gravity (−) Dip Components to Focal Depth and Geographic Area.

Area	Focal Depth, km.														Total	
	Normal		100		200		300		400		500		600			
	+	-	+	-	+	-	+	-	+	-	+	-	+	-	+	-
New Zealand to Samoa	4	3	3	-	3	-	2	1	-	-	1	-	1	1	14	5
New Hebrides, Solomon Islands	10	1	2	1	3	1	1	-	-	-	-	-	-	-	16	3
Marianas, Bonins	1	-	-	1	-	-	-	1	-	1	-	-	-	1	1	4
Japan to Kamchatka	2	8	2	-	-	1	1	1	-	-	1	-	-	-	6	10
Aleutians	3	5	-	1	-	-	-	-	-	-	-	-	-	-	3	6
Alaska to Panama	9	9	-	-	-	-	-	-	-	-	-	-	-	-	9	9
Continental North America	1	4	-	-	-	-	-	-	-	-	-	-	-	-	1	4
Caribbean	-	-	1	-	-	-	-	-	-	-	-	-	-	-	1	-
South America	1	3	1	1	-	-	-	-	-	-	-	-	1	-	3	4
New Guinea to Sumatra	8	6	3	1	1	2	-	-	-	1	1	1	-	4	13	15
Central Asia	-	3	-	-	1	1	-	-	-	-	-	-	-	-	1	4
Mediterranean	2	8	-	-	-	-	-	-	-	-	-	-	1	-	3	8
Totals	41	50	12	5	8	5	4	3	-	2	3	1	3	6	71	72

Dip Vectors and Null Vectors

A General Discussion

In the earlier paper two quantities were defined, known as the dip vector and the null vector. These terms derived logically from the techniques of the solutions. As an example the reader is referred to Figure 9 of that earlier paper (Hodgson, 1957) which shows a typical solution. In that figure, circles *a* and *b* represent planes. The direction of dip of these planes is obtained by drawing the diameters of the corresponding circles through the origin; the tangent of the dips of the planes is proportional to the length of these diameters. The direction of dip is thus given by the direction of a line and the amount of dip by its length. It is therefore logical to call the directed line segment a vector—the *dip vector.*

The line joining the points of intersection of the two circles is the projection of the line of intersection of the corresponding planes. The trend of this line of intersection is given by the azimuth of its projection, and the tangent of its plunge is proportional to the length of the projection. Again it is logical to call the directed segment a vector— the *null vector*, the term *null* deriving from the fact that the line of intersection of the two planes undergoes no displacement during the earthquake.

In the earlier paper it was suggested that the strike directions of the planes in the various circum-Pacific areas were random, but that the dip vectors and null vectors showed patterns. These patterns were demonstrated by treating the dip or null vectors as free, and drawing them from a single point by means of the projection shown in Figure 1a. If in this figure we regard PQ as the vector, then it projects into the segment OQ', or simply into the point Q'. If we regard PQ as the trace of a plane drawn perpendicular to the paper, then the plane projects into a line through Q'. Parallel planes having different dips project into parallel lines at distances from the centre proportional to the dips of the corresponding planes.

McIntyre and Christie (1957) in a discussion of that earlier paper made an important contribution to the understanding of the physical significance of the null vector. They also made a number of criticisms, most of them very helpful, one or two of them pedantic. In the latter category must be their objection to the term "vector" as used in dip vector and null vector. These terms have been defended in the foregoing paragraphs. Perhaps this in itself is pedantic; it matters little what they are called so long as their significance is understood. More pertinently McIntyre and Christie pointed out that the separate analysis of strike and dip is a serious defect in procedure, since these are two aspects of a single concept—the attitude of the plane. In structural geology it is usual to define attitude by plotting the pole of the plane in a stereographic projection. This brings us to the question of projections and to the most serious criticism of their Discussion.

Structural geologists have long been accustomed to dealing with the orientation in space of lines and planes. This has been done with the stereographic projection shown in Figure 1b. Lines are drawn from the centre of the figure to meet the lower hemisphere as at Q. This point

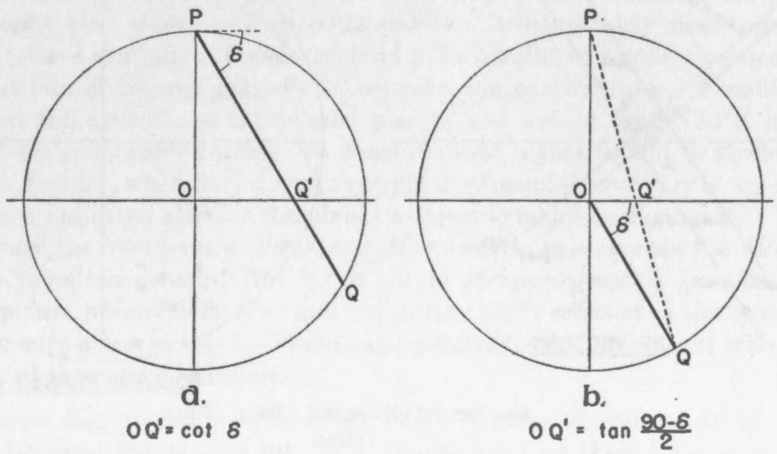

Figure 1. A comparison of the two alternate projections. In each case the heavy line is to be projected on the diametral plane drawn perpendicular to the paper through O. *a* is the projection used in the earlier paper, *b* is the projection normally used by structural geologists.

is then joined to the pole P to intersect the mapping plane at Q'. The line OQ thus projects into the line OQ', or simply into the point Q'. To plot a plane, the plane is imagined to pass through the origin and the downward normal is drawn; this is a line similar to OQ, and it is projected as before. The point Q' would be called the *pole* of a plane perpendicualr to OQ. McIntyre and Christie suggested that, since the study of the fault planes is a study in structural geology, the projection favoured by structural geologists should be used. They suggest indeed that the projection shown in Figure 1a, which was used in the earlier paper, leads to self-deception.

Before examining this criticism it should be pointed out that McIntyre and Christie have clarified the meaning of the dip vector: the dip vector defines the attitude of the fault plane, for its azimuth is perpendicular to the strike of the plane and its dip is the complement of the dip of the plane. It defines attitude just as well, although less conventionally, than the poles do. Indeed, as it turns out, it does it better.

This is shown in Figure 2, where the attitude of the planes in the New Zealand-Tonga sector are defined by dip vectors (a) and by poles (b). In b the poles lie close to the periphery of the diagram, indicating that the planes are steeply dipping, and they are drastically spread out in azimuth indicating a lack of uniformity in strike direction. It labours the very points which McIntyre and Christie sought to avoid. Figure 2a, on the other hand, shows that there is a system to the attitude of the planes—that planes which deviate from a preferred strike direction have a very steep dip.

The null vectors are plotted in the two projections in Figure 3. In the projection used in Figure 3a the distance of a point from the centre is equal to cot δ, which can vary from zero to infinity. The points are much more extended in the favoured direction than in Figure 3b where the distance of a point, being equal to tan $(90-\delta)/2$, can vary only from zero to one. This extension is not scientifically dishonest; where there is no pattern it also magnifies the confusion. But the most important point about the projection used in *a* is that parallel planes project into parallel lines instead of into arcs of circles as in *b*. This is a great convenience since we propose to search for properties related to parallel planes. I conclude that while McIntyre and Christie may properly use their favourite projection in carrying out their very valuable analysis of the fault-plane results, its advantages are not sufficiently obvious to require a change from the projection already adopted.

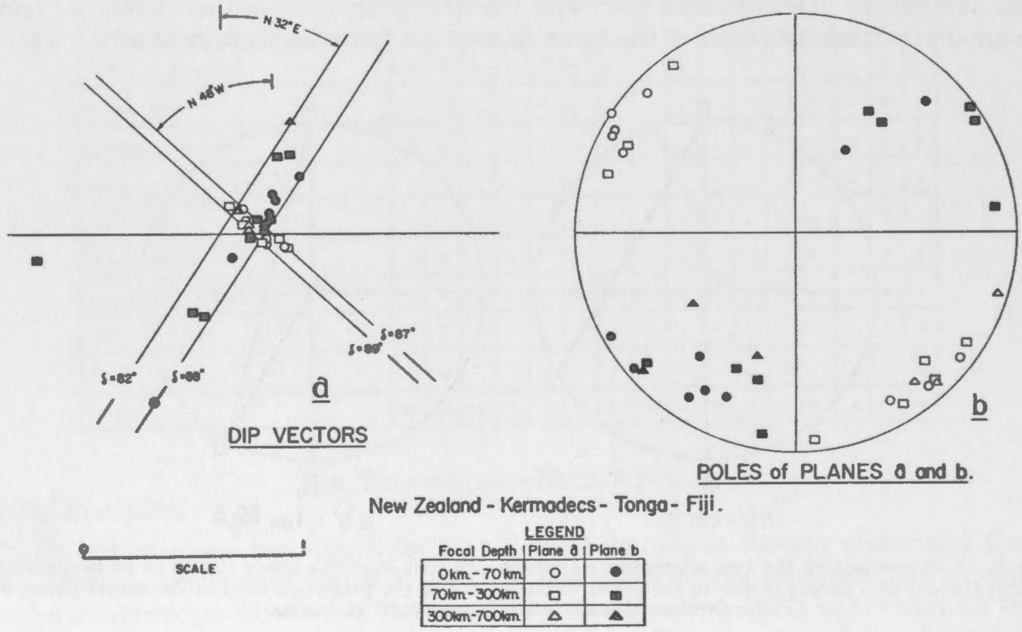

Figure 2. The attitudes of the fault planes determined in the New Zealand—Tonga sector as defined by (*a*) dip vectors and the projection of Figure 1*a* and by (*b*) poles and the projection of Figure 1*b*.

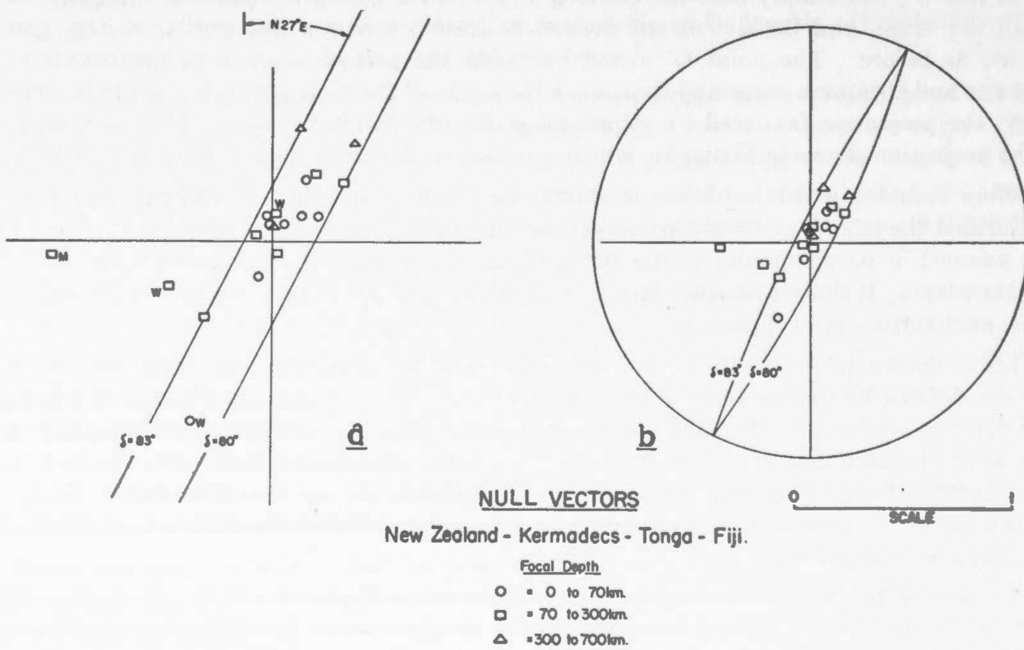

Figure 3. Null vectors and their enveloping planes as defined by (*a*) the projection of Figure 1*a* and (*b*) the projection of Figure 1*b*. Letters *M*, *W*, beside symbols indicate solutions by Mühlhäuser (1957) and Webb (1954) respectively.

Areas with Simple Null Vector Patterns

It will be a thesis of this paper, as it was of the earlier one, that the null vector has definite tectonic significance in the New Zealand-Tonga sector, in the New Hebrides, and in South America. If this can be accepted it is a most important conclusion; these areas are the most difficult ones in which to obtain solutions because of the small numbers of seismic stations within even moderate distance of the epicentres. If the results in these areas can be shown to be tectonically valid there can be little doubt that the solutions in other areas are dependable. Considering the conflict between the results of the fault-plane work and the theories of many tectonophysicists it is extremely important to establish this point.

The dip vector and null vector diagrams for the first of these areas, the New Zealand-Tonga sector, have already been shown in Figures 2*a* and 3*a*. It seems fairly clear that the dip vectors for the *b* planes (closed symbols in Figure 2*a*) tend to lie parallel to a nearly vertical plane, striking N32°E. All but two of twenty symbols lie between the parallel lines. Recalling that the dip vectors represent the attitude of the related planes, and noting that N32°E is approximately the direction of the geographic feature, we conclude that planes *b* tend to strike at right angles to the geographic feature; when they do not so strike they usually have very steep dip. A favoured direction has been indicated also for the planes *a* (open symbols in Figure 2*b*). This is not well supported, because the vectors are too steep. If, however, one accepts the direction, it would follow that the favoured direction for the *a* planes is approximately parallel to the feature. It is this set of planes which McIntyre and Christie (1957) selected as the more probable fault planes; they are supported in this by Wellman (personal communication) who is an authority on the tectonics of the area in question.

The null vector diagram for the area (Figure 3*a*) seems equally clear. All but two of nineteen null vectors lie between the parallel lines, and the direction of these lines, as was shown in the earlier paper, is approximately that of the associated geographic feature. It would certainly be desirable to establish the best direction of the lines statistically and indeed to establish that parallel lines provide the best system; these are difficult statistical problems. It must also be admitted that, whereas the typical fault in the area is a steeply dipping strike-slip one, the direction of the pattern is controlled by the distant points, and these derive from the less strongly strike-slip faults with the less steeply dipping planes. In this sense, the pattern which is being proposed as typical for the area derives from the least typical earthquakes. Despite these objections, when one considers that the points in Figure 3*a* might lie anywhere in the plane, the pattern is impressive.

The dip vector pattern for the New Hebrides is shown in Figure 4*a*, the null vector pattern in Figure 4*b*. The directions which have been suggested for the dip vector pattern are less well defined than those in the New Zealand-Tonga sector, and they are less easy to interpret. The diagram would suggest that the favoured direction for faulting is about N43°E and N66°W, and since the mean direction of the geographic feature is about N22°W, these are neither normal nor tangential to the feature. It should be pointed out that the two directions suggested in this diagram are very similar to the dip vector directions for the New Zealand-Tonga sector as shown in Figure 2*a*. This suggests the possibility that the favoured direction for the strike of the fault planes is related in the two areas.

It might be argued that a more westerly inclination to the parallel lines would fit the pattern of null vectors better than that selected. At least it seems clear that the pattern will be a NW-SE one, which is in good agreement with the strike of the geographic feature. Twelve of the fifteen points fit the pattern selected and two others come very close to doing so. This pattern is exactly parallel to the feature. Admitting the limitations of the analysis already outlined, the correlation is reasonably satisfactory.

The tectonic pattern in South America is relatively simple, but the area is so large that diagrams similar to those used in the southwest Pacific are not satisfactory. It is better to

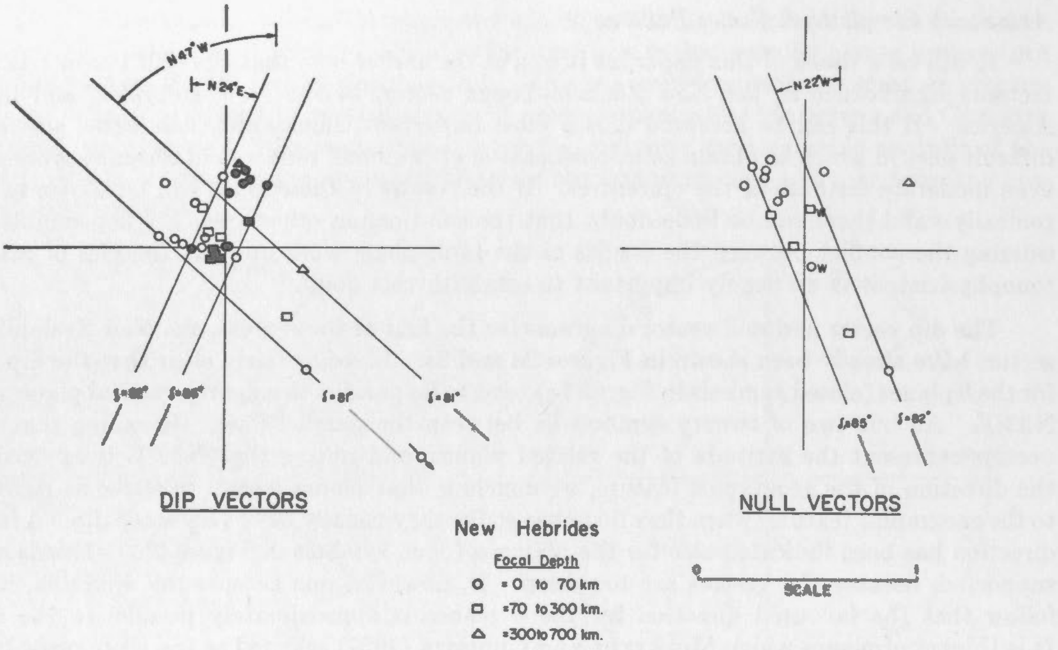

Figure 4. Dip vectors and null vectors for earthquakes in the New Hebrides. The letter *W* beside a symbol represents a solution by WEBB (1954). In the dip vector diagram open symbols refer to planes *a*, closed symbols to planes *b*.

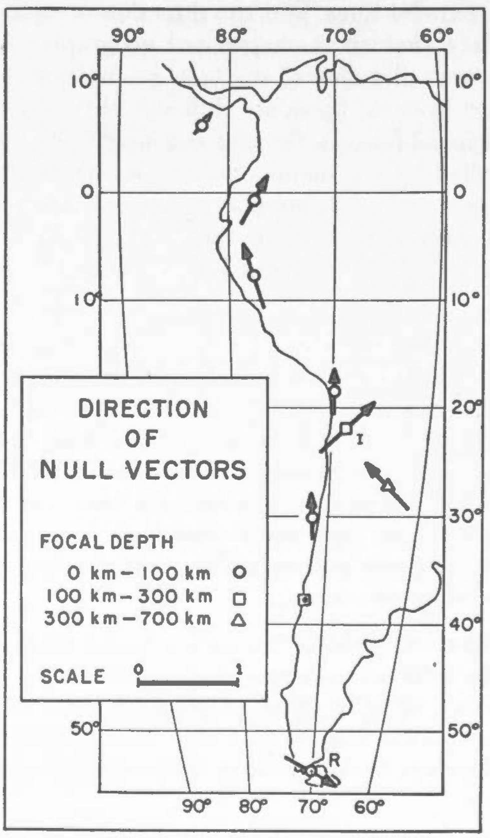

Figure 5. Null vectors for South American earthquakes. The lengths of the vectors are obtained by the projection of Figure 1*a*. The letter *I* identifies a solution by INGRAM (1957), the letter *R* one by RASCHER (1952).

plot the null vectors on a map. This has been done in Figure 5. With the exception of the solution by INGRAM the arrows are very satisfactorily parallel to the tectonic fabric of the country; even the swirl at the southern tip of the continent is followed by the null vector of RASCHER's solution. The solution by INGRAM is a very well defined and well supported one, and there can be no question about its accuracy. The epicentre lies at the junction of the northern and southern systems, and the null vector direction is probably significant.

This discussion of South American earthquakes concludes the most direct evidence for the significance of the null vector. It is submitted that the null vectors have shown a strong tendency to lie parallel to the tectonic pattern in the New Zealand-Tonga sector and in South America, and a less definite but still well defined tendency in the New Hebrides. It is further submitted that this cannot be an accidental matter and that, since it occurs in the regions where solutions are most difficult to obtain, the techniques of the fault-plane project must be thereby confirmed. We conclude that the null vector must have tectonic significance, and we shall use it to examine areas which are less simple tectonically.

Areas with Double Null Vector Pattern

There are two Pacific areas in which the null vectors suggest a double pattern, as if two different failure systems were in simultaneous operation. The first such area is the northwest Pacific. The dip and null vector patterns for these areas, shown in Figure 6 are considerably different than those given in the earlier paper. This has come about because of the large number of new solutions many of which, having strong dip components, have their vector points far off-scale. These off-scale points dictate the directions of the parallel lines.

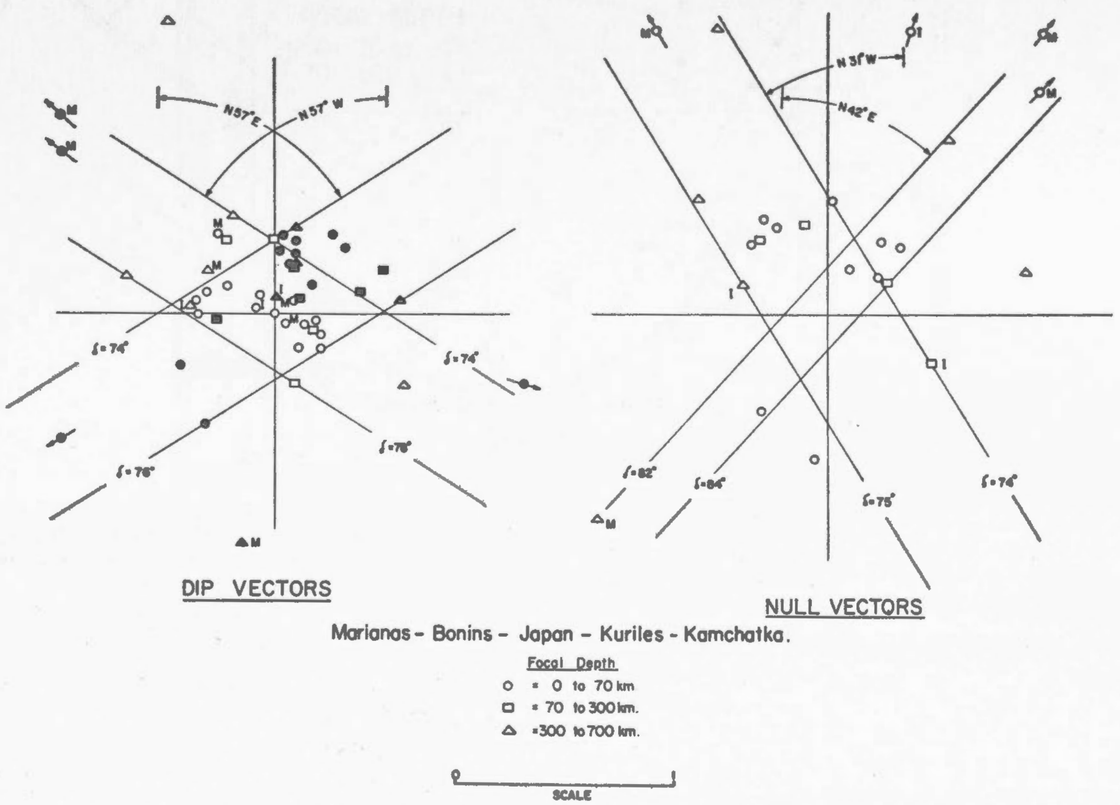

Figure 6. Dip vectors and null vectors for earthquakes in the northwest Pacific. The letter *M* identifies points from solutions by MÜHLHÄUSER (1957), the letter *I* points from solutions by ICHIKAWA (1955).

In the dip vector diagram open symbols refer to planes *a*, closed symbols to planes *b*.

The pattern selected for the dip vectors is a highly symetrical one, with deviations of about 15° from vertical planes striking 57° east and west of north. All but three of forty-nine dip vectors adhere to this pattern. This suggests that the favoured direction of faulting is either N33°W or N33°E. The former direction is inclined at 20° to the mean normal to the arc. I have elsewhere published evidence (Hodgson 1958), based largely on Russian solutions, that this is the probable direction of the faults of the area.

The null vector diagram (Figure 6*b*) suggests however that the problem is not so simple. In the southwest Pacific the null vectors defined a single direction for each arc; here two directions appear to be defined. All but three of twenty-four null vectors fit the suggested pattern, the directions of which are dictated by the off-scale points. These directions are somewhat different than those determined in the earlier paper, but they give a better fit to the geographic directions there selected (Hodgson, 1957, p. 636) of N38°E and N30°W.

A second area with an apparently dual null vector pattern is the Pacific coast of North America, the diagrams for which are shown in Figure 7; note that in this figure the scale for the null vector diagram is only one-fifth of that used in the other diagrams.

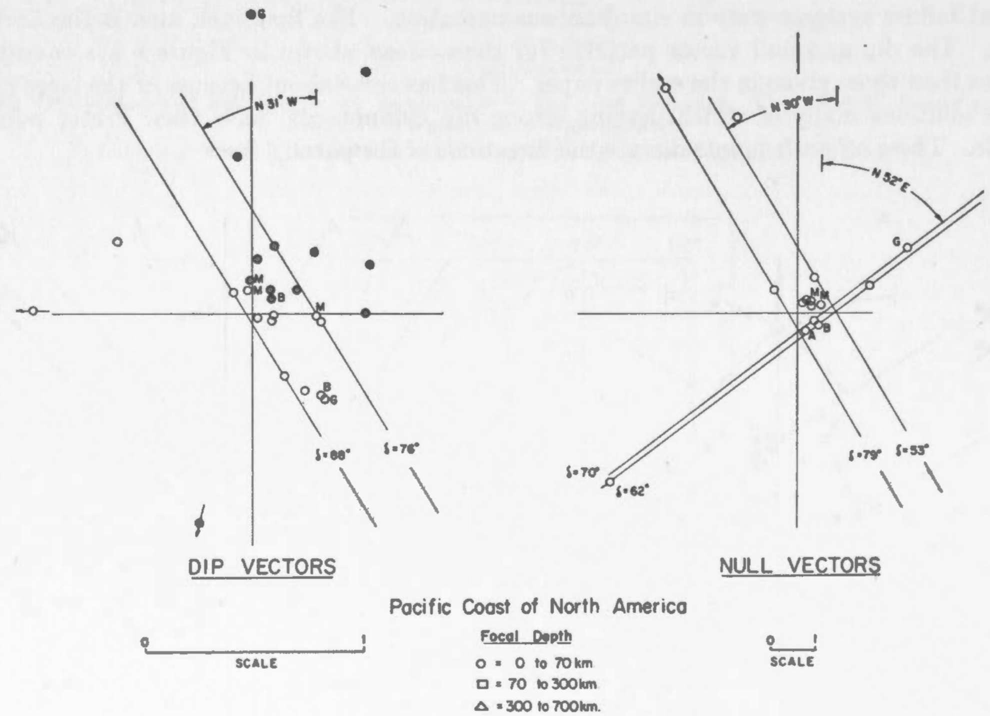

Figure 7. Dip vectors and null vectors for earthquakes on the Pacific coast of North America. Note the special scale used in the null vector diagram. The letters *A*, *B*, *G* and *M* indicate that the points come from solutions by Adkins (1940), Byerly (1938), Gutenberg (1955) and Mühlhäuser (1957) respectively.

In the dip vector diagram open symbols refer to planes *a*, closed symbols to planes *b*.

A direction N31°W has been selected as the best direction for the dip vectors of plane *a*. This is not a well defined direction, a much more westerly trend would be equally easy to defend. Indeed it may well be that there is no favoured direction for the *a* dip vectors; there is certainly no direction evident for the *b* set. There does, however appear to be some evidence for a dual pattern in the null vector diagram, even when we bear the reduced scale in mind. The significance of the two directions suggested was discussed in the earlier paper. It is worth noting that the better defined of the two planes is not vertical, but dips at about 66° to the southeast.

It is much too early to suggest the significance of the dual null vector pattern found in the two north Pacific areas. If one is prepared to accept the patterns it must follow that, in each of these vast areas, the tectonics may be considered as a whole; in the next section we shall see that in other much smaller areas this cannot be done. It must also follow that, in each area, there are two different families of earthquakes. It seems certain that these families must be regarded separately in studies such as those which McIntyre and Christie (1957) made in the southwest Pacific. It is possible that they should be considered separately also in constructing strain release diagrams.

Areas with Complex Null Vector Pattern

We now turn our attention to certain other areas in which, considering the section as a whole, no null vector pattern can be found. The first such area is the Aleutians, for which the null vectors have been shown on in Figure 8. If there is any pattern in the null vectors it seems to be quite different from that in the south Pacific, for here the more prominent vectors are perpendicular rather than parallel to the features. It is probably more significant that adjacent null vectors are nearly parallel: for example the three vectors on the Alaskan mainland are approximately parallel to each other, and so are the vectors for the next two earthquakes to the west. This suggests that in this particular area the tectonics of different small sections must be considered separately.

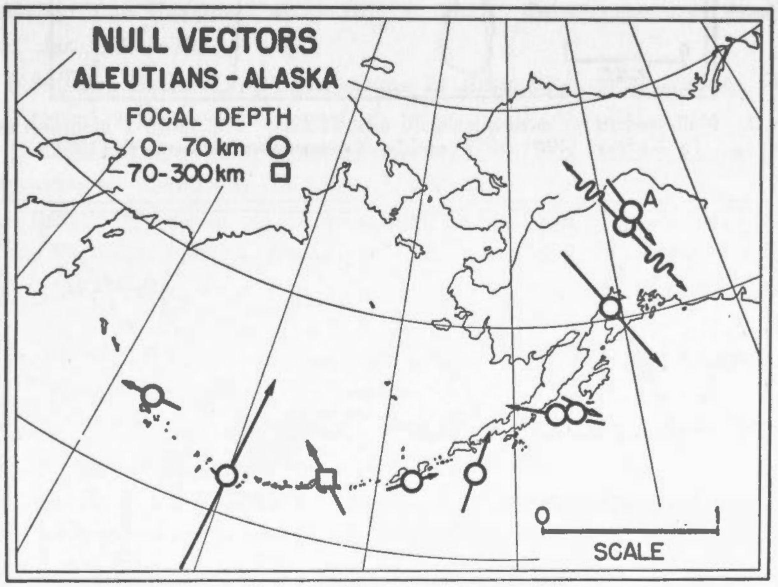

Figure 8. Null vectors for Aleutian earthquakes. The symbol designated *A* represents a solution by Adkins (1940). In this, and in subsequent diagrams, null vectors of greater than unit length have been indicated by a compressed arrow.

In the version of this paper that was read at the Meetings it was suggested that the New Guinea-Indonesia area was similar in its complexity. In his contribution to this symposium Ritsema has shown that the null vectors in the area of his interest probably have a pattern, not as simple as that in the southwest Pacific, but a good deal more regular than I had supposed. The reader is referred to his very complete discussion, to which nothing can be added here.

Null vectors for earthquakes in central Asia are shown in Figure 9, those for the Mediterranean in Figure 10. Again it seems clear that there is no over all pattern in these large areas but that these areas must be subdivided for discussions of their tectonics.

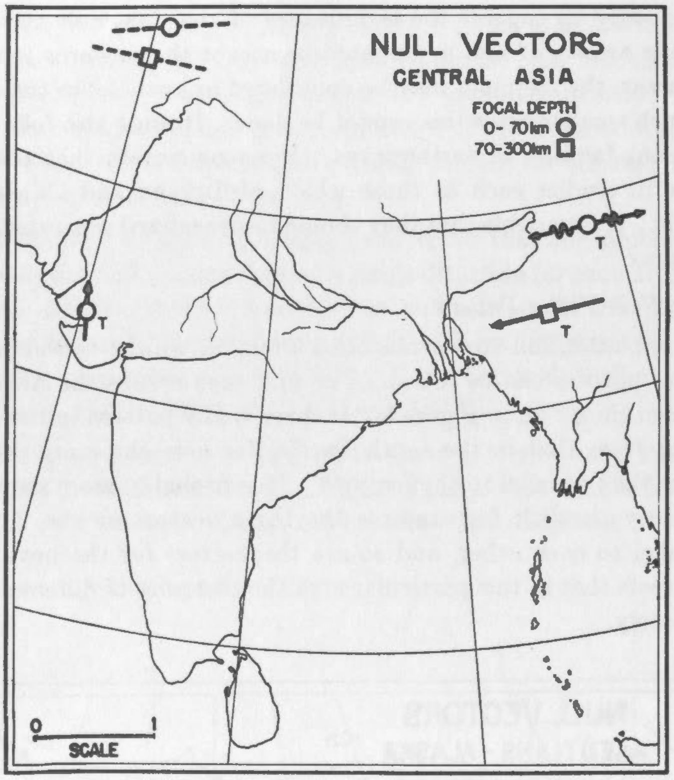

Figure 9. Null vectors for earthquakes in central Asia. The letter *T* identifies solutions by Tandon (1954, 1957) and by Tandon and Mukherjee (1956).

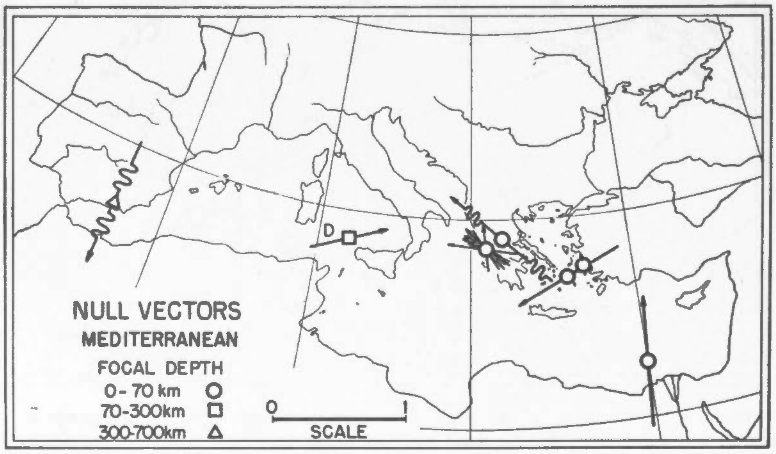

Figure 10. Null vectors for Mediterranean earthquakes. The letter *D* identifies a solution by DiFilippo (1950a).

SUMMARY AND CONCLUSIONS

Eighty-six fault-plane solutions, from various sources, have been listed; combining these with the 75 solutions given earlier yields 161 earthquakes for analysis.

From the combined results it appears that strike-slip faulting is by far the most common, but that there are certain areas in which the faulting in not exclusively strike-slip. Among these areas are Alaska and British Columbia, central Asia, the zone from the Marianas to Japan, and southeast Asia. The latter two are newly defined as areas in which the faulting is not exclusively strike-slip. The addition of two such large areas to the previous small list must raise the question whether the importance of strike-slip faulting has been overemphasized. It now appears possible that a disproportionate number of solutions have been made in areas in which the faulting is exclusively strike-slip.

There is no support for the contraction hypothesis from the analysis of the direction of dip-slip.

The null vectors for tectonically simple areas show simple patterns related to the geographic features. This inspires some confidence in the null vector as a diagnostic tool. So used it suggests that a double failure system has developed in the northeast and northwest Pacific, while the Aleutians, central Asia and the Mediterranean are so tectonically complex that only limited areas of them can be considered at one time.

ACKNOWLEDGEMENTS

I am very much indebted to Miss Anne Stevens for the help she gave in preparing and checking the tables and diagrams included in this paper.

References

ADKINS, J. D. (1940): The Alaskan Earthquake of July 22, 1937. *Bull. Seismol. Soc. Am.*, **30**, 353–376.

BYERLY, P. (1938): The Earthquake of July 6, 1934: Amplitudes and First Motion. *Bull. Seismol. Soc. Am.*, **28**, 1–13.

DIFILIPPO, D. (1950*a*): Sulla Rappresentazione in Superficie della Natura Dinamica di una Scossa con Ipocentro Profondo. *Annali di Geofisica*, **3**, 379–391.

DIFILIPPO, D. (1950*b*): Sulla Rappresentazione in Superficie della Natura Dinamica di una Scossa all'Ipocentro. *Annali di Geofisica*, **3**, 263–279.

GUTENBERG, B. (1955): The First Motion in Longitudinal and Transverse Waves of the Main Shock and the Direction of Slip. *Bulletin 171, State of California Division of Mines*, 165–170.

HODGSON, J. H. (1957): Nature of Faulting in Large Earthquakes. *Bull. Geol. Soc. Am.*, **68**, 611–643.

HODGSON, J. H. (1958): Direction of Displacements in Western Pacific Earthquakes. *Gutenberg Testimonial Volume*, Pergamon Press, London.

HODGSON, J. H., and W. M. ADAMS (1958): A Study of the Inconsistent Observations in the Fault-Plane Project. *Bull. Seismol. Soc. Am.*, **48**, 17–31.

HODGSON, J. H., and J. I. COCK (1957): Direction of Faulting in the Larger Earthquakes of 1954-1955. *Publications of the Dominion Observatory*, Ottawa, **19**, 221–258.

HODGSON, J. H., and A. E. STEVENS (1958): Direction of Faulting in the Larger Earthquakes of 1955-56. *Publications of the Dominion Observatory*, Ottawa, **19**, 281–317.

ICHIKAWA, M. (1955): On the Distribution of the Initial Shock of the P-Wave. *Quarterly Journal of Seismology, Japan*, **20**, No. 4. (*Note:* A translation of this paper, in English, is available from the Dominion Observatory, Ottawa).

INGRAM, R. E., S.J. (1957): Fault Plane of the Chile Earthquake, December 7, 1953. *Bull. Seismol. Soc. Am.*, **47**, 281–285.

MCINTYRE, D. B., and J. M. CHRISTIE (1957): A Discussion of 'Nature of the Faulting in Large Earthquakes'. *Bull. Geol. Soc. Am.*, **68**, 645–652.

MÜHLHÄUSER, S. (1957): Herdmechanische Vorgänge bei einigen Zirkumpazifischen Erdbeben. *Tellus*, **9**, 104–117.

RASCHER, W. F. (1952): *The Direction of Faulting in some South American Earthquakes*. B. Sc. Thesis, Saint Louis University.

RITSEMA, A. R. (1956): The Mechanism in the Focus of 28 South-east Asian Earthquakes. *Verhandelingen 50, Meteor. and Geophys. Institute, Djakarta.*

ROMNEY, C. (1957): Seismic Waves from the Dixie Valley—Fairview Peak Earthquakes. *Bull. Seismol. Soc. Am.*, **47**, 301–319.

SCHEIDEGGER, A. E. (1957): The Geometrical Representation of Fault-Plane Solutions of Earthquakes. *Bull. Seismol. Soc. Am.*, **47**, 89–110.

SHOR, G. G., Jr., and E. ROBERTS (1958): San Miguel, Baja California Norte, Earthquakes of February, 1956. *Bull. Seismol. Soc. Am.*, in press.

TANDON, A. N. (1954): Direction of Faulting in the Great Assam Earthquake of 15 August 1950. *Indian Journ. Meteor. Geophys.*, **6**, 61–64.

TANDON, A. N. (1957): The Rann of Cutch Earthquake of 21st July, 1956. *Indian Journ. Meteor. Geophys.*, in press.

TANDON, A. N., and S. M. MUKHERJEE (1956): The Manipur-Burma Border Earthquake of 22 March 1954. *Indian Journ. Meteor. Geophys.*, **7**, 1–10.

TOCHER, D. (1955): *Seismic Velocities and Structure in Northern California and Nevada.* Doctoral Thesis, University of California.

WEBB, J. P. (1954): *A Seismological Study of the Tectonics of a Portion of the Southwest Pacific.* Doctoral Thesis, Saint Louis University.

The Kinematics of Faulting from Seismic Data

BY DONALD B. MCINTYRE and JOHN M. CHRISTIE
Pomona College, Claremont, California.

ABSTRACT

The attitude of a fault and the nature of the slip on it can be determined from the pattern of distribution over the globe of compressional and dilatational first motions of P waves. The method as used by BYERLY and HODGSON gives two possible solutions for each earthquake. The writers have already demonstrated that in an area showing a certain type of structural homogeneity, the ambiguity might be resolved by consideration of the geometrical relations between the pairs of solutions: it was concluded that in the southwest Pacific the movement was on steep strike-slip faults striking parallel to the physiographic feature. In the present paper solutions from other areas are discussed.

On the assumption that the ambiguity of the results of a P-wave analysis can be resolved by study of the first motions of S waves, KOGAN has derived unique solutions for the northwest Pacific. It is shown that KOGAN's results for the Japan-Kamchatka area differ markedly from HODGSON's solutions for the same region and time interval based on P-wave records obtained at stations distributed all over the world. Similarly the solutions of HONDA *et al* for the same area and time interval differ markedly from the solutions of both HODGSON and KOGAN.

The value of solutions for an earthquake sequence is emphasized and an analysis of a series of Greek earthquakes (1953) is attempted.

INTRODUCTION

If an earthquake is generated by movement on a fault, and if the orientations of the fault and of the slip on it are known, then it is possible to predict the distributions of stations receiving respectively compressional and dilatational first motions of the P phase. Conversely, from an adequate distribution of data concerning the observed signs of the first motion of P, the orientation of the generating fault and the nature of the slip on it may be determined. The method, originated by BYERLY, and developed especially by HODGSON, is now well known. Unfortunately, the symmetry of the data is such that two solutions are always possible; the orientations of two planes are found, one of these is the fault and the other is the plane normal to the direction of slip. Using kinematic reference axes*, we can say that, whereas the B axis is uniquely determined as the intersection of the two planes, it is not possible to distinguish between the planes and hence between the A and C axes.

Perhaps the greatest interest in the results obtained by HODGSON and his collaborators is the unambiguous demonstration that the B axes are usually steep (MCINTYRE and CHRISTIE, 1957, Figure 1) and hence that the fault movements which give rise to major earthquakes are predominantly strike-slip. As a result of the ambiguity between A and C inherent in the method, there is uncertainty about the relative orientations of the faults and the approximately rectilinear or arcuate physiographic features with which they are associated. It has been claimed that for any area the B axes tend to lie parallel to a vertical plane having the direction of the associated feature. The fault-plane solutions give in each case two perpendicular planes, one of which is the fault plane; the present writers examined the structure resulting from one of the two sets of planes for all solutions in a single arc, and then from the other. This was done by means of β diagrams; that set of planes which gave a β maximum coinciding with the maximum of B axes for the arc was taken to represent the faults†.

---

*A = motion direction in the fault plane;
B = normal to A in the fault plane (equal to null vector);
C = normal to the fault plane (AB).

†One of the conditions which must be fulfilled but which was not stated explicity (MCINTYRE and CHRISTIE, 1957, p. 651), is that the planes must fall into two groups. These groups may be defined statistically but in such a case ambiguity will remain for any planes which do not belong to these groups.

It is essential that the solutions with which such an analysis is made are derived from faults which belong to a genetically related series, such as the faults constituting a movement zone like the San Andreas Rift. The selection of areas for analysis is therefore a matter of critical importance, for if an area includes two or more unrelated systems of faults, a simple result could not be expected using this technique. It seems to have been generally assumed that the long, gently-curving island arcs of the circum-Pacific region represent such simple systems. However, it is not unlikely that some of the island arcs are more complex than this, and close to the intersections of arcs complication of the kinematic picture must certainly exist. These complexities may account for the failure of our analyses in some of the areas selected, though lack of data is considered to be a more important cause. Old fault planes or other planes of weakness unrelated to the main fault system may become active during a sequence of movements if the resolved shear stress on any of these becomes sufficiently great. Solutions obtained for movements on such planes might vitiate the patterns obtained for an area.

The best results are to be expected from series of shocks belonging to a single earthquake sequence, for we consider that in a localized sequence there is the greatest likelihood of the movements being kinematically related. One such sequence (in the Greek Islands, August 1953) is analyzed below and it is shown that the data could be interpreted in terms of movement with the same sense and more or less the same direction on a group of sub-parallel planes. Eyewitness accounts indicate that at least some of the movements followed the pattern deduced. It is to be hoped that solutions will be obtained for other sequences of this type, such as the remarkable series of shocks which occurred in the Aleutians in March, 1957. Where sequences of shocks are not available, considerable advantage should be gained by subdividing the areas at present used for analysis; some of these are island arcs almost 3,000 miles long. This procedure has already been employed by HONDA (1957) in his analysis of movements in the region of Japan. By separate analysis of solutions for smaller areas and shorter intervals of time it may be possible to resolve the complexity in some of the areas so far considered. An ideal case would be a number of foreshock-main shock-aftershock sequences in a limited area.

NEW ZEALAND-KERMADEC-TONGA-FIJI

When the available data were plotted on equal area projections, it was found that only for HODGSON's New Zealand-Kermadec-Tonga-Fiji group was the claim justified that in any one area the B axes defined a plane. In the other areas the number of analyses was as yet too small. In the New Zealand-Fiji area, the B axes define a vertical plane striking parallel to the trend of the feature and containing a single strong maximum (MCINTYRE and CHRISTIE, 1957, Figures 2–4); the A and C axes (which of course cannot be distinguished from one another) fall into two groups, normal and parallel respectively to the plane of the B axes. Whereas the group of planes which are parallel to the plane of the B axes gives a β maximum of nearly 30 per cent per 1 per cent area coinciding with the B maximum, the other planes give two much smaller β maxima which do not coincide with B. Hence it was concluded that the group of planes parallel to the physiographic feature probably represent the faults.

Dr. HODGSON has since made available to us a large number of new solutions. Four of these are from the New Zealand-Kermadec-Tonga area and they are shown in Figure 1*a*. The result of adding these new analyses to the thirteen previously available is to maintain the two groups of planes (Figure 1*b*), and to increase the strength of the β maximum for the northeast-striking planes while weakening the B maxima for the northwest-striking planes (compare Figures 1*c* and *d* with MCINTYRE and CHRISTIE, 1957, Figures 3 and 4).

At the time of writing our contribution to the discussion of HODGSON's paper (HODGSON, 1957), we did not have data on the sense of movement implied by our selection of a northeasterly strike for the faults. This important information has fortunately been included in the table of data accompanying the published paper (HODGSON, 1957, Table 1), and is also available for HODGSON's new analyses (personal communication). There are seventeen solutions for the New

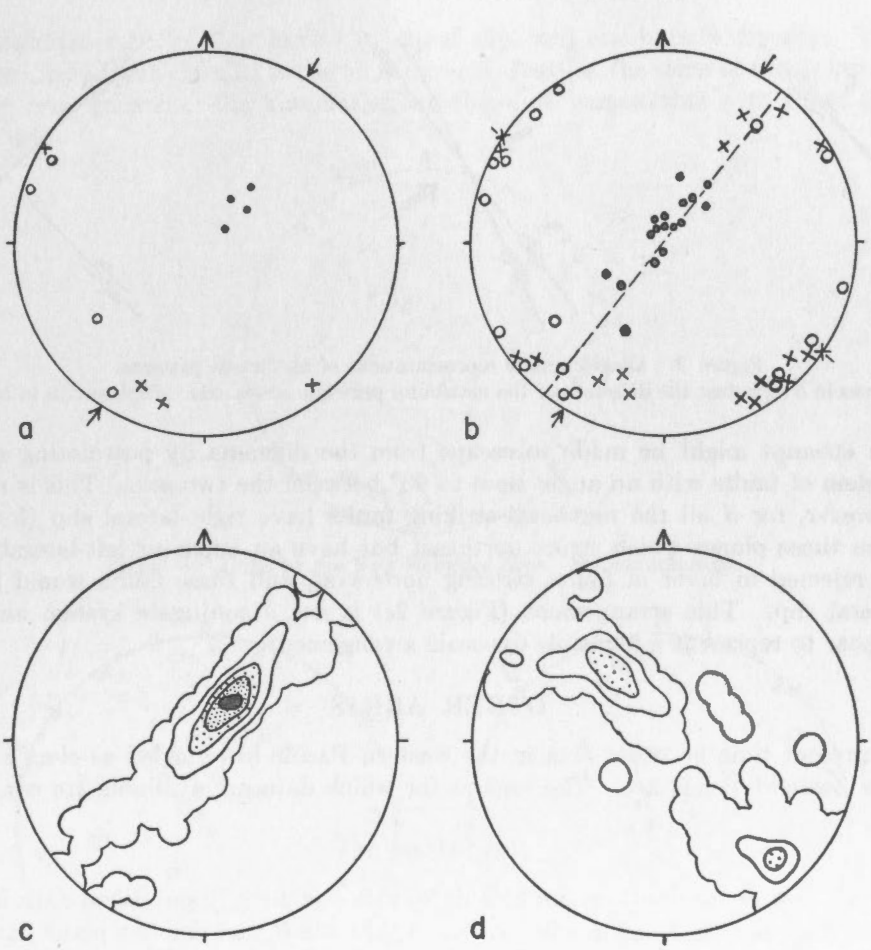

Figure 1. **Data for the New Zealand-Kermadec-Tonga-Fiji arc.**
a. Four new solutions.
b. Total of seventeen solutions.
c. β diagram for group of planes with northeast strike.
Contours: 30, 20, 10, 5, 3/4 per cent per 1 per cent area.
d. β diagram for group of planes with northwest strike.
Contours: 10, 5, 3/4 per cent per 1 per cent area.

The following symbols are used in all the projections except where otherwise stated:
● ***B* axis.**
⊗ **Pole of a plane with pure dip-slip movement.**
○ **Pole of a plane with right-lateral strike-slip component of movement.**
× **Pole of a plane with left-lateral strike-slip component of movement.**
Arrows indicate the mean trend of the associated physiographic feature in each area.
All data are plotted in the lower hemisphere of an equal-area projection; the primitive circle is horizontal with north at the top.

Zealand-Tonga area and of these nine have right-lateral slip and eight have left-lateral slip. There are several possible interpretations of this interesting result:

i) The large earthquakes may all result from slip on essentially parallel faults on which the sense of slip oscillates between right and left lateral (Figure 2*a*).

ii) The faults may constitute a system of two sets of slip surfaces inclined at small angles to each other and with opposite senses of slip (Figure 2*b*). This would imply a higher degree of plasticity than seems probable, and in the available data there is no indication of two such sets of faults.

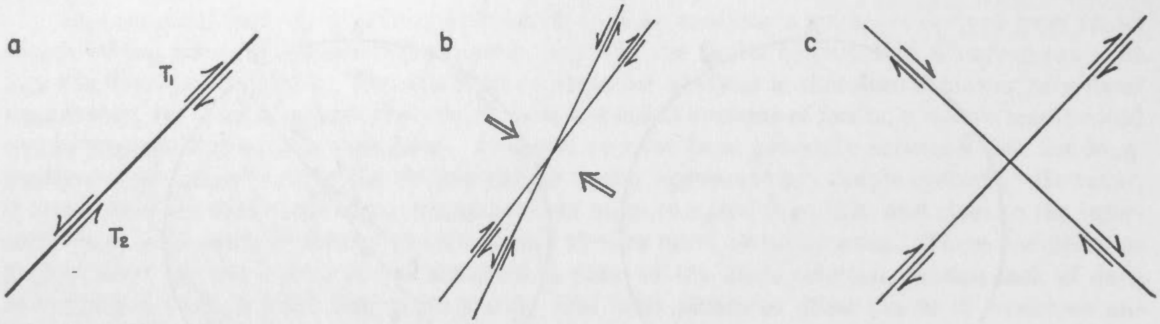

Figure 2. Diagrammatic representations of movement patterns.
Arrows in *b* represent the direction of the maximum principle stress axis. Explanation in text.

iii) An attempt might be made to escape from the dilemma by postulating a conjugate system of faults with an angle close to 90° between the two sets. This is not possible however, for if all the northeast-striking faults have right-lateral slip (for example), then those planes which strike northeast but have an apparent left-lateral slip would be rejected in favor of faults striking northwest, and these faults would have right-lateral slip. This arrangement (Figure 2*c*) is not a conjugate system and does not appear to represent a plausible dynamic arrangement.

OTHER AREAS

At the present time no other area in the western Pacific has yielded as clear a pattern as has the New Zealand-Tonga arc. The regions for which data are available are commented on briefly.

New Hebrides

Hodgson's new determinations are combined with the already published data in Figure 3. The pattern is now more in keeping with the claim that the *B* axes define a plane parallel to the physiographic feature, but the scatter is considerable and the poles of the planes do not fall into two distinct groups. The data do not fulfill the conditions previously outlined and an analysis cannot be made for this area.

Sumatra-Timor

Ritsema (1956) has published seventeen solutions for the Sumatra-Timor arc and these are shown in Figure 4*a*. The *B* axes do not define a plane and analysis of the type employed for the New Zealand-Tonga arc is not applicable in this area.

Phillipines-New Guinea

Nine solutions for this arc have been published by Ritsema (1956). Eight of the *B* axes define a plane striking north-northwest, a little oblique to the trend of the physiographic feature (Figure 4*b*). The remaining earthquake had a horizontal *B* axis nearly normal to this plane; the movement on this fault is so different from the pattern given by the other earthquakes that it has been omitted from the analysis. The poles of the planes given by the eight solutions fall into two groups, representing planes striking northwest and northeast respectively. The northwest-striking planes, which are parallel to the general trend of the feature, give a β maximum of 21 per cent per 1 per cent area coinciding with the *B* maximum (Figure 4*c*), whereas the northeast-striking planes give a weaker β maximum ($17\frac{1}{2}$ per cent) nearly normal to the *B* maximum (Figure 4*d*).

Although there is still a scarcity of data from this arc, the existing data may be interpreted in an analogous manner to those from the New Zealand-Fiji arc; the planes striking parallel to the physiographic feature appear to be the faults. It is interesting to observe that of these, three have right-lateral slip, four have left-lateral slip, and one is pure dip-slip. Thus, if the fault planes are indeed sub-parallel to the physiographic feature, the sense of slip in this movement zone has not been constant; the kinematics are therefore comparable with those of the New Zealand-Fiji arc.

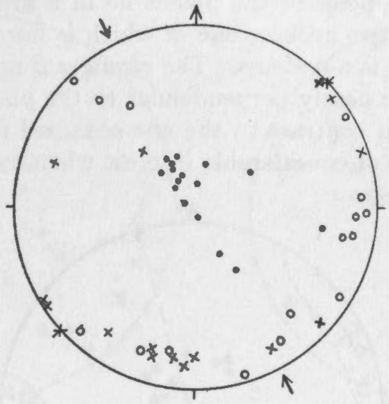

Figure 3. Data for the New Hebrides Area. Sixteen solutions.

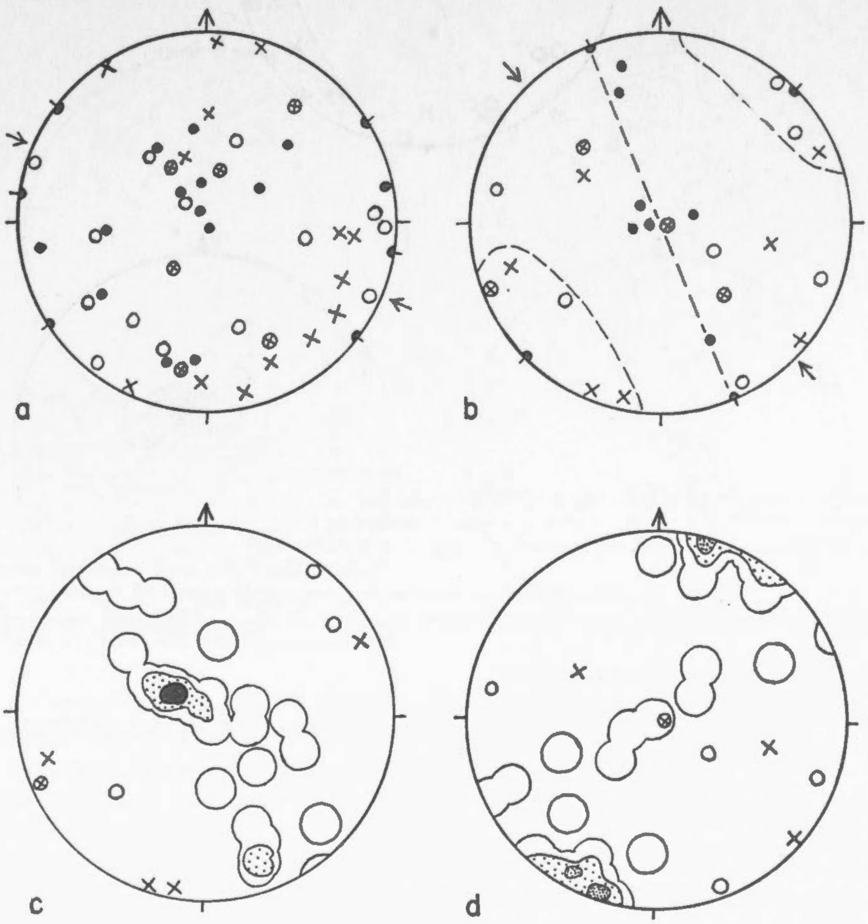

Figure 4. Data for the Sumatra-Timor and Philippines-New Guinea arcs.
a. Seventeen solutions for the Sumatra-Timor arc.
b. Nine solutions for the Philippines-New Guinea arc.
c. β diagram for planes with northwest strike (poles enclosed by broken line in b). Contours: 21, 10½, 3½ per cent per 1 per cent area.
d. β diagram for planes with northeast strike. Contours: 17½, 10½, 3½ per cent per 1 per cent area.

Kuriles-Kamchatka

From the data now available from this arc (Figure 5*a*) it might be claimed that the *B* axes define a vertical plane, but the definition is very poor; the *B* axes tend rather to lie in a single maximum. In consequence the poles of the planes lie in a great circle about this maximum. The poles may be divided into two groups, one of which is normal to the plane of the *B* axes, but the separation of the groups is not sharp. The stronger β maximum (Figure 5*c*) is obtained for the planes which strike more nearly perpendicular to the plane of the *B* axes, and for these planes $\beta = B$. This result is in contrast to the one obtained for the areas already described. The patterns for this arc will be of considerable interest when more data are available.

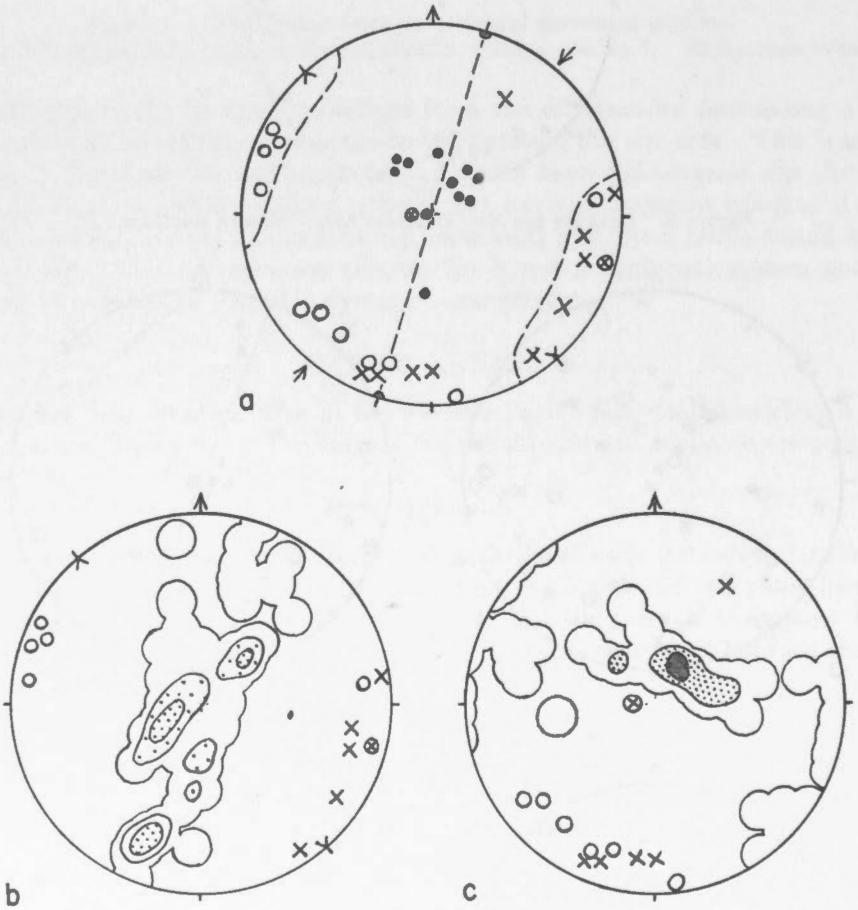

Figure 5. Data for the Kuriles-Kamchatka arc.
a. Total of twelve solutions.
b. β diagram for group of planes enclosed by broken line in a. Contours: 10, 6, 1½ per cent per 1 per cent area.
c. β diagram for other group of planes. Contours 18, 10, 1½ per cent per 1 per cent area.

Comparison of Solutions from Different Sources

Three groups of workers have published solutions for the Mariana-Bonin-Japan-Kamchatka area and their results are shown in Figure 6. Hodgson and co-workers (Hodgson, 1957, and unpublished data) have utilized reports, obtained in response to questionnaires, from stations with world-wide distribution. Miss Kogan, working with Dr. Keylis-Borok in Moscow (Kogan, 1954, cited by Scheidegger, 1957) made use of records from stations in the U.S.S.R. and the scanty data available in the literature for other stations. Honda and his colleagues (Honda, *et al.*, 1957) appear to have used data from Japanese stations alone.

HODGSON included thirteen solutions from the Bonins, Japan and Kamchatka in his 1957 paper and has since supplied us with seven additional solutions. These are all shown in Figure 6*a*. The pattern is characterized by steep *B* axes which do not define a plane.

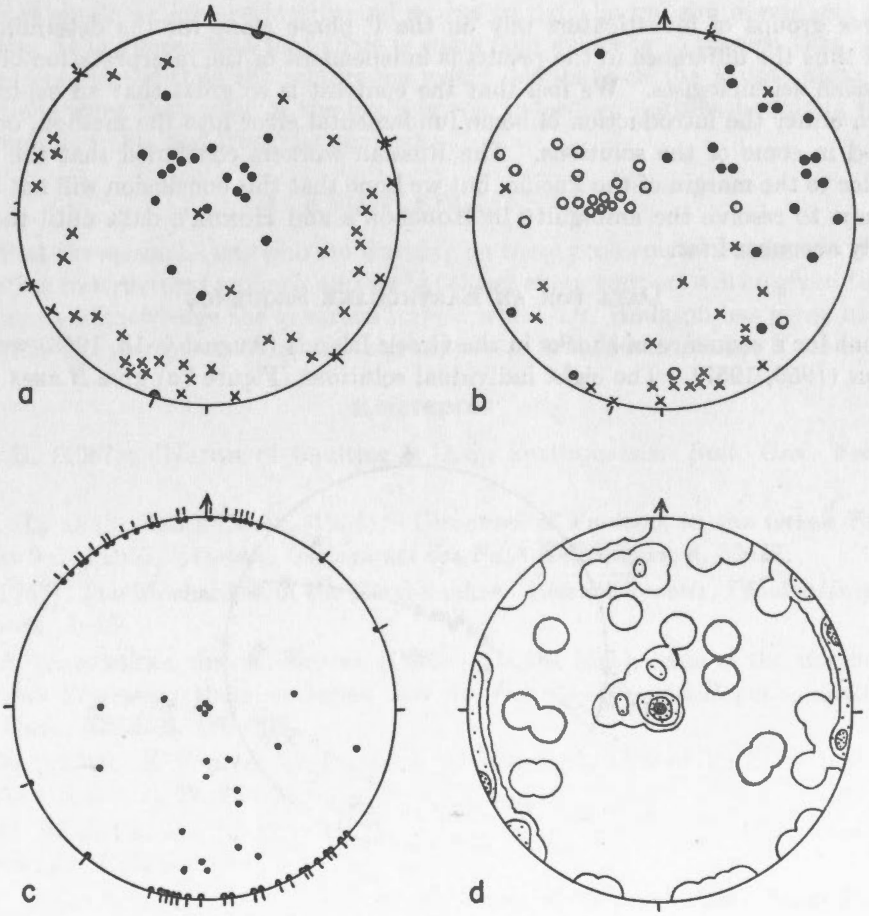

Figure 6. Comparison of data from different sources.

a. Twenty solutions by HODGSON for the Mariana-Bonin-Japan-Kamchatka area. Planes are not distinguished on the basis of type of movement: crosses represent poles of all planes (*A* and *C* axes).

b. Twenty-one solutions by KOGAN for same area. Crosses represent poles of faults (*C* axes) and open circles are movement directions (*A* axes).

c. Forty-three *B* axes from solutions by HONDA, *et al.*, for same area.

d. Eighty-six poles of planes (*A* and *C* axes) from the forty-three solutions represented in c. Contours: 20, 10, 5, 1½ per cent per 1 per cent area.

A number of solutions for earthquakes in this area have been determined by KOGAN. The Russian workers employed the first motion of the P phase to determine the orientations of the two planes and then distinguished the fault plane from the auxiliary plane by study of the S phase. Thus, provided an adequate distribution of data regarding P was available, and the intrepretation of S is reliable, a unique solution is found for each earthquake. On Figure 6*b* are shown KOGAN's twenty-one solutions for the same area as covered by HODGSON's data (Figure 6*a*).

HONDA, *et al.* (1957, Table I) have listed the maximum pressure and the maximum tension which they inferred from their data. This has enabled us to determine the attitudes of the *B* axes and nodal planes for each of forty-three earthquakes in the vicinity of Japan. The *B* axes for these solutions are represented in Figure 6*c* and the poles of planes are shown in the contoured diagram (Figure 6*d*).

The contrast between the three groups of solutions is remarkable, although each group shows strong preferred orientations of *B* axes. Whereas the *B* axes determined by HODGSON are characteristically steep, those found by KOGAN are gently plunging; the pattern of *B* axes of HONDA and his colleagues is similar to neither of these.

All three groups of investigators rely on the P phase alone for the determination of the *B* axis, and thus the difference in the results is independent of the interpretation of the S phase by the Russian seismologists. We feel that the contrast is so great that an explanation must be sought in either the introduction of some fundamental error into the method, or inadequacy of data used in some of the solutions. The Russian workers concluded that the faults strike perpendicular to the margin of the Pacific, but we hope that this conclusion will not be employed in an attempt to resolve the ambiguity in HODGSON's and HONDA's data until the contrast is satisfactorily accounted for.

DATA FOR AN EARTHQUAKE SEQUENCE

Solutions for a sequence of shocks in the Greek Islands (August 9–13, 1953) were published by HODGSON (1956, 1957). The eight individual solutions (Figure 7*a*) give *B* axes which define

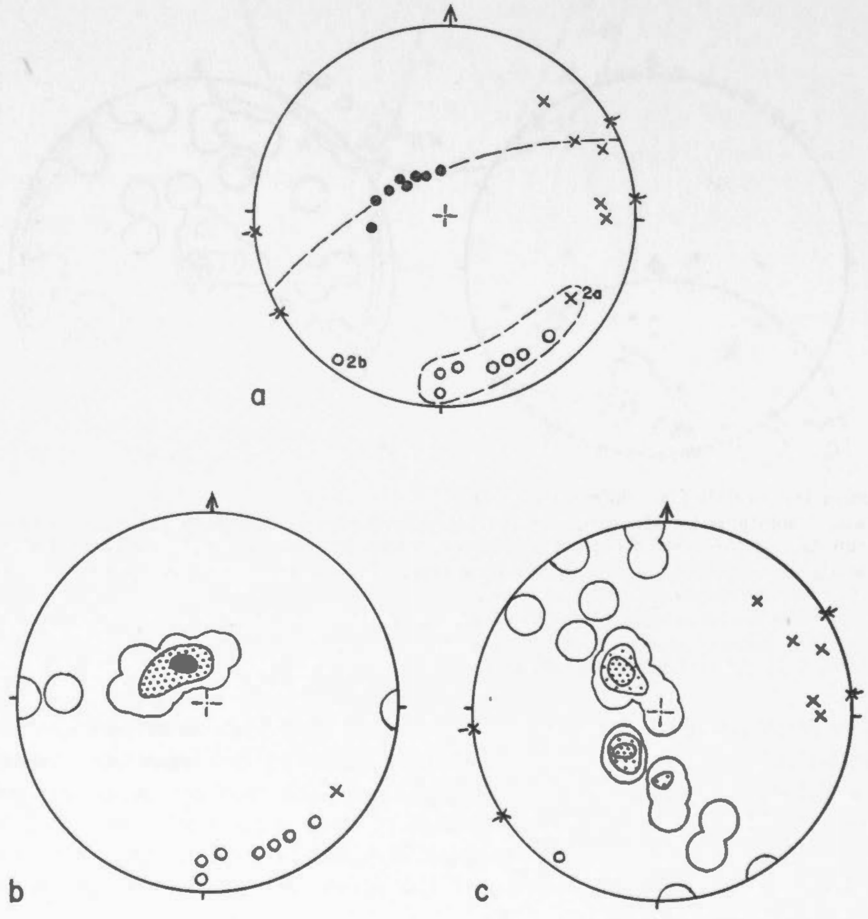

Figure 7. Analysis of the Greek earthquake sequence of August 9-13, 1953.
a. Solutions for eight shocks.
b. β diagram for planes with northeast strike (poles enclosed by broken line in a). Contours: 50 per cent, 25 per cent, 3½ per cent per 1 per cent area.
c. β diagram for planes with northwest strike. Contours 21 per cent, 10½ per cent, 3½ per cent per 1 per cent area.

No linear physiographic feature is present in the area covered by the epicenters of these shocks.

a plane dipping steeply towards the northwest, and the planes can be grouped into two broad orientations, one of which strikes approximately parallel to the plane of the B axes. This group gives a β maximum $= B$, whereas there is no strong β maximum for the other group. The spread of these two groups is such that HODGSON's planes 2*a* and 2*b* could be interchanged so that all the earthquakes might be interpreted as due to right-lateral slip movement on a single group of faults. It is appreciated that there is some field evidence to suggest that the faulting may be more complicated than the picture we would deduce from the P data alone. But the field observations show that most of the faulting was indeed on northeast-striking planes, and this is the conclusion obtained from the analysis.

ACKNOWLEDGMENTS

We feel that the seismologists who are working on these problems are making a very important contribution to structural geology, and we hope that every support will be given to this work. It is a pleasure to acknowledge the generous way in which Dr. Hodgson has given us data, help and advice. The authors are working with the support of a National Science Foundation grant.

References

HODGSON, J. H. (1957): Nature of Faulting in Large Earthquakes. *Bull. Geol. Soc. Am.* **68**, 611–643.

HODGSON, J. H., and J. IRMA COCK, (1956): Direction of Faulting in the Greek Earthquakes of August 9–13, 1953. *Annales Géologiques des Pays Helléniques*, **8**, 29–47.

HONDA, H. (1957): The Mechanism of the Earthquakes. *Science Reports, Tôhoku Univ., Ser. 5*, **9**, Supplement, 1–46.

HONDA, H., A. MASATSUKA, and K. EMURA (1956): On the Mechanism of the Earthquakes and the Stresses Producing them in Japan and its Vicinity, (Second Paper). *Science Reports Tôhoku Univ., Ser 5*, **8**, 186–205.

KOGAN, S. D., (1954): K Voprosu ob Izuchenii Mekhanizma Glubokikh Zemletryasenii, *Dokl. Akad. Nauk S.S.S.R.*, **99**, 385–388.

MCINTYRE, D. B., and J. M. CHRISTIE (1957): A Discussion of 'Nature of the Faulting in Large Earthquakes'. *Bull. Geol. Soc. Am.*, **68**, 645-652.

RITSEMA, A. R. (1956): The Mechanism in the Focus of 28 South-East Asian Earthquakes. *Verhandelingen 50, Meteor. and Geophys. Institute, Djakarta.*

SCHEIDEGGER, A. E. (1957): Table of Russian Fault Plane Solutions. *Publications of the Dominion Observatory, Ottawa*, **19**, 99–109.

[illegible]

[illegible]

References

Hodgson, J. H. (1957): Nature of Faulting in Large Earthquakes. Bull. Geol. Soc. Am., 68, 611–643.

Hodgson, J. H., and J. Ibsen Cock (1956): Direction of Faulting in the Greek Earthquakes of August 9–13, 1953. Annales Géologiques des Pays Helléniques, 8, [illegible]

Honda, H. (1957): The Mechanism of the Earthquakes. Science Reports, Tôhoku Univ., Ser. 5, 9, Supplement, [illegible]

Honda, H., A. Masatsuka, and K. Emura (1956): On the Mechanism of the Earthquakes and the Stresses Producing them in Japan and its Vicinity (Second Paper). Science Reports Tôhoku Univ., Ser. 5, 8, 186–205.

[illegible] (1954): [illegible]

McIntyre, D. B., and J. M. Christie (1957): A Discussion of [illegible] of the Faults [illegible] Earthquakes. Bull. Geol. Soc. Am., 68, [illegible]

Ritsema, A. R. (1956): The Mechanism of [illegible] Verhandelingen [illegible]

Scheidegger, A. E. (1957): [illegible]

Circum-Pacific Tectonics*

BY HUGO BENIOFF

Seismological Laboratory, California Institute of Technology.

ABSTRACT

A study of the Kamchatka aftershock sequence by BÅTH and BENIOFF provided the basis for distinguishing between the two possible fault-plane solutions for the principal shock given by HODGSON. Thus, this great earthquake was generated by a right-handed slip on a 1000-km. fault segment lying parallel to the trench. With this observation, data are now available for the direction of slip on the shallow components of nearly all the principal circum-Pacific faults. This includes Japan, Philippines, Tonga-Kermadec, New Zealand, the Aleutian Arc, Alaska, northwest Pacific, California and possibly the western coast of South America. In all of these regions the principal fault lies parallel to the coast and the slip is right-handed. Secondary faulting, such as represented by the Garlock fault in California, strikes transverse to the coast line and in many cases is left-handed. Although the principal movement is strike-slip in nature, smaller dip-slip components also occur and these are responsible for the relief which takes the form of oceanic deeps and associated mountain ranges. The circum-Pacific tectonic activity now in progress can thus be described as a tangential, clockwise rotation of the continental margins relative to the oceanic mass, together with a radial movement of the margins toward the oceanic mass. If the tangential slip is constant around the margins, with a rate equal to that of the San Andreas, the time for a complete revolution is approximately 3×10^9 years.

The observational data from which we attempt to determine the tectonic behavior patterns of the circum-Pacific marginal province are the surface geology (when accessible), the spatial and chronological distribution of earthquake foci, and the observed or calculated directions of earthquake fault slips. The problem is rendered difficult by small scale complexities of the patterns which tend to obscure or conceal the principal mass movements. Moreover, the methods for calculating the fault-slip geometry at the source from initial seismogram trace displacements are not entirely satisfactory, owing to instrumental and transmission complications or to departures of the source mechanism from the simple form assumed in the theory. In this paper an attempt is made to derive the principal tectonic patterns from the portions of the available data considered to be most reliable or pertinent.

The western marginal region of North America, extending from a point off the coast of Oregon to the southern end of the Gulf of California, is tectonically dominated by the San Andreas fault or fault system. The relative crustal movements involved in this system are horizontal, with the oceanic block moving northwestward relative to the continental mass. The fault is thus of the right-hand (dextral) strike-slip or transcurrent type. The great San Francisco earthquake of 1906 was caused by a slip on its northern segment. The visible trace extended 400 km. northward from San Juan to Point Arena and from there possibly an unknown distance under the ocean. The maximum relative displacement was 6.5 meters. In the earthquake of 1857 a segment of approximately the same length and slip displacement was active from the vicinity of San Bernardino northward. In addition to these two great earthquakes many smaller ones have occurred in the system, clearly indicating extension of the fault zone northward under the ocean to a point approximately $\phi = 44.5°$, $\lambda = 130°$, and southward under the Gulf of California to its southern limit as shown by the map of epicenters Figure 1. The epicenters are taken from GUTENBERG and RICHTER (1949). Although over most of its length the fault is quite straight, a substantial flexure occurs in the vicinity of Gorman where the southern segment appears to have been moved eastward relative to the northern segment. Near the curved region another fault, the Garlock fault, originates and extends approximately eastward for about 250 km. Although no earthquakes of consequence have taken place on this

*Publications of the Division of the Geological Sciences, California Institute of Technology, Pasadena, California, Contribution No. 857.

fault during the 100 years or so of historical time, the geological evidence indicates that it is an active strike-slip fault with left-hand polarity. The Garlock fault does not cross the San Andreas fault. However, some 8 km. north of the point of intersection, the Pine fault takes off on the western side of the San Andreas fault in a direction roughly parallel to the Garlock

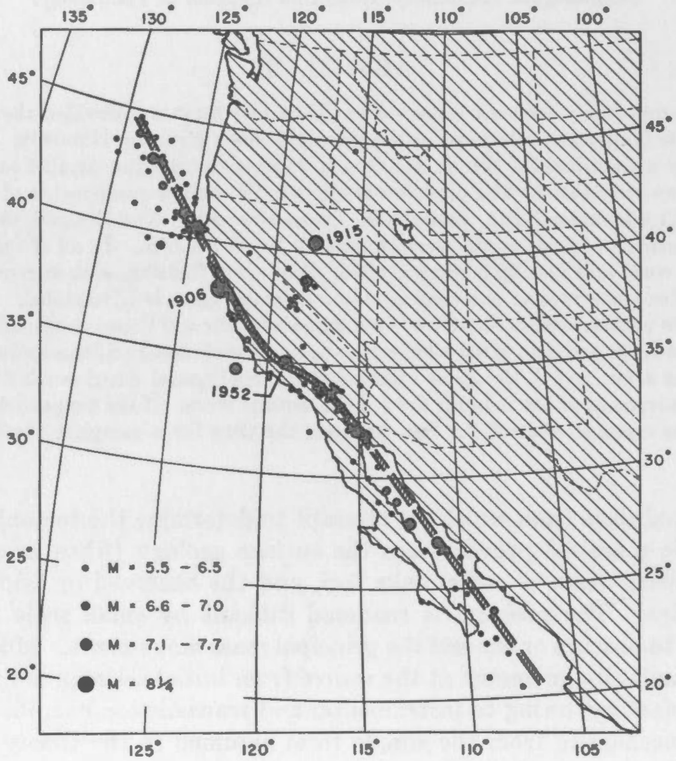

Figure 1. San Andreas fault and earthquake epicenters.

fault. It also exhibits sinestral polarity. A number of authors and more recently Hill and Dibblee (1953) have interpreted the San Andreas, Garlock and Pine configuration as a conjugate shear fracture pattern generated by a single horizontal north-south crustal stress acting throughout the region. This interpretation appears untenable to this writer for the following reasons:

1. The angles between the two components and the assumed direction of stress is too large.

2. The concept of conjugate fractures is derived from laboratory experiments on small homogeneous samples in which the two components break simultaneously. In a large body such as the portion of the earth's crust represented by the San Andreas system, the material cannot be sufficiently homogeneous for simultaneous conjugate fractures to occur. Owing to the existence of joints, crystal imperfections and variations in composition, the failure response to an increasing uni-directional stress can only begin as a single fracture. Once such an initial break has formed the local stress pattern becomes modified in such a way as to reduce the conjugate stress component and to prevent the formation of a conjugate fracture.

3. The curvature in the vicinity of the intersection is not compatible with a uni-directional stress.

4. Hill and Dibblee (1953) present arguments for a total accumulated displacement on the San Andreas fault of at least 550 km. If this is true, the Garlock and Pine faults should be offset relative to each other by this amount since the two original conjugate fractures must necessarily be simultaneous.

5. The geologic evidence indicates that movement on the Garlock-Pine faults has amounted to at least a kilometer and possibly more (HILL, DIBBLEE, 1953 p. 451). This movement should have offset the San Andreas fault.

It is clear that conjugate fractures can exist only as initial breaks within a very small region in a homogeneous material. Subsequent movements on both components are incompatible—one or other initial break must take over for large accumulated displacements.

Without prior knowledge as to the origin of the tectonic forces involved, it is not possible to derive the primary stress pattern from observations of the fracture pattern in fault systems such as the San Andreas. Thus a compressional stress, such as sometimes envisaged as the cause of the San Andreas system of fractures, might be produced by a horizontal gradient in viscous drag between the under surface of the crust and a subcrustal current flowing parallel to the assumed direction of the simple linear stress. On the other hand, the San Andreas fracture may just as well have been generated by a shear stress pattern produced by a subcrustal current flowing parallel to the fault having a viscous drag gradient at right angles to the direction of flow, as illustrated in Figure 2. In view of the marginal nature of the San Andreas fault, the

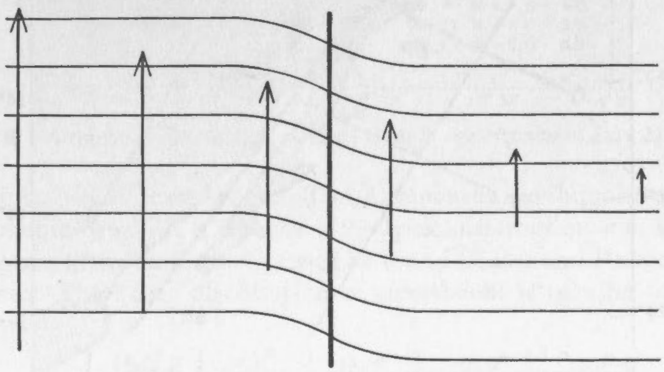

Figure 2. Plan of stress gradient normal to a fault.

generating stress might also originate in body forces acting differentially on continental and oceanic land masses. With the present state of our ignorance of the origin of tectonic forces, the writer prefers to confine considerations to observable tectonic movements, displacements and strains, rather than to attempt to derive the generating stress patterns from incomplete observational data.

The principal tectonic movements of the western continental margin from the lower limit of the Gulf of California to a position corresponding with the northern limit of the San Andreas system are, therefore, a horizontal dextral displacement parallel to the margin of the oceanic mass relative to the continental mass, and a sinistral displacement of the northern portion relative to the southern, in a direction perpendicular to the margin. These two movements are indicated by the arrows in Figure 3. It should be noted that the arrows represent velocity vectors and not stresses. The transverse movement is indicated by the Garlock-Pine fault displacements and by the curvature of the San Andreas fault. Since movements on the two faults are mutually incompatible, the San Andreas system exhibits branches in the southern part, west of the original break. Thus it appears that the San Jacinto, Elsinore and Inglewood branch-faults represent the tendency of the San Andreas fault to maintain a straight course in spite of the transverse distortion.

The White Wolf fault, on which the Kern County earthquake of 1952 occurred, is a reverse fault with a small average sinistral strike-slip component. This fault is also a result of the incompatibility of the two principal movements, (BENIOFF, 1955). The portion of the north-eastern block of the San Andreas fault which moves along the flexure is subjected to a local distortion in the form of a north-south compression, and this accounts for the combined reverse and sinistral strike-slip characteristic of the White Wolf fault. The White Wolf fault is thus an auxiliary fracture, and its orientation and slip are not direct indicators of the regional stress system but are, instead, expressions of a small local distortion resulting from two primary components of the regional flux pattern. It may be concluded, therefore, that fault-plane solutions

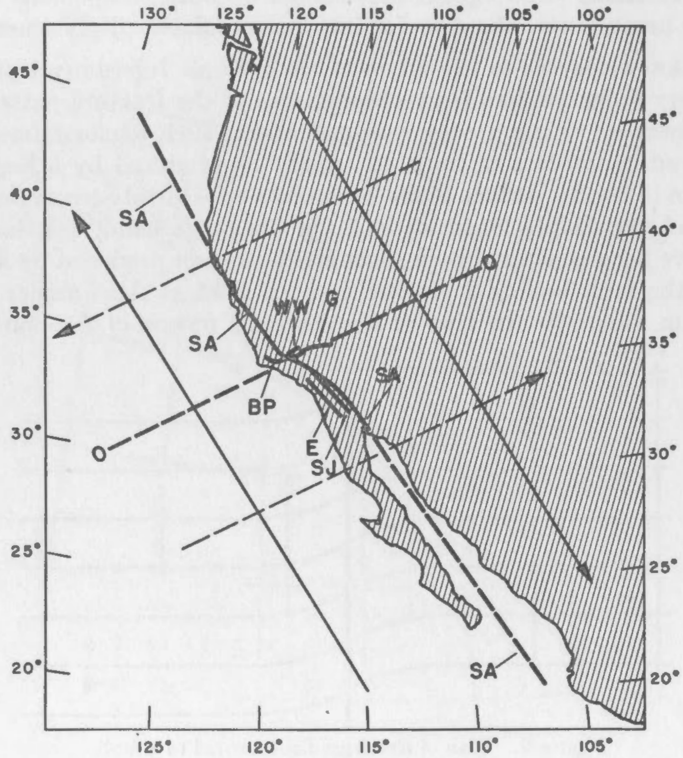

Figure 3. Large scale dynamic pattern of San Andreas province.

of earthquake fault characteristics cannot be relied upon indiscriminately for deriving the principal stress or flux patterns of a large region unless additional pattern information is available from other sources. The fault-plane evidence is reliable in great earthquakes only, since in these the extent of faulting is large enough to eliminate the effects of local distortions, and thus to indicate the character of the prevailing tectonic flux of the region. It should be noted, however, that there is no *a priori* reason for assuming that the primary stress patterns do not change with time. A pattern responsible for the generation of a given fault system may change in magnitude or direction with time. Consequently, once a fracture pattern has been established, subsequent movements on the faults may bear no simple relation to the original generating stress.

The Kern County shock of July 21, 1952 was the first earthquake in which precise epicentral locations of aftershocks were available together with visible evidence for the extent of faulting. A group of portable seismographs were rushed into the area within a few hours and these, together with the permanent network of stations of the California Institute of Technology, provided the necessary observations for precise aftershock epicenter determinations with errors not greater than about ± 1 km. as reported by C. F. Richter (1955). Figure 4 is a map of the region showing the principal shock epicenter, the observed extent of faulting and the aftershock epicenters. In this earthquake the extent of faulting coincides with the long dimension of the aftershock epicenter distribution area. That aftershocks would define the extent of faulting in the principal earthquake has long been suspected by the writer on the basis of partial evidence, but this is the first instance in which the evidence was complete. Assuming that this relationship holds generally, we can determine the extent of faulting in other earthquakes where the

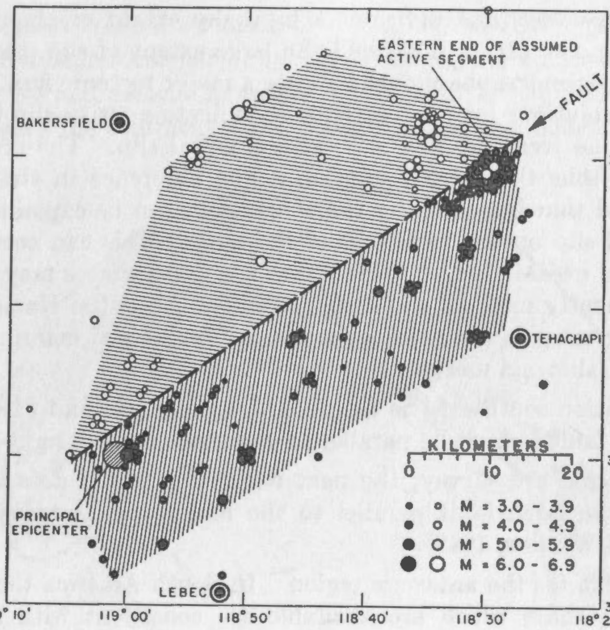

Figure 4. Aftershock distribution of Kern County earthquake of July 21, 1952.

fault is not accessible to visual observation. The Kamchatka earthquake of November 4, 1952 provided the first example in which a reliable aftershock distribution was available from which the extent of faulting in a great earthquake could be found (BÅTH and BENIOFF, 1958). Figure 5 is a map of the region. The linear distribution of aftershocks is parallel to the general coastal

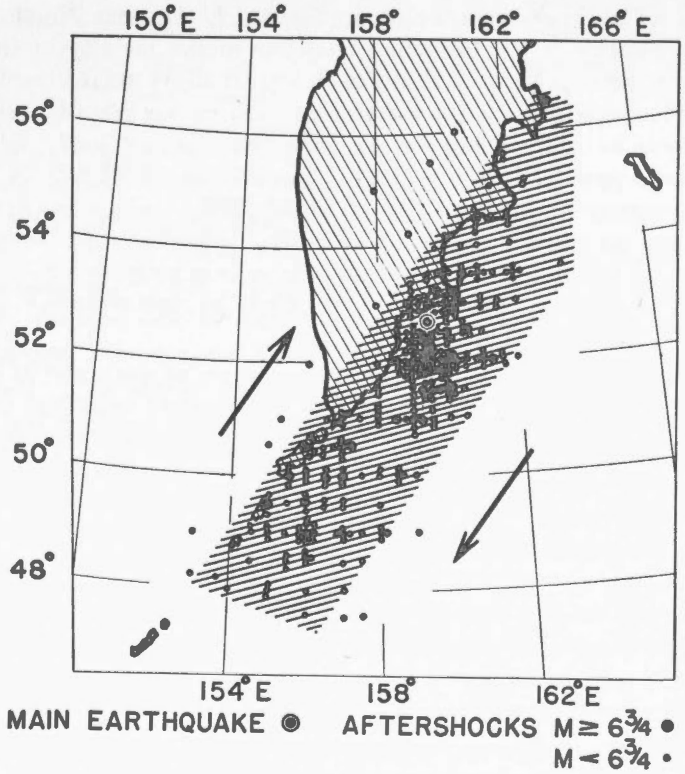

Figure 5. Aftershock distribution of Kamchatka earthquake of November 4, 1952.

trend of the principal features, and indicates a total slip extent of about 1000 km. In view of the size of the earthquake ($M = 8.25$) and the large extent of slip, the fault-plane solution from first P motions on seismographs should indicate a major tectonic flux pattern of the region. HODGSON'S (1956) two solutions for this earthquake indicate a strike-slip fault trending N10°E with dextral slip, and one trending N84°.5W with sinistral slip. The one with strike N10°E and dextral polarity is thus the correct solution. The difference in strike direction between his solution, N10°E, and that indicated by the aftershocks can be explained, partially at least, on the basis of unequal slip on the two faces of the fault. This can occur in marginal faults between continental and oceanic land masses where the two surfaces may have unequal elastic coefficients and consequently unequal slip displacements. Thus the Kamchatka arc is moving relatively to the oceanic mass in a direction parallel to the coastal margin. The slip is dextral as in the San Andreas California margin.

Directing our attention southward to the Japan segment, we find (TSUBOI—personal communication) that those faults which lie parallel to the coast exhibit right-hand strike slip also.

Continuing our Pacific arc survey, the next region for which data are available is New Zealand, where again the large fault parallel to the major axis is transcurrent with dextral polarity (WELLMAN and WILLET, 1942).

No data are available for the antarctic region. In South America the data are inadequate for final evaluation but those which are available are consistent with right-hand strike-slip movement. INGRAM (1957) derived a fault-plane solution for the Chilean earthquake of December 7, 1953 ($\phi = 22°S$, $\lambda = 68\frac{1}{2}°W$, $M = 7.1$) with one plane striking N66°W and the other N32°E. Assuming that the plane N32°E, more nearly parallel with the coast, is the fault plane, his results indicate dextral transcurrent slip. The solution for the Ancash, Peru, shock of November 10, 1946, derived by HODGSON and BREMNER (1953) and indicating principally transcurrent faulting, departs so far from the visible vertical fault displacement (SILGADO, 1951) that it cannot be trusted.

Passing over the California region already discussed, the next North American segment for which data are available is the Canadian coastline in the vicinity of the Queen Charlotte Islands. The evidence here from the earthquake of August 22, 1949 (HODGSON and MILNE, 1951) indicates dextral strike slip parallel to the margin. Also in the northern Canadian Pacific margin, Alaska, and the Aleutian arc, the geological evidence (ST. AMAND, 1957) indicates large dextral strike-slip displacement parallel to the margin. The solution of HODGSON and MILNE (1951) for the Aleutian earthquake of April 1, 1946 ($\phi = 53° 30N$, $\lambda = 163°W$) indicates principally transcurrent slip, either on a plane striking N22° 30′E or N65°W. In this region the N22° 30′E direction is more nearly parallel with the arc and these data indicate left-hand polarity. However, since this shock is not large ($M = 7.3$) it may not be representative of the whole region, especially in view of the geological evidence.

The fault-slip characteristics of the circum-Pacific margins discussed in the preceding paragraphs are indicated on the map of Figure 6. The solid arrows represent movements believed to be reliably known: the dashed arrows refer to assumed movements for which the observations are inadequate. On the basis of the evidence here presented, it appears that the principal tectonic movement of the circum-Pacific region is a clockwise rotation of the continents relative to the enclosed oceanic mass. The observed data are not sufficient to determine which of the two structures is moving in an absolute sense relative to coordinates fixed with respect to the earth's axis of rotation. The rate of movement has been measured geodetically in one region only—California (C. A. WHITTEN, 1955)—and here it amounts to approximately 5 cm. per year. If this represents a mean constant rate applicable to the whole system, the time required for a complete relative rotation is about 10^9 years.

It was noted in an earlier paragraph that in California, in addition to the principal movement parallel to the margin, there is a second movement approximately normal to the margin. Viewed in relation to the whole circum-Pacific arc this movement is radial. The marginal segment from

California to Alaska differs from the remainder of the circum-Pacific arc in that it contains no oceanic trenches and no deep-focus earthquakes. This may be a chronological difference only. The presence of trenches and associated coastal uplift, and the dip under the continents of the marginal contact between the continental and oceanic masses, as defined by the foci of the deep

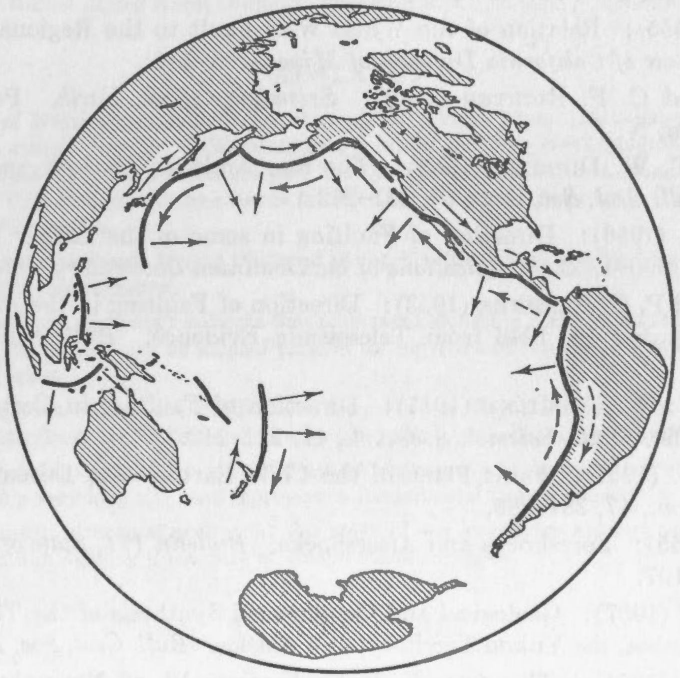

Figure 6. Principal fault slip pattern of the circum-Pacific margins.

earthquakes, have been taken as evidence for radial motion (BENIOFF, 1954) at the margin. It was assumed that since the continental mass is less dense than the oceanic mass, the radial movement causes the former to override the latter at the margins. The oceanic mass is thus forced downward to form the trench and the continental mass is uplifted to form the mountains. The amount of radial movement required to form the marginal relief is small compared with tangential movements which have been suggested on the basis of geological evidence—560 km. for the San Andreas fault (HILL and DIBBLEE, 1953) and 240 km. for the Alaskan faults (ST. AMAND, 1957). This corresponds with HODGSON's fault-plane data which indicate that the total amount of dip slip is small; the dip-slip faults are few in number and the strike-slip faults have small dip components. The energy required in dip-slip movements to produce relief is very much larger than that required for equal strike-slip tectonic displacements. Neglecting the elastic energy contribution, the energy required to produce, against gravity, an oceanic trench and associated uplift of 1000 km. extent and 5 km. departure from sea level, is of the order of 10^{30} ergs, about equivalent to the elastic energy of 10^6 magnitude 8 earthquakes. Thus assuming an average of 2 meters slip per earthquake, the energy required to produce the relief of an average trench and mountain chain against gravity could produce a total horizontal slip of about 1000 km. if expended in strike-slip faulting. In the light of these considerations, radial movement of the continental margins relative to the ocean mass continues to be a reasonably satisfactory hypothesis for the origin of the circum-Pacific marginal relief. As mentioned earlier (BENIOFF, 1954, p. 396) the movement which generates the relief originally may not continue indefinitely. In time, reverse or other movements may occur tending to restore the original level contours, or bring about other modifications.

References

BÅTH, MARCUS, and HUGO BENIOFF (1958): The Aftershock Sequence of the Kamchatka Earthquake of November 4, 1952. *Bull. Seismol. Soc. Am.*, **48**, 1–15.

BENIOFF, HUGO (1954): Orogenesis and Deep Crustal Structure—Additional Evidence from Seismology. *Bull. Geol. Soc. Am.*, **65**, 386–400.

BENIOFF, HUGO (1955): Relation of the White Wolf Fault to the Regional Tectonic Pattern. *Bulletin 171, State of California Division of Mines*, 203–204.

GUTENBERG, B. and C. F. RICHTER (1949): *Seismicity of the Earth.* Princeton University Press, Princeton, N. J.

HILL, M. L. and T. W. DIBBLEE (1953): The San Andreas, Garlock and Big Pine Faults, California. *Bull. Geol. Soc. Am.*, **64**, 221–242.

HODGSON, JOHN H. (1956): Direction of Faulting in some of the Larger Earthquakes of the North Pacific, 1950–1953. *Publications of the Dominion Observatory, Ottawa*, **18**, 217–252.

HODGSON, J. H. and P. C. BREMNER (1953): Direction of Faulting in the Ancash, Peru, Earthquake of November 10, 1946 from Teleseismic Evidence. *Bull. Seismol. Soc. Am.*, **43**, 121–125.

HODGSON, J. H. and W. G. MILNE (1951): Direction of Faulting in Certain Earthquakes of the North Pacific. *Bull. Seismol. Soc. Am.*, **41**, 221–242.

INGRAM, R. E., S.J. (1957): Fault Plane of the Chile Earthquake, December 7, 1953. *Bull. Seismol. Soc. Am.*, **47**, 281–285.

RICHTER, C. F. (1955): Foreshocks and Aftershocks. *Bulletin 171, State of California Division of Mines*, 177–197.

ST. AMAND, PIERRE (1957): Geological and Geophysical Synthesis of the Tectonics of Portions of British Columbia, the Yukon Territory, and Alaska. *Bull. Geol. Soc. Am.*, **68**, 1343–1370.

SILGADO, ENRIQUE (1951): The Ancash, Peru, Earthquake of November 10, 1946. *Bull. Seismol. Soc. Am.*, **41**, 83–100.

WELLMAN, H. W. and R. W. WILLETT (1942): The Geology of the West Coast from Abut Head to Milford Sound, Part I. *Trans. Royal Soc., New Zealand*, **71**, 282–306.

WHITTEN, C. A. (1955): Measurements of Earth Movements in California. *Bulletin 171, State of California Division of Mines*, 75–80.

Circum-Pacific Orogeny

BY PIERRE ST. AMAND

United States Naval Ordnance Test Station, China Lake, California.

ABSTRACT

The Pacific coast of North America is fringed by a series of right lateral faults sub-parallel to the coastline. The San Andreas fault extends from Baja California to a point off the Oregon-Washington coast. Near this point, the Alaskan fault complex begins and continues past the Queen Charlotte Islands, along the coast and inland to join the Denali fault. This zone of faulting extends for more than 2100 km. from Lynn Canal, by the north face of Mt. McKinley, to the Bering Sea.

Faulting on the Alaska peninsula having the trend of the Aleutian Island arc has been mapped as right lateral faulting with concomitant overthrusting.

First motion results from seismology indicate that movement along the Aleutian arc, the Kamchatka-Kurile arc and elsewhere around the Pacific may be aligned parallel to the strike of the island arcs or mountain chains, and is often of right lateral sense.

The conclusion is presented that the Pacific basin from at least Baja California to a point beyond the Kurile Islands is rotating counterclockwise. The rest of the Pacific basin is probably also rotating in the same sense.

The Rocky Mountain Trench and sub-parallel features between it and the coast indicate that this type of movement has been going on a very long time and represents a fundamental type of orogeny.

The results of field and structural geology at this stage of our knowledge support the basic work of BYERLY and of HODGSON, and aid in defining the nature of circum-Pacific orogeny.

INTRODUCTION

STATEMENT OF INTENT

For several years seismologists have been reporting that many earthquakes are produced by lateral movements on faults. These investigators have been courageously flying in the face of geological and geophysical tradition. They have contended that a predominant portion of present day tectonic activity has been due to lateral faulting and some of them have even expressed surprise that this much lateral faulting exists. Although lateral faults have been recognized in California, Canada, Alaska, Scotland and elsewhere, the importance of these faults has scarcely been appreciated by geologists and largely ignored by geophysicists. Recently, however, HILL and DIBLEE (1953), MOODY and HILL (1956), and ALBERDING (1957) have published papers showing the importance of lateral faulting. In this discussion I wish to assemble a few of the main facts pertaining to the distribution of faulting around the northern and eastern edges of the Pacific basin and to demonstrate as best I can that this faulting forms a consistent pattern and that this pattern is consistent with the observations of seismologists. In order to do this it will be necessary to discuss the subjects of geology and geomorphology to some extent. The object of the fault-plane work is to discover the nature of the present day mountain building processes and that is a geologic goal.

RECOGNITION OF LATERAL FAULTS

General Remarks

It is difficult to recognize a lateral fault in the field, unless one has learned a few diagnostic geomorphic criteria essential to the recognition of such features. An actual proof of lateral movement on a fault is even more difficult. ANDERSON's work (1942) on the Great Glenn fault forms one of the finest examples of such a demonstration. In most cases the lateral component of motion cannot be shown from stratigraphic evidence. Often the stratigraphic evidence has

55092-1—12

been explained away by assuming vertical movement to have been responsible for all the displacement. The San Andreas fault of California and Baja California is now considered by all geologists to be primarily strike-slip in nature but it is doubtful if the lateral habit would have been recognized if the fault had not actually slipped several times in recorded history. Once the lateral nature of faulting was known, it was easy to distinguish those geomorphic criteria by which lateral faults may be recognized.

The most striking property of large lateral faults is the consistent straightness, or the smooth and gradual curvature, of the strike of the feature. Another, not always present, is the occurrence of a trough along the strike of the fault. This trough is found along portions of the San Andreas, Garlock, Great Glenn and Denali faults, to name a few. The troughs have a comparatively straight trend, are usually filled with alluvium and are often not recognized as being the locus of a fault. Small scale features attributable to smaller scale faulting are often found within the trough; examples are the upthrusting of minor fault slices or the formation of small grabens. There have been instances where geologists have mapped such minor features in considerable detail and have made desperate attempts to understand the stratigraphy without ever recognizing the fact that they were working in a large fault zone.

The trough may be developed by erosion of crushed rock in the zone of the fault, or in some instances, such as the Koehn Valley trough of the Garlock fault by development of a graben through normal faulting on both sides of a lateral fault. Such troughs may also develop along the sides of thrust faults associated with lateral faulting, as is the case of a portion of the White Wolf fault. The width of the trough along the course of a lateral fault may be several tens of miles.

Such faults often exhibit many branches and it is frequently difficult to tell if there is a main fault. An example is to be found in the San Andreas in the southernmost part of California where ALLEN (1957) has remarked that the entire area, over 50 miles in width between the Elsinore fault on the west and the eastern edge of the Salton depression should properly be called the San Andreas fault zone.

Other geomorphic features often cited are shutter ridges, formed by the displacement of one part of a ridge with respect to another so that a ridge blocks the drainage of an established stream. Upthrusting of fault slices may also produce ridges lying athwart the drainage of a major mountain mass. This situation gives rise to offset streams and these are a commonly cited criterion. Offset streams commonly occur also in the trough of the fault, and the direction of offset is often taken as being indicative of the direction of displacement on the fault. This is not a reliable indication unless one is able to establish that a major valley has been offset.

The extent of a lateral fault is often underestimated because the faulting has been recognized by apparent vertical offset along one portion of the fault, and the fault considered to be terminated, when actually there are other evidences of faulting of a less spectacular nature. There is a small lateral fault near Little Lake, California, at least 30 miles long, yet it cannot be followed for more than a few thousand feet by any one criterion. A few of the features along the fault will be cited. This fault intersects the main body of the Sierra Nevada at an oblique angle with but little change in the general slope of the mountain front. The fault is noticeable by a series of oases aligned along the trace and by an occasional small col and butt. A few thousand feet south it may be seen in a road cut, a little farther along it is marked by some ridges in a lava flow, a small cinder cone, a series of sag ponds in the surface of a basaltic lava bed, and eventually a scarp produced by a flexure in some lake bed sediments, compressed in a direction parallel to the strike of the fault. Hereafter the fault is lost beneath the alluvium for several miles but reappears to form a trough-like valley across a minor mountain block. This fault has been active since the end of the ice age and yet if a geologist were to look at any one part of it, it is unlikely that he would recognize it as a fault, much less an important lateral fault.

I will not discuss this sort of geomorphology in detail, and cite these examples only to show that the problem of recognizing lateral faults is not a simple one. In my opinion, any fault having a straight trace more than a few miles in length has undergone lateral movement. The reason that the prevalence of lateral faulting surprises seismologists, particularly from elsewhere than California, is because geologists have not recognized this type of faulting often enough.

Figure 1. The path of the San Andreas fault across California, with a few of the more important active or recent faults shown. The path of the San Andreas in the ocean is deduced from seismological evidence.

DISCUSSION OF REGIONAL STRUCTURAL GEOLOGY OF THE PACIFIC COAST OF NORTH AMERICA

What is now known of the faulting around a portion of the Pacific margin will be discussed, and on the basis of regional geology an attempt will be made to understand the nature of the orogeny. We will begin with the San Andreas fault zone and work our way around the Pacific to the north and west.

San Andreas Fault

The San Andreas fault and features similar to it, Figure 1, dominate the structural geology of the west coast of North America. The San Andreas fault has moved several times in recorded history, each time displaying right lateral strike-slip motion along one or more of its many branches. The main zone begins in the Gulf of California, continues through the Imperial Valley of California, crosses the Transverse Ranges and the Coast Ranges, and enters the sea north of San Francisco. It continues under the sea, where it may be followed by a line of epicenters to the vicinity of 45°N, 130°W.

Basin Range Area

Structures with the San Andreas trend exist in the Basin Range area. In the southern part of this province these faults are currently active and demonstrate right lateral movement. The magnificent normal faulting found in the Basin Range province has distracted attention

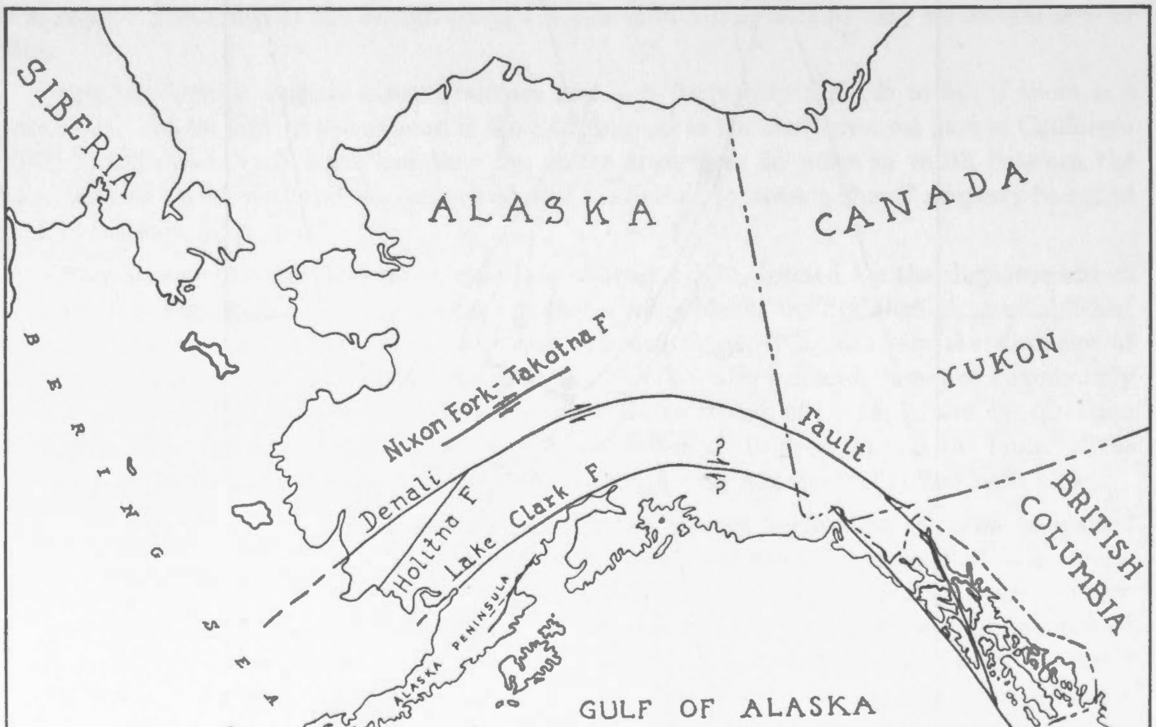

Figure 2. The principal faults in the southern part of Alaska and British Columbia.

from the lateral faulting. This region has been, and is being, deformed as if it were undergoing dextral shear by a couple aligned roughly east-west, the western end of which is being pulled north.

An example that might be cited is the Fairview Peak earthquake of 1954, where a fault displayed a right lateral displacement of about 10 feet. Lateral movement accompanied the great earthquake of 1872 in Owens Valley, but unfortunately it seems impossible to decide the sense of the main faulting from the printed accounts. It does appear that the movement was right lateral and of the order of 18 feet, both horizontally and vertically.

Alaskan System

To the north and east of the termination of the San Andreas system, the Alaskan system (Figure 2) begins. This is traceable under the ocean floor by an alignment of epicenters reaching to the Alaskan coast on the oceanward side of the Queen Charlotte Islands. The main line of activity runs northward along the coast, forming the seaward shores of Baranof and Chichagof Islands, and then passes inland to beyond the head of Yakutat Bay. This fault was probably the causative agent of the great Yakutat Bay earthquakes of 1899.

The fault branches at the mouth of Christian Sound, one important branch passing up Lynn Canal and joining the Denali fault. This gigantic feature, somewhat circular in plan, extends from the region of Lake Dezadeash, past the northern front of Mt. McKinley, and reaches the shores of the Bering Sea in Kuskokwim Bay. This fault appears to be right lateral in habit, as does the rest of the Alaskan fault system. It has a major thrust branch, the Holitna fault, that strikes to the southwest away from the Denali fault.

The massif of Mt. McKinley appears to have been upraised along gigantic thrust faults lying along the eastern edge of the massif and oriented in a southwesterly direction. These thrusts appear to have undergone a great deal of lateral displacement, although the sense of the displacement is not known. The details of this faulting in Alaska have been explored in a preliminary way, and the documentation given, in a paper by St. Amand (1957).

There is a second major fault south of the Denali fault, and sub-parallel thereto. This fault seems to be lateral in habit, but nothing can be told of the sense of movement as yet. This is called the Lake Clark fault zone because Lake Clark lies in the trough of this fault.

Displacement on Alaskan System

The evidence upon which the sense of the displacement of the Denali fault is based is scant. The Mt. McKinley massif appears to have been offset, along the Denali fault, from the Mt. Hess-Mt. Hayes massif by about 150 miles. A tectonic map by Cady, Wallace, Hoare and Webber (1956) shows that the division between the rocks of the primary and secondary geosyncline of the Kuskokwim region are offset 150 miles along the Denali fault. While a large part of this displacement may be due to vertical movements, it is interesting and probably significant that the same dividing line is offset another 150 miles in a right lateral sense across the Nixon Fork-Iditarod alignment—another huge fault displaying all the geomorphic and stratigraphic relations commonly found on lateral faults.

Aleutian Islands

Knappen (1929) describes the structure of the Alaskan peninsula in the Katmai region. Here he finds the predominate faulting to be right lateral with concomitant overthrusting. The lateral faulting is aligned at a slight angle to the Aleutian arc. The volcanoes in this region appear to have been developed along conjugate tensional shears where these intersect other fractures. The geology of the rest of the Aleutian Islands is not known well, but it has been proposed by Gibson and Nichols (1953) that a continuous fracture runs the full length of the

Island chain. The maps of the Aleutians show many faults, some of which are aligned parallel to the strike of the islands. It is difficult to tell if the faults have undergone lateral displacement or not. Indeed, it is almost impossible to recognize lateral faulting in a volcanic terrain.

Fault-Plane Solutions and Fault Movement

The seismic evidence for displacement on these faults, to be found in the papers of Hodgson and others, indicates that the major movement is lateral. One of the two solutions for most of the earthquakes indicates a right lateral movement aligned along the general trend of the fault. Usually, the motion makes a slight angle with the arc or with the most prominent nearby geologic structure. Benioff and Båth (1958) have recently demonstrated that the major Kamchatka faulting was parallel to the arcuate structure, and this permits making a choice as to one of Hodgson's solutions for this earthquake. This has been pointed out by Benioff in another paper in this symposium.

ROTATIONAL MOVEMENT AS A SOLUTION

Consistent Right Lateral Displacement

The consistent movement from the Mexican coastal region, along the San Andreas system, including the great Basin faults, the Alaskan system, the Aleutian arc and the Kurile-Kamchatka system, clearly indicates that the ocean basin is rotating counterclockwise (Figure 3) with respect to the continents for at least that far. The work of Wellman (1955) in New Zealand also indicates the right lateral nature of the faulting in that area. It hence appears as a possible solution that the whole of the Pacific basin is rotating counterclockwise. These conclusions have also been reached independently by Benioff and by St. Amand (1957).

It will be necessary to study in detail the geology of Kamchatka, the Kuriles, Japan, the Pacific islands and South America in order to establish that the rest of the Pacific is so rotating. There are other fault systems in the Pacific area, some of which are left lateral in nature. These are usually associated with the fracture zones beneath the Pacific as described by Menard (1955) and form the transverse ranges of North America.

Movement in the Past

There are on the North American continent a number of features similar to the San Andreas and Denali fault systems. The most prominent of these is the Rocky Mountain Trench. Although the matter of movement and the nature of this feature, or of the several parallel to it and the western coast, has not been clearly demonstrated it seems likely that they are lateral faults. Should the movement on these prove to have been right lateral, then it is clear that the Pacific rotational orogeny has been going on for a very long time indeed.

It appears, further, that the orogenic zone on the eastern side of the Pacific may have moved westward as time went by, abandoning former planes of movement as they became too stiff to displace, or as the agency producing the force moved westward.

POSSIBLE CAUSE OF THE OROGENIC FORCES

Convection Currents

At this stage, one can only guess as to the source of the movements and forces causing them. A possible source of the orogenic forces is a convergent sub-crustal current moving from the continents toward the oceans. This should produce a Coriolis force of the same sense as is observed. Objections to this hypothesis are that it is contrary to ideas developed from heat-flow measurements and evidence as discussed by Menard (1957).

It is also possible that some sort of magneto-hydrodynamic forces are producing the rotation.

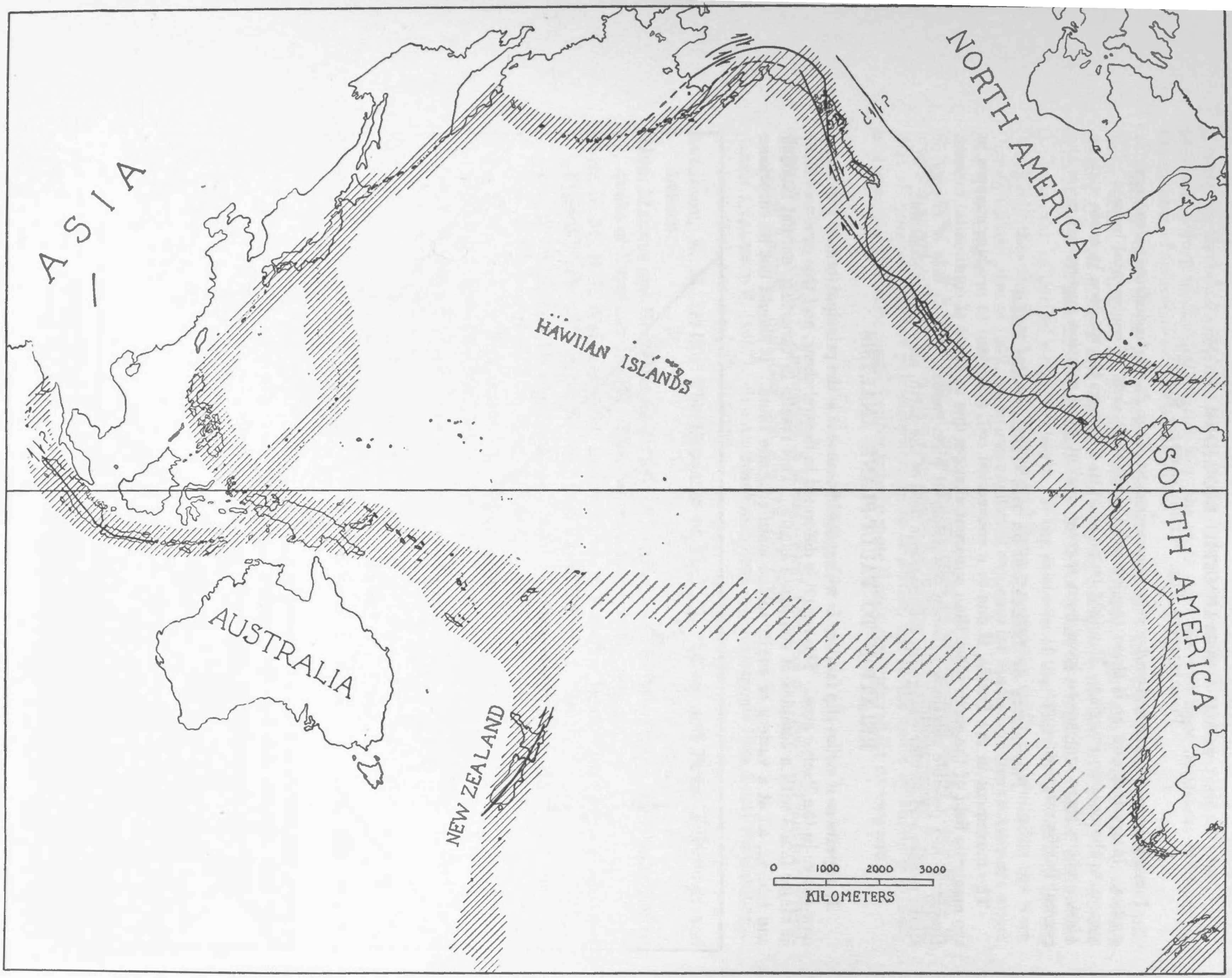

Figure 3. Circum-Pacific orogenic zone, the hatched portions representing seismically active areas. It is felt that the orogenic zone in the southern half is spread between a zone through Antarctica and the Easter Island zone nearer the equator. It appears as if the whole ocean basin on both sides of the equator is rotating in the same sense, counter-clockwise with respect to the continents. It appears also as if the portion north of the equator has been shoved west with respect to that half south of the equator. Such a movement would agree with the movement on the transverse ranges of the North American coast.

SOME GEOMAGNETIC CONSIDERATIONS

Possibilities For Paleomagnetic Study

It might be possible to find evidence for the movement of the Pacific basin from paleomagnetic studies. It appears now as if these require some large scale drift of continental masses with respect to the oceanic margins. It might be possible to check on the rotation in areas such as Alaska where there appears to have been a great deal of local rotation superposed upon the general Pacific rotation.

Possibility of Influence on the Geomagnetic Field

The movement in the Pacific, if due to a convection cell, is certain to produce changes in the magnetic field of the earth other than apparent changes due to drifts of continental masses. Research into possible relations between seismological phenomena, such as rate of energy or strain release and secular changes in the magnetic field of the earth, may prove profitable.

RELATION TO FAULT-PLANE ANALYSIS

It appears as if strike-slip faulting is widespread because it is the principal form of distortion now active in the Pacific area. The region is deformed in dextral shear, and this produces a set of major faults with a complex of conjugate shears. This results in thrusting, normal faulting and folding, all at a variety of angles to the main orogenic trend. It should not be surprising

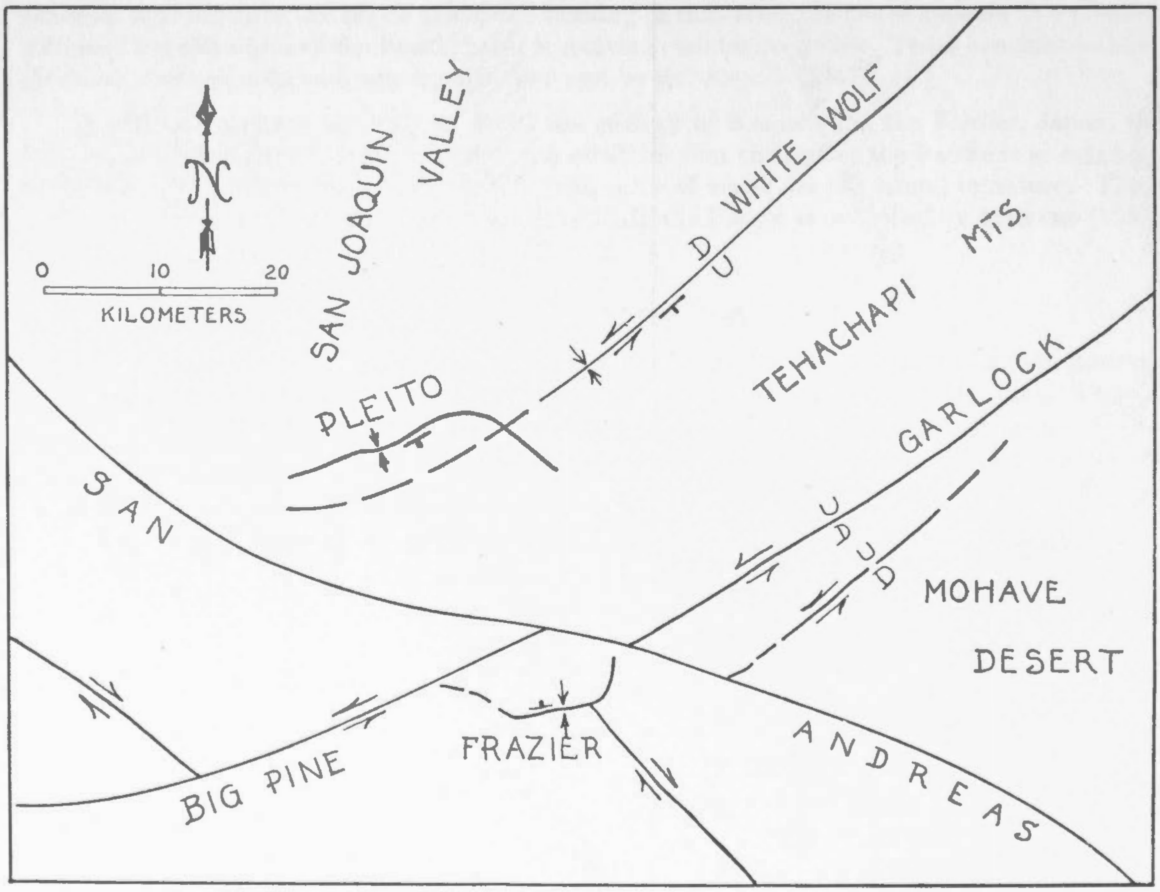

Figure 4. The plexus of faults near the intersection of the San Andreas and Garlock systems. Any of the faults shown are capable of producing large earthquakes. Conclusions based on fault-plane work in this area would lead to possible erroneous conclusions if the structural geology were not known.

if many earthquakes appear to be on faults difficult of explanation on a regional basis. The previous history of the deformation and the local structure will have important influence in the manner of failure in individual localities.

The existence of the left lateral fracture zones in the transverse ranges, such as the Garlock fault, further complicate the picture. An example that one might cite is the White Wolf fault (Figure 4). The strike of this feature is almost at right angles to the San Andreas, the movement is an oblique, left lateral, reverse displacement. This occurs in a region dominated by the San Andreas fault of dextral strike-slip habit. If the existence of the White Wolf were not known, it is likely that the San Andreas fault would have received the credit for producing the Kern County earthquakes of 1952. A serious conflict of evidence for the San Andreas movement would then have arisen.

It seems as if a knowledge of local geology must be incorporated in the final analysis of orogenic movements, as based upon fault-plane solutions. The solutions should first be made, if at all possible, without preconceptions as to structure, but in the end a synthesis of geology and seismology must be made if either is to be more than a game played for its own end.

References

ALBERDING, H. (1957): Application of Wrench-Fault Tectonics of Moody and Hill to Northern South America. *Bull. Geol. Soc. Am.*, **68**, 785–790.

ALLEN, CLARENCE R. (1957): San Andreas Fault Zone in San Gorgonio Pass, Southern California. *Bull. Geol. Soc. Am.*, **68**, 315–350.

ANDERSON, E. M. (1942): The Dynamics of Faulting. Oliver and Boyd, Edinburgh and London.

BÅTH, MARKUS and HUGO BENIOF (1958): The Aftershock Sequence of the Kamchatka Earthquake of November 4, 1952. *Bull. Seismol. Soc. Am.*, **48**, 1–16.

CADY, W. M., R. E. WALLACE, J. M. HOARE, and E. J. WEBBER (1956): *The Central Kuskokwim Region, Alaska.* U.S. Geol. Survey, Prof. Paper 268.

GIBSON, WILLIAM, and HAVEN NICHOLS (1953): Configuration of the Aleutian Ridge, Rat Islands-Semisopochnoi I. to West of Buldir I. *Bull. Geol. Soc. Am.*, **64**, 1173–1188.

HILL, M. L., and T. W. DIBBLEE, Jr. (1953): San Andreas, Garlock and Big Pine Faults, California. *Bull. Geol. Soc. Am.*, **64**, 443–458.

KNAPPEN, RUSSELL S. (1929): *Geology and Mineral Resources of the Aniakchak District.* U. S. Geol. Survey Bull. 797.

MENARD, HENRY W. (1955): Deformation of the Northeastern Pacific Basin and the West Coast of North America. *Bull. Geol. Soc. Am.*, **66**, 1149–1198.

MOODY, J. D., and M. J. HILL (1956): Wrench-Fault Tectonics. *Bull. Geol. Soc. Am.*, **67**, 1207–1246.

ST. AMAND, PIERRE (1957): Geological and Geophysical Synthesis of the Tectonics of Portions of British Columbia, the Yukon Territory and Alaska. *Bull. Geol. Soc. Am.*, **68**, 1343–1370.

WELLMAN, H. W. (1955): New Zealand Tectonics. *Geologische Rundschau*, **43**, 248–257.

Current Status of Fault-Plane Studies—A Summing Up

BY JOHN H. HODGSON

Dominion Observatory, Ottawa, Canada.

ABSTRACT

The paper attempts to state the present position of the fault-plane work, as defined by the contributions to this Symposium. The conclusions are:

1. There is a fundamental disagreement about mechanism which must be solved before the results may be interpreted unambiguously. The disagreement involves the interpretation of S.

2. Assuming a fault mechanism, faulting is predominantly strike-slip except in limited areas. Where unambiguous solutions have been obtained they usually suggest displacement perpendicular to the feature.

3. Assuming the alternative force mechanism, the principal forces appear to act normal to the geographic feature in most areas.

4. The most pressing need of the fault-plane work is agreement on the interpretation of S. This should be sought through detailed studies in theoretical and model seismology and by the careful examination of many seismograms.

During the past few years the study of the mechanism of earthquakes has been increasingly occupying seismologists. Four principal "schools" have grown up, one in Japan, one in Holland, one in the Soviet Union and one, of broad geographical distribution, made up of followers of BYERLY. These different groups have worked independently of each other, and comparison of techniques and results has been difficult. The present volume is the first to contain contributions from each of these groups, as well as papers interpreting the fault-plane results in terms of tectonophysics. In order to define areas of agreement and disagreement between the several authors and to give direction to future work, it seemed desirable to provide a summary of these papers, a task that could best be performed by the Editor. The review has been criticized in manuscript by all of the contributors; it is hoped that it has thereby gained in objectivity.

THEORY

At the outset we must record a disagreement between various investigators in the fundamental matter of assumed mechanism. Two alternative mechanisms have been mentioned repeatedly throughout this volume. They may conveniently be referred to in the notation of HONDA*: type I a single couple, type II a pair of perpendicular coplanar couples. These mechanisms both yield a pair of planes in which the P amplitude becomes zero, but the pattern for S waves is different in the two cases. For type I the magnitude of S is a maximum in the auxiliary plane and a minimum in the fault plane, in type II both nodal planes represent maxima in the magnitude of S waves. It should therefore be possible to decide which mechanism is appropriate from a study of the S waves.

This volume shows complete disagreement in the results of such studies. HONDA, working with records obtained close to the epicentre, finds that a mechanism of type II is demanded by Japanese earthquakes of all focal depths. KEYLIS-BOROK reports that Soviet seismologists, working with more than 300 earthquakes both near to and distant from their stations, find that almost without exception these are due to a mechanism of type I. RITSEMA, instead of using the first motion of S, determines the line of polarization of the S waves from questionnaires from distant stations and the records of nearby ones. He reports that twelve of the earthquakes which he studied were clearly due to type I; results for the remainder were inconclusive.

*Where no specific paper is mentioned, the reference is to the particular author's contribution to this Symposium.

How are we to account for these conflicting findings? It is possible, although improbable, that different mechanisms are active in different parts of the world. The model studies of PRESS, in which the S waves fail to produce a node on the fault plane, even when the fault has been carefully cemented, seem to point to a more logical explanation. If the nodal plane for shear waves is displaced from that for P waves by as much as 35°, and if a maximum thereby appears on the fault plane, it would be very easy to confuse the pattern with that expected from a model of type II. It may be objected that the model used by PRESS is too simple; the excellent agreement between the model studies and the theory for the P amplitudes argues against this. In any event the work suggests that the theory for S amplitudes should be re-examined.

If the failure of different investigators to agree on mechanism is due to the inadequate understanding of the S waves, the possibility must be considered that studies which have been based to any considerable extent on S may be in error. In the present state of knowledge it appears desirable to define the nodal lines by use of P data only, and to use the S data to distinguish the fault plane from the auxiliary plane. Even this process of selection must be suspect in the light of the findings of PRESS and the equivalent work of KATO and TAKAGI (1957).

The paper by BYERLY and STAUDER suggests that North American seismologists, influenced by the San Francisco earthquake, have accepted a mechanism of type I without question. This is certainly true of those of us who have been followers of BYERLY. We have been content to accept the mechanism and to search for confirmation of our fault-plane solutions in observed faulting. I have listed elsewhere (HODGSON, 1957) ten solutions in which the fault strike was confirmed by field observation; my paper in the present volume lists an eleventh. As BYERLY and STAUDER have stated, this agreement would not be expected under a mechanism of type II, for in that case the fault would be inclined to the nodal plane at an angle of 20° or more. In this connection it is interesting to note that HONDA lists two earthquakes, the North Idu earthquake of Nov. 25, 1930, and the North Tango earthquake of March 7, 1927, in which the observed faulting is almost coincident with one of the P nodal planes. This suggests a type I mechanism, yet even in these cases HONDA says the general features of the geodetic deformations, in the region not very close to the fault, are best explained by type II mechanism. North American seismologists would regard the fault as the basic concept, the surface distortion as a secondary effect in which the basic displacement is influenced by surface material, topography, and elastic afterworking.

It seems clear that this problem of mechanism, and the associated problem of the reliability of S waves, is the most pressing matter currently facing investigators. The theory of the S amplitudes should be re-examined, experimental studies using more sophisticated models should be encouraged and, in the words of HONDA, "further and minute investigations of the initial motion of the S waves observed at stations over the world are desired".

TECHNIQUE

In discussing technique one must recognize two classes of solutions, those based on data from nearby stations only and those based principally on data from distant stations. In the former case the information is usually plotted on ordinary maps, in the latter case some special projection must be used. The matter of projections has been competently discussed by SCHEIDEGGER (1957). Whether one uses the Wulff projection or the BYERLY projection the results are the same and the amount of work involved is comparable. So far as projection is concerned one may combine all results based on observations at distant stations into a single catalogue; indeed there is no theoretical reason why all solutions, whether they are based on near or on distant stations, should not be combined.

In practice the results from the different groups of investigators do not seem to be strictly comparable, as has been pointed out by McINTYRE and CHRISTIE. Ottawa solutions, largely for earthquakes from the circum-Pacific zone, have shown a preponderance of strike-slip faulting on steeply dipping planes. RITSEMA, working with earthquakes of the East Indies, found a much smaller percentage of strike-slip faults. In the area from Japan to Kamchatka, in which the Ottawa group has found so many examples of strike-slip faulting on steeply dipping planes, Soviet studies (KOGAN, 1954) have also shown strike-slip faulting but on less steeply dipping planes. Japanese solutions, on the other hand, generally show nodal planes very steeply dipping. The amount of strike-slip motion is a very important matter in the interpretation of the fault-plane results, and these differences should not go unmentioned.

The Ottawa group has obtained only five solutions in the area from the Solomons to New Guinea, probably too few to permit a valid comparison with RITSEMA's results. Of these five, one indicated normal faulting, one thrust faulting, one strike-slip faulting, and two strike-slip faulting with a strong thrust component. These results are sufficiently similar to RITSEMA's to suggest that our techniques are probably consistent, and that RITSEMA is working in an area in which the mechanics of failure differ somewhat from the Pacific zone.

I had thought at first that the difference between KOGAN's solutions and my own was due to the fact that she was using S extensively. Dr. KEYLIS-BOROK tells me that this is not so, that the nodal lines were defined largely by the P waves and that the S waves were used only to select the fault plane. He suggests another reason. When the Soviets were developing their techniques, KOGAN examined the Soviet records, covering a very long period of time, for all earthquakes in the north Pacific, but was able to obtain solutions only for a small percentage of these earthquakes. KEYLIS-BOROK suggests that this selection favoured the less steeply-dipping planes for some reason. This seems probable, and I am able to suggest a reason. KOGAN was dependent largely on the records of Soviet stations, with limited help from bulletins. Planes which were dipping so steeply as to be defined in the PKP range or at the greater distance of the P range would lie beyond the range of the Soviet stations and so escape her notice. She would therefore obtain a preponderance of solutions in which the circles were defined at intermediate distances.

An analogous reason explains the very steep dips found by the Japanese. With their close networks of stations near to the epicentre they can define the quadrants very accurately and so obtain a good definition of strike. With only nearby stations however they cannot define the curvature of the nodal lines; any steeply dipping plane will appear to define a straight line on the surface, and all steeply dipping planes will be called vertical for want of definition. This does not seriously vitiate the conclusions from such studies, but renders exact comparison unprofitable.

From the foregoing it appears probable, but by no means certain, that the work of the various "schools" is comparable. It is sometimes suggested that each group working in fault-plane studies should be assigned an area for which they will be responsible and on which other investigators will not encroach. At the present time this does not seem to be desirable. It is better for each group to work independently until, by comparison of results, the equivalence of technique is established beyond question. In the meantime one is probably justified in combining results for most sorts of studies. It must always be remembered that any investigator may occasionally produce an erroneous solution. The data are never as complete as one would like, and in making the best fit to an incomplete set of data, errors must occasionally occur.

So much for the larger aspects of technique. It is interesting that these major aspects have become generally accepted and that it is the refinements which are now coming in for study. INGRAM's paper, which looks forward to the time when fault-plane studies will be less of an art and more of a science, is a case in point. We in Ottawa have examined the reliability of secondary arrivals as reported in questionnaires and have found this to be unsatisfactory (HODGSON and ADAMS, 1958). RITSEMA gives somewhat analagous evidence. But in neither case is there any evidence that past use of secondary phases has caused solutions to be seriously in error. Soviet seismologists have examined the effects of refracting boundaries close to the source, of crustal layers including low-velocity layers, and of materials which are not perfectly elastic. From a practical point of view they find that these effects are likely to be serious only for near earthquakes or for certain phases such as PcP in the event that the core is not perfectly elastic. Sutton and Berg (1958) have examined the effect of crustal structures of various degrees of complexity on some solutions published by the Ottawa group. They find that the effect of allowing for the crust would be to increase the strike-slip component of the solutions. Since the solutions have been criticized for having too high a strike-slip component the results of the refinement have not been in the desired direction. To sum up, it appears that the refinements and the critical examination of details have not vitiated any of the main conclusions of the fault-plane work.

RESULTS AND INTERPRETATION

From the time when fault-plane solutions became available in many parts of the world it has been apparent that strike-slip faulting has a larger importance in tectonics than had been anticipated. This conclusion is so inconsistent with existing theories that many tectonophysicists have refused to accept it. We have already seen that the papers of the present volume give no reason to doubt the theory or techniques of the method. Do the results taken as a whole justify the conclusion?

It should first be stressed that the conclusion depends on the assumption of a mechanism of type I. If a mechanism of type II is assumed instead the nodal plane is no longer a fault, and one thinks in terms of the forces bisecting the angles between the nodal planes. In Japan, as Honda has shown, these pressures lie approximately normal to the trends of the deep and intermediate earthquake zones. Ritsema also finds that, assuming a mechanism of type II, there is "a tendency for all maximum pressure components to concentrate in directions about perpendicular to the general trend of the seismic zone". It seems probable that if the results of other investigators were treated in the same way similar conclusions might be reached. Since most theories of mountain building or of island arc formation require forces normal to the feature, most tectonophysicists would be happier with the assumption of a mechanism of type II.

Returning to the fault interpretation, all studies seem to point to the great importance of strike-slip faulting. Normal faults become important at great depths in the East Indies, dip-slip faults occur profusely in the Hindu Kush and in the Pamir Knot area and occasionally in the Bonins and off the coast of British Columbia. Elsewhere strike-slip faulting does appear to be the rule. How is this fact to be reconciled with the crustal shortening evident in island arcs and mountain ranges? There are many variations of thought on these matters, many of them heard in discussion rather than read in print, but most thinking seems to derive from one or other of two models.

The first model is the San Andreas fault. This is a strike-slip fault parallel to the continental boundary; by inference one group of thinkers would argue that the strike-slip faults found in the fault-plane work should lie parallel to the continental margin or to the island arc. Where fault-plane solutions are based on P waves only, and so are ambiguous, it is usually possible to select one plane which approximately fits this criterion. Wellman, in several private communications, has favoured this interpretation of the fault-plane results in the southwest Pacific; his interpretation is based on an intimate knowledge of the geology of the area rather than on philosophical arguments. McIntyre and Christie arrive at a similar conclusion from interpretation of the null vector. Two of the interpretive papers in the present volume, those by Benioff and by St. Amand, have been along these lines; both these papers have been based only partly on fault-plane results and have depended more on large-scale evidence and on detailed knowledge of the regional geology.

The "San Andreas" model has difficulty in producing adequate crustal shortening. Benioff has overcome this by postulating a second movement radial to the Pacific, by which the ocean basin underthrusts the continents. Others, following Anderson (1942), have suggested that strike-slip faults are usually hinged and that there is enough vertical motion involved to account for deeps and mountains. However the problem does bring us to the second model.

The second model is the ordinary island arc. There is a vast literature on island arcs, in most of which it is implicit that they are the product of pressures normal to themselves. If strike-slip faulting develops from such a force ti should be inclined at a small angle, perhaps 30°, to the normal to the feature. Where fault-plane solutions are ambiguous one may usually select a plane which fits this requirement. With planes so selected, the direction of material transport is approximately in the direction of the normal, that is in the direction of the postulated major force.

The fault-plane literature, including that in the present volume, is inclined in favour of this second model. Soviet solutions are based on S and so are unambiguous. In the Pacific those solutions favour faulting approximately perpendicular to the arcs (KOGAN, 1954). RITSEMA, who has used S, finds that strike-slip faults tend to be perpendicular, and dip-slip faults parallel, to the seismic zones so that, in his own words, "almost all fault displacements are directed approximately perpendicular to the (seismic) zone". I have shown elsewhere (HODGSON, 1958) that my own results in the northwest Pacific may be interpreted to give displacements normal to the arc in almost exactly the same direction as KOGAN'S, and that the solutions in the south Pacific may be similarly interpreted. HONDA, while admitting that other possible interpretations of his data exist, says that there "seems to exist the general tendency for the Pacific side to be relatively forced downward and toward the Asiatic continental side."

The second model seems to present the least difficulty in interpreting the fault-plane results. We postulate a force normal to the feature, so that folds, troughs and similar features will have axes parallel to the feature. In some areas this force gives rise to dip-slip faults striking parallel to the feature but more usually it causes strike-slip faults inclined at small angles to the normal to the feature. There is nothing in this inconsistent with conventional geological theories on the failure of material. We even, as I have shown in the paper already referred to, get dextral and sinistral faults developed in about equal numbers, so that by interfingering we obtain the necessary crustal shortening. MCINTYRE and CHRISTIE have discussed the difficulties posed by the development of dextral and sinistral faults in about equal numbers. These difficulties are much less severe in the second model.

The papers by BENIOFF and by ST. AMAND in the present volume present evidence for the first, or "San Andreas" model, but little of this evidence is from the fault-plane work. Where the seismic solutions are ambiguous they have selected the solution best fitted to the other evidence, and they have ignored the evidence of the unambiguous solutions that displacement is perpendicular to the geographic features. BENIOFF has given some thought-provoking reasons to justify this. He suggests that fault-plane solutions should not be used by themselves to derive the principal stresses in a region, because they may only be expressions of small local distortion. Only the fault-plane solutions for the largest earthquakes, in which the extent of faulting is large enough to eliminate local effects, are to be depended upon and even here the movement may be along fractures established under an earlier system of forces. DIX has suggested other reasons why fault planes determined from first motion may not always coincide with actual faulting. These arguments are extremely discouraging to the fault-plane seismologists, and most of us would repudiate them where a statistical number of solutions are involved. Nevertheless we must make it clear that a large gulf still exists between the findings of the fault-plane seismologists and the theories of the tectonophysicists.

Finally we must mention the contribution of MCINTYRE and CHRISTIE, who have brought the disciplines of structural geology to the interpretation of the null vector. The null vector was originally introduced as evidence that the fault-plane solutions were self-consistent and related to the topography. While MCINTYRE and CHRISTIE have not accepted this conclusion in all areas, they have given a geological interpretation to the null vector and have used it as a basis for selecting the fault plane. Unless the use of S can be established beyond question, so that unambiguous solutions become available, their technique will become very important. Solely on the basis of this evidence they have been independently led to the "San Andreas" model in those areas where their results are definite.

Clearly, no final conclusions on interpretation can yet be drawn. Seismologists must devote much more effort to the study of the S waves, so that they may come to an agreement on the fundamental mechanism and eliminate the ambiguity of the fault-plane solutions. In the meantime tectonophysicists should not ignore those solutions from which the ambiguity has already been eliminated, but should seek some interpretation of the available data which is acceptable to both disciplines.

CONCLUSIONS

1. There is disagreement on the fundamental mechanism of energy release. Efforts to resolve this disagreement have not been successful. Studies in model seismology suggest that this may be due to inadequacy of the theory. This is the most important problem facing fault-plane seismologists at the present time, and it should be attacked as energetically as possible.

2. On the fault hypothesis faulting is strike-slip in most areas; exceptions are deep-focus earthquakes in the East Indies, and earthquakes of various focal depths in the Hindu Kush, the Pamir Knot, the Bonins and off the coast of British Columbia. Refinements of technique and slight differences between different groups of investigators do not alter this conclusion. On the alternative hypothesis (type II), forces generally act normal to the associated feature.

3. Enough differences exist between the results of the several "schools", that no effort should be made to limit duplication of effort. Only by duplication can comparison be obtained.

4. Where unambiguous solutions have been obtained they suggest that displacement is perpendicular to the associated feature in most areas. This may be accomplished by having dip-slip faults striking parallel to the feature or strike-slip faults striking perpendicular to it. Ambiguous results may be given a similar interpretation.

5. When agreement has been obtained on the interpretation of S, uniquely defined solutions should be aimed at.

References

Anderson, E. M. (1942): *The Dynamics of Faulting.* Oliver and Boyd, Edinburgh and London.

Hodgson, J. H. (1957): Nature of Faulting in Large Earthquakes. *Bull. Geol. Soc. Am.*, **68**, 611-643.

Hodgson, J. H. (1958): Direction of Displacements in Western Pacific Earthquakes. *Gutenberg Testimonial Volume*, Pergamon Press, London.

Hodgson, J. H., and W. M. Adams (1958): A Study of the Inconsistent Observations in the Fault-Plane Project. *Bull. Seismol. Soc. Am.*, **48**, 17–31.

Kato, Y., and A. Takagi (1957): Seismic Studies, Part 3. *Science Reports, Tôhoku Univ., Ser. 5*, **8**, 212–224.

Kogan, S. D. (1954): K Voprosu ob Izuchenii Mekhanizma Glubokikh Zemletryasenii. *Dokl. Akad. Nauk SSSR*, **99**, 385–388.

Scheidegger, A. E. (1957): The Geometrical Representation of Fault-Plane Solutions of Earthquakes. *Bull. Seismol. Soc. Am.*, **47**, 89–110.

Sutton, G. H., and E. Berg (1958): Direction of Faulting from First-Motion Studies. *Bull. Seismol. Soc. Am.*, **48**, 117–129.